REPORT NO.
UCB/EERC-78/28
DECEMBER 1978

EARTHQUAKE ENGINEERING RESEARCH CENTER

CYCLIC LOADING TESTS OF MASONRY SINGLE PIERS
VOLUME 2 – HEIGHT TO WIDTH RATIO OF 1

by
SHY-WEN J. CHEN
PEDRO A. HIDALGO
RONALD L. MAYES
RAY W. CLOUGH
and
HUGH D. McNIVEN

Report to:

National Science Foundation
Masonry Institute of America
Western States Clay Products Association
and the
Concrete Masonry Association of California and Nevada

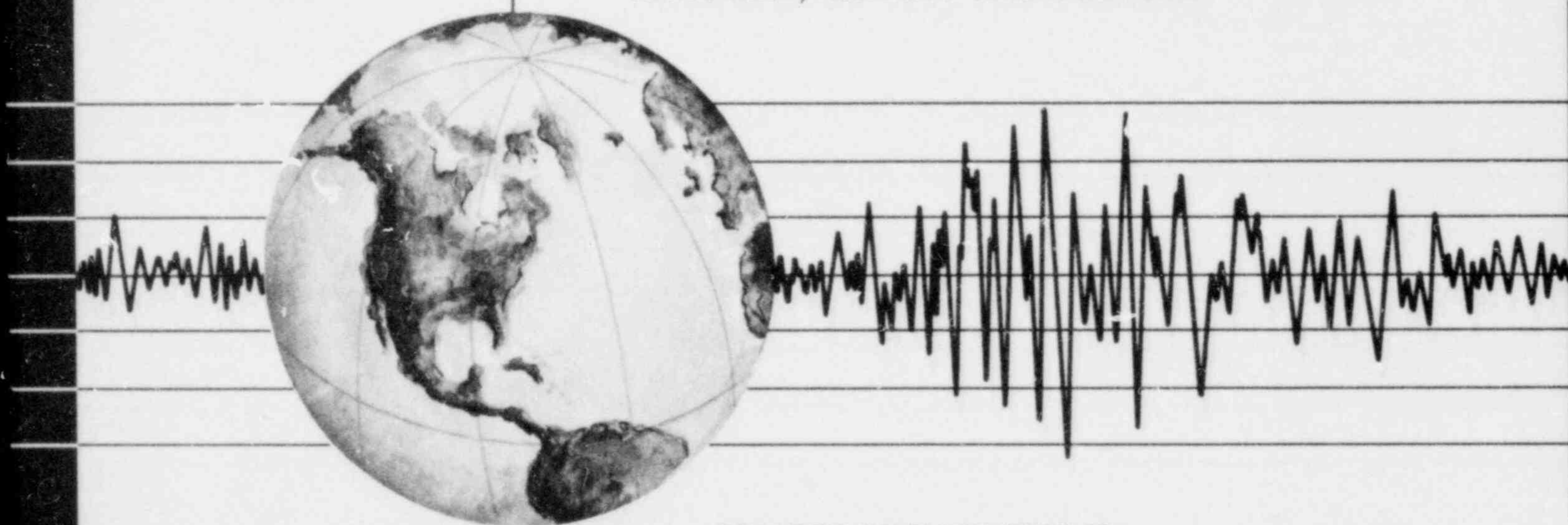

COLLEGE OF ENGINEERING

UNIVERSITY OF CALIFORNIA · Berkeley, California

CYCLIC LOADING TESTS OF MASONRY SINGLE PIERS
VOLUME 2 - HEIGHT TO WIDTH RATIO OF

by

Shy-Wen J. Chen

Pedro A. Hidalgo

Ronald L. Mayes

Ray W. Clough

and

Hugh D. McNiven

Report to

National Science Foundation
Masonry Institute of America
Western States Clay Products Association
Concrete Masonry Association of California and Nevada

Report No. UCB/EERC-78/28

Earthquake Engineering Research Center
College of Engineering
University of California
Berkeley, California

December, 1978

ABSTRACT

This report presents the results of thirty-one cyclic, in-plane shear tests on fixed ended masonry piers having a height to width ratio of 1. These thirty-one tests form part of a test program consisting of eighty single pier tests. A previous report presented the results of fourteen tests of piers having a height to width ratio of 2 and subsequent reports will present the test results of the remaining thirty-five tests.

The test setup was designed to simulate insofar as possible the boundary conditions the piers would experience in a perforated shear wall of a complete building. Each test specimen was a full scale pier 56 inches high and 40 inches wide. Three types of masonry construction were used; hollow concrete block and hollow clay brick, both with 8 inch wide units, and a double wythe grouted core wall, 10 inches thick, that consisted of two clay brick wythes 3¼ inches thick and a 3½ inch grouted core. The other variables included in the investigation were the quantity of reinforcement and the type of grouting.

The results are presented in the form of hysteresis envelopes, graphs of stiffness degradation, energy dissipation and shear distortion, and tabulated data on the ultimate strength and hysteresis indicators. A discussion of the test results is presented but no definitive conclusions are offered. These will be included in a final report at the completion of the eighty tests.

ACKNOWLEDGEMENTS

This investigation was jointly sponsored by the National Science Foundation under Grant ENV76-04265, the Masonry Institute of America, the Western States Clay Products Association and the Concrete Masonry Association of California and Nevada. The authors wish to express their appreciation for technical advice and encouragement received from Mr. Walter Dickey, Mr. John Tawresey, Mr. Donald Wakefield, Mr. Dick Wasson, Mr. James Amrhein, Mr. Stuart Beavers and Mr. Don Prebble. D. A. Sullivan and Co. constructed all the test specimens. Many thanks also are due to Messrs. David Steere, Ivo Van Asten, Robert Robinson, Derald Clearwater, John McNab and Steve Miller of the Earthquake Engineering Research Center for their electronic and machine shop work. The authors also wish to thank the students A. Anvar, J. Kubota, A. Agarwal, A. Shaban, B. Sveinsson, F. Medina, J. Baniesrael and J. Pfeiffer for their help in performing the tests and reducing the test data, and Mrs. B. Bolt for reviewing the manuscript. The computing facilities to reduce the data were provided by the Computer Center at the University of California, Berkeley.

The typing was done by Ms. Toni Avery and the drafting by Ms. Gail Feazell.

TABLE OF CONTENTS

LIST OF TABLES

LIST OF FIGURES

1. INTRODUCTION

1.1. The Multistory Masonry Building Research Program

A multistory masonry building research program was initiated at the Earthquake Engineering Research Center in September 1972, and has continued for the past six years. After an extensive review of literature [4,5]* dealing with resistance of masonry to earthquakes, it was concluded that shear walls penetrated by numerous window openings (Fig. 1.1) were the components of multistory masonry buildings most frequently damaged in past earthquakes, and it was decided that an experimental study of the seismic behavior of such components was necessary.

Two types of structural components can be identified in the shear wall of Fig. 1.1, the piers and the spandrel beams. In order to study the pier behavior, a testing fixture was designed to subject typical full-scale double pier specimens to combined static vertical (gravity) and cyclic lateral (seismic) loads (Fig. 1.2). The results obtained from seventeen such specimens have been reported by Mayes et al.[7,8]. These results show significant variations in the pier behavior with the various test parameters including the type of grouting, types of reinforcement and the rate of loading. The results were not conclusive and demonstrated the need for more extensive tests to establish definitive parametric relationships.

The cost of the double pier tests, both in money and time, precluded carrying out extensive parametric variations with the double pier test setup and, consequently, a single pier test system was designed which greatly simplified the investigation (Fig. 1.3). A series of eighty

---

* References are arranged in alphabetical order of the authors names, and are listed at the end of the text.

single pier tests was planned, which included the following test parameters: type of masonry construction, height to width ratio of the piers, type of grouting, and amount and distribution of both vertical and horizontal steel reinforcement. The present report deals with the experimental results of specimens with a height to width ratio of 1.

1.2 Objectives and Scope of the Single Pier Test Program

In determining the shear strength of masonry piers and panels, the first step is to evaluate the mode of failure. Because most failures in past earthquakes have been characterized by diagonal cracks, many research programs have concentrated on this type of failure mechanism. Test techniques used by Blume[1], Greenley and Cactaneo[2], and others induce the diagonal tension or shear mode of failure. Scrivener[13], Meli[10], Williams[14] and Priestley and Bridgeman[11] recognized that there are two possible modes of failure for cantilever piers. In addition to the shear or diagonal tension mode, they recognized that for certain piers, a flexural failure occur. This mechanism is characterized by yielding of the tension steel of the wall, followed by a secondary failure at the compressive toe, with associated buckling of the reinforcement once confinement is lost. Meli[10] described the flexural failure as similar to that of an under-reinforced concrete beam; i.e., extensive flexural cracking and strength limited by yielding of the reinforcement with failure finally due to crushing of the compressive corner or to rupture of the extreme bars.

Because the double pier tests were the first fixed ended piers to be tested cyclically, the objective of those tests was to determine the effect of various parameters and compare the results with those obtained by others on cantilever piers. Both the shear and flexural modes of failure were included in that investigation.

One of the main objectives of the single pier test program was to investigate thoroughly the effects of different parameters on the behavior shown with the shear mode of failure. It was evident from the double pier test program that the flexural mode of failure in a fixed ended pier has desirable inelastic characteristics, although these are not as desirable as those obtained by Priestley[12] in cantilever piers. Furthermore, it was recognized that for fixed ended piers, with height to width ratios commonly found in multistory buildings, the amount of horizontal reinforcement required to induce a flexural mode of failure is substantially greater than that required by current codes. Therefore, it was decided to investigate the effects of lesser amounts of horizontal reinforcement on the shear mode of failure to determine if desirable inelastic behavior could be obtained.

The thirty-one tests reported herein are a part of a total program of eighty single pier tests; a matrix characterizing the first sixty-three tests is shown in Table 1.1. The parameters for the remaining seventeen tests will be selected after an evaluation of these sixty-three. The test parameters, other than the type of construction and height to width ratio, include the amount of reinforcement and the effect of partial grouting. Hollow concrete block piers having height to width ratio of 2 were not included in the single pier test program because such piers were investigated in the original double pier tests.

This report presents the results for piers with a height to width ratio of 1 of which eleven tests were performed on hollow concrete block specimens (HCBL), thirteen on hollow clay brick specimens (HCBR) and seven on double wythe grouted core clay brick specimens (CBRC). A previous report[3] presented the results obtained from piers with height to width ratio of 2, and a subsequent report will present the results obtained from the single pier specimens with height to width ratio of 0.5. The results from the series of seventeen specimens which will complete the proposed research program also will be presented in a separate report. The organization of the present report is similar to the previous one on piers with height to width ratio of 2[2]. The general background of the single pier test program has been included again in order to make this report as self-contained as possible.

TABLE 1.1

SINGLE PIER TEST PROGRAM*
(Number of test specimens)

HEIGHT: WIDTH RATIO / TYPE OF MASONRY	HOLLOW CLAY BRICK (HCBR)	DOUBLE WYTHE GROUTED CORE CLAY BRICK (CBRC)	HOLLOW CONCRETE BLOCK (HCBL)	TOTAL NUMBER
2 : 1	9	5	0	14
1 : 1	13	7	11	31
1 : 2	6	6	6	18

*Last 17 tests to be decided after this phase is completed

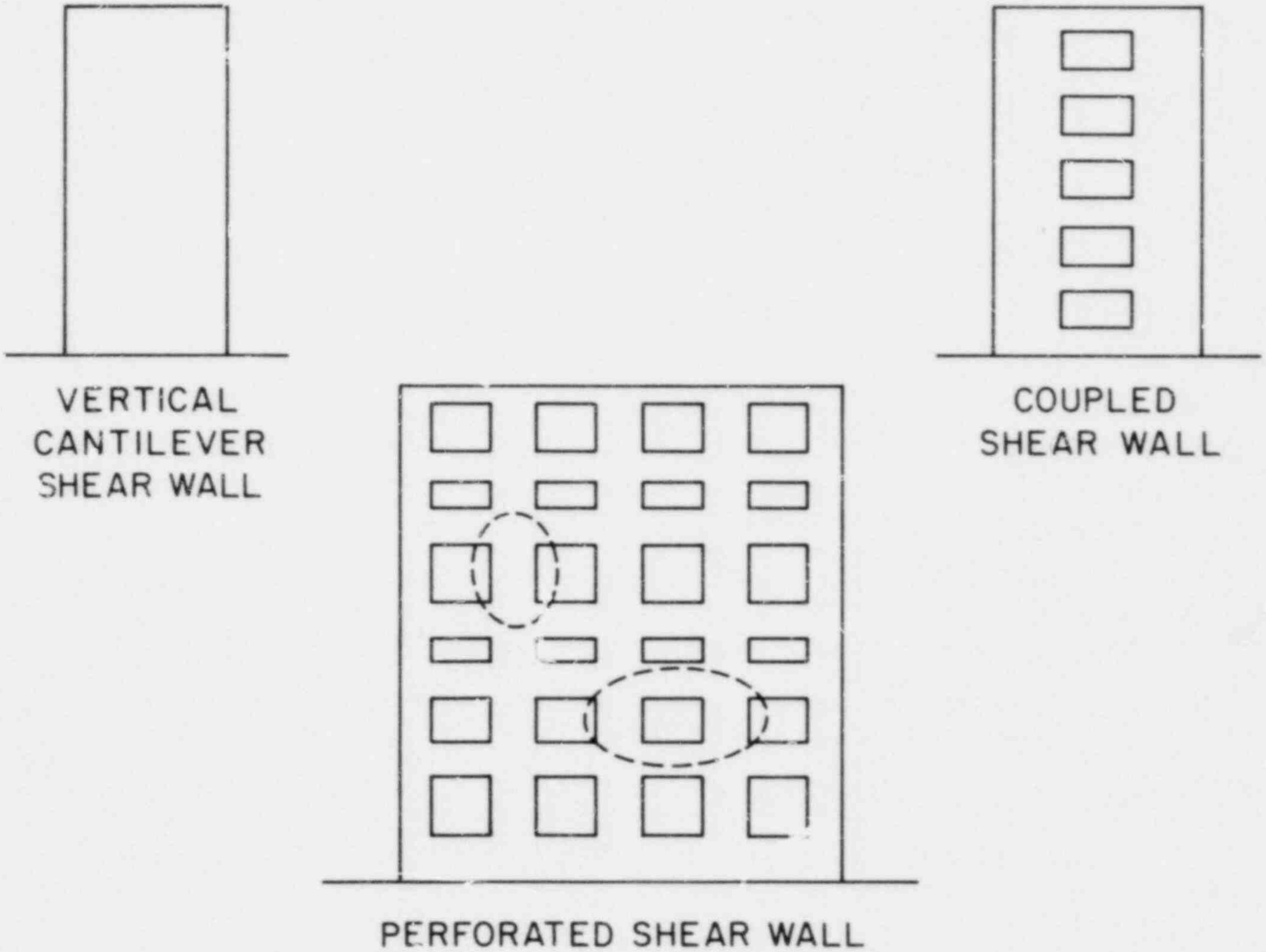

FIG. 1.1 TYPICAL SHEAR WALLS

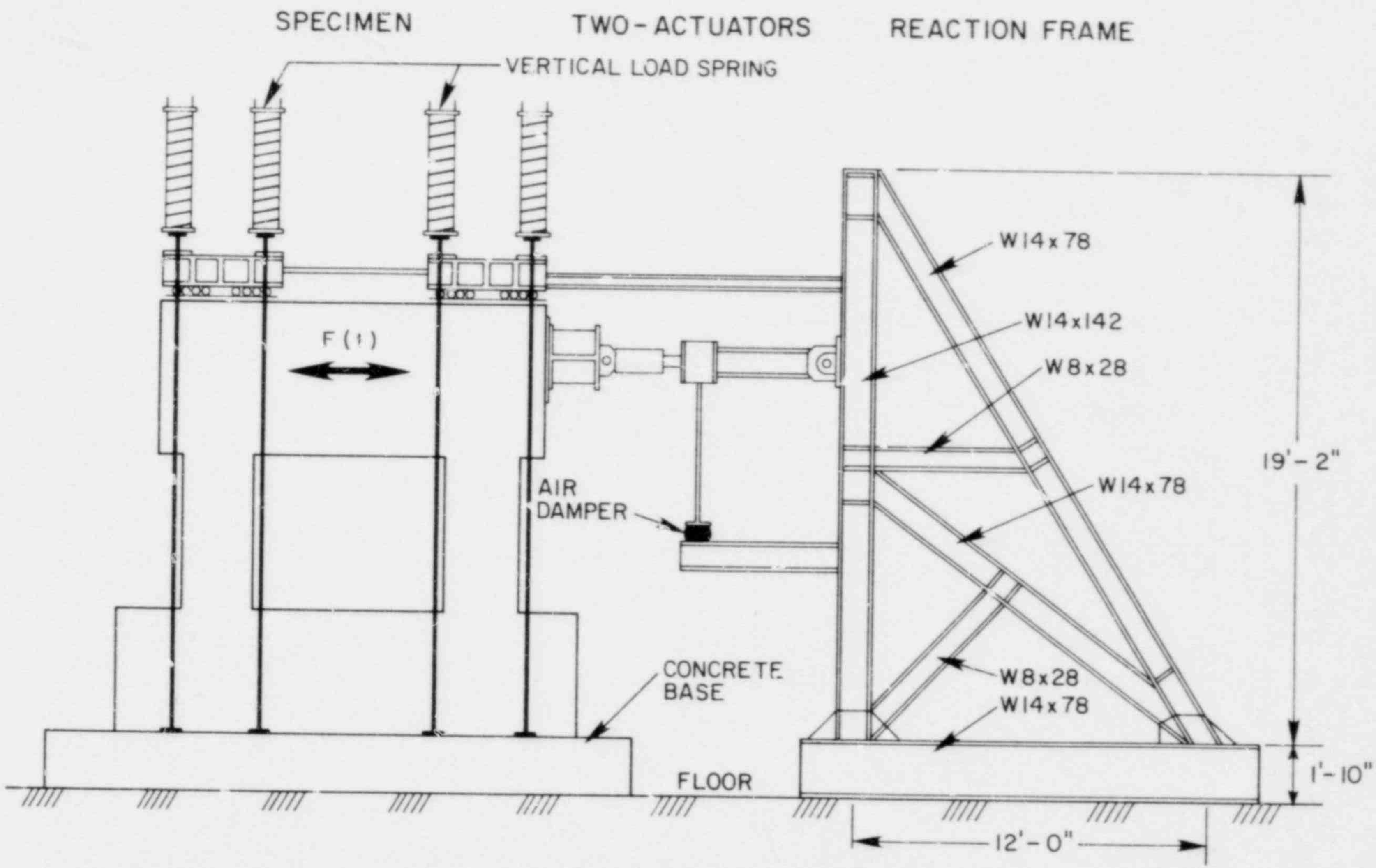

FIG. 1.2 DOUBLE PIER TEST SETUP

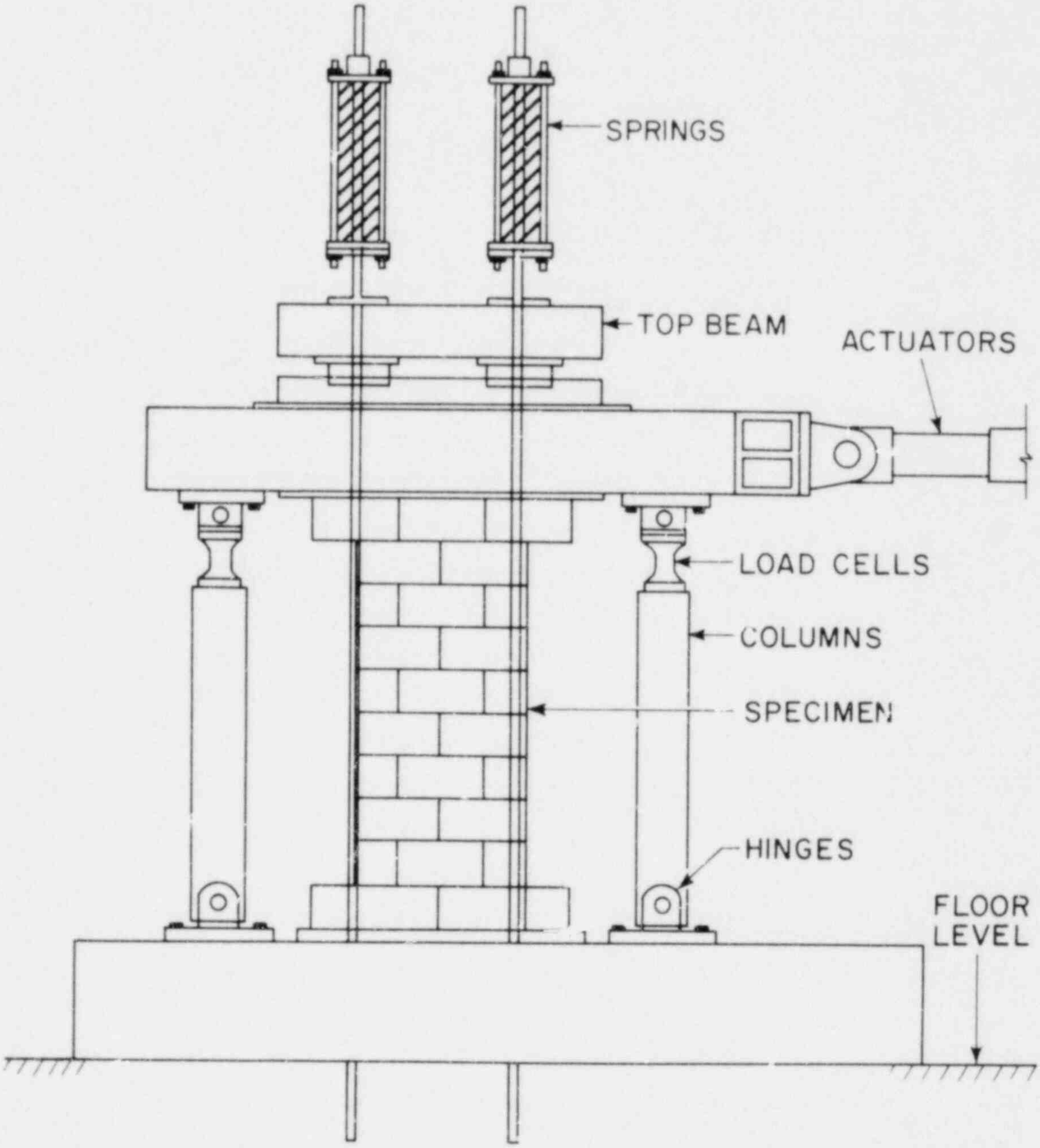

FIG. 1.3 SINGLE PIER TEST SETUP

2. TEST SPECIMENS

2.1 Design and Construction of Specimens

The overall dimensions of the test specimens discussed here are shown in Fig. 2.1. They are the same for all thirty-one piers except for the thickness, which is 7 5/8 inches for the hollow concrete block piers (HCBL), 7 3/8 inches for the hollow clay brick piers (HCBR) and 10 inches for the double wythe grouted core clay brick piers (CBRC).

The HCBL panels were constructed from standard two-core hollow concrete blocks nominally 8 inches wide x 8 inches high x 16 inches long, as shown in Fig. 2.3(a). The cored area of each block is approximately 50.6 square inches and the ratio of net to gross area is 58%.

The HCBR piers were constructed from standard two-core hollow clay bricks nominally 8 inches wide x 4 inches high x 12 inches long, as shown in Fig. 2.3(b). The cored area of each brick is approximately 57.4 square inches and the ratio of net to gross area is 67%.

The CBRC piers were constructed from two wythes of solid clay bricks nominally 4 inches wide x 4 inches high x 12 inches long, as shown in Fig. 2.3(c). The grouted space between the wythes was 3 1/2 inches wide and was filled after the steel reinforcement had been placed in position.

The piers were constructed on 0.75 inch thick steel plates as shown in Fig. 2.2. A similar plate was added on top of the pier after the grout was poured. Both plates had holes to permit anchorage of the vertical steel reinforcement and keys to provide an adequate shear transfer between the masonry pier and the steel plate. The plates also had welded bolts and holes to anchor the pier to the test rig.

Seven of the eleven HCBL piers and nine of the thirteen HCBR piers were fully grouted. The remaining four piers in each of the HCBL and HCBR series were partially grouted. Partial grouting consisted of grouting the cores containing vertical reinforcement and the bond beams containing horizontal reinforcement. All the CBRC piers had the 3 1/2 inch core between the wythes fully grouted and have been termed "solid grouted".

The series of tests was planned to determine the effect of the quantity of steel reinforcement and of partial grouting on the strength and deformation properties of the piers, considering combinations of steel and grouting as shown in Table 2.1. Details of the reinforcing bar arrangements are shown in Fig. 2.4(a) for the HCBL piers, in Fig. 2.4(b) for the HCBR piers and in Fig. 2.4(c) for the CBRC piers. The actual position of the vertical reinforcement is indicated in Fig. 2.1. When horizontal reinforcement was used, the bars were evenly distributed over the height of the pier.

2.2 Material Properties

Table 2.2 shows the mechanical properties of the materials used in the construction of the test specimens. The specimens used to determine the material properties are shown in Figs. 2.3(a), (b) and (c).

The tests of the single masonry units followed the ASTM C67-73 Specification[9] and were based on five samples for each test.

The joint mortar was specified as standard ASTM type M (i.e., 1 Cement : 1/4 Lime : 2 1/4 - 3 Sand, by volume), with a minimum compressive strength of 2,500 psi at 28 days. The grout was specified as 1 Cement : 3 Sand : 2 G, where G refers to 10mm maximum size local gravel. Because the specimens were not constructed or grouted at the same time, the mortar and grout strength varied according to normal workmanship. A minimum of three samples of both mortar and grout was taken from each batch used during construction.

ASTM A615 steel was specified for both the vertical and horizontal steel reinforcement. Yield and ultimate strengths are listed in Table 2.2.

Three prisms for uniaxial compression tests (Fig. 2.5) and three square panels for diagonal tension tests (Fig. 2.7) were constructed from the same mortar and grout used in each set of wall panels. All the prisms were fully grouted and had a height-to-thickness ratio of 5. Their compression tests were performed at a loading rate of 12,000 lb/min, and the compressive strengths are shown in Table 2.2. In the case of the HCBL prisms, the compression tests were also used to determine the modulus of elasticity as shown in Fig. 2.5. The axial deformations were measured with mechanical gages attached to both sides of the prisms, over a length of 12 inches. The readings were averaged and plotted as indicated in Fig. 2.6. The average modulus of elasticity for six samples was 1,140 ksi.

The square panels were tested as shown in Fig. 2.7 at a loading rate of 8,000 lb/min, and the ultimate load is shown in Table 2.2. A modified diagonal tension test setup was also used to duplicate some of the simplified tests. The modification was intended to provide better boundary conditions for the application of the shear load, and is discussed in detail in reference[8]. However the time and cost spent on the modified diagonal tension tests were not worth the small improvement obtained in the test results when compared with the simplified test setup. Because of this, the use of the modified diagonal tension test in the single pier test program was discontinued.

The mortar, grout, prism and square panel samples were cured under the same normal atmospheric conditions as the piers; also the prism and square panel tests were performed during the tests of the corresponding piers.

TABLE 2.1

TEST PROGRAM

Pier General Characteristics	Specimen Designation	Test Frequency (cps)	Grouting Full (F) Partial (P) Solid (S)	Reinforcing Steel	
				Vertical	Horizontal
Masonry type: Hollow Concrete Block	HCBL-11-1	1.5	F	No	No
Pier height: H = 56 in	-2	1.5	P	No	No
Pier width: D = 48 in	-3	1.5	F	2#5	No
Pier thickness: 7.625 in	-4	1.5	F	2#5	1#5
Gross section area: 366 in^2	-5	1.5	P	2#5	1#5
Bearing load: 20 kip	-6	1.5	F	2#5	4#5
Bearing stress: 55 psi	-7	1.5	F	2#8	No
	-8	1.5	P	2#8	No
	-9	1.5	F	2#8	2#5
	-10	1.5	P	2#8	2#5
	-11	1.5	F	2#8	4#6
Masonry type: Hollow Clay Brick	HCBR-11-1	0.02	F	No	No
Pier height: H = 56 in	-2	0.02	P	No	No
Pier width: D = 48 in	-3	0.02	F	2#5	No
Pier thickness: 7.375 in	-4	0.02	F	2#5	1#5
Gross section area: 354 in^2	-5	0.02	P	2#5	1#5
Bearing load: 20 kip	-6	0.02	F	2#5	5#5
Bearing stress: 56 psi	-7	0.02	F	2#5	5#5
	-8	0.02	F	2#8	No
	-9	0.02	P	2#8	No
	-10	0.02	F	2#8	2#5
	-11	0.02	P	2#8	2#5
	-12	0.02	F	2#8	5#6
	-13	0.02	F	2#8	5#6
Masonry type: Double Wythe Grouted	CBRC-11-1	0.02	S	No	No
Core Clay Brick	-2	0.02	S	2#5	No
Pier height: H = 56 in	-3	0.02	S	2#5	1#5
Pier width: D = 48 in	-4	0.02	S	2#5	5#5
Pier thickness: 10 in	-5	0.02	S	2#8	No
Gross section area: 480 in^2	-6	0.02	S	2#8	2#5
Bearing load: 20 kip	-7	0.02	S	2#8	5#6
Bearing stress: 42 psi					

TABLE 2.2

MATERIAL PROPERTIES

Specimen	Masonry Unit: Gross Compressive Strength (psi)	Masonry Unit: Net Tensile Strength (psi)	Mortar Compressive Strength (psi)	Grout Compressive Strength (psi)	Prism (5:1) Compressive Strength (psi)	Ultimate Load of Sq. Panel (kip)	Vertical Reinforcement: Yie'd Strength (ksi)	Vertical Reinforcement: Ultimate Strength (ksi)	Horizontal Reinforcement: Yield Strength (ksi)	Horizontal Reinforcement: Ultimate Strength (ksi)
HCBL-11-1			2754.	3810.	1330.	58.4	---	---	---	---
-2			2754.	3810.	---	---	---	---	---	---
-3			2965.	4020.	1833.	64.5	70.81	108.71	---	---
-4			2965.	4020.	1833.	64.3	70.81	108.71	47.91	75.65
-5			2754.	3810.	---	---	70.81	108.71	47.91	75.65
-6			2965.	4020.	1833.	63.4	70.81	108.71	47.91	75.65
-7			2322.	6895.	1905.	78.1	69.20	105.91	---	---
-8			2942.	6860	---	---	69.20	105.91	---	---
-9			2942.	6860.	1905.	78.1	69.20	105.91	47.91	75.65
-10			2322.	6895.	---	---	69.20	105.91	47.91	75.65
-11			2322.	6895.	1330.	62.7	69.20	105.91	73.85	102.25
Average	1800	293	2728.	5263.	1710.	67.	69.9	107.2	52.2	80.1
HCBR-11-1			3840.	4225.	2535.	144.1	---	---	---	---
-2			3840.	4225.	---	---	---	---	---	---
-3			3840.	4225.	2535.	144.1	75.00	113.00	---	---
-4			3044.	4327.	2722.	185.8	71.34	108.07	70.00	109.04
-5			3838.	5780.	---	---	71.34	108.07	70.00	109.04
-6			4316.	4857.	2722.	171.9	71.34	108.07	64.20	100.33
-7			1870.	4225.	2535.	144.1	75.00	113.00	72.60	109.7
-8			3080.	4207.	2866.	149.9	69.20	105.91	---	---
-9			3838.	5780.	---	---	69.20	105.91	---	---
-10			3044.	4327.	2722.	185.8	72.87	112.19	68.71	95.32
-11			3044.	4327.	---	---	72.87	112.19	68.71	95.32
-12			1870.	4225.	2535.	144.1	76.00	108.20	73.85	102.25
-13			3044.	4327.	2722.	185.8	72.87	112.19	74.66	109.89
Average	5816	466	3270.	4543.	2655.	162.	72.5	109.7	70.3	103.9
CBRC-11-1			2640.	4230.	2507.	142.0	---	---	---	---
-2			2640.	4230.	2507.	142.0	71.72	110.11	---	---
-3			2640.	4230.	2507.	142.0	71.72	110.11	68.28	102.37
-4			2640.	4230.	2507.	152.5	71.72	110.11	68.28	102.37
-5			2640.	4230.	2507.	142.0	72.87	112.19	---	---
-6			2640.	4230.	2507.	152.5	72.87	112.19	73.87	106.46
-7			2640.	4230.	2507.	152.5	72.87	112.19	74.66	109.89
Average	5443	253	2640.	4230.	2507.	147.	72.3	111.2	71.3	105.3

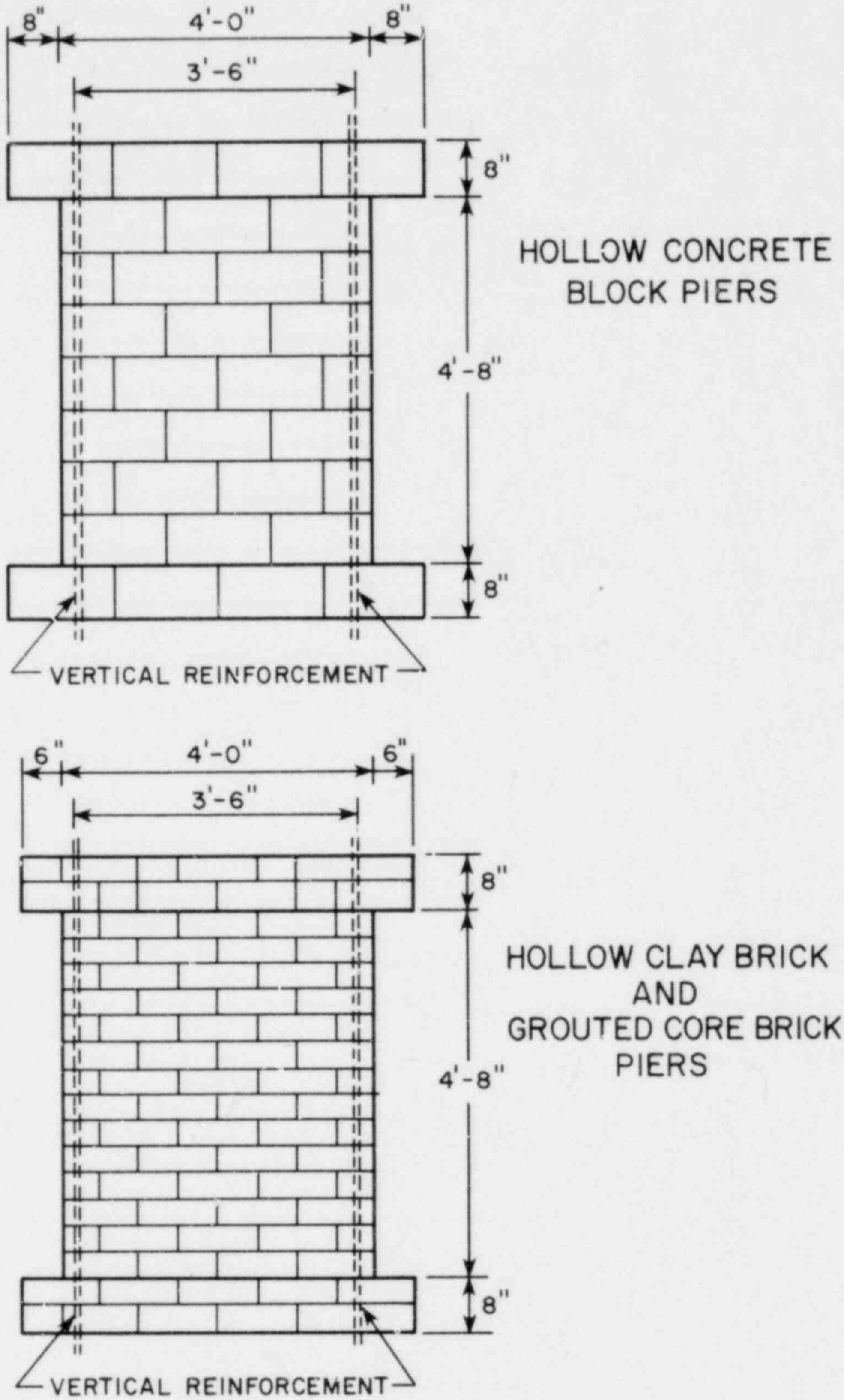

FIG. 2.1 PIER DIMENSIONS

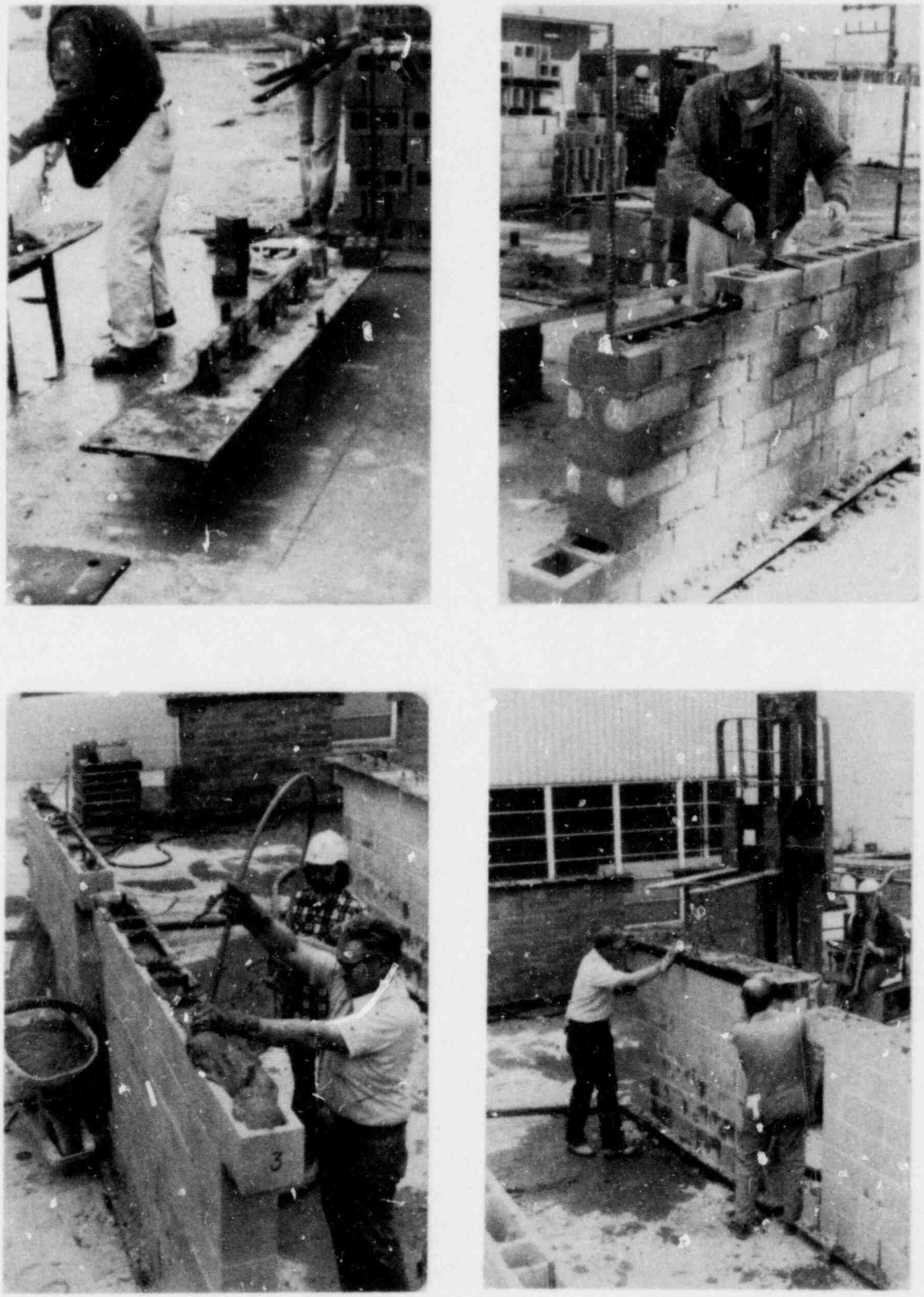

FIG. 2.2 CONSTRUCTION OF TEST SPECIMENS

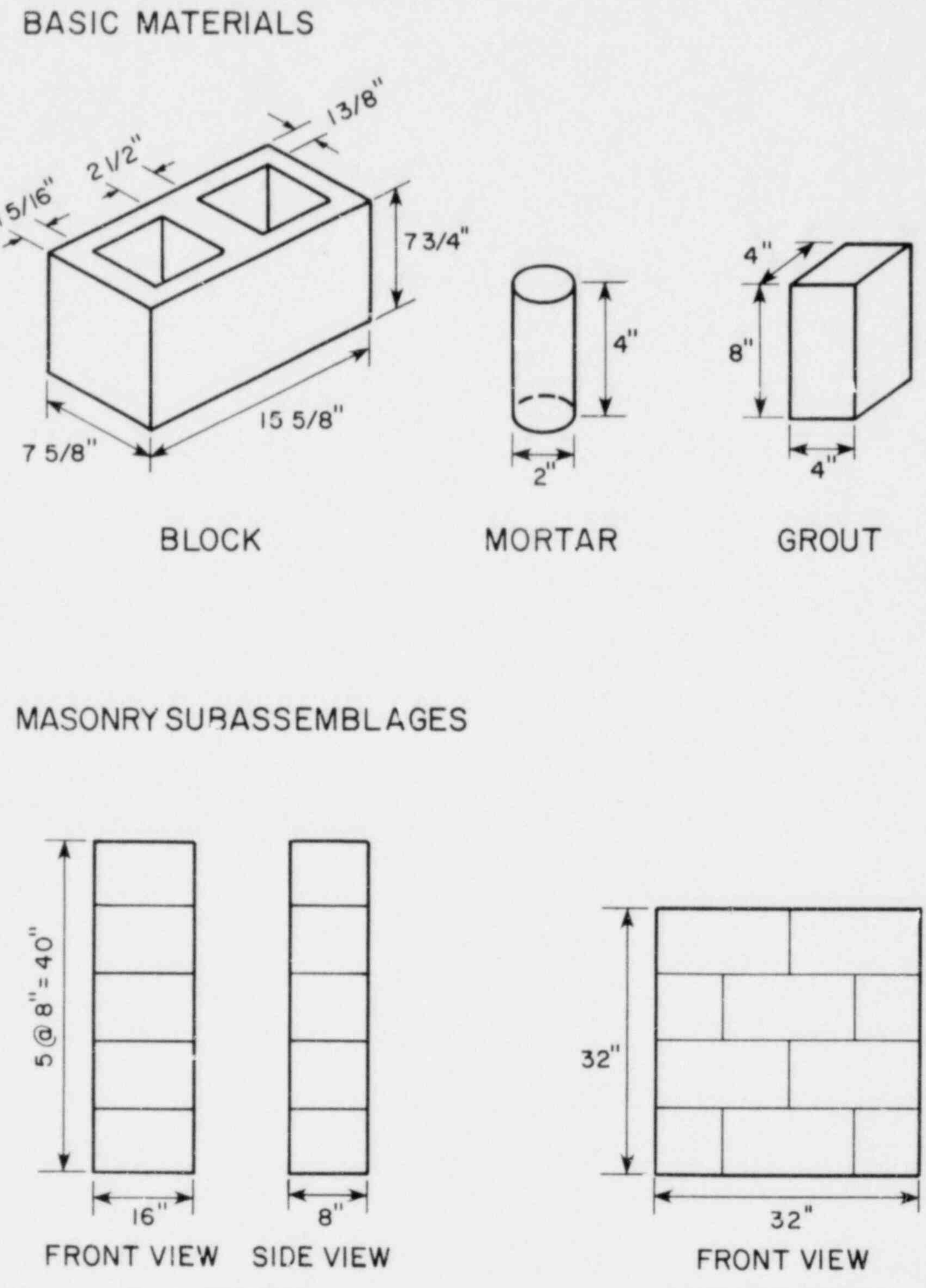

FIG. 2.3(a) SPECIMENS TO DETERMINE MATERIAL PROPERTIES (HCBL)

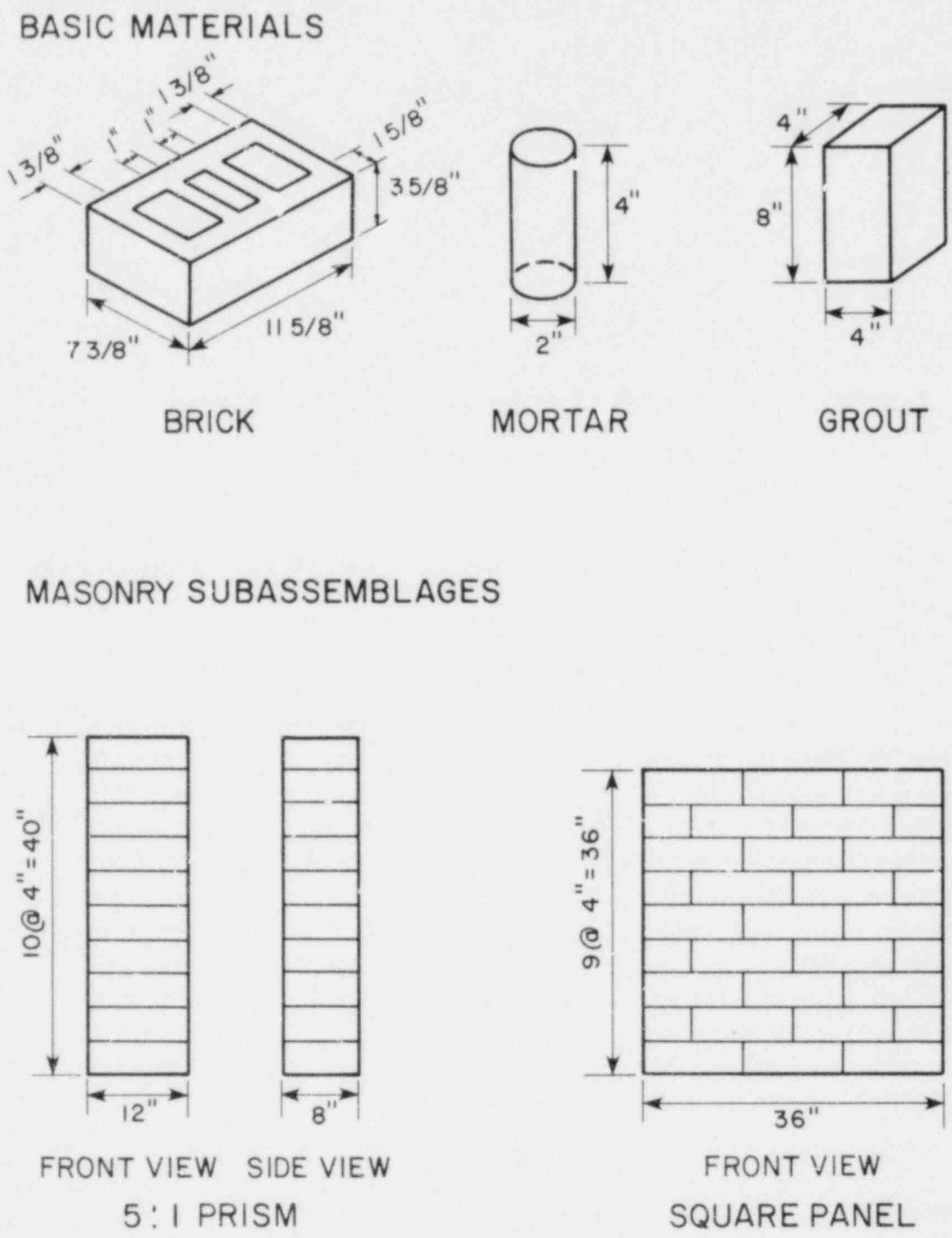

FIG. 2.3(b) SPECIMENS TO DETERMINE MATERIAL PROPERTIES (HCBR)

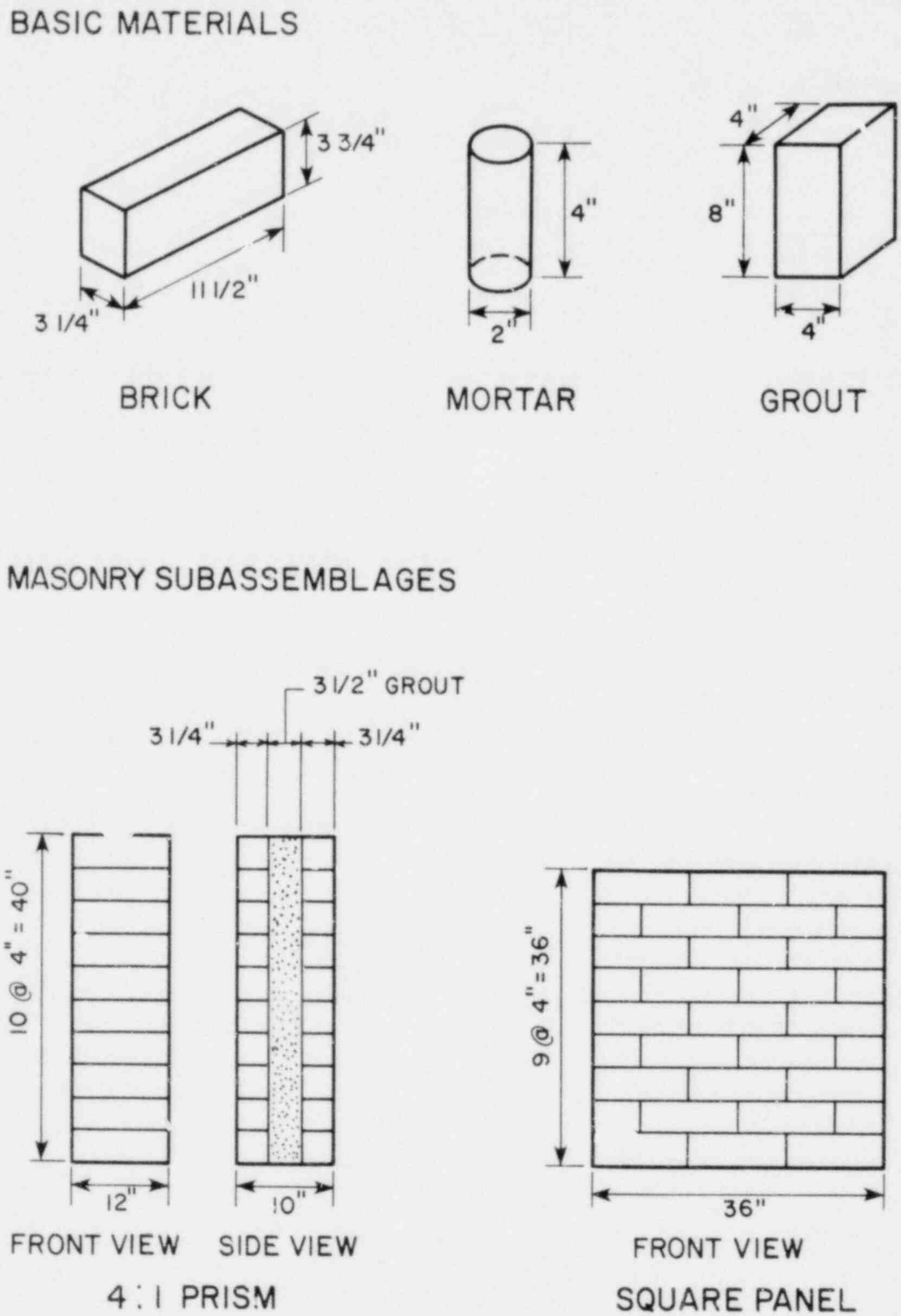

FIG. 2.3(c) SPECIMENS TO DETERMINE MATERIAL PROPERTIES (CBRC)

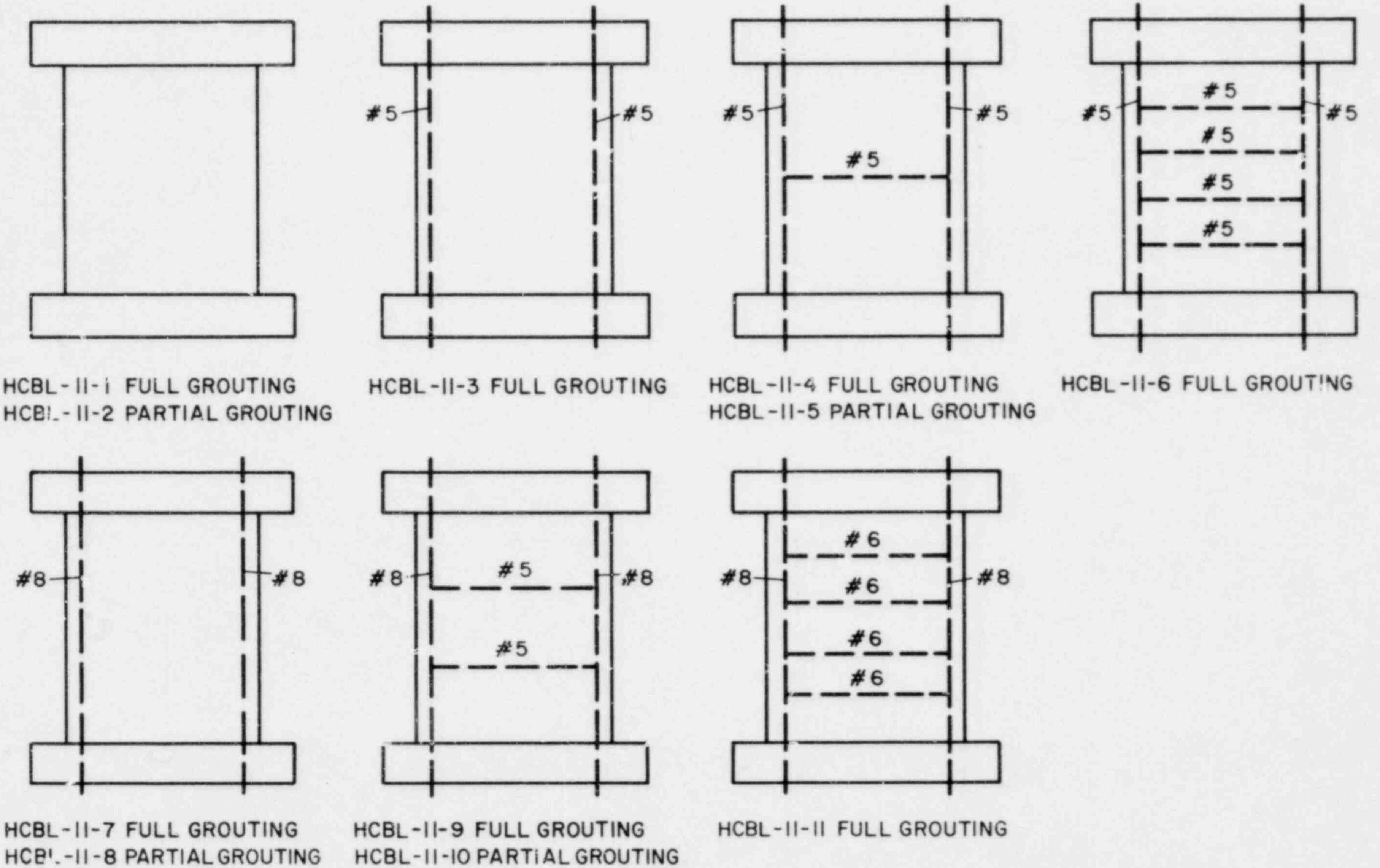

FIG. 2.4(a) REINFORCING STEEL ARRANGEMENTS FOR HOLLOW CONCRETE BLOCK PIERS (HCBL)

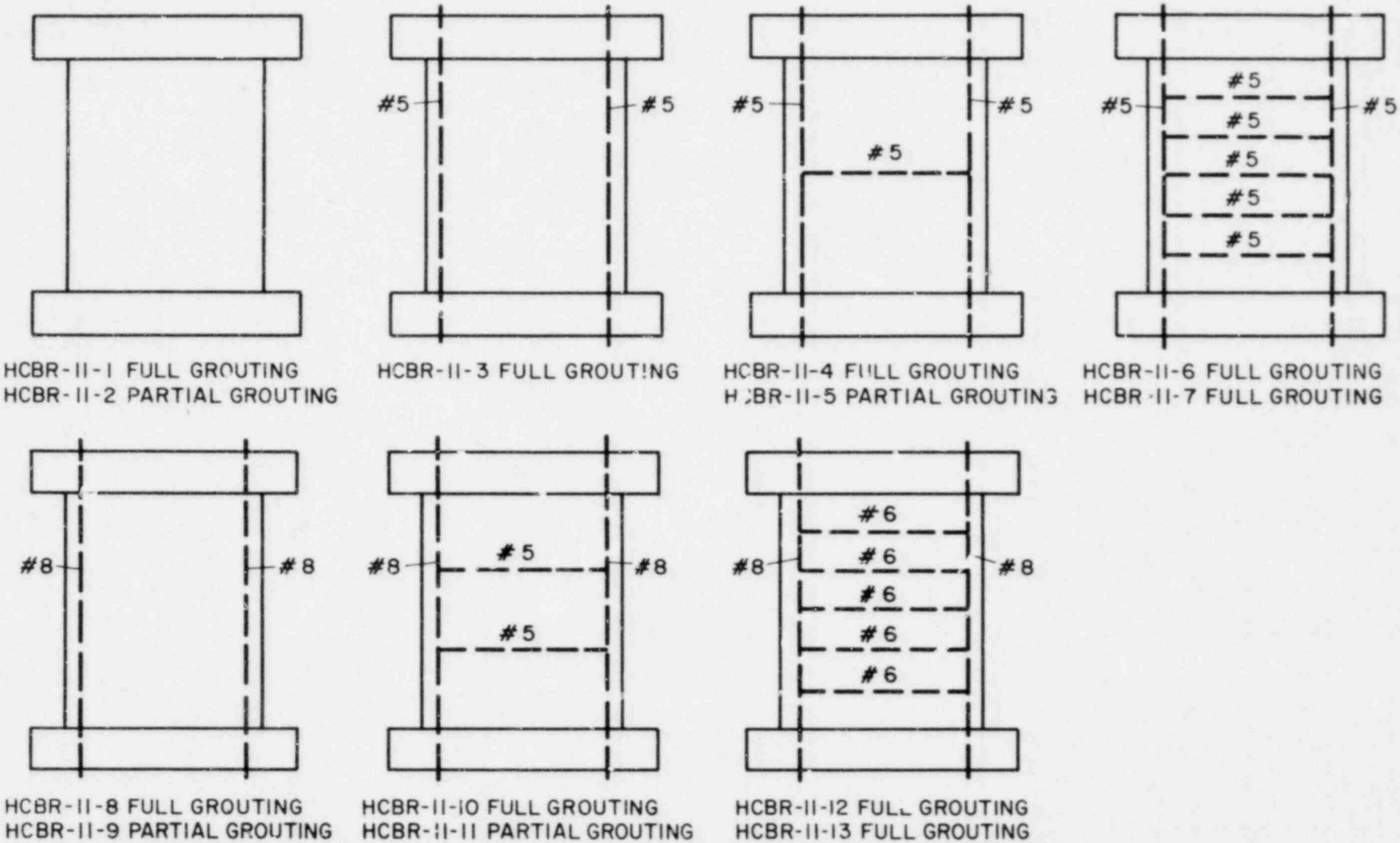

FIG. 2.4(b) REINFORCING STEEL ARRANGEMENTS FOR HOLLOW CLAY BRICK PIERS (HCBR)

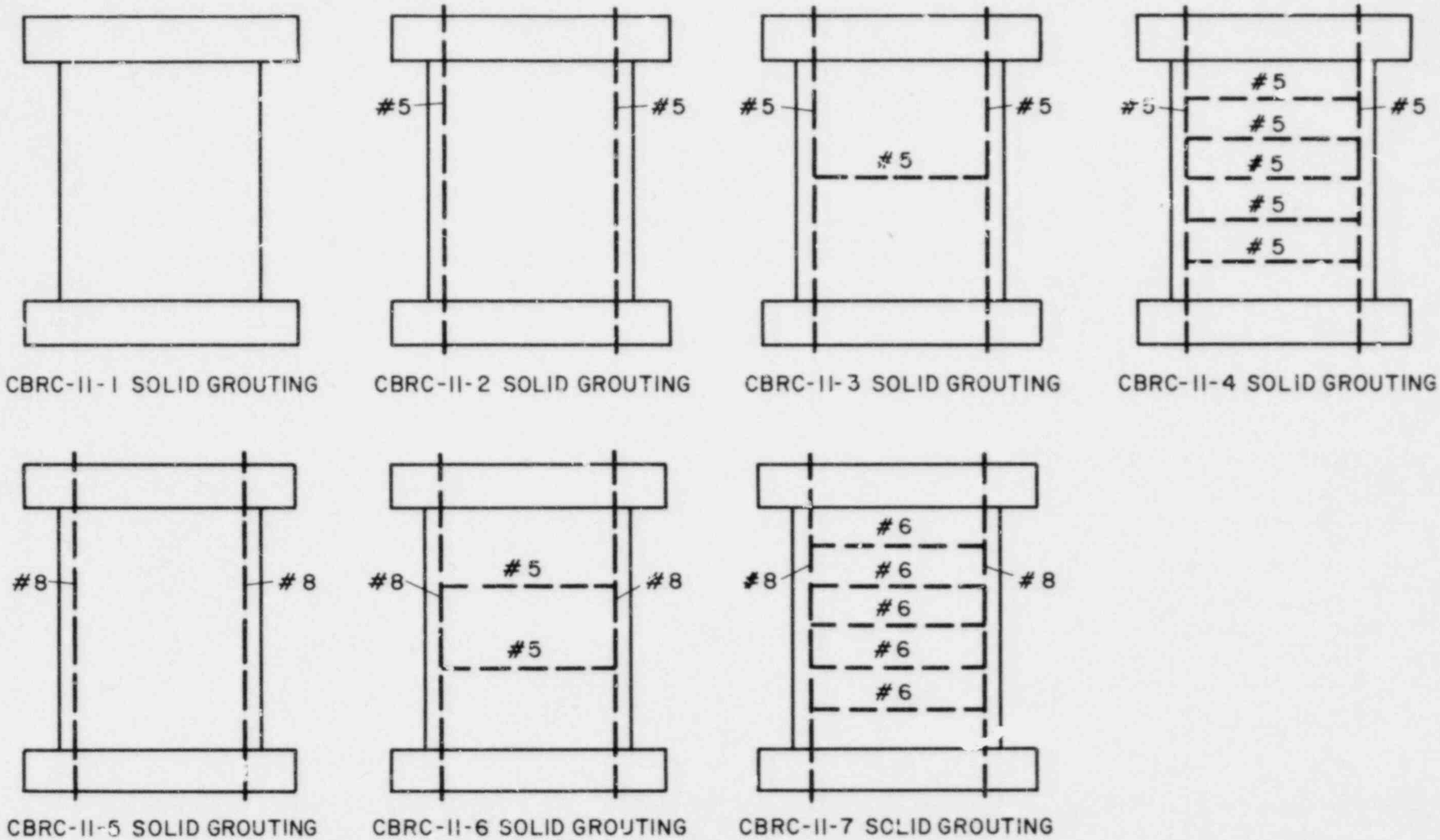

FIG. 2.4(c) REINFORCING STEEL ARRANGEMENTS FOR GROUTED CORE BRICK PIERS (CBRC)

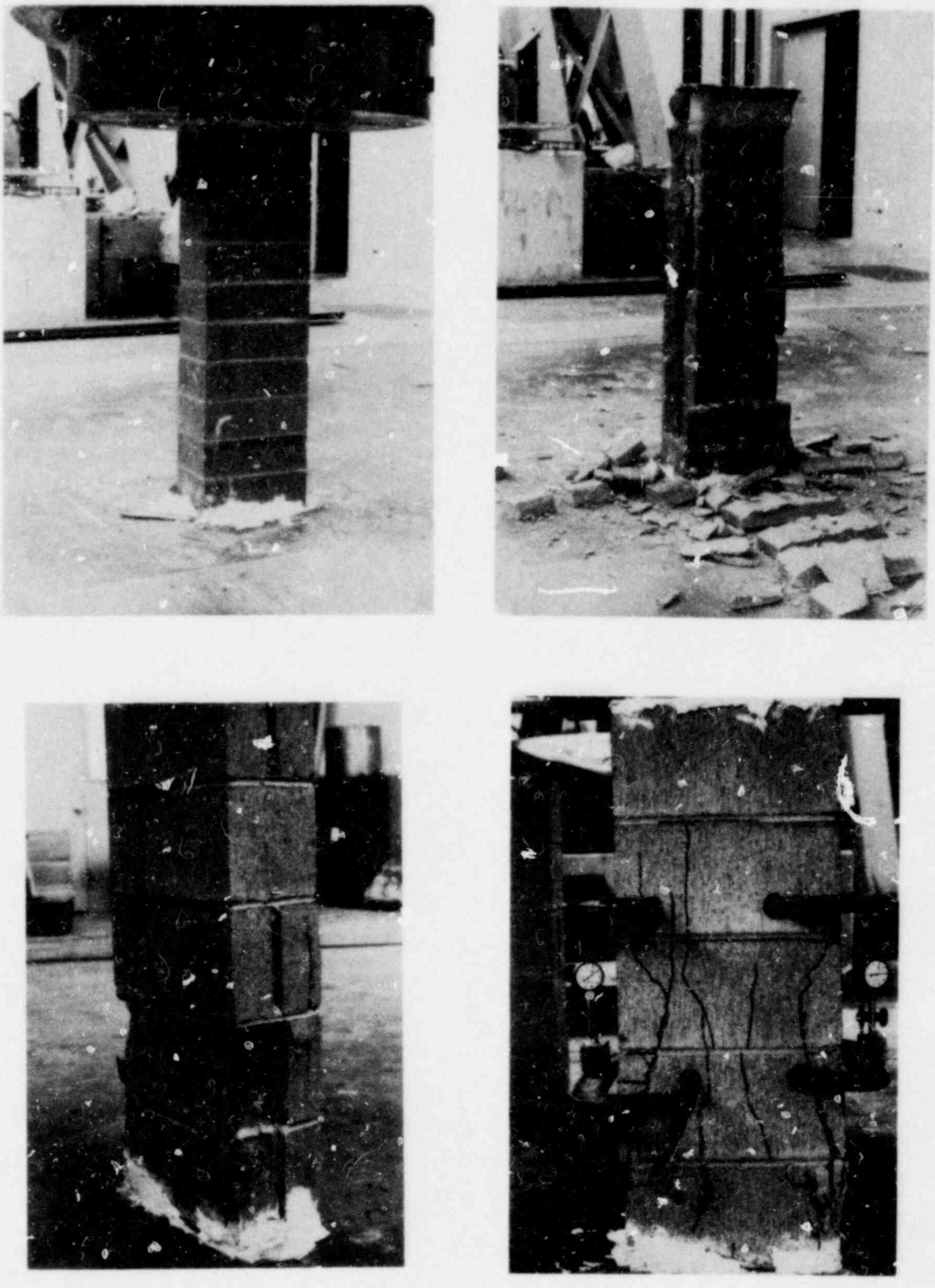

FIG. 2.5 PRISM TEST AND MODULUS OF ELASTICITY MEASUREMENT

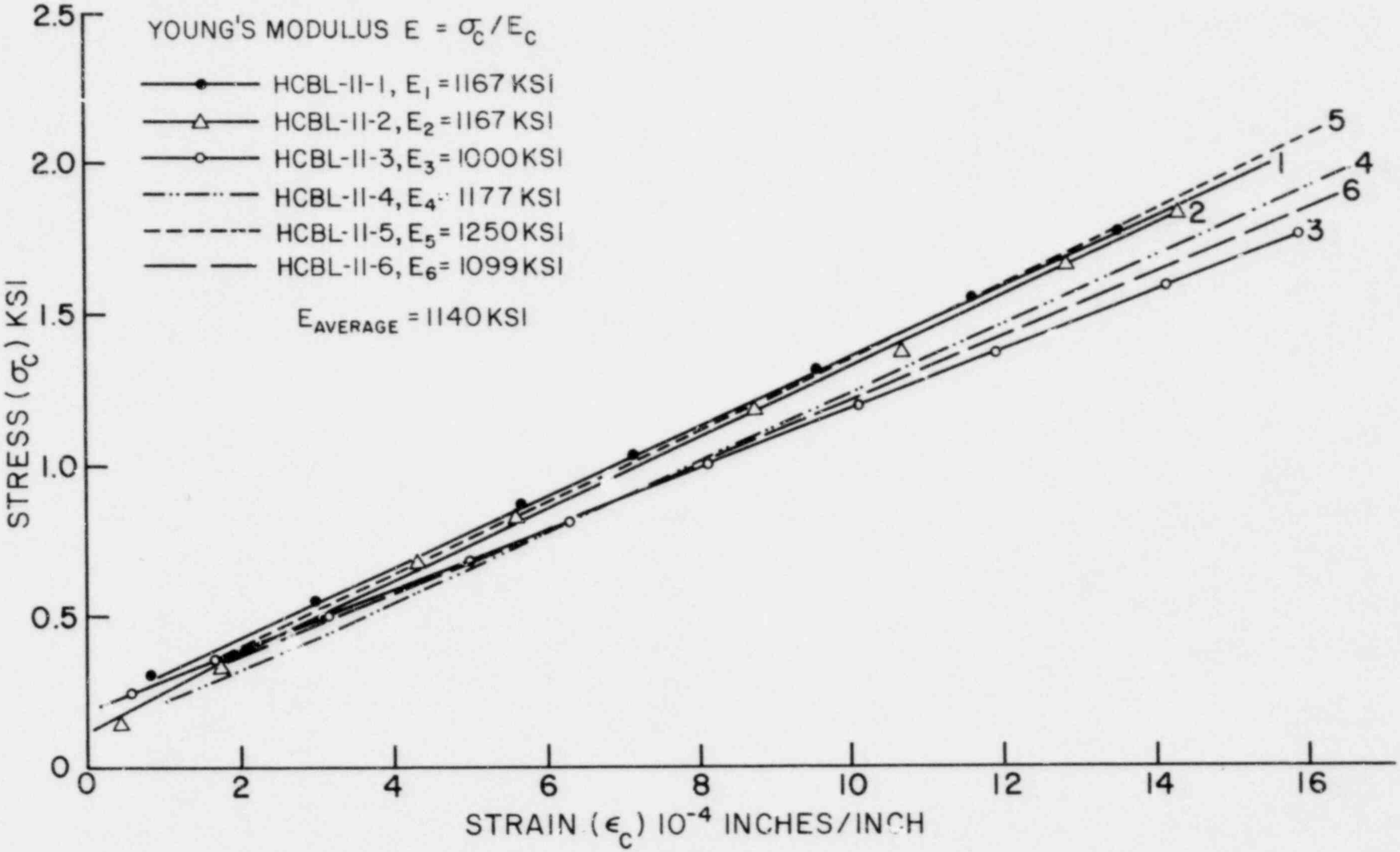

FIG. 2.6 MODULUS OF ELASTICITY MEASUREMENTS FOR HOLLOW CONCRETE BLOCK PIERS

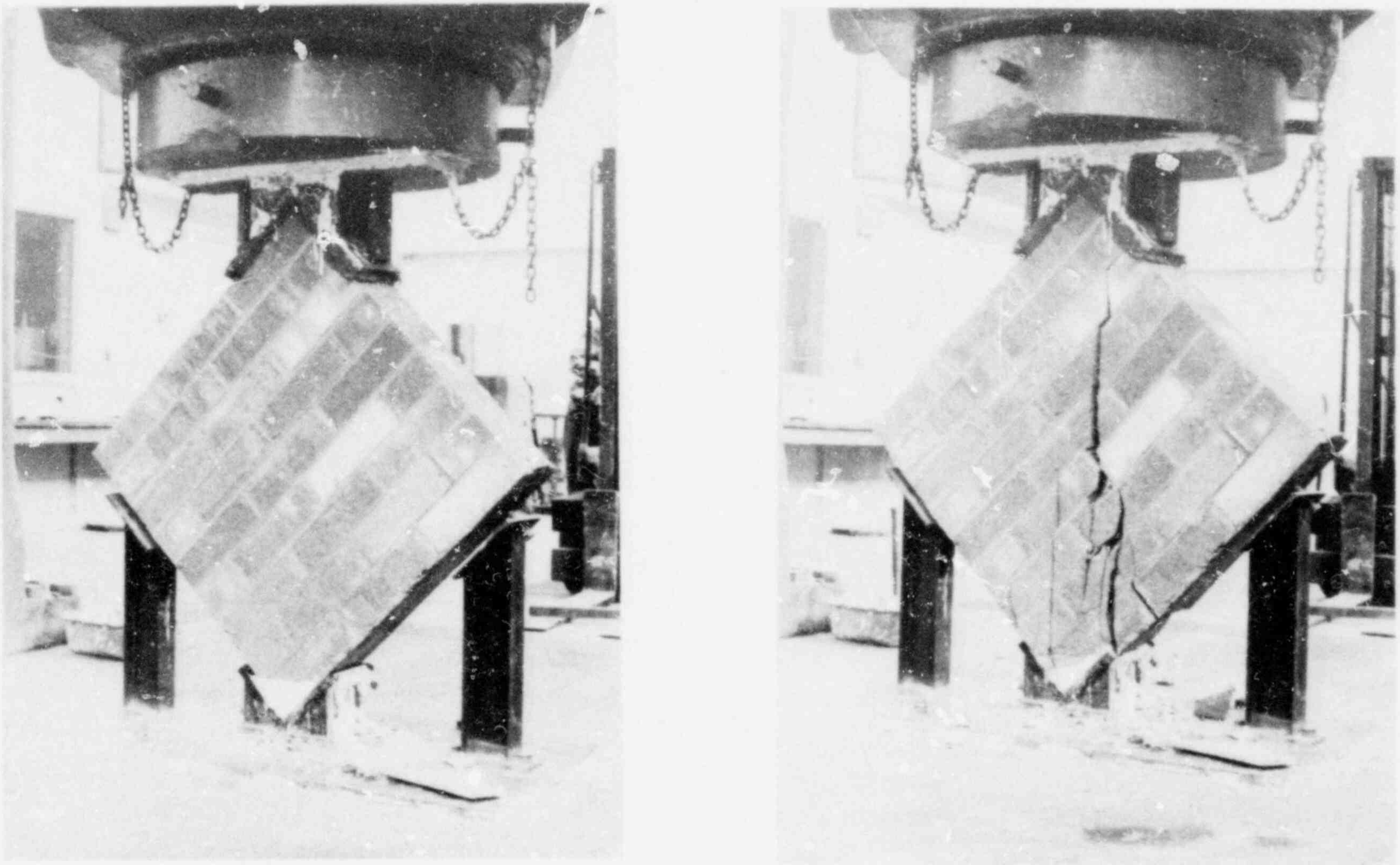

FIG. 2.7 SQUARE PANEL TEST

3. TEST EQUIPMENT AND PROCEDURE

3.1 Test Equipment

The test equipment shown in Figs. 3.1 and 3.2 permits lateral loads to be applied in the plane of the piers in a manner similar to which a floor diaphragm would load the piers during earthquake excitation. It consists of two 20 feet high, heavily-braced reaction frames supporting a pair of horizontally acting hydraulic actuators; a mechanism capable of applying vertical bearing loads similar to the gravity loads experienced by the piers in an actual structure; a bottom beam composed of a concrete base and a wide flange steel beam which provides anchorage to the test floor and suitable connection holes to the bottom plate of the specimen; and a top beam fabricated from two wide flange, steel beams as shown in Fig. 3.1. The top and bottom beams simulate the action of the spandrel beams in actual masonry construction; they are connected by two steel columns located 10 feet 7 inches apart, which prevent rotation of the top beam and thus provide approximate fixed-fixed end conditions during the test.

The maximum dynamic load which may be developed by each of the horizontal actuators is 75 kips, using a hydraulic pressure of 3,000 psi. The maximum stroke is ± 6 inches, the maximum piston velocity is 26 in./sec and the flow capacity of the servovalves is 200 gpm. Either displacement or load can be controlled with these actuators. Their operational capabilities are limited by the above mentioned force capacity, and also by a frequency limitation of about 5 Hz. The actuator control consoles are shown in Fig. 3.5.

A vertical load up to 160 kips can be applied to the pier through the springs and rollers shown in Fig. 3.2. The Thomas Dual Roundway

Bearings connecting the springs to the top of the panel allow the panel to move freely with minimal friction force. The coefficient of friction of bearings is purported to be 0.007.

An additional vertical, compressive load results from the characteristics of this test setup. As significant lateral displacements are imposed on the top beam by the hydraulic actuators, the constraint provided by the side columns forces the top beam to move in a circular arc. The vertical component of this motion is opposed by the axial stiffness of the pier, resulting in a compressive load being applied to the pier. The significance of this additional, cyclic varying compressive load on the test results is discussed in Chapter 5.

Each pier was constructed on a 0.75 inch thick steel plate and had a similar plate on top, as discussed in Section 2.1. This allowed the piers to be moved into place before each test and bolted to the bottom and top steel beams. Prior to the bolting process, hydrostone was placed between the surfaces of the plates and beam flanges as well as between the top plate and the top brick course of the pier.

3.2 Loading Sequence

Each pier was subjected to a series of displacement controlled, in-plane shear loads. The full sequence of loading consisted of sets of three sinusoidal cycles of loading at a specified actuator displacement amplitude. The specified amplitude was gradually increased; the full loading sequence is given in Table 3.1. After each stage, (one set of three sinusoidal displacements at the same amplitude), the walls were visually inspected and the crack pattern identified and photographed. The sinusoidal cycles were applied at the frequency of 1.5 cycles per second during the HCBL pier tests and at 0.02 cycles per second for the remainder of the test program.

The test of each pier had a duration of 2½ to 3 hours. The test was usually terminated when the shear strength of the pier had dropped below one third of the maximum shear strength. At this stage the pier generally was not capable of supporting significant vertical loads. All the tests were carried out under a constant primary bearing stress of 55 psi (HCBL piers), 56 psi (HCBR piers) or 42 psi (CBRC piers). Additional cyclic vertical compressive loads were developed during the test, as described in Section 3.1 and discussed further in the following chapters.

Partially grouted piers were subjected to maximum input displacement amplitudes of 0.20 inch to 0.45 inch. Fully or solid grouted piers failed at input amplitude displacements ranging from 0.30 inch to 0.80 inch.

Because of the flexibility of the reaction frame and other load transferring devices, the lateral displacement actually experienced by the pier was always less than the actuator input displacement, this difference being smaller towards the end of the test when the pier stiffness had attained its lowest values. There was also a slight difference between the maximum loads developed during the push and pull half cycles due to the different type of stress placed on the bolting system and to the different pier stiffness associated with non-symmetric crack patterns.

3.3 Instrumentation

The total horizontal load applied by the hydraulic actuators, as well as the vertical forces developed by the side columns, were measured using pre-calibrated load cells. Each pier was instrumented as indicated in Fig. 3.3.

DCDT's (direct current differential transformers) H_1 and H_2 were attached to an external reference frame in order to measure the lateral deformation of the pier during each sequence of loading. The difference between H_1 and H_2 was used to indicate the relative lateral deflection of each pier. DCDT's D_1 and D_2 measured the changes in distance between points along the diagonals of the pier and were used to indicate the shear distortion of the pier as defined in Fig. 3.4.

3.4 Data Acquisition and Data Processing

Two different data acquisition systems were used during the test program. The main one consisted of a high speed scanner able to handle up to 25 channels of information, and the corresponding tape recording system (Fig. 3.5). Three computer programs were used to read the original tape, input the calibration values and geometrical data of each pier and to reduce the response data to their final presentation in computer plots.

The second data acquisition system was used to monitor the progress of the test and to act as a back-up system in case of any failure in the main system. It consisted of a direct writing oscillograph (visicorder) and was used only to record the most important data; namely, forces at the actuators and side columns, actuator stroke and lateral displacement of the pier. This second data acquisition system proved to be extremely useful in detecting occasional malfunctions of the actuators or the instruments attached to the pier and provided excellent visualization of the behavior of the pier as the test progressed.

TABLE 3.1

LOADING SEQUENCE

STAGE*	INPUT DISPLACEMENT AMPLITUDE (in)
1	0.02
2	0.04
3	0.08
4	0.10
5	0.12
6	0.14
7	0.16
8	0.20
9	0.25
10	0.30
11	0.35
12	0.40
13	0.45
14	0.50
15	0.55
16	0.60
17	0.70
18	0.80
19	0.90
20	1.00
21	1.10
22	1.20

*Each stage consists of three sinusoidal cycles at the amplitude shown

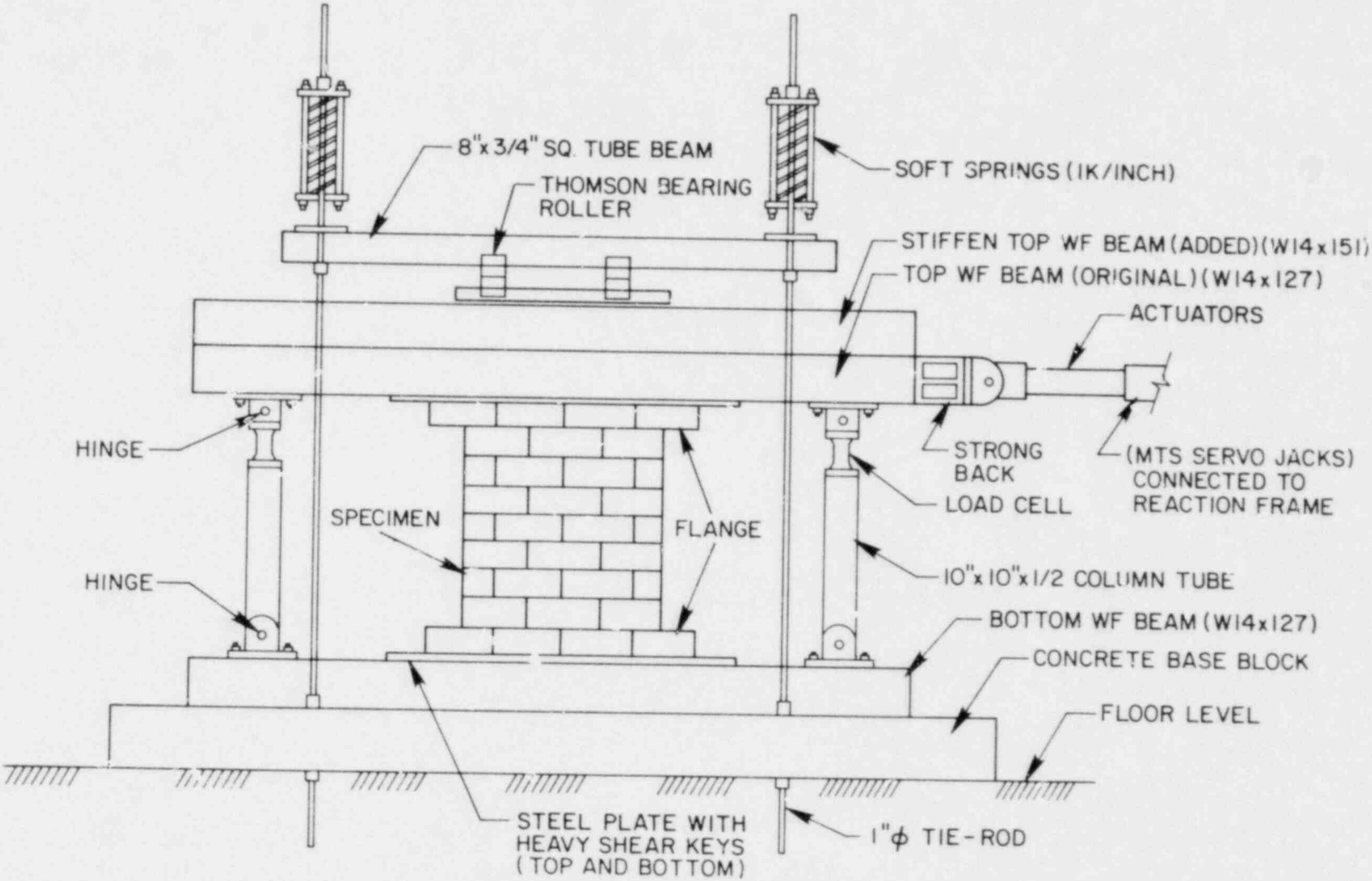

FIG. 3.1 SCHEMATIC ILLUSTRATION OF SINGLE PIER TEST

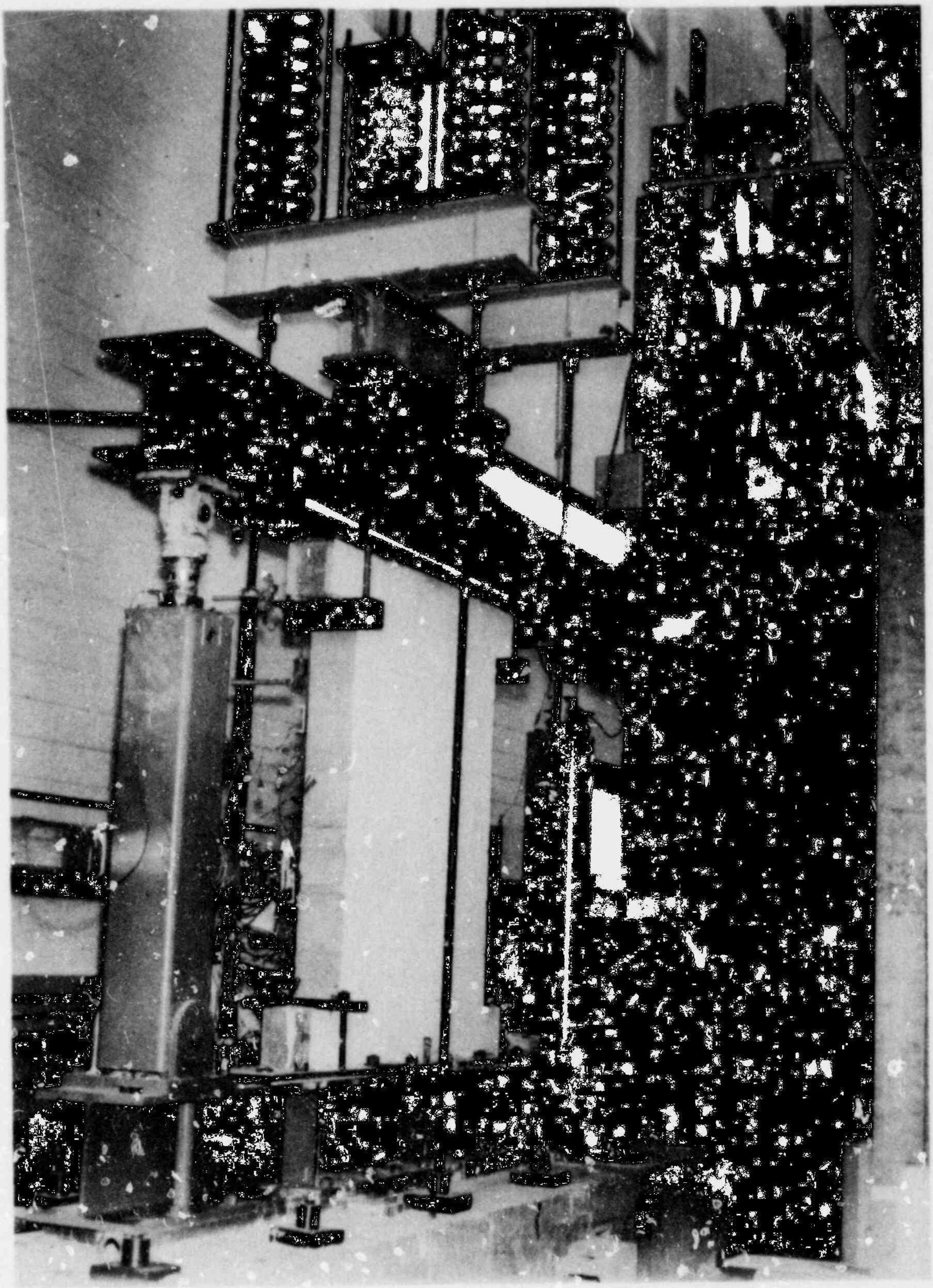

FIG. 3.2 OVERVIEW OF SINGLE PIER TEST

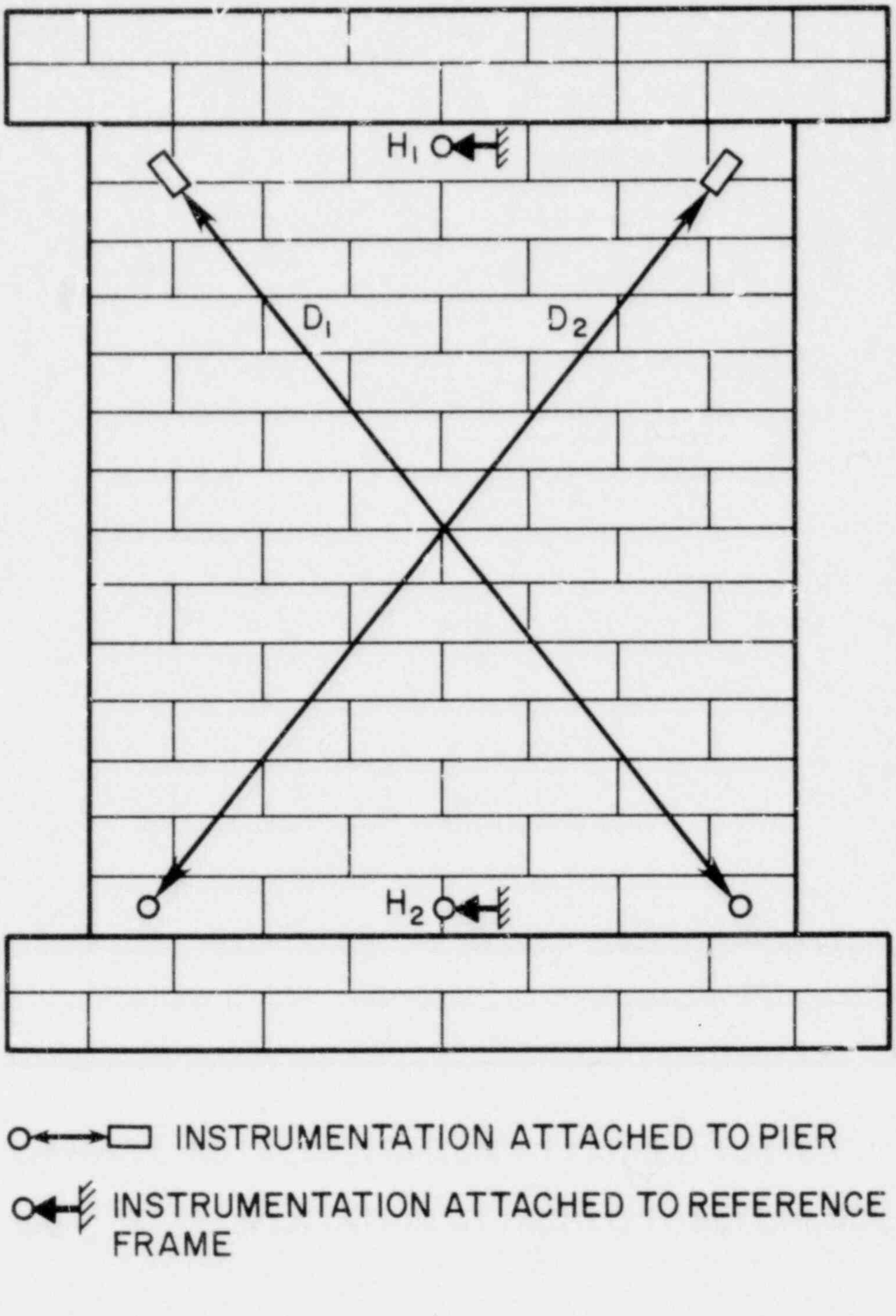

FIG. 3.3 PIER INSTRUMENTATION

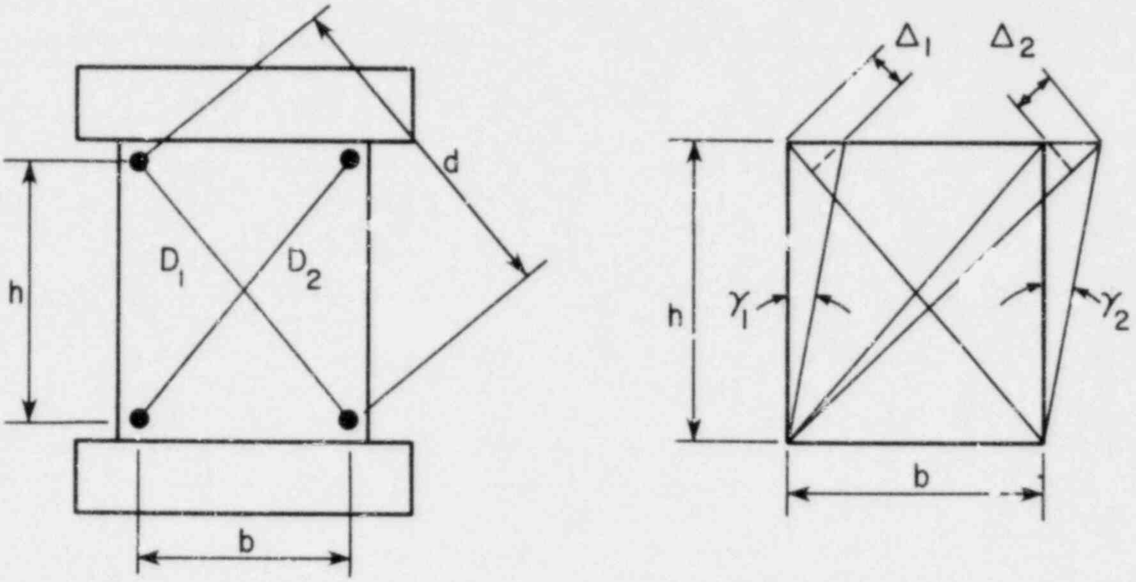

b, h, d = AVERAGE PIER DIMENSIONS

Δ_i = LENGTH CHANGE IN DIAGONAL D_i

γ_i = SHEAR ROTATION

$\gamma_{AVG.}$ = AVERAGE SHEAR ROTATION

δ_s = AVERAGE SHEAR DISTORTION

$$\gamma_i = |\Delta_i| \cdot \frac{d}{b.h} \qquad i = 1, 2$$

$$\gamma_{AVG.} = \frac{1}{2} \sum_{i=1}^{2} \gamma_i$$

$$\delta_s = \gamma_{AVG.} \cdot h$$

FIG. 3.4 MEASUREMENT OF AVERAGE SHEAR DISTORTION

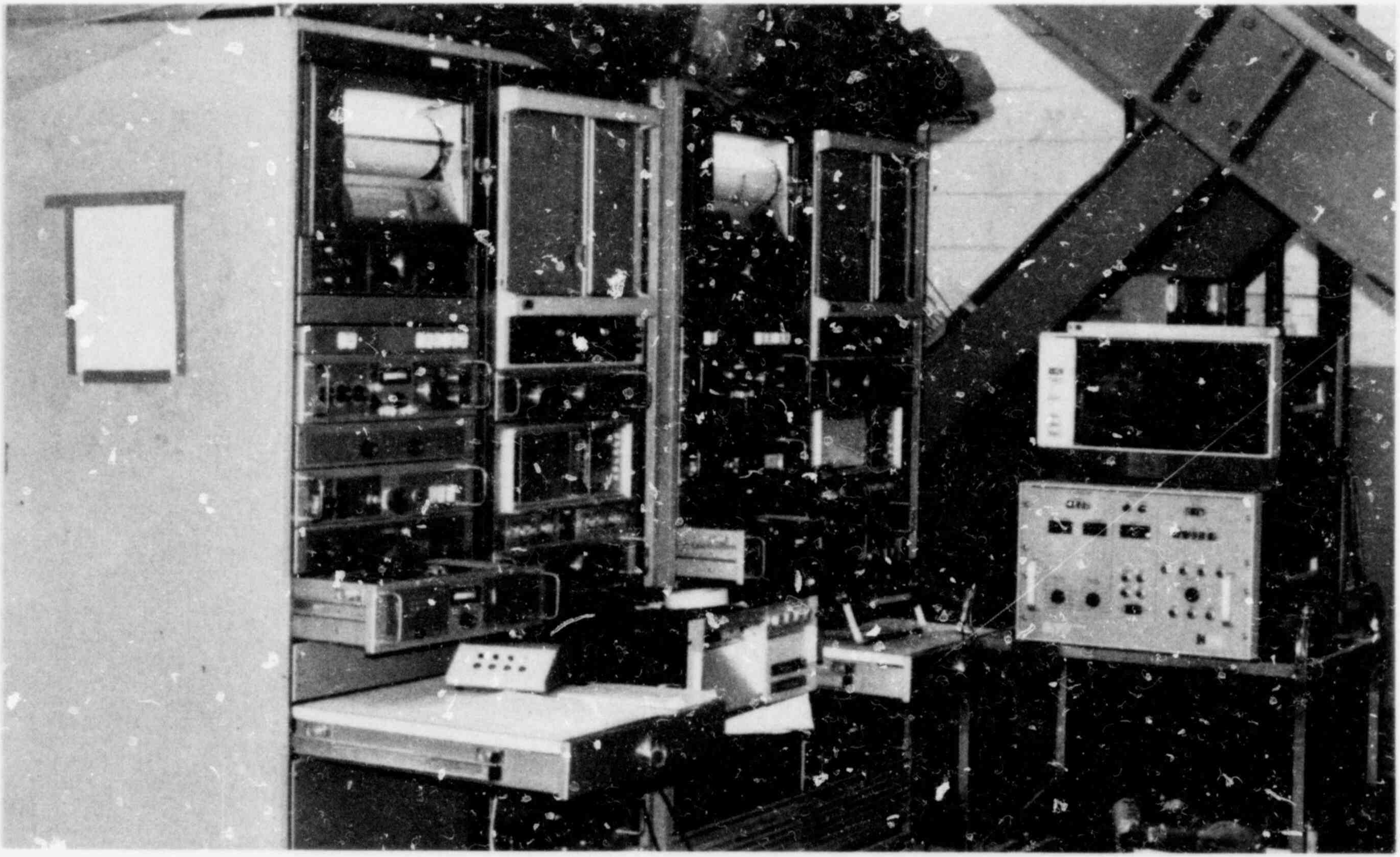

FIG. 3.5 TEST CONTROL CONSOLES AND DATA ACQUISITION SYSTEM

4. TEST RESULTS

4.1 Introduction

The experimental results for the thirty-one piers having a height to width ratio of 1 are presented in the form of hysteresis loops, hysteresis envelopes, stiffness degradation properties, energy dissipation characteristics, and relative shear distortion. In addition a sequence of photographs of the successive crack patterns is given for each test. An explanation of how each of the graphs was obtained and the meaning of the terms used above is included in Section 4.3. The complete presentation of the figures and photographs has been arranged by test numbers and is included in Appendix A.

In addition, data on the ultimate strength and hysteresis indicators for each test are listed in Tables 4.1(a), (b) and (c). A discussion of the modes of failure observed follows in Section 4.2 and a discussion of the test results is presented in Chapter 5.

4.2 Modes of Failure

All the thirty-one piers displayed a shear mode of failure (Fig. 4.1). This is characterized by early flexural cracks at the toes of the pier (horizontal cracks) and later augmented with diagonal cracks that extended through a partial zone of the pier. As the horizontal load increases, as a consequence of the increase in the flexural moment capacity of the sections of the pier the diagonal tensile stress reaches the tensile strength capacity of the masonry with resulting large diagonal cracks characteristic of the shear mode of failure (Fig. 4.1). The diagonal tension or shear failure generally coincided with the ultimate strength of the pier and was followed by a strength degradation characterized by the opening of diagonal cracks and the inability of the walls to maintain a serviceable condition.

In some of the fully grouted specimens (HCBL-11-6, HCBR-11-3, 4, 6 and 7, and CBRC-11-2, 3, 4, 6 and 7) the shear failure was accompanied by yielding of the vertical steel reinforcement. This is what has previously been called a combined shear and flexural mode of failure[7]. After the first flexural cracks occurred at the toes of the pier and as the horizontal load increased, the vertical steel began to yield and the corners of the pier developed high compressive stresses. The additional compressive load, induced by the test setup with the increase in lateral deflection, allowed the critical moment sections (top and bottom of the pier) to increase their flexural moment capacities thus enabling the horizontal load to increase while the vertical reinforcement sustained further yield deformation. This process continued until the shear strength of the pier was attained and full diagonal cracks developed as in the shear mode of failure.

The partially grouted piers (HCBL-11-2, 5, 8, 10 and HCBR-11-2, 5, 9 and 11) showed a shear mode of failure. These piers required much less horizontal load to develop the ultimate shear strength and as a result no yielding of the vertical reinforcement occurred. Correspondingly the amount of compressive load developed at the ultimate load was generally smaller than that for the tests of the fully grouted piers.

The solid grouted core clay brick piers displayed a shear failure characterized by a split between the grouted core and the brick wythe, as shown in Fig. 4.1.

4.3 Load-Displacement Characteristics

As mentioned before, Tables 4.1 (a), (b) and (c) summarize the strength and hysteresis characteristics of the piers and Appendix A presents the test results for each of the specimens.

The details of the derivation of each of the figures compiled in Appendix A is discussed in the following sections.

a) Hysteresis Loops (Shear Force vs. Lateral Deflection Diagram)

This graph was obtained by plotting the horizontal load against the relative lateral displacement of the pier for the whole duration of the test. The horizontal shear force was directly obtained from the load cell readings. The relative lateral displacement was computed from the difference between the lateral deflections at the top and bottom of the pier ($H_1 - H_2$ as defined in Fig. 3.3).

b) Hysteresis Envelopes

This plot was obtained from the hysteresis loops by averaging the absolute values of the three extreme positive and the three extreme negative forces and the corresponding absolute values of the relative lateral displacement, for each stage of the test at a given input displacement. One point on the hysteresis envelope was obtained for each stage of 3 cycles of loading. The average lateral displacement obtained in the hysteresis envelope is always less than the input displacement, as explained in Section 3.2.

The maximum strength obtained from the hysteresis envelope is indicated in Tables 4.1 (a), (b) and (c) under "average ultimate shear force or stress", (the stress values are computed by dividing the horizontal force by the cross section area of the pier). The "peak ultimate shear force or stress" values that appear in Tables 4.1(a), (b) and (c) were obtained from the maximum force (stress) developed in any one cycle of loading. The average value is always less than the peak value, varying from 81% to 98% of the peak value. The compressive load at ultimate indicated in Tables 4.1 (a), (b) and

(c) corresponds to the maximum axial compressive load developed during each of the tests. This maximum value usually occurred at the same time as the peak ultimate shear force, and is computed from the readings of the load cells located in the vertical columns plus the bearing load applied prior to each test (Table 2.1).

The last two columns of Tables 4.1 (a), (b) and (c) correspond to hysteresis indicators obtained from the hysteresis envelopes and defined in Fig. 4.2. The level of $0.70P_u$ used to define these indicators, where P_u is the maximum strength indicated by the hysteresis envelope, was arbitrarily chosen. Indicator h_1 tells how much the pier has deviated from its initial, theoretical stiffness, and indicator d_2 gives an indication of the deformation capability of the pier. The initial theoretical stiffness of the pier was computed with the assumption that the piers were fixed against rotation at both the top and bottom. The moment of inertia was calculated using the gross, uncracked section, neglecting the effect of steel reinforcement; the modulus of elasticity was taken from the measured values (Fig. 2.6 for the HCBL piers, Tables 2.3 (a) and (b) in reference [3] for the HCBR and CBRC piers, respectively), and the Poisson's ratio was assumed to be 0.15. Further discussion of the correlation of the theoretical stiffness and the measured stiffness is presented in Chapter 5.

c) Stiffness Degradation

A cyclic definition of the stiffness, as indicated in Fig. 4.3, was used to measure the stiffness of the piers throughout each test. The three cyclic stiffness values obtained from each stage of loading were averaged and plotted against the average gross shear stress and the relative lateral displacement.

d) Energy Dissipation

The energy dissipated per cycle of loading was expressed in terms of an equivalent damping ratio, which can be related to a dimensionless energy dissipation ratio EDT, as shown in Fig. 4.3. EDT is defined as the ratio of the energy dissipated to the total stored strain energy per cycle and is diagrammatically shown in Fig. 4.3. The three damping values obtained for each stage of loading were averaged and plotted against the average lateral displacement.

e) Shear Distortion

The values of the shear distortion, δ_s, were calculated as indicated in Fig. 3.4. The absolute values of δ_s corresponding to the three extreme positive and three extreme negative forces were averaged for each stage of the test, and plotted against the respective average relative lateral displacement, (total deformation of the pier), obtained from the hysteresis envelope. The plot depicts how much of the total deformation of the pier is due to shear distortion as defined in Fig. 3.4. Since the instruments used to measure the diagonal deformations were usually removed three or four stages before the end of the tests, the number of stages used to plot this graph is usually smaller than the number used for the previous graphs.

TABLE 4.1(a)

PIER CHARACTERISTICS AND TEST RESULTS - HCBL

(Gross cross section of wall=366 in^2.
Net cross section area (bedded plus grouted cell area) = 220 in^2).

Specimen	Test Frequency (cps)	Grouting Full (F) Partial (P) Solid (S)	Vert. reinf. steel		Horizontal reinforcing steel				Ratio of Total Area of Steel to Gross Area of Wall $p_v + p_h$	Average Ultimate Shear Force (kip)	Average* Ultimate Shear Stress (psi)	Peak Ultimate Shear Force (kip)	Peak* Ultimate Shear Stress (psi)	Compressive Load at Ultimate (kip)	Bearing* Stress at Ultimate (psi)	Hysteresis Indicators	
			No. of Bars	$p_v = \frac{A_{vs}}{A_g}$	No. of Bars	Yield Strength (ksi)	$p_h = \frac{A_{hs}}{A_g}$	$A_{hs} f_{hy}$ (kip)								h_1	d_2 (in)
HCBL-11-1	1.5	F	No	---	No	---	---	---	---	45.2	123	49.5	135	44.0	120	4.8	0.38
-2	1.5	P	No	---	No	---	---	---	---	25.2	115(69)	26.3	120(72)	42.2	192(115)	3.9	0.34
-3	1.5	F	2#5	0.0017	No	---	---	---	0.0017	46.3	127	49.1	134	25.1	69	3.7	0.45
-4	1.5	F	2#5	0.0017	1#5	47.9	0.0008	14.8	0.0025	60.3	165	62.7	171	39.1	107	3.9	0.39
-5	1.5	P	2#5	0.0017	1#5	47.9	0.0008	14.8	0.0025	46.8	213(128)	49.6	226(136)	30.2	137(83)	3.1	0.31
-6	1.5	F	2#5	0.0017	4#5	47.9	0.0034	59.4	0.0051	72.8	199	82.7	226	52.7	144	5.6	0.64
-7	1.5	F	2#8	0.0043	No	---	---	---	0.0043	53.6	146	65.8	180	33.3	91	3.4	0.35
-6	1.5	P	2#8	0.0043	No	---	---	---	0.0043	36.8	167(101)	37.9	172(104)	29.2	133(80)	4.2	0.29
-9	1.5	F	2#8	0.0043	2#5	47.9	0.0017	29.7	0.0060	53.6	146	56.9	155	41.9	114	6.1	0.40
-10	1.5	[illegible]	[illegible]	0.0043	2#5	47.9	0.0017	29.7	0.0060	48.7	222(133)	50.2	228(137)	31.2	142(85)	3.2	0.30
-11	1.5	F	2#8	0.0043	4#6	73.9	0.0048	130.1	0.0091	84.5	231	87.7	240	50.8	139	4.8	0.62

* Partially grouted pier stresses computed using net areas. Values in parentesis indicate gross area stresses.

TABLE 4.1(b)

PIER CHARACTERISTICS AND TEST RESULTS - HCBR

(Gross cross section of wall = 354 in^2).
Net cross section area (bedded plus grouted all earea) = 189 in^2).

Specimen	Test Frequency (cps)	Grouting Full (F) Partial (P) Solid (S)	Vert. reinf. steel: No. of Bars	Vert. reinf. steel: $p_v = \frac{A_{vs}}{A_g}$	Horizontal reinforcing steel: No. of Bars	Horizontal reinforcing steel: Yield Strength (ksi)	Horizontal reinforcing steel: $p_h = \frac{A_{hs}}{A_g}$	Horizontal reinforcing steel: $A_{hs}\ f_{hy}$ (kip)	Ratio of Total Area of Steel to Gross Are. of Wall $p_v + p_h$	Average Ultimate Shear Force (kip)	Average* Ultimate Shear Stress (psi)	Peak Ultimate Shear Force (kip)	Peak* Ultimate Shear Stress (psi)	Compressive Load at Ultimate (kip)	Bearing* Stress at Ultimate (psi)	Hysteresis Indicators: h_1	Hysteresis Indicators: d_2 (in)
HCBR-11-1	0.02	F	No	---	No	---	---	---	---	90.1	255	98.5	278	116.1	328	8.4	0.36
-2	0.02	F	No	---	No	---	---	---	---	---	---	26.6	141(75)	76.5	405(216)	---	---
-3	0.02	F	2#5	0.0018	No	---	---	---	0.0018	94.4	267	98.9	279	52.3	148	6.6	0.23
-4	0.02	[illegible]	2#5	0.0018	1#5	70.0	0.0009	21.7	0.0026	119.3	337	124.8	353	114.3	323	5.5	0.55
-5	0.02	P	2#5	0.0018	1#5	70.0	0.0009	21.7	0.0026	45.4	240(128)	52.4	278(148)	53.7	284(152)	5.1	0.29
-6	0.02	F	2#5	0.0018	5#5	64.2	0.0044	99.5	0.0061	116.2	328	122.4	346	61.9	175	8.0	0.52
-7	0.02	F	2#5	0.0018	5#5	72.6	0.0044	112.5	0.0061	94.6	267	99.2	280	85.3	241	5.3	0.38
-8	0.02	F	2#8	0.0045	No	---	---	---	0.0045	80.4	227	85.6	242	43.4	123	7.4	0.34
-9	0.02	P	2#8	0.0045	No	---	---	---	0.0045	43.0	228(121)	49.1	260(139)	37.3	198(105)	3.4	0.25
-10	0.02	F	2#8	0.0045	2#5	68.7	0.0018	42.6	0.0062	101.6	287	104.8	296	54.2	153	7.4	0.52
-11	0.02	P	2#8	0.0045	2#5	68.7	0.0018	42.6	0.0062	46.0	244(130)	51.9	275(147)	26.7	141(75)	5.2	0.30
-12	0.02	F	2#8	0.0045	5#6	73.9	0.0062	162.6	0.0107	94.3	266	97.2	275	85.0	240	4.9	0.45
-13	0.02	F	2#8	0.0045	5#6	74.7	0.0062	164.3	0.0107	113.3	320	116.3	329	110.6	312	5.9	0.38

*Partially grouted pier stresses computed using net areas. Values in parenthesis indicat gross area stresses.

TABLE 4.1(c)

PIER CHARACTERISTICS AND TEST RESULTS - CBRC

(Gross cross section of wall = 480 in^2)

Specimen	Test Frequency (cps)	Grouting Full(F) Partial(P) Solids(S)	Vert. reinf. steel		Horizontal reinforcing steel				Ratio of Total Area of Steel to Gross Area of Wall $p_v + p_h$	Average Ultimate Shear Force (kip)	Average Ultimate Shear Stress (psi)	Peak Ultimate Shear Force (psi)	Peak Ultimate Shear Stress (psi)	Compressive Load at Ultimate (kip)	Bearing Stress at Ultimate (psi)	Hysteresis Indicators	
			No. of Bars	$p_v = \frac{A_{vs}}{A_g}$	No. of Bars	Yield Strength (ksi)	$p_h = \frac{A_{hs}}{A_g}$	$A_{hs}\ f_{hy}$ (kip)								h_1	d_2 (in)
CBRC-11-1	0.02	S	No	---	No	---	---	---	---	114.9	239	118.6	247	141.9	296	6.3	0.43
-2	0.02	S	2#5	0.0013	No	---	---	---	0.0013	106.0	221	117.0	244	92.7	193	4.8	0.28
-3	0.02	S	2#5	0.0013	1#5	68.3	0.0006	21.2	0.0019	106.7	222	114.5	239	89.5	186	5.4	0.38
-4	0.02	S	2#5	0.0013	5#5	68.3	0.0032	105.9	0.0045	124.4	259	128.6	268	132.5	276	6.2	0.63
-5	0.02	S	2#8	0.0033	No	---	---	---	0.0033	102.0	213	104.3	217	76.4	159	4.0	0.26
-6	0.02	S	2#8	0.0033	2#5	73.9	0.0013	45.8	0.0046	128.3	267	130.4	272	100.3	209	4.1	0.32
-7	0.02	S	2#8	0.0033	5#6	74.7	0.0046	164.3	0.0079	115.7	241	123.3	257	80.9	169	4.4	0.39

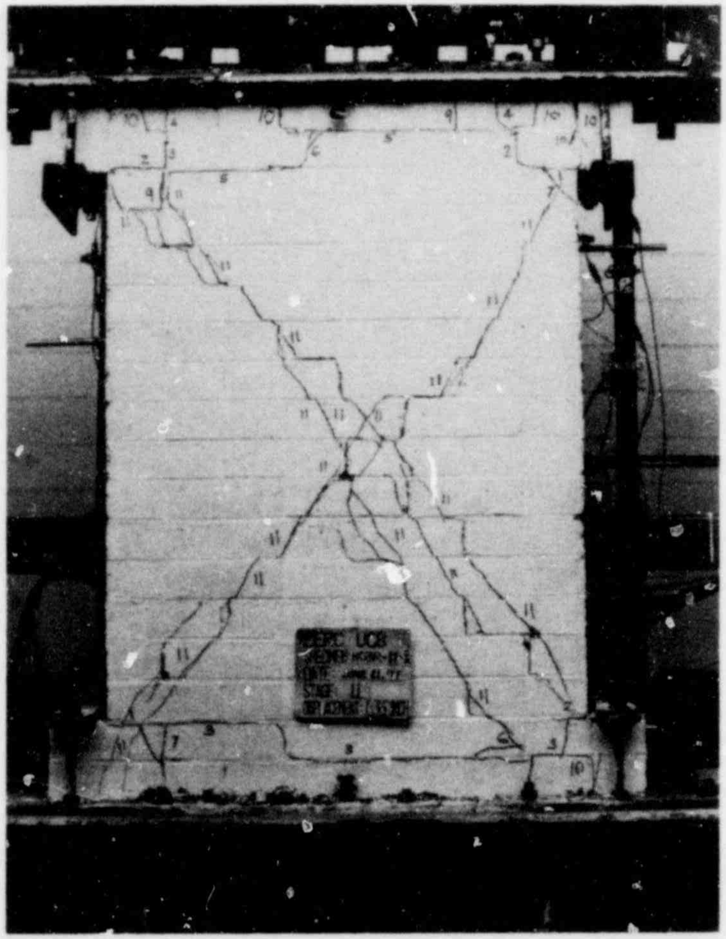

SHEAR MODE OF FAILURE

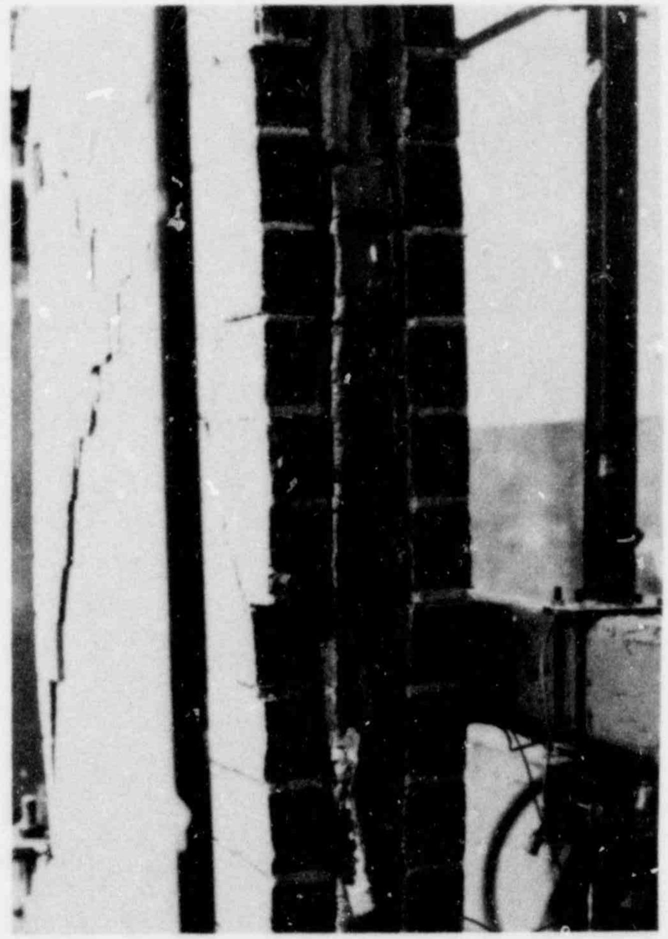

CORE SPLIT IN GROUTED CORE BRICK WALLS

FIG. 4.1 MODES OF FAILURE

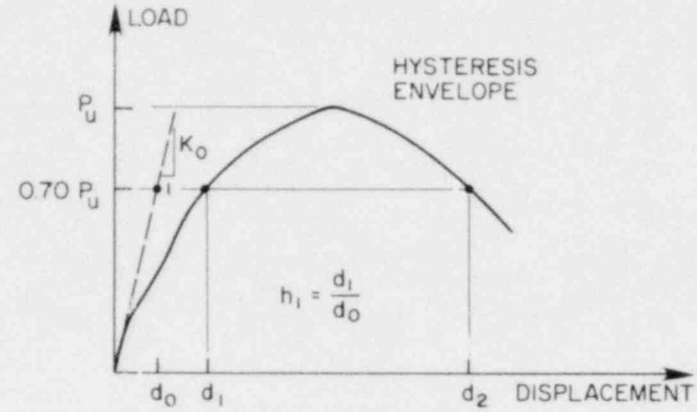

DEFINITION OF HYSTERESIS INDICATORS h_1 AND d_2

COMPUTATION OF INITIAL STIFFNESS K_o

$$K_o^{-1} = \frac{L^3}{12EI} + 1.2\ \frac{L}{AG}$$

L = height of pier

E = modulus of elasticity

$G = \frac{E}{2(1+\nu)}$ shear modulus

D = width of pier

t = thickness of pier

SPECIMEN	L (in)	D (in)	t (in)	I (in^4)	A (in^2)	E (Ksi)	ν	K_o (Kip/in)
HCBL-11 Full grouting	56	48	7.625	70272	366.0	1140	0.15	1808
HCBL-11 Partial grouting	56	48	7.625	59303	219.8	1140	0.15	1200
HCBR-11 Full grouting	56	48	7.375	67968	354.0	2450	0.15	3759
HCBR-11* Partial grouting	56	48	7.375	48355	188.8	2450	0.15	2185
CBRC-11 Solid grouting	56	48	10.0	92160	480.0	1720	0.15	3577

* Bedded plus grouted cell area considered

FIG. 4.2 DEFINITION OF HYSTERESIS INDICATORS AND COMPUTATION OF INITIAL STIFFNESS

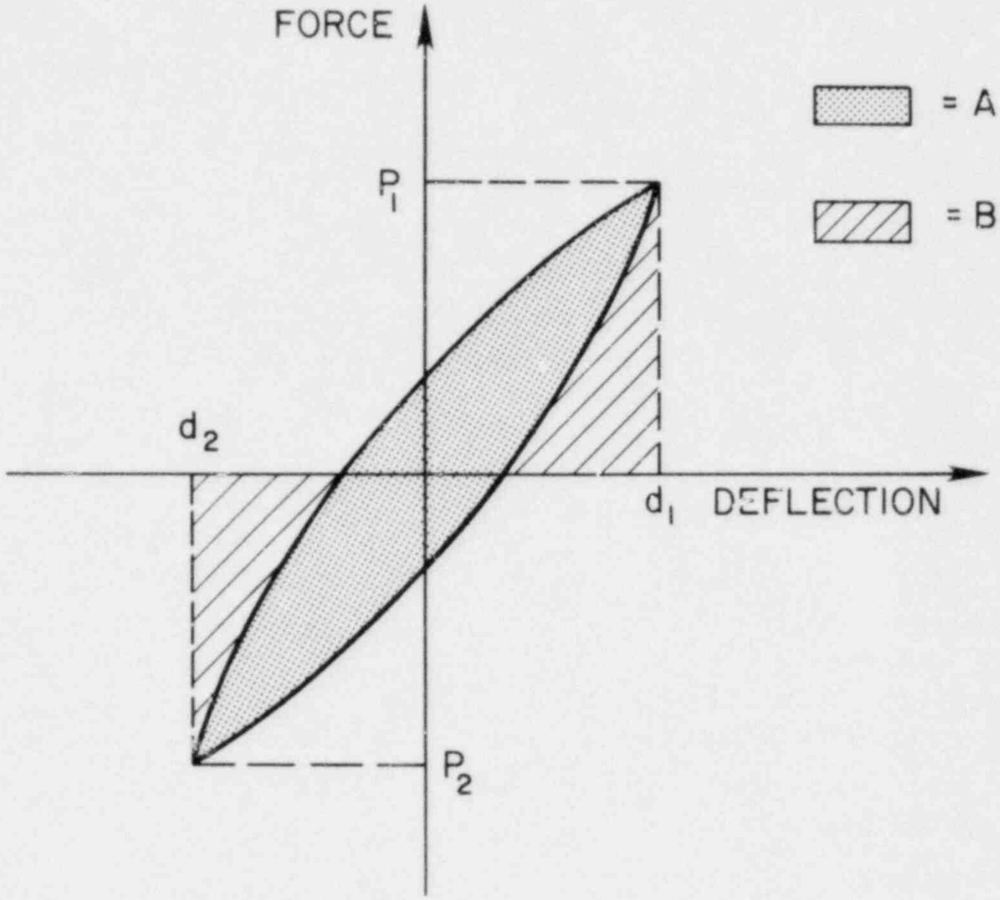

ENERGY DISSIPATION RATIO:

$$EDT = \frac{\text{DISSIPATED ENERGY}}{\text{TOTAL STORED ENERGY}} = \frac{A}{A+B}$$

EQUIVALENT DAMPING RATIO:

$$\xi_{EQ} = \frac{1}{2\pi} \cdot \frac{A}{A+B} = \frac{1}{2\pi} EDT$$

PIER STIFFNESS:

$$K = \frac{|P_1 - P_2|}{|d_1 - d_2|}$$

P_1, P_2, d_1, d_2 MUST BE TAKEN WITH THEIR OWN SIGN

FIG. 4.3 DEFINITIONS OF ENERGY DISSIPATION AND PIER STIFFNESS

5. DISCUSSION OF TEST RESULTS

5.1 Introduction

The test results presented in Appendix A and Tables 4.1 (a), (b) and (c) are discussed in this chapter with reference to the three parameters that were varied during these thirty-one tests; namely, the amount of vertical reinforcement, the amount of horizontal reinforcement and the type of grouting. Other parameters, such as the initial bearing stress and the test cyclic frequency, which were varied in the first seventeen double pier tests[7], were held constant during these thirty-one tests. The test frequency was not originally intended to be held constant during these tests. However, after the HCBL pier tests were performed using a test frequency of 1.5 cycles per second, it was observed that the anchorage of the vertical bars, (provided by the top and bottom steel girders), became precarious as soon as the vertical reinforcement began to yield. For this reason the test frequency was changed to 0.02 cycles per second for the HCBR and the CBRC pier tests.

It is also important to note that the results presented herein were obtained from a particular loading sequence. The choice of this loading sequence has been discussed previously[7]. Other types of load sequences are to be used in some of the additional thirty-five tests that complete the single pier test program.

In considering the results of these thirty-one tests on 1:1 piers it is important to realize that conclusions which appear valid for these tests may not hold for tests on piers with other height to width ratios. The complexity of the problem requires the completion of the test program (eighty tests) before valid conclusions concerning an adequate design of masonry structural elements can be made.

Finally, it is important to recall that all of the thirty-one piers showed a shear mode of failure, sometimes combined with flexural yielding of the vertical reinforcement. The ultimate strength always occurred when diagonal cracks developed over the full height of the pier in both directions of horizontal loading.

5.2 Ultimate Strength

5.2.1 Effect of Vertical Reinforcement

No significant difference was observed in the ultimate strengths of the HCBL, HCBR and CBRC piers as the amount of vertical steel was increased from two No. 5 to two No. 8 steel bars (reinforcement ratios and ultimate strengths are shown in Tables 4.1 (a), (b) and (c)). The reason for this result is that the ultimate strength is determined by the shear strength of the piers which is not influenced by the vertical steel. It was expected before the tests that the piers with two No. 5 steel bars as vertical reinforcement would have their strength controlled by the yielding strength of the vertical bars, (flexural mode of failure), as opposed to the shear mode of failure expected from the piers with two No. 8 steel bars. However, the presence of the additional compressive load, discussed in Sections 3.1 and 4.2, produced an increase in the horizontal load capacity of the piers and suppressed the flexural mode of failure (see Section 5.6 in reference [3]), thus offsetting the effect of reducing the amount of vertical reinforcement.

5.2.2 Effect of Horizontal Reinforcement

The results obtained for the average ultimate shear stresses of fully grouted piers (Tables 4.1 (a), (b) and (c)) indicate no consistent relation between the amount of horizontal reinforcement and the ultimate strength of the piers. In all cases, the piers with horizontal reinforcement had equal or more strength than the corresponding piers with no horizontal reinforcement. However, this increase does not appear to be a function of the amount of horizontal reinforcement. For instance, for the HCBR piers with two No. 5 bars as vertical reinforcement, specimens with one or five No. 5 horizontal bars (HCBR-11-4 and 6) had the same strength which was 25% more than the specimen with no horizontal reinforcement (HCBR-11-3); nevertheless the other specimen with five No. 5 horizontal bars (HCBR-11-7) had the same strength as the nonreinforced specimen (HCBR-11-3). Similar inconsistencies can be found for the HCBR piers with two No. 8 vertical bars and the CBRC piers with two No. 5 or two No. 8 vertical bars. The only case where some consistent trend is observed is that of the HCBL piers; in this case the specimens with four No. 5 or four No. 6 (HCBL-11-6 and 11) horizontal bars had 58% higher strength than the corresponding piers with no horizontal reinforcement (HCBL-11-3 and 7). However, while the pier with one No. 5 horizontal bar (HCBL-11-4) had 30% higher strength than the corresponding non-reinforced pier (HCBL-11-3), the specimen with two No. 5 horizontal bars (HCBL-11-9) had the same strength as the nonreinforced one (HCBL-11-7).

The average ultimate shear stress values obtained for the fully grouted specimens was 162 psi for the HCBL piers, 284 psi for the HCBR piers and 237 psi for the CBRC piers.

5.2.3 Effect of Partial Grouting

The ultimate shear stress of partially grouted HCBL piers, computed using net areas, was about 22% higher than the stress of comparable fully grouted piers. In the case of the HCBR piers the partially grouted specimens had an average ultimate shear stress about 23% less than the value obtained for comparable fully grouted piers.

5.3 Inelastic Behavior

The hysteresis envelopes (average maximum force-deflection curves) are used as a frame of reference to discuss the inelastic behavior of the piers. The question of what can be considered a desirable hysteresis envelope has been discussed in reference [7] pp. 68-70 in qualitative terms. It is appropriate to recall that the usefulness of the hysteresis envelopes is that they provide visual comparisons of ductility and ultimate strength; however, they give no indication of the energy dissipated per cycle and consideration of this parameter in conjunction with the ultimate strength, the deformation capacity and comparison of crack patterns at equal displacements is necessary to evaluate completely the inelastic characteristics of the pier behavior.

In order to quantify the deformation capabilities of the piers, hysteresis indicators defined in Section 4.3 are listed in the last two columns of Tables 4.1 (a), (b) and (c).

5.3.1 Effect of Vertical Reinforcement

No difference can be observed in the hysteresis envelopes of the HCBL, HCBR and CBPC piers (Figs. 5.1, 5.2 and 5.3, respectively) as the amount of vertical reinforcement increases from two No. 5 to two No. 8 bars. The same can be said for the inelastic behavior as reflected by the hysteresis indicators h_1 and d_2. It is clear, however, that the ability of the vertical reinforcement to control the inelastic behavior of a masonry pier is not well reflected by these results because of the effect of the additional compressive load developed during the tests, as explained in Section 5.2.1.

5.3.2 Effect of Horizontal Reinforcement

Figures 5.1, 5.2 and 5.3 show the changes in the hysteresis envelopes as the amount of horizontal reinforcement varies. The influence of the amount of horizontal reinforcement on the inelastic behavior of the piers is not well defined and although there is a trend indicating a positive correlation between them, this trend is not consistent as some of the specimens with a large amount of horizontal reinforcement, (i.e. HCBR-11-7 and HCBR-11-13), display less desirable inelastic behavior than specimens with considerably less horizontal reinforcement, (i.e. HCBR-11-4 and HCBR-11-10). Hysteresis indicator h_1 has values ranging from 3.4 to 8.0 and d_2 from 0.23 inch to 0.64 inch; piers with the largest amount of horizontal reinforcement, (over four No. 5 steel bars), generally present the largest inelastic deformation capacities, as indicated by d_2.

The strength degradation characteristics, after the ultimate strength is attained, are more favorable for the HCBL piers than for the HCBR and CBRC piers. However, the amount of horizontal reinforcement appears to have no influence in controlling this strength degradation.

5.3.3 Effect of Partial Grouting

Figure 5.4 shows the comparison of hysteresis envelopes of fully and partially grouted HCBL piers using both gross and net shear stresses. Figure 5.5 does the same for the HCBR piers. For the HCBL series, the inelastic behavior of the partially grouted piers based on net stresses is better (particularly in the piers with horizontal reinforcement) than the fully grouted piers. For the HCBR series, the fully grouted piers have better (particularly with horizontal reinforcement) inelastic behavior than the partially grouted piers. For both the HCBL and HCBR tests partial grouting reduces the deformation capability of the piers. The hysteresis indicator, d_2, of the partially grouted specimens has an average value only 82% of that of the fully grouted piers in the case of the HCBL piers and 62% in the case of the HCBR piers. As was true of the ultimate strength, the effect of partial grouting is detrimental to the inelastic behavior of HCBR piers but does not significantly affect the inelastic behavior of HCBL piers.

5.4 Stiffness Degradation

All the piers suffered substantial stiffness degradation when subjected to gradually increasing lateral displacements. Table 5.1 summarizes this effect and shows two sets of results. The first is a comparison between the theoretical initial stiffness and the maximum stiffness measured during the early stages of the test. The theoretical initial stiffness has been computed in Fig. 4.2 and the assumptions used are indicated in Section 4.3(b). The measured value is almost always smaller than the theoretical value and it ranges from 38% to 102% for the HCBL partially grouted piers, from 34% to 65% for the HCBL fully grouted piers, from 25% to 115% for the HCBR partially grouted piers, from 23% to 46% for the HCBR fully grouted piers and from 36% to 52% for the CBRC piers. These large differences in the two values are attributed to the flexibility of the boundary conditions at small lateral displacements, as discussed in Section 5.8 of reference[3]. Unlike the double pier test results[8], the assumed fixed-fixed rotation conditions at the top and bottom of the pier do not appear to be achieved for small lateral displacements and hence the discrepancy between the calculated and measured values.

The second set of results presented in Table 5.1 provides a comparison of the measured stiffnesses of all piers at applied shear stresses of 50 psi and 100 psi, and also shows the percentage decreases in stiffness at these stress levels with respect to the maximum initial measured value. The average percentage decreases at 50 psi were 24%, 16% and 19% for the HCBL, HCBR and CBRC piers, respectively. The corresponding average percentage decreases at 100 psi were 51%, 35% and 33%.

It must be noted that all the stiffness degradation results have been obtained using displacement increments that gradually increase. Later tests will determine if the type of degradation observed is similar under a more random type of loading sequence.

5.4.1 Effect of Reinforcement

Figures 5.6, 5.7 and 5.8 present the stiffness degradation curves for different amounts of vertical and horizontal reinforcement in the HCBL, HCBR and CBRC piers, respectively. It is difficult to identify any consistent relation between the amount of vertical or horizontal reinforcement and the rate at which stiffness degrades.

5.4.2 Effect of Partial Grouting

Figures 5.9 and 5.10 compare the stiffness degradation curves for fully and partially grouted HCBL and HCBR piers, respectively. The trend of these degradation results is similar and appears to be independent of the type of grouting.

5.5 Energy Dissipation

The effect of reinforcement on the equivalent damping or energy dissipation ratio is shown in Figs. 5.11, 5.12 and 5.13 for the HCBL, HCBR and CBRC piers, respectively. The effect of partial grouting is shown in Figs. 5.14 (HCBL piers) and 5.15 (HCBR piers).

Results show that the energy dissipation capacity of all the piers increases as the lateral displacement increases. This is attributed to the effect of progressive cracking. However, the amount of both vertical and horizontal reinforcement and the type of grouting appear to have little effect on the rate at which the energy is dissipated, except for the partially grouted HCBR piers (Fig. 5.15) which show a sudden increase in the energy dissipation at the 0.10 inch lateral displacement level, relative to the corresponding fully grouted piers.

As with the stiffness degradation property, investigation of the energy dissipation characteristics of the piers under a more random load sequence is necessary before analytical models based on the results are formulated.

5.6 Effect of Compressive Load on Inelastic Behavior

The additional compressive load imposed by the columns during the tests has been briefly mentioned in Sections 3.1 and 4.2 and has been discussed and analyzed in detail in Section 5.6 of reference [3]. Therefore, only the specific results from the thirty-one piers with height to width ratio of 1 will be presented here.

Even though the initial bearing stress for all the tests was set at 50 psi, the additional compressive load resulting from the test fixture caused this bearing stress to increase to 150 psi for the HCBL piers, to 325 psi for the HCBR piers and to 275 psi for the CBRC piers. As expected, these maximum values are lower than the maximum bearing stresses obtained for the piers with height to width ratio of 2, because of the smaller value of lateral displacement at which these maximum bearing stresses were recorded. As was observed before, (piers with height to width ratio of 2), the piers with no reinforcement at all developed larger maximum bearing stresses than the values obtained for the rest of the piers, which are indicated above.

Figure 5.16 shows a free-body diagram at the bottom section of the pier and the necessary equations to determine the amount of horizontal load that can be associated with the additional compressive load. This analysis, which is subject to the limitations established in Section 5.6 of reference [3], permits prediction of the pier behavior if this additional vertical load were not present. The results for specimens HCBL-11-6 and HCBR-11-6 are indicated in Fig. 5.17. The procedure followed to obtain the hysteresis envelopes shown in Fig. 5.17 is explained in detail in reference [3], the only difference being in the determination of the commencement of yielding in the tension vertical reinforcement; static equilibrium equations and experimental yield stresses for the vertical reinforcement were used instead of strain gage readings and experimental yield strains.

The onset of yield in the vertical reinforcement from Fig. 5.17 shows that the lateral force required to produce yield was 70 kip for specimen HCBL-11-6 and 81 kip for HCBR-11-6. If only the initial compressive load were considered, the theoretical yielding lateral force for HCBL-11-6 and HCBR-11-6 would be 52.5 kip. Future tests, with a modified test setup to remove this axial force effect, will be performed to validate these theoretical estimates.

5.7 Correlation Between Critical Tensile Strengths of Square Panels and Piers

This correlation is presented in Table 5.2 and is discussed in more detail in reference [8]. The purpose of this investigation was to evaluate an alternative and more rational test procedure for establishing the code allowable shear strength of masonry walls. Currently, the code allowable strength is based on the compressive strength of a masonry prism.

The square panel measure of critical tensile strength was determined from a study made by Blume[1], who proposed the expression shown in Table 5.2. The ultimate load P was taken from the experimental values indicated in Table 2.2.

The critical tensile strength indicated by the pier tests was computed at the neutral axis of the pier sections, following the simple beam theory for a section under combined flexure, shear and axial force. A parabolic distribution of shear stresses over the cross section was assumed. The piers developed shear cracks at the same time the ultimate shear strength was attained; therefore, the peak shear force and the corresponding compressive load from Tables 4.1 (a), (b) and (c) were used to evaluate the pier critical tensile strength.

The square panels were all fully grouted; for this reason the correlation only considers fully grouted HCBL and HCBR piers and all the CBRC piers. The correlation is considered to be reasonable. This type of analysis will continue to be performed throughout the pier test program. The consideration of the whole set of results will permit a better assessment of this test method in predicting the shear strength of masonry walls.

5.8 Other Test Results

The last graph in the test results (Appendix A) shows a comparison between the lateral displacement of the piers and the percentage of this displacement that can be attributed to shear distortion as defined in Fig. 3.4. These results reflect the amount of diagonal cracking present at each stage of the test. It is interesting to note that in the initial stiffness computed in Fig. 4.2, the flexural and shear components of the deformation are in the ratio of 1:2 for fully or solid grouted piers while the ratio is 1:2.8 for the partially grouted HCBL and HCBR piers.

TABLE 5.1

EFFECT OF SHEAR STRESS, STEEL REINFORCEMENT AND TYPE OF GROUTING OF STIFFNESS DEGRADATION
(Net areas used for partially grouted piers)

Specimen	Grouting Full(F) Partial(P) Solid(S)	Vertical Steel Reinforcement	Horizontal Steel Reinforcement	Theoretical Initial Stiffness (kip/in)	Measured Maximum Initial Stiffness (kip/in)	Stiffn at 50 psi		Stiffness at 100 psi	
						Measured (kip/in)	Percentage Decrease (%)	Measured (kip/in)	Percentage Decrease (%)
HCBL-11-1	F	No	No	1808	916	534	42	324	65
-2	P	No	No	1200	455	124	73	-	-
-3	F	2#5	No	1808	646	620	4	466	28
-4	F	2#5	1#5	1808	1071	952	11	540	50
-5	P	2#5	1#5	1200	905	630	29	470	48
-6	F	2#5	4#5	1808	927	840	9	564	39
-7	F	2#8	No	1808	610	472	23	290	53
-8	P	2#8	No	1200	1066	770	28	274	74
-9	F	2#8	2#5	1808	637	514	19	298	53
-10	P	2#8	2#5	1200	1227	1102	10	486	60
-11	F	2#8	4#6	1808	1176	1050	11	606	42
HCBR-11-1	F	No	No	3759	1046	1015	3	595	43
-2	P	No	No	2185	2523	204	92	-	-
-3	F	2#5	No	3759	1240	1070	14	714	42
-4	F	2#5	1#5	3759	1717	1530	11	1008	41
-5	P	2#5	1#5	2185	554	543	2	474	14
-6	F	2#5	5#5	3759	855	828	3	612	28
-7	F	2#5	5#5	3759	1611	1448	10	807	50
-8	F	2#8	No	3759	1156	1140	1	636	45
-9	P	2#8	No	2185	807	780	3	630	22
-10	F	2#8	2#5	3759	1170	924	21	618	47
-11	P	2#8	2#5	2185	706	*	*	654	7
-12	F	2#8	5#6	3759	1494	1377	8	1004	33
-13	F	2#8	5#6	3759	1262	900	29	600	53
CBRC-11-1	S	No	No	3577	1798	1208	33	778	57
-2	S	2#5	No	3577	1554	1353	13	1027	34
-3	S	2#5	1#5	3577	1802	1143	37	912	49
-4	S	2#5	5#5	3577	1354	1140	16	963	29
-5	S	2#8	No	3577	1281	1224	4	1140	11
-6	S	2#8	2#5	3577	1861	1515	19	1236	34
-7	S	2#8	5#6	3577	1406	1287	8	1143	19

*Maximum initial stiffness obtained after 50 psi.

TABLE 5.2

CORRELATION BETWEEN SQUARE PANEL AND PIER CRITICAL TENSILE STRENGTH

Specimen	SQUARE PANEL (1)				PIER (2)						$\frac{\sigma^0_{tcr}}{\sigma_{tcr}}$
	Ultimate Load P(kip)	Side Area A(in^2)	$\tau = \frac{P}{\sqrt{2}A}$ (psi)	Blume's Formula $\sigma^0_{tcr} = 0.734\tau$ (psi)	Ultimate Shear Force P(kip)	Compressive Load at Ultimate N(kip)	Cross Section A(in^2)	Ultimate Shear Stress $\frac{P}{A}$ (psi)	Bearing Stress at Ultimate $\frac{N}{A}$ (psi)	Critical Strength σ_{tcr} (psi)	
HCBL-11-1	58.4	244	169.2	124.2	49.5	44.0	366	135.2	120.2	151.4	0.82
-3	64.5		186.9	137.2	49.1	25.1		134.2	68.6	169.9	0.81
-4	64.3		186.3	136.8	62.7	39.1		171.1	106.8	209.0	0.65
-6	63.4		183.7	134.9	82.7	52.7		226.0	144.0	274.6	0.49
-7	78.1		226.3	166.1	65.8	33.3		179.8	91.0	228.0	0.73
-9	78.1		226.3	166.1	56.9	41.9		155.5	114.5	182.9	0.91
-11	62.7		181.7	133.4	87.7	50.8		239.6	138.8	296.6	0.45
HCBR-11-1	144.1	265.5	383.8	281.7	98.5	116.1	354	278.2	328.0	284.4	0.99
-3	144.1		383.8	281.7	98.9	52.3		279.4	147.7	351.7	0.80
-4	185.8		494.8	363.2	124.8	114.3		352.5	322.9	391.4	0.93
-6	171.9		457.8	336.0	122.4	61.9		345.8	174.9	438.1	0.77
-7	144.1		383.8	281.7	99.2	85.3		280.2	241.0	316.7	0.89
-8	149.9		399.2	293.0	85.6	43.4		241.8	122.6	306.5	0.96
-10	185.8		494.8	363.2	104.8	54.2		296.0	[illegible]	374.[illegible]	0.97
-12	144.1		383.8	281.7	97.2	85.0		274.6	240.1	309.0	0.91
-13	185.8		494.8	363.2	116.3	110.6		328.5	312.4	360.7	1.01
CBRC-11-1	142.0	360	278.9	204.7	118.6	141.9	480	247.1	295.6	251.2	0.81
-2	142.0		278.9	204.7	117.0	92.7		243.8	193.1	281.7	0.73
-3	142.0		278.9	204.7	114.5	89.5		238.5	186.5	276.5	0.74
-4	152.5		299.5	219.9	128.6	132.5		267.9	276.0	286.9	0.77
-5	142.0		278.9	204.7	104.3	76.4		217.3	159.2	255.9	0.80
-6	152.5		299.5	219.9	130.4	100.3		271.7	209.0	316.2	0.70
-7	152.5		299.5	219.9	123.3	80.9		256.9	168.5	310.2	0.71

(1) Square Panel Critical Tensile Strength

Blume's formula: $\sigma^0_{tcr} = -0.582\frac{P}{A} - \frac{\sigma_c}{2} + \frac{1}{2}\sqrt{4.849\left(\frac{P}{A}\right)^2 + \sigma_c^2}$

If edge pressure $\sigma_c = 0$, $\tau = 0.734\frac{P}{\sqrt{2}A}$

(2) Pier Critical Tensile Strength

Assuming a parabolic distribution of shear strisses

$$\sigma_{tcr} = -\frac{\sigma_c}{2} + \sqrt{(1.5\tau)^2 + \left(\frac{\sigma_c}{2}\right)^2}$$

$\sigma_c = \frac{N}{A}$: applied compressive stress

$\tau = \frac{P}{A}$: average shear stress

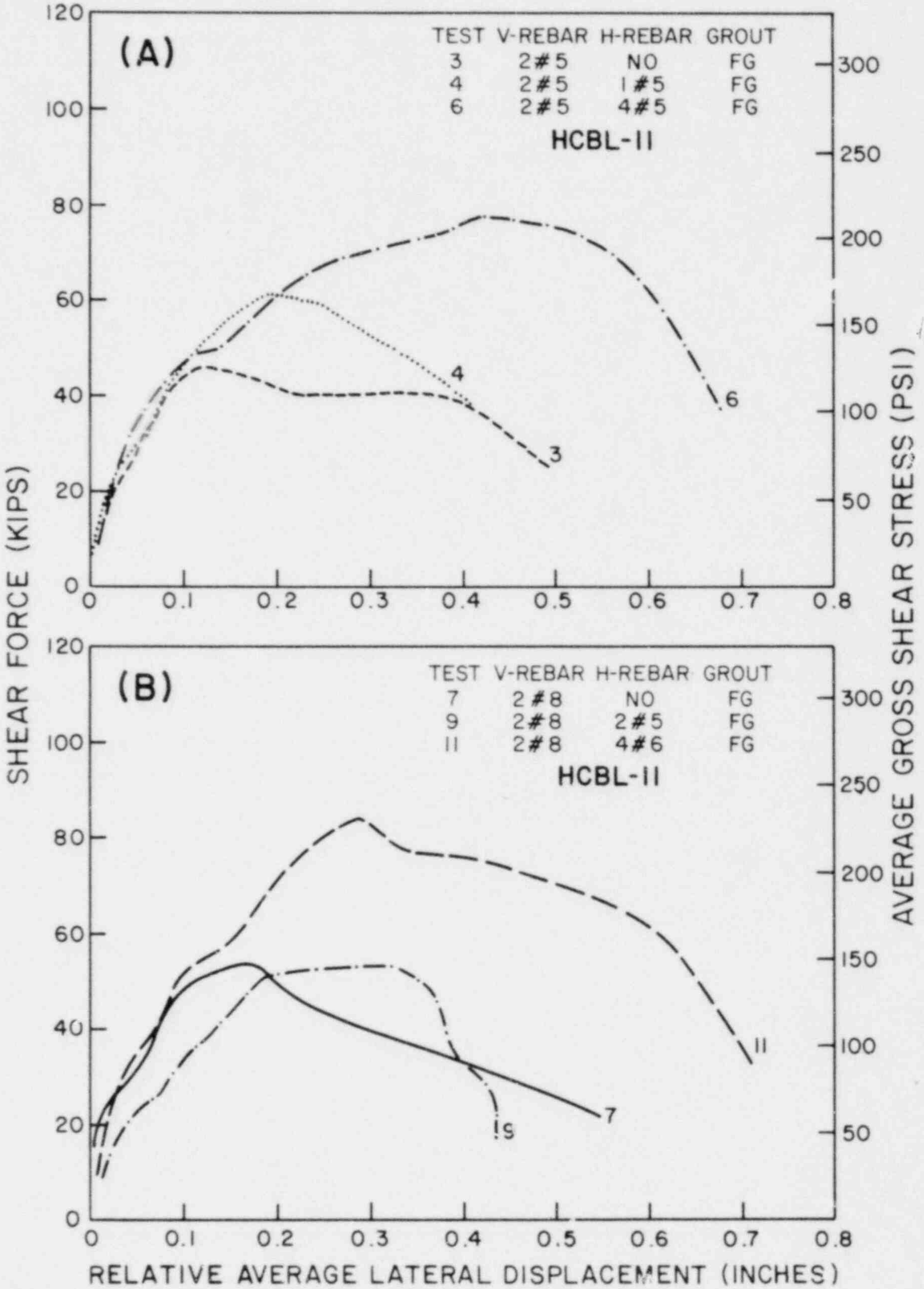

FIG. 5.1 EFFECT OF HORIZONTAL REINFORCEMENT ON HYSTERESIS ENVELOPE (HCBL)

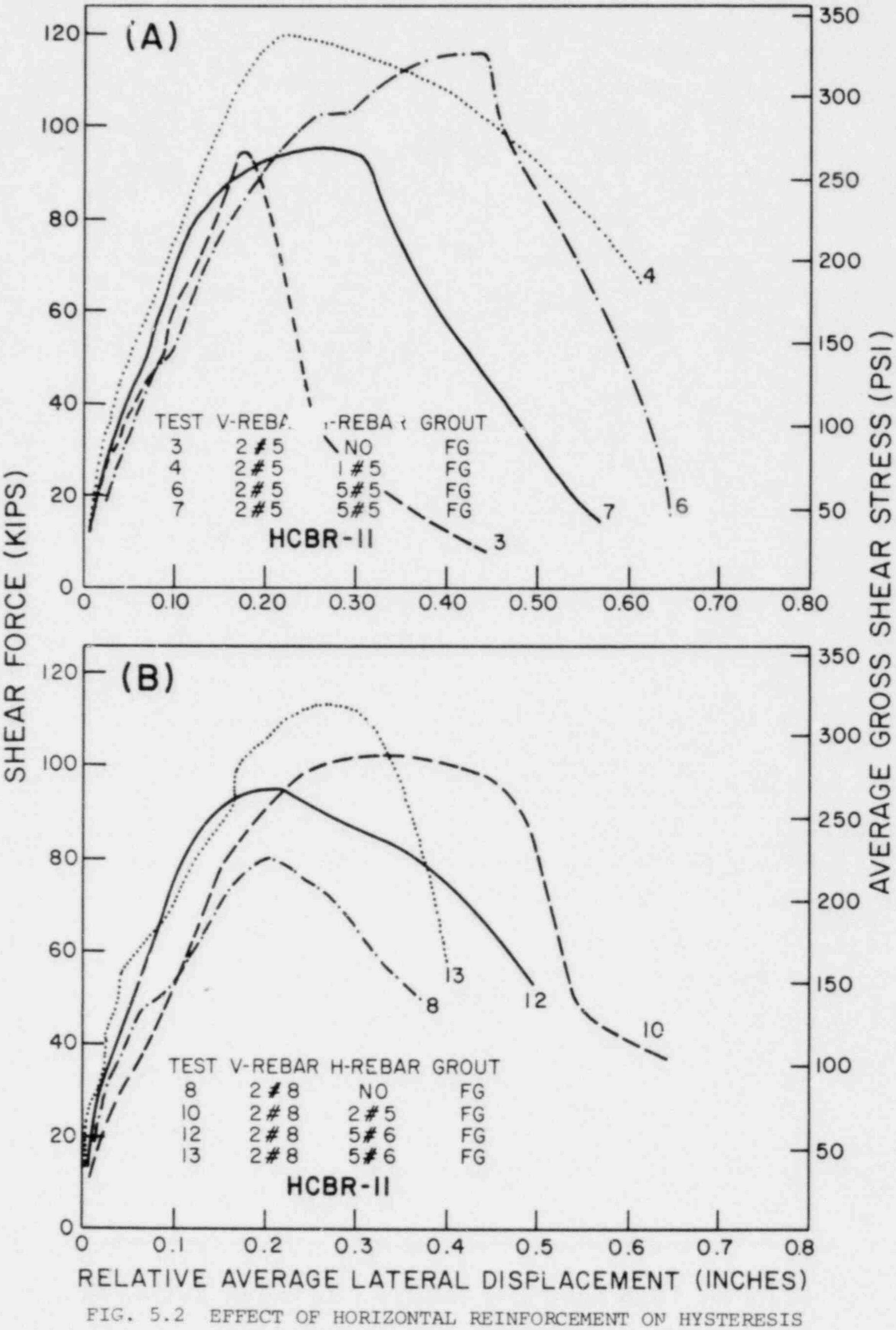

FIG. 5.2 EFFECT OF HORIZONTAL REINFORCEMENT ON HYSTERESIS ENVELOPE (HCBR)

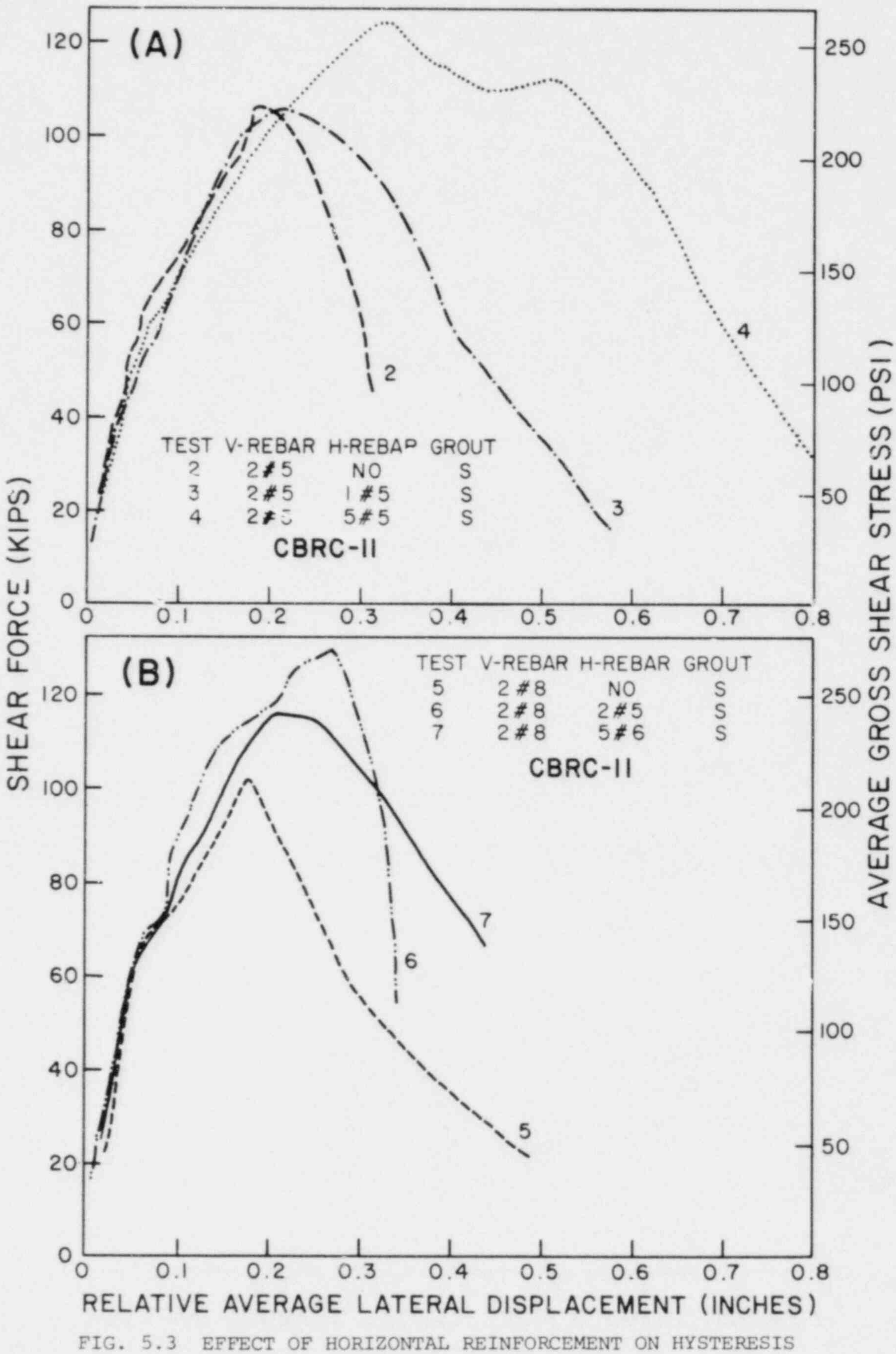

FIG. 5.3 EFFECT OF HORIZONTAL REINFORCEMENT ON HYSTERESIS ENVELOPE (CBRC)

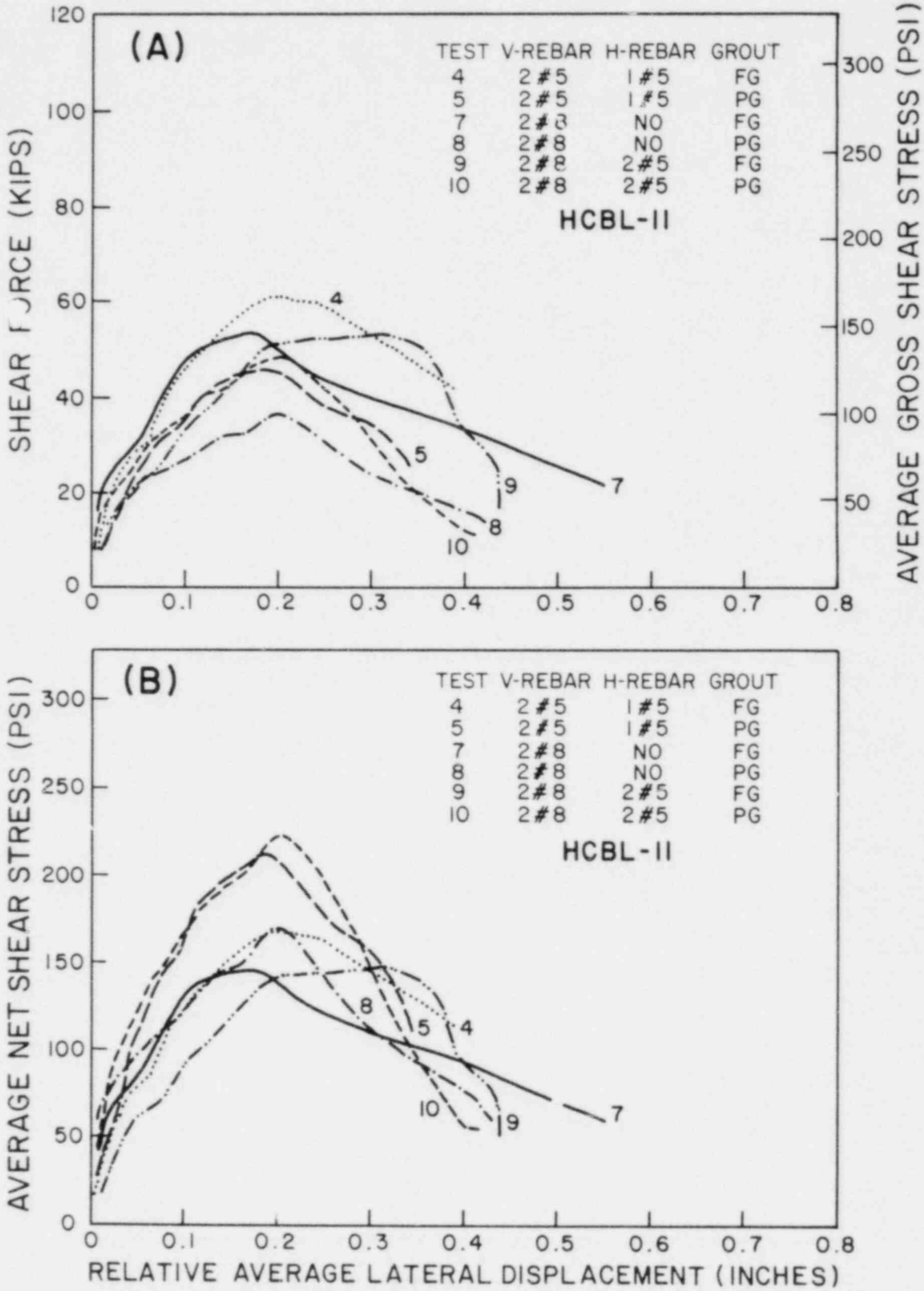

FIG. 5.4 EFFECT OF PARTIAL GROUTING ON HYSTERESIS ENVELOPE (HCBL)

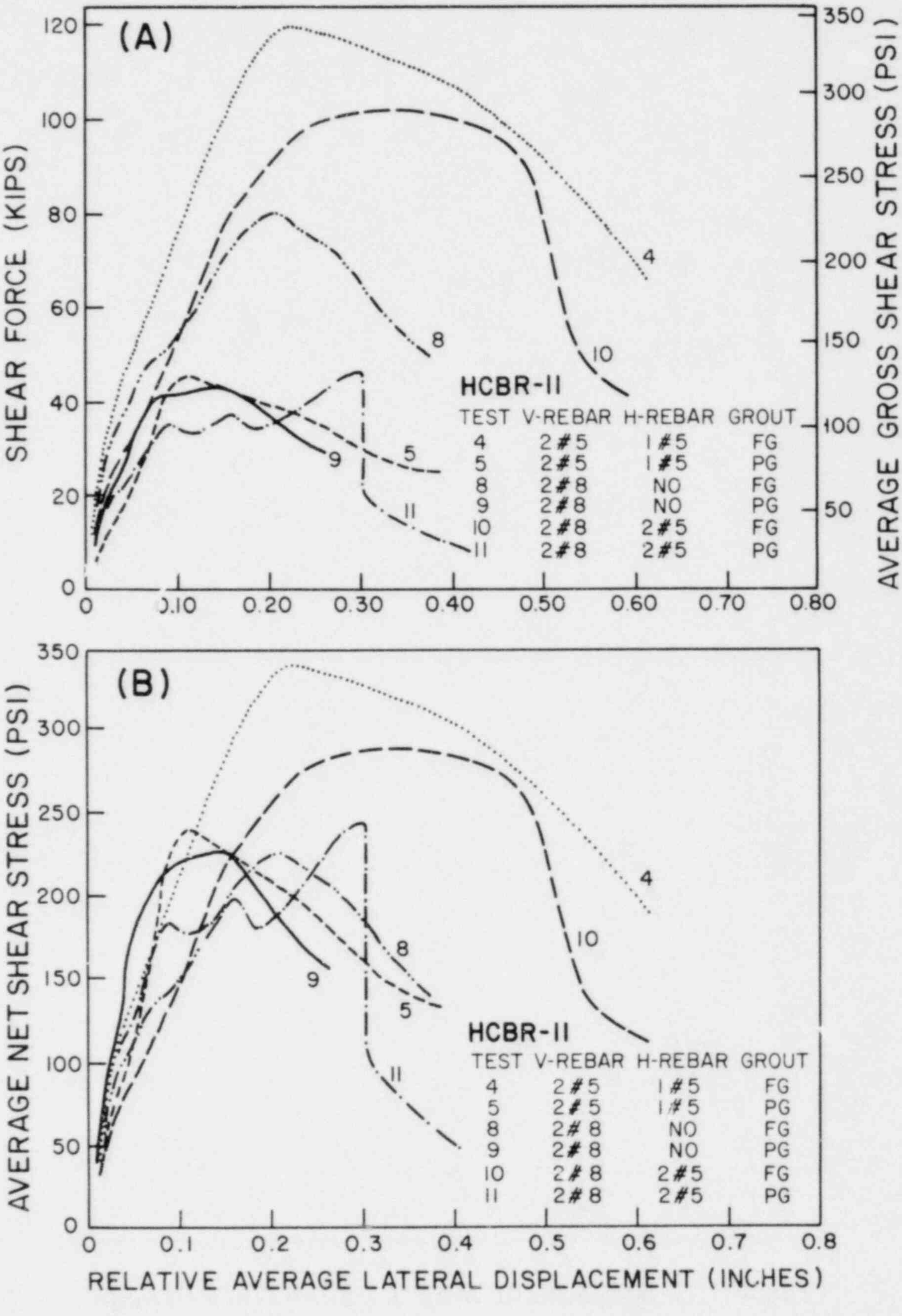

FIG. 5.5 EFFECT OF PARTIAL GROUTING ON HYSTERESIS ENVELOPE (HCBR)

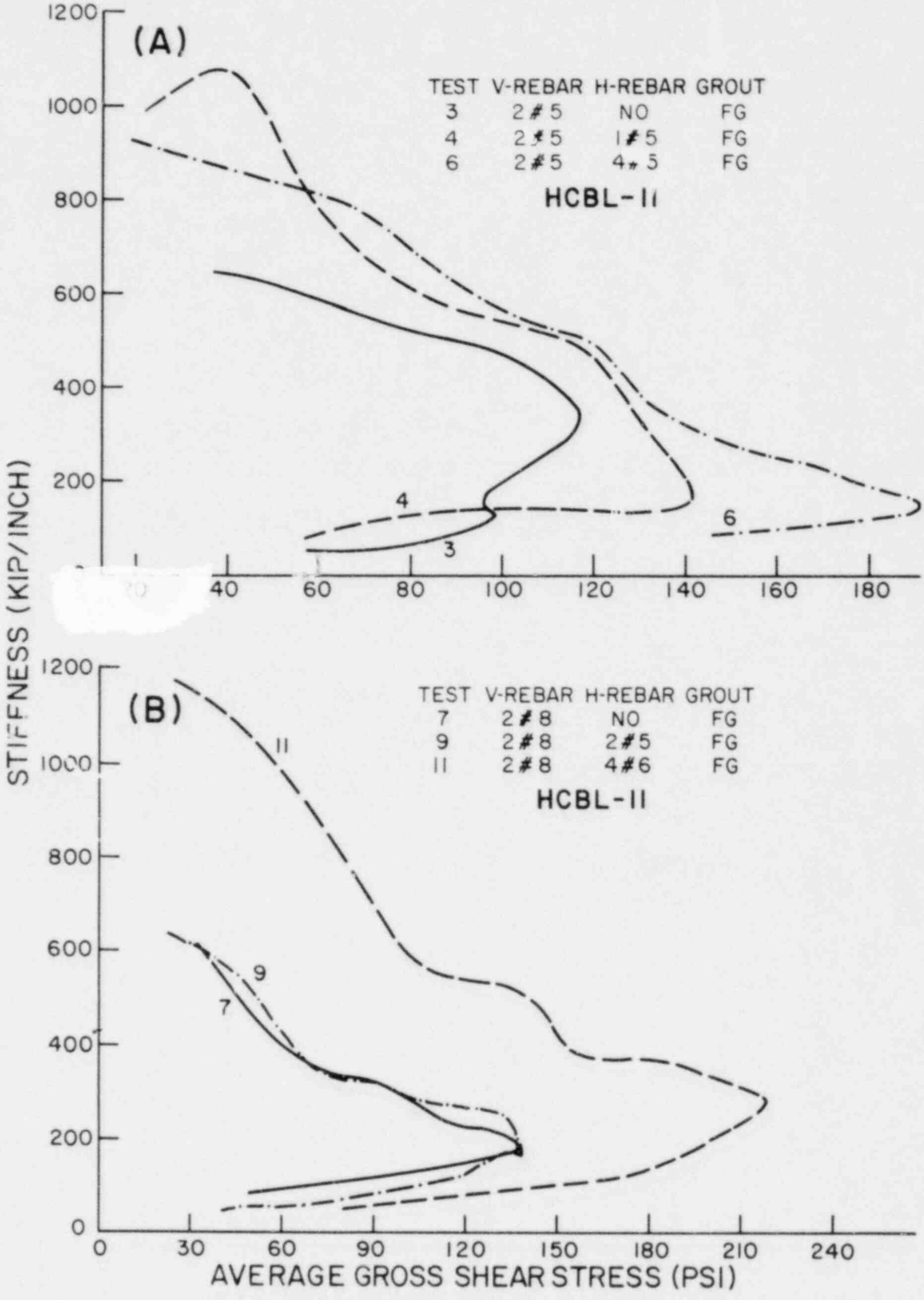

FIG. 5.6 EFFECT OF HORIZONTAL REINFORCEMENT ON STIFFNESS DEGRADATION (HCBL)

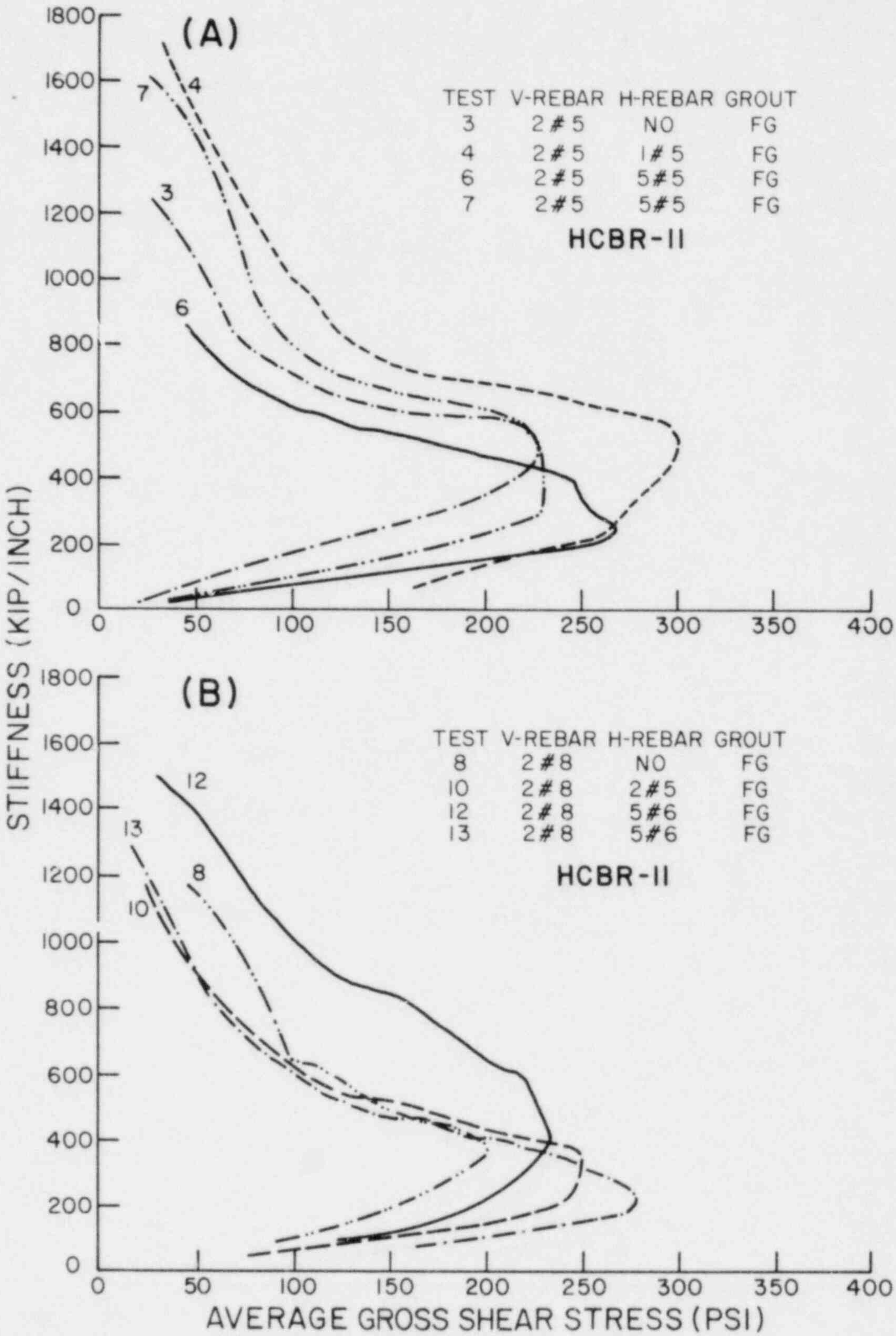

FIG. 5.7 EFFECT OF HORIZONTAL REINFORCEMENT ON STIFFNESS DEGRADATION (HCBR)

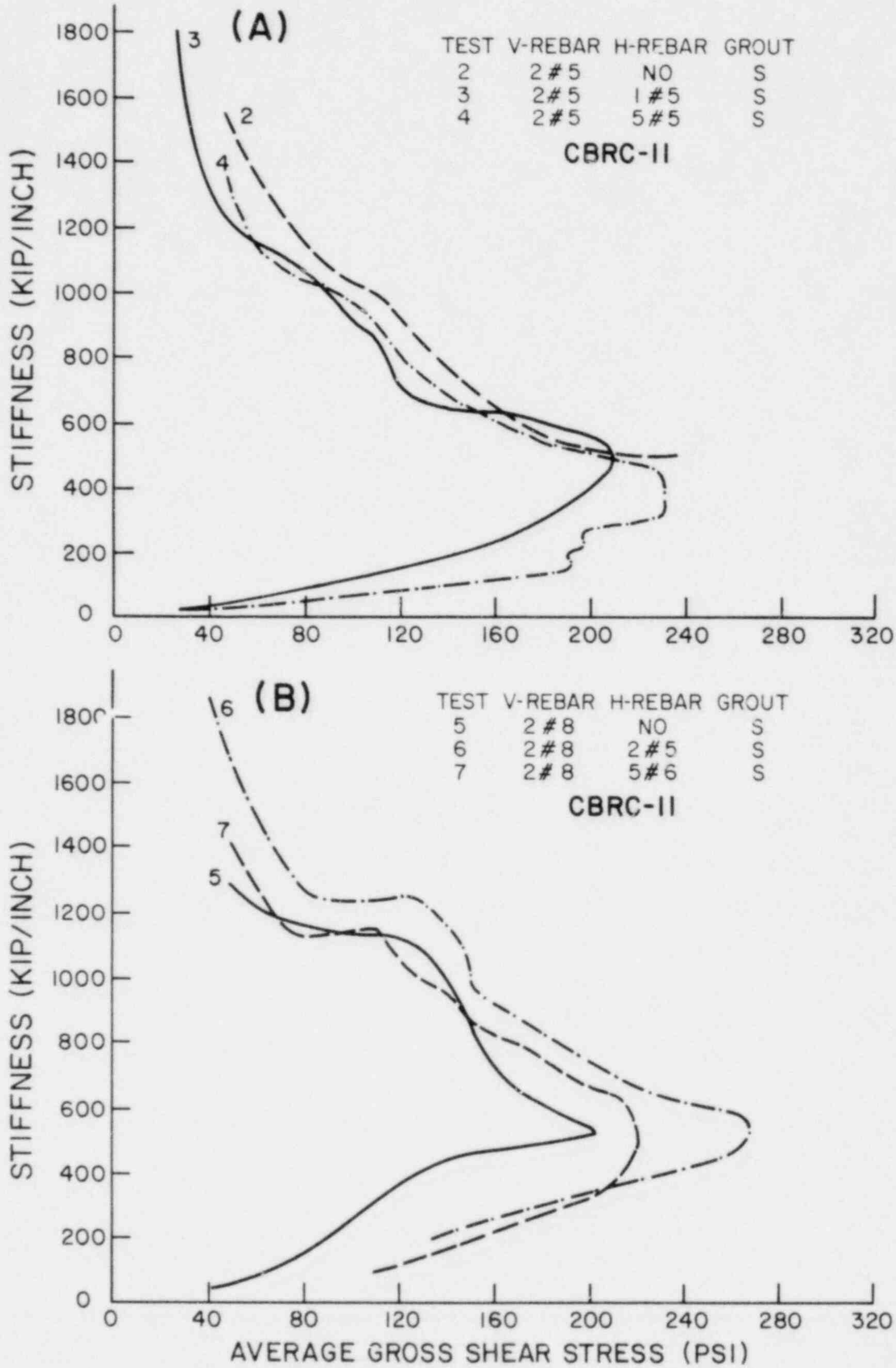

FIG. 5.8 EFFECT OF HORIZONTAL REINFORCEMENT ON STIFFNESS DEGRADATION (CBRC)

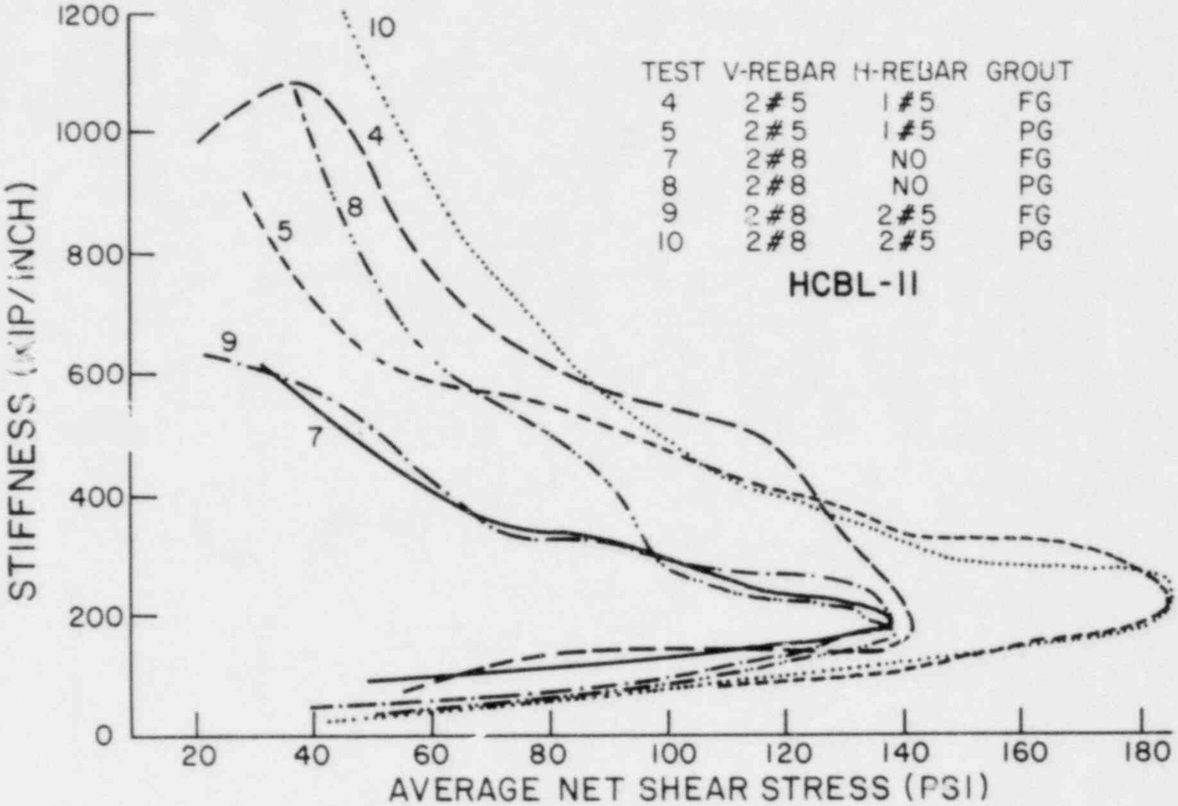

FIG. 5.9 EFFECT OF PARTIAL GROUTING ON STIFFNESS DEGRADATION (HCBL)

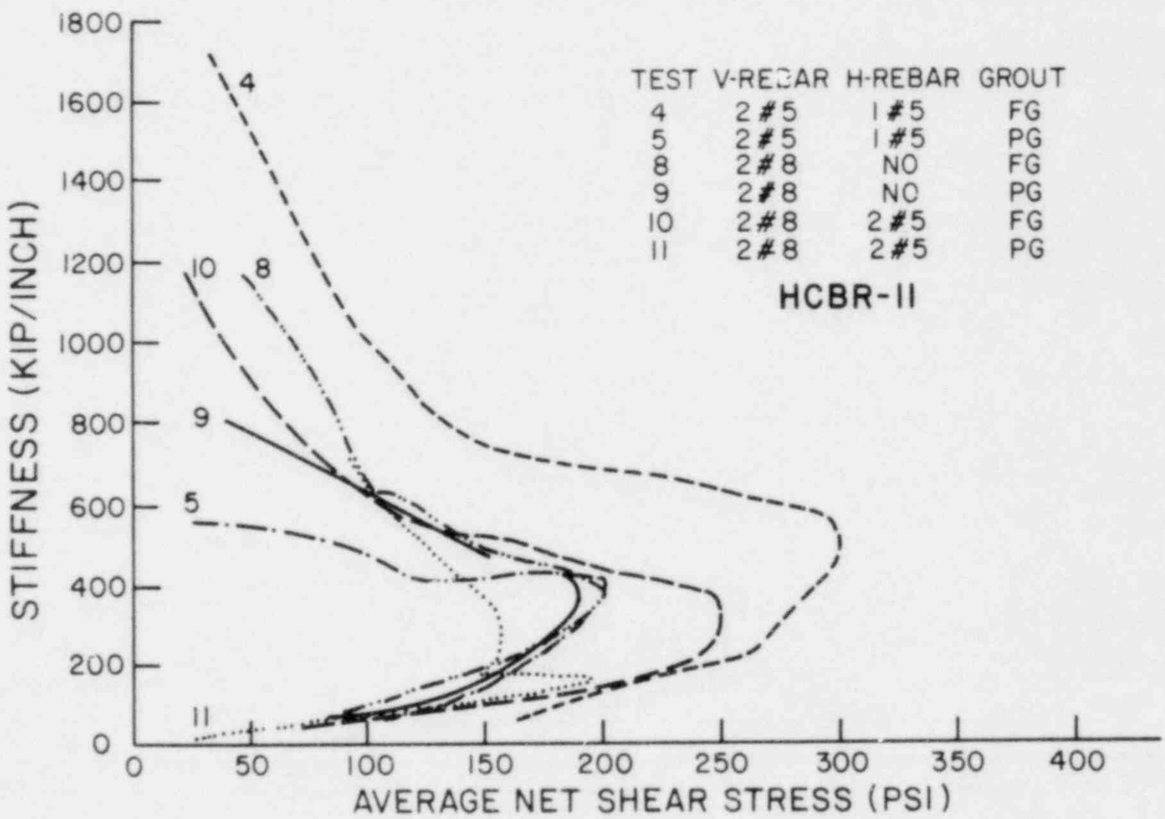

FIG. 5.10 EFFECT OF PARTIAL GROUTING ON STIFFNESS DEGRADATION (HCBR)

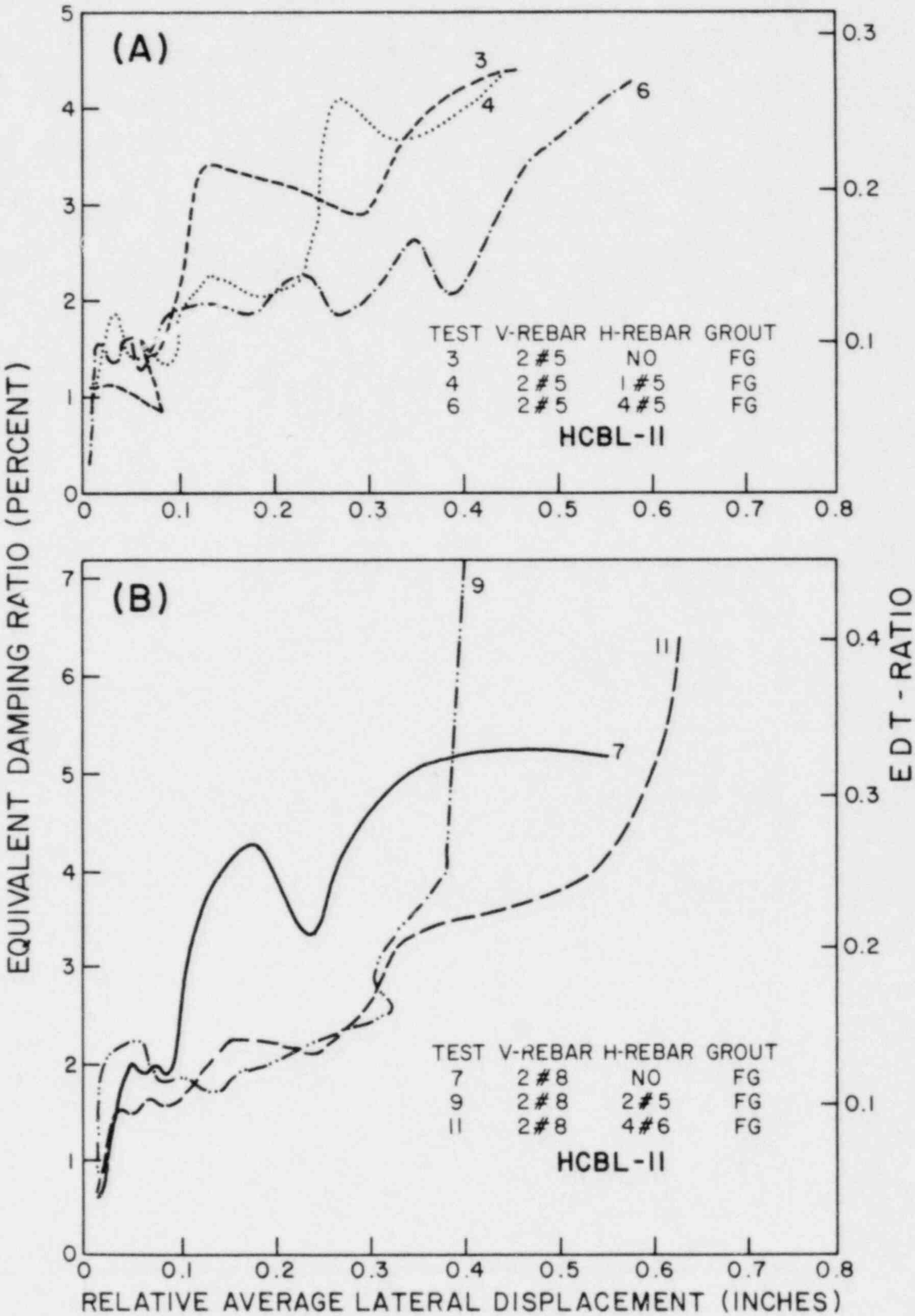

FIG. 5.11 EFFECT OF HORIZONTAL REINFORCEMENT ON ENERGY DISSIPATION (HCBL)

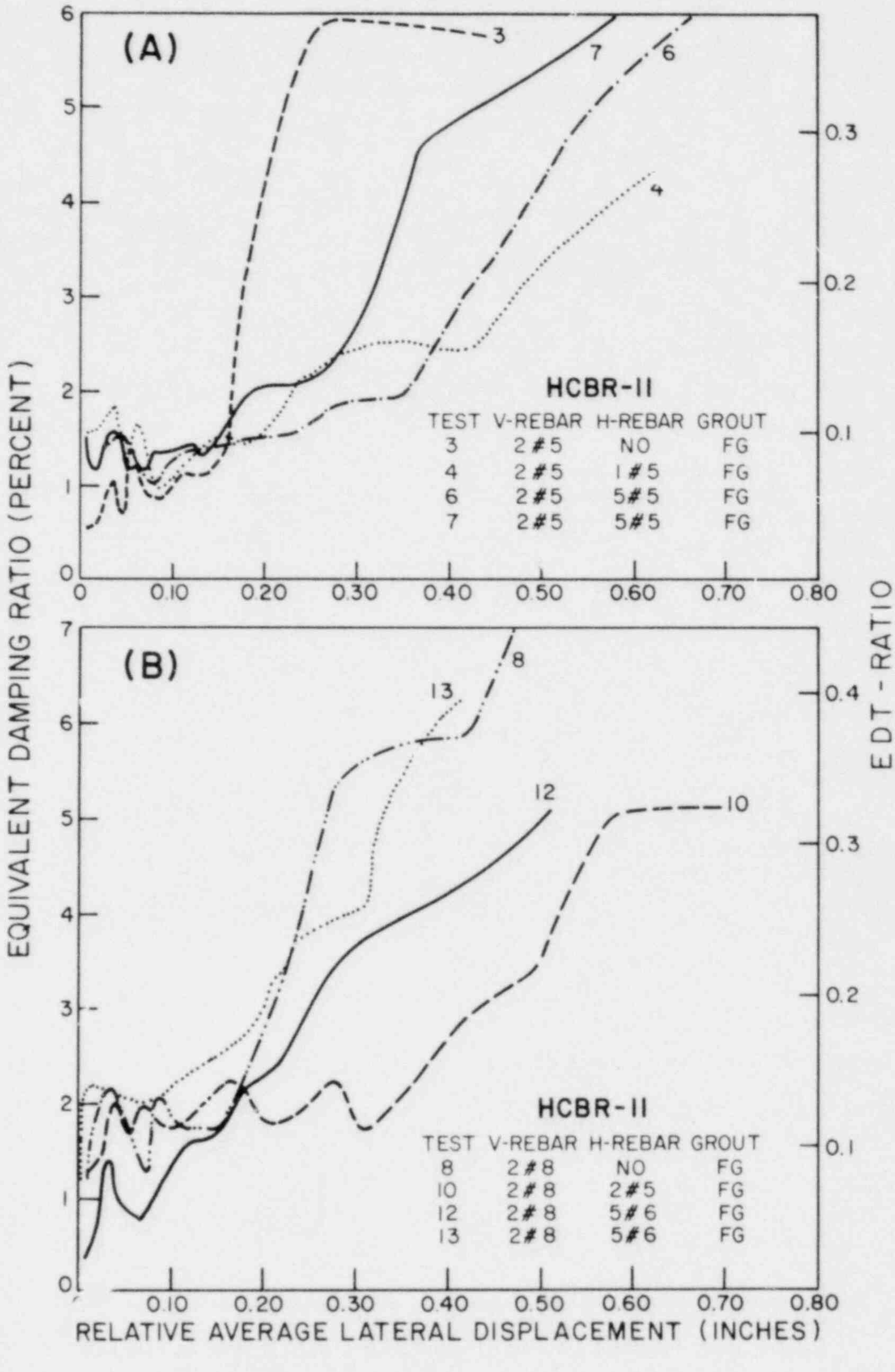

FIG. 5.12 EFFECT OF HORIZONTAL REINFORCEMENT ON ENERGY DISSIPATION (HCBR)

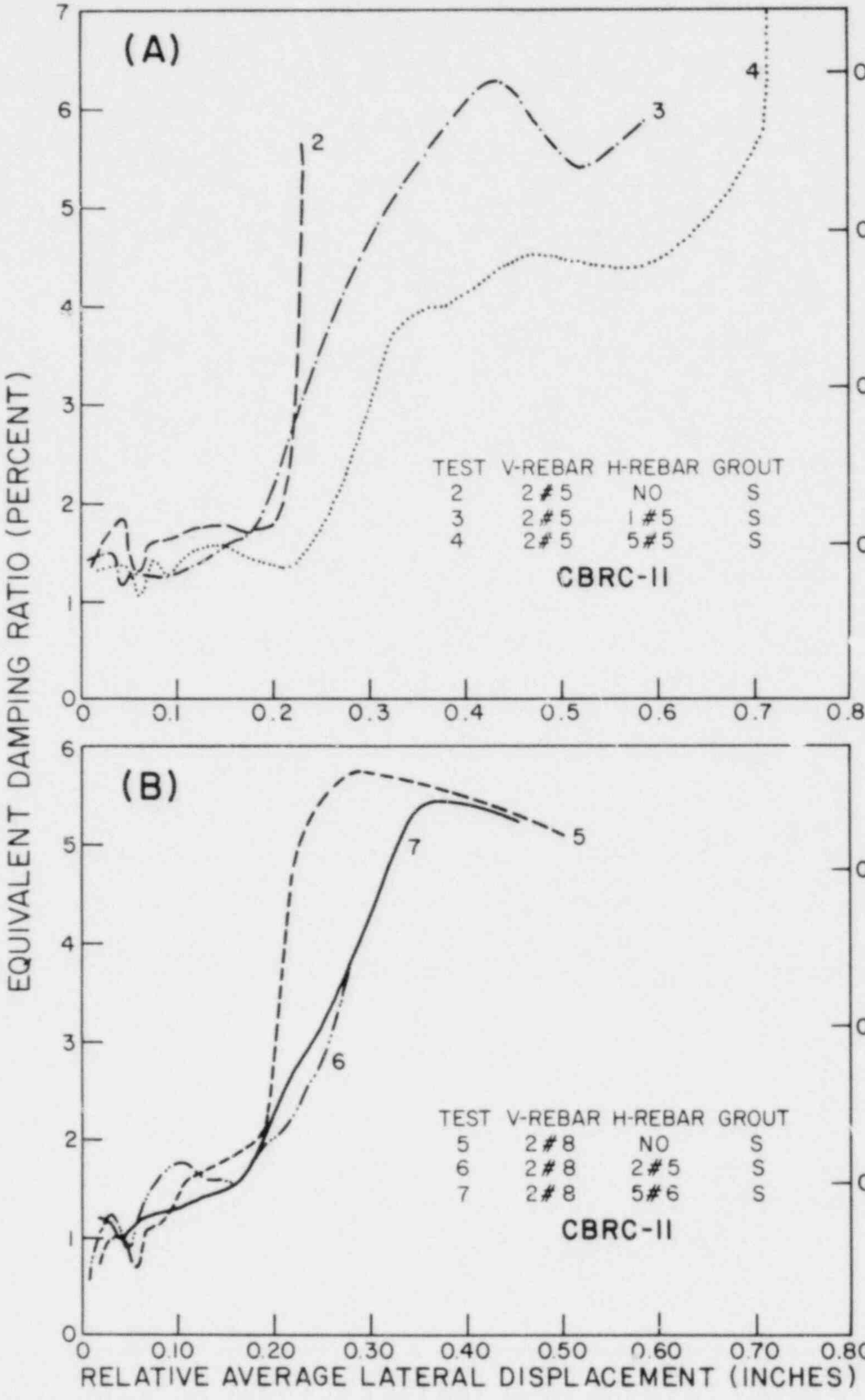

FIG. 5.13 EFFECT OF HORIZONTAL REINFORCEMENT ON ENERGY DISSIPATION (CBRC)

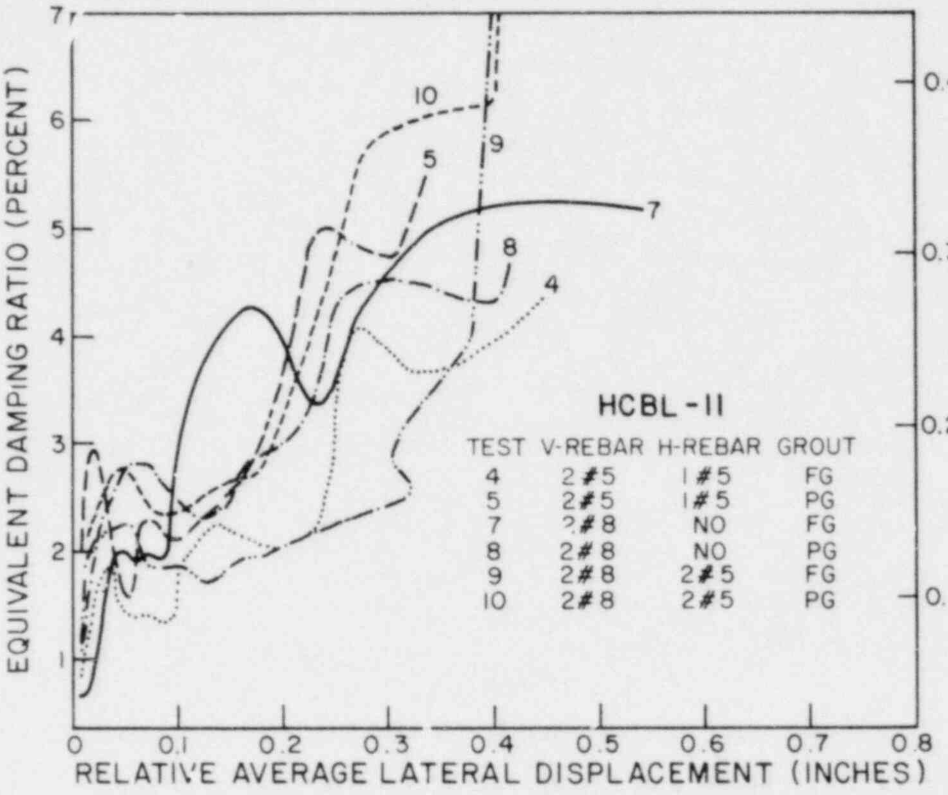

FIG. 5.14 EFFECT OF PARTIAL GROUTING ON ENERGY DISSIPATION (HCBL)

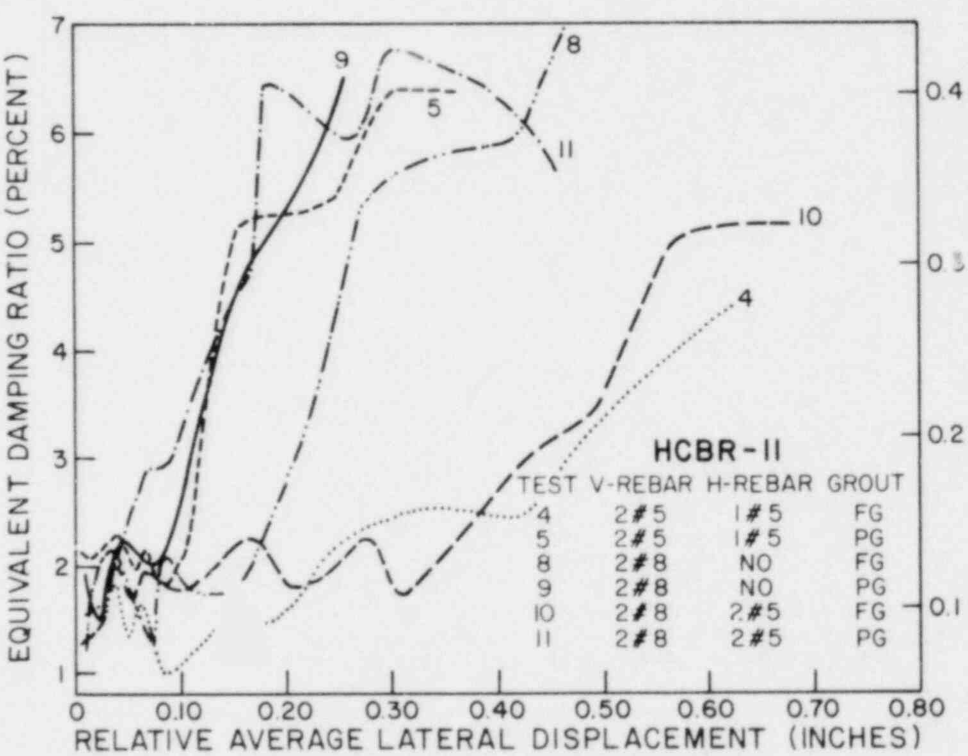

FIG. 5.15 EFFECT OF PARTIAL GROUTING ON ENERGY DISSIPATION (HCBR)

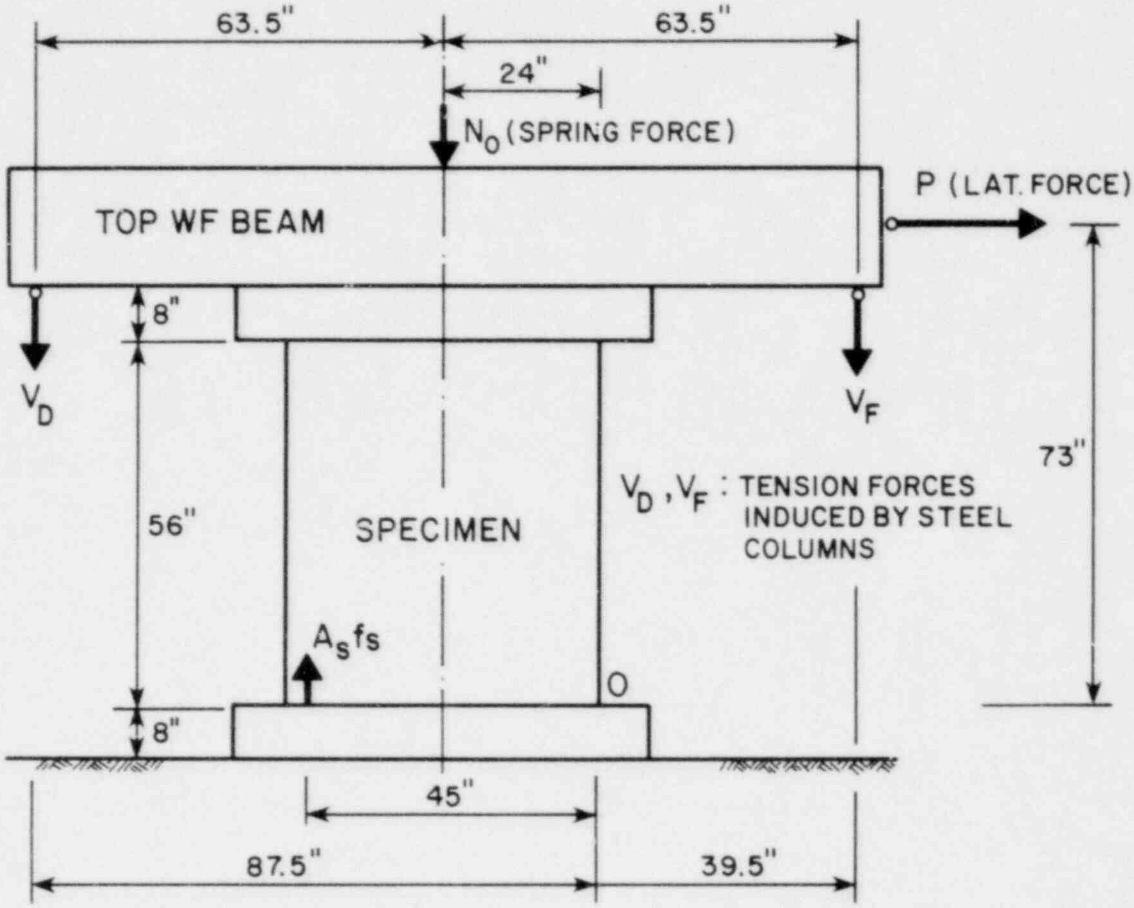

AXIAL COMPRESSIVE FORCE $= N_O + V_D + V_F$

GENERAL MOMENT EQUATION ABOUT 0 (center of compressive force) : $P \times 73 - (N_O + V_D + V_F) \times 24 - (V_D - V_F) \times 63.5 = A_S f_S \times 45$

AT INITIATION OF YIELDING : $P_Y \times 73 - (N_O + V_{DY} + V_{FY}) \times 24 - (V_{DY} - V_{FY}) \times 63.5 = A_S f_Y \times 45$

FOR ANY SUBSEQUENT STAGE WHERE THE STEEL CONTINUES YIELDING ($f_S = f_Y$) : $\underbrace{(P-P_Y)}_{\Delta P} \times 73 - (\underbrace{V_D + V_F - V_{DY} - V_{FY}}_{\Delta N}) \times 24 - (\underbrace{V_D - V_F - V_{DY} + V_{FY}}_{\Delta M}) \times 63.5 = 0$

$$\Delta P = \underbrace{\Delta N \frac{24}{73}}_{(\Delta P)_N} + \underbrace{\Delta M \frac{1}{73}}_{(\Delta P)_M}$$

FIG. 5.16 INFLUENCE OF AXIAL FORCE ON PIER LATERAL STRENGTH

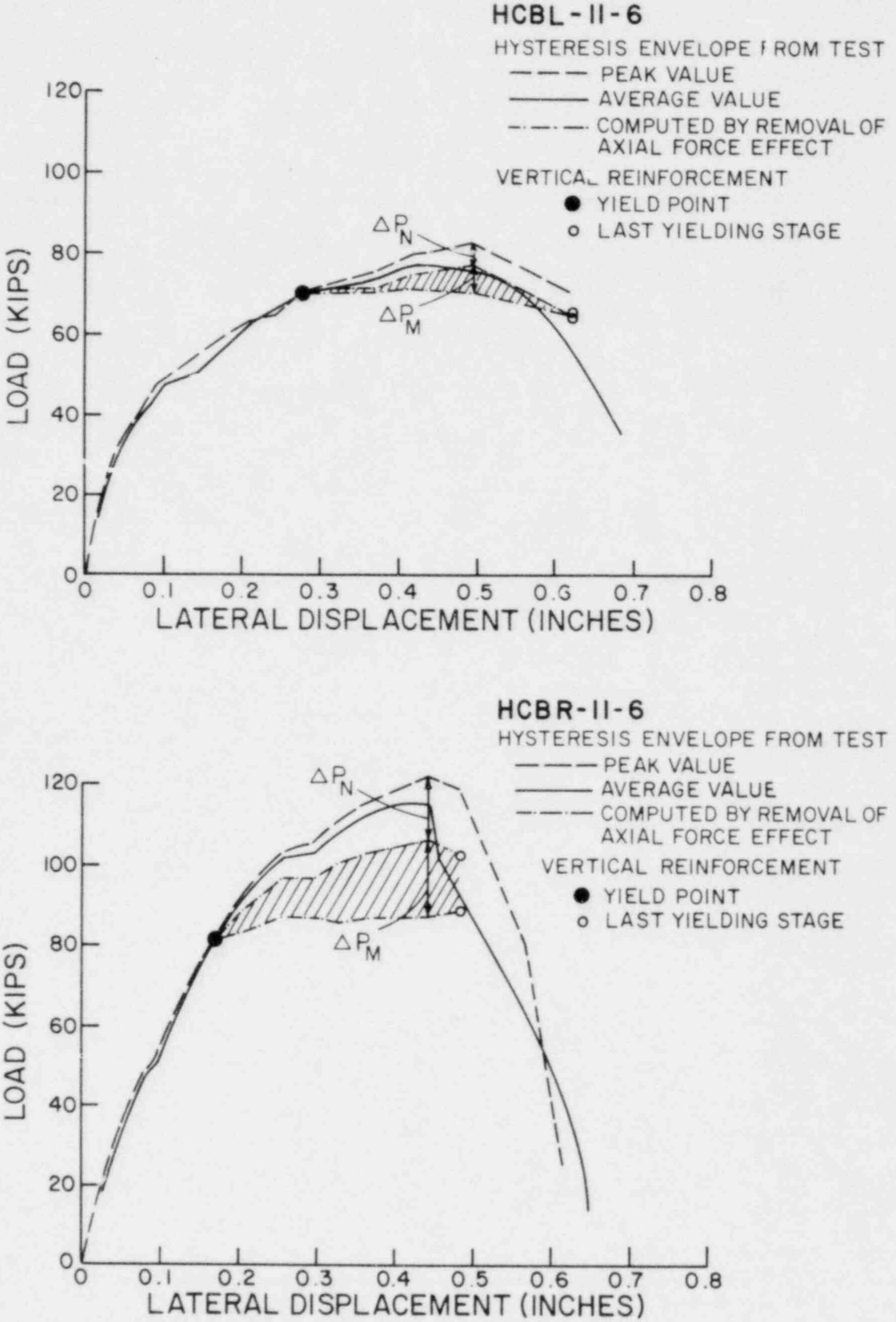

FIG. 5.17 INFLUENCE OF AXIAL FORCE ON PIER BEHAVIOR

REFERENCES

1. Blume, J.A., and Prolux, J., "Shear in Grouted Brick Masonry Wall Elements," Report to Western States Clay Products from J.A. Blume and Associates, 1968.

2. Greenley, D.G. and Cattaneo, L.E., "The Effect of Edge Load on the Racking Strength of Clay Masonry," Proceedings, Second International Brick Masonry Conference, Stoke-on-Trent, 1970.

3. Hidalgo, P.A., Mayes, R.L., McNiven, H.D. and Clough, R.W., "Cyclic Loading Tests of Masonry Single Piers, Volume 1 - Height to Width Ratio of 2," EERC Report No. 78-27, University of California, Berkeley, 1978.

4. Mayes, R.L. and Clough, R.W., "A Literature Survey-Compressive, Tensile, Bond and Shear Strength of Masonry," EERC Report No. 75-15, University of California, Berkeley, 1975.

5. Mayes, R.L. and Clough, R.W., "State-of-the-Art in Seismic Strength of Masonry--An Evaluation and Review," EERC Report No. 75-21, University of California, Berkeley, 1975.

6. Mayes, R.L., Omote, Y., Chen, S.W. and Clough, R.W., "Expected Performance of Uniform Building Code Designed Masonry Structures," EERC Report No. 76-7, University of California, Berkeley, 1976.

7. Mayes, R.L., Omote, Y. and Clough, R.W., "Cyclic Shear Tests of Masonry Piers, Volume I--Test Results," EERC Report No. 76-8, University of California, Berkeley, 1976.

8. Mayes, R.L., Omote, Y. and Clough, R.W., "Cyclic Shear Tests on Masonry Piers, Volume II - Analysis of Test Results," Report No. EERC 76-16, 1976.

9. 1977 Masonry Codes and Specifications, Published by the Masonry Industry Advancement Committee, California, 1977.

10. Meli, R., "Behaviour of Masonry Walls under Lateral Loads," Proceedings of the Fifth World Conference on Earthquake Engineering, Rome, 1973.

11. Priestley, M.J.N. and Bridgeman, D.O., "Seismic Resistance of Brick Masonry Walls," Bulletin of the New Zealand National Society for Earthquake Engineering, Vol. 7, No. 4, 1974.

12. Priestley, M.J.N., "Seismic Resistance of Reinforced Concrete Masonry Shear Walls with High Steel Percentages," Bulletin of the New Zealand National Society for Earthquake Engineering, Vol. 10, No. 1, 1977.

13. Scrivener, J.C., "Concrete Masonry Wall Panel Tests with Predominant Flexural Effect," New Zealand Concrete Construction, 1966.

14. Williams, D.W., "Seismic Behaviour of Reinforced Masonry Shear Walls," Ph.D. Thesis, University of Canterbury, Christchurch, New Zealand, 1971.

APPENDIX A

CATALOG OF TEST RESULTS

The experimental results are arranged in three pages for each test, containing six photographs of the successive crack patterns and six graphs obtained from the data collected during the test. These graphs include the hysteresis loops, the hysteresis envelope, stiffness degradation, equivalent damping ratio and amount of shear distortion as compared with total deformation.

In order to show the relation between the photographs of the crack patterns and the diagrams showing the results, a black dot has been drawn on the graphs and next to the corresponding picture of the crack pattern.

The details on how each of the diagrams was obtained are presented in Chapter 4.

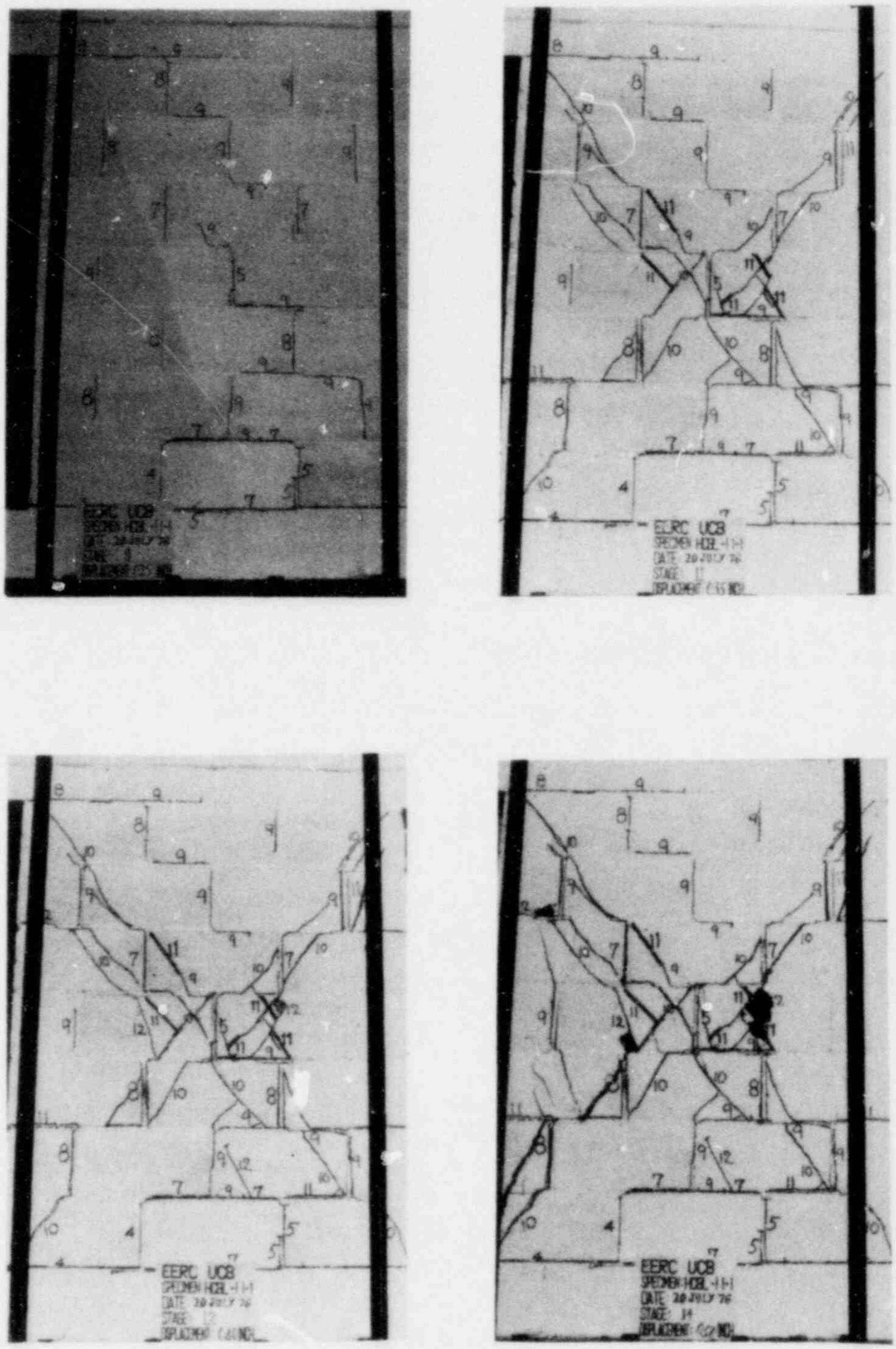

FIG. A.1 SUCCESSIVE CRACK FORMATION
AND EXPERIMENTAL RESULTS
TEST HCBL-11-1

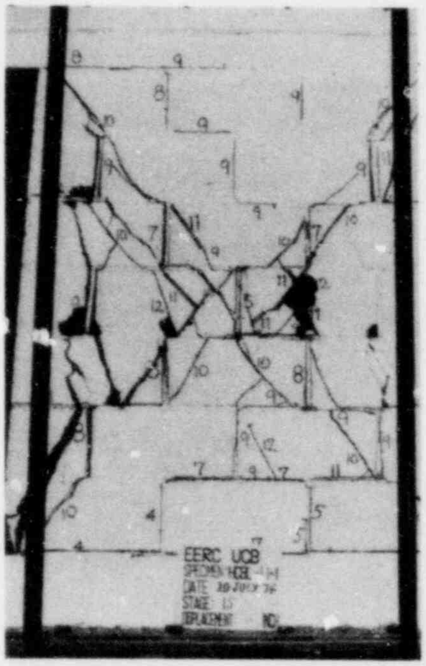

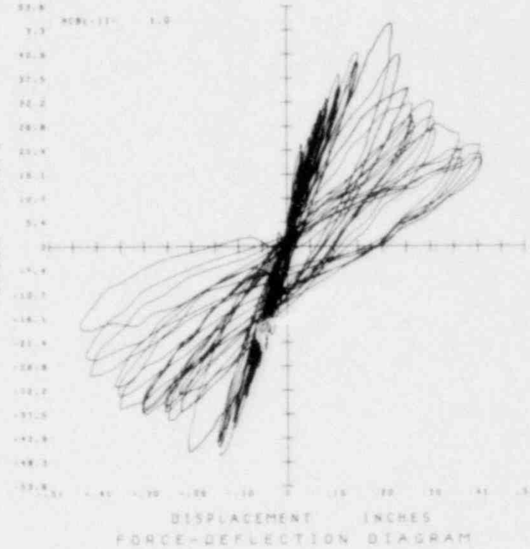

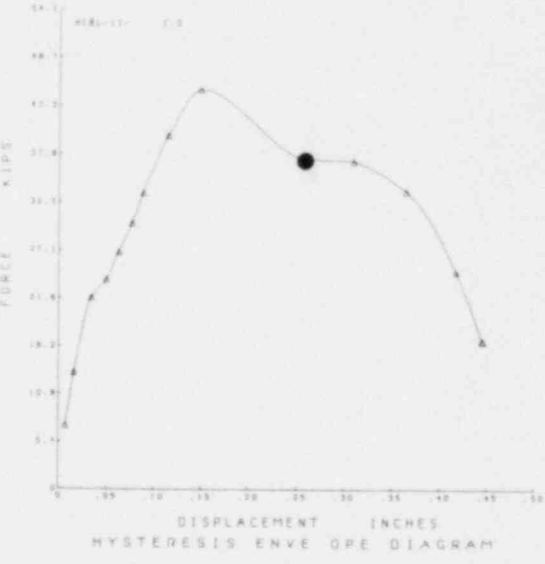

FIG. A.1 CONTINUE HCBL-11-1

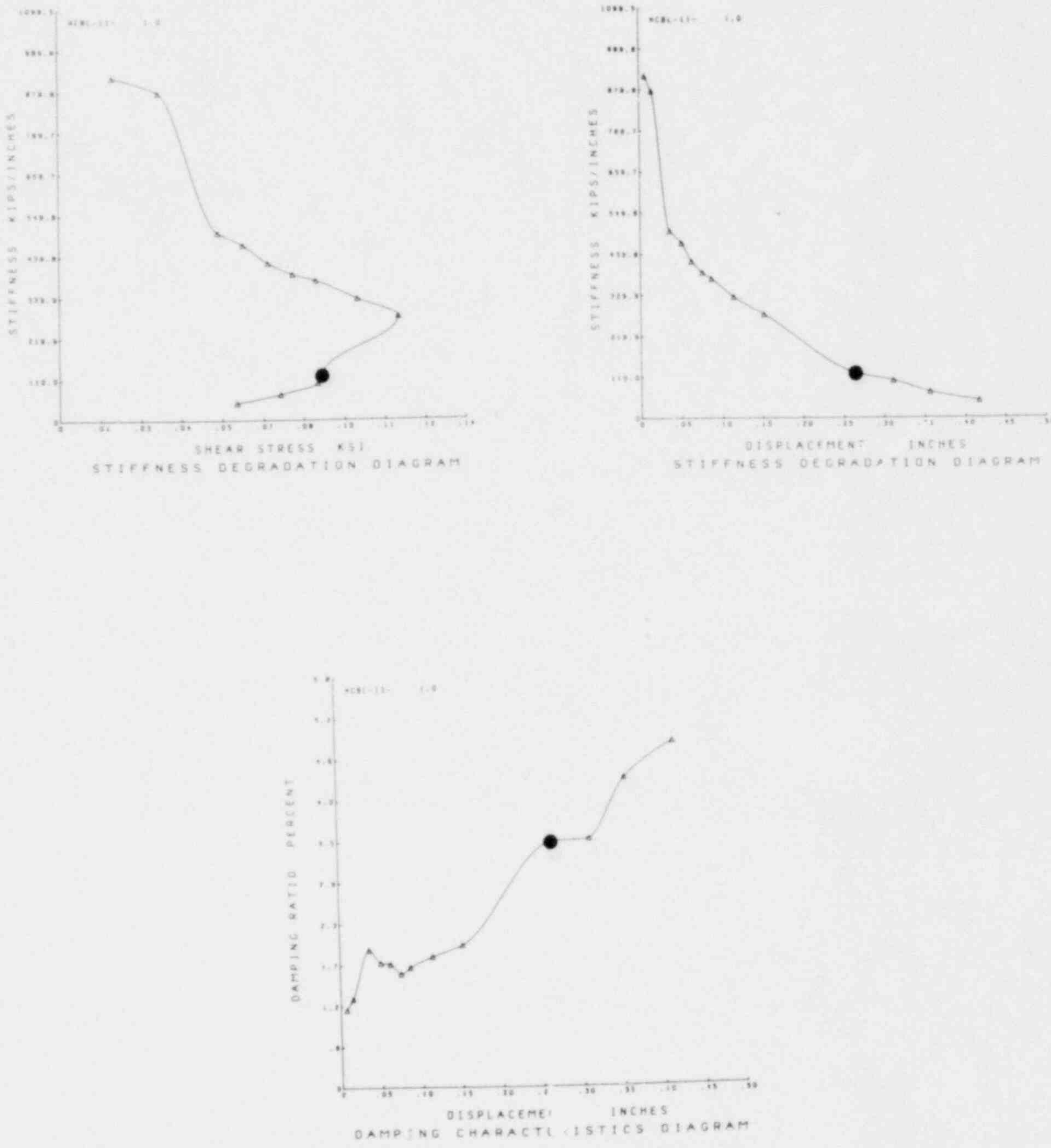

FIG. A.1 CONTINUE HCBL-11-1

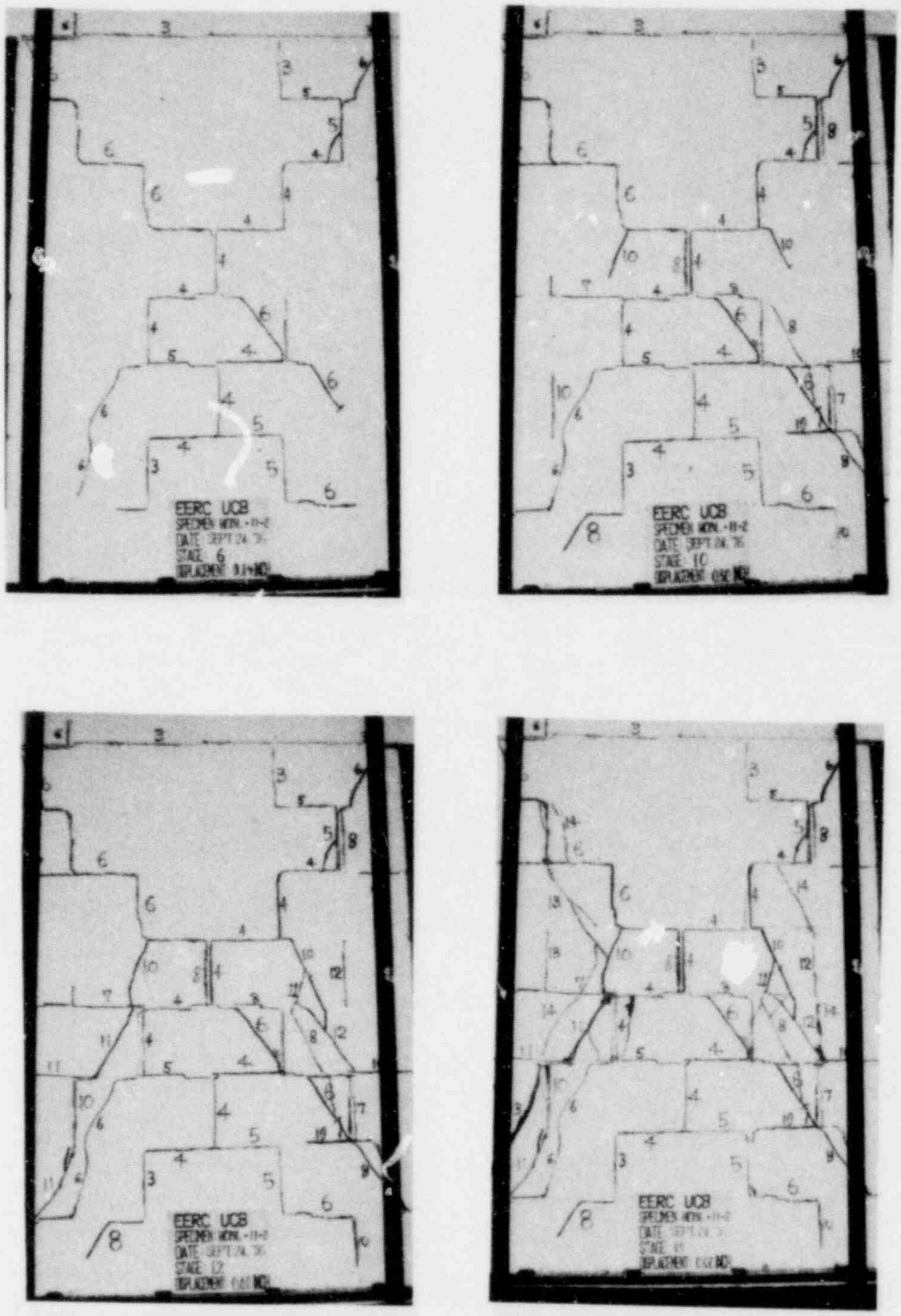

FIG. A.2 SUCCESSIVE CRACK FORMATION
AND EXPERIMENTAL RESULTS
TEST HCBL-11-2

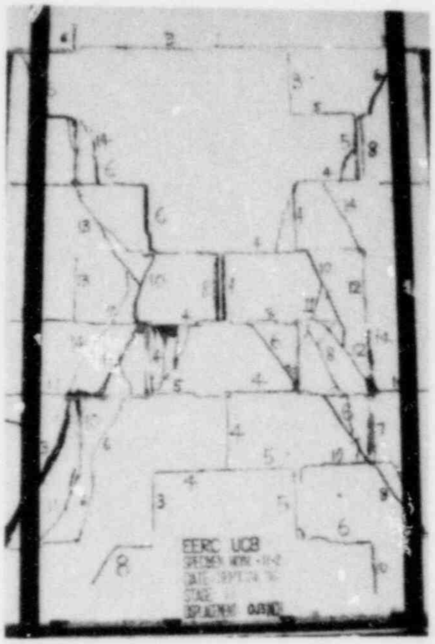

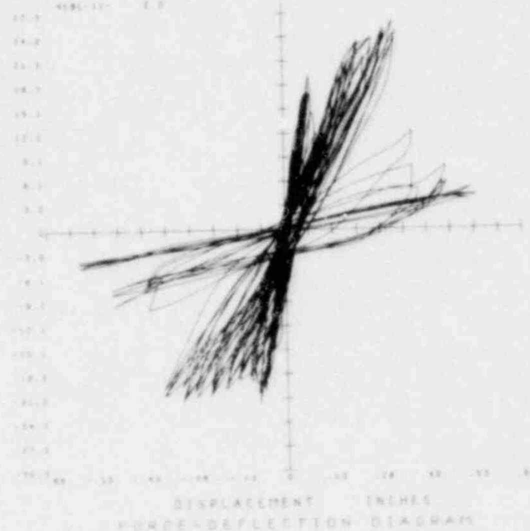

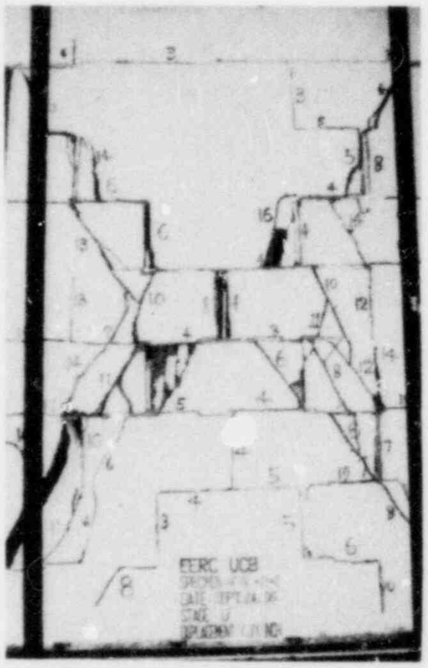

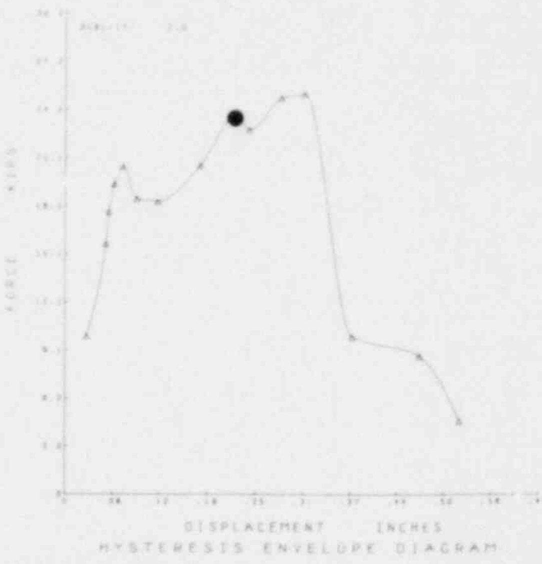

FIG. A.2 CONTINUE HCBL-11-2

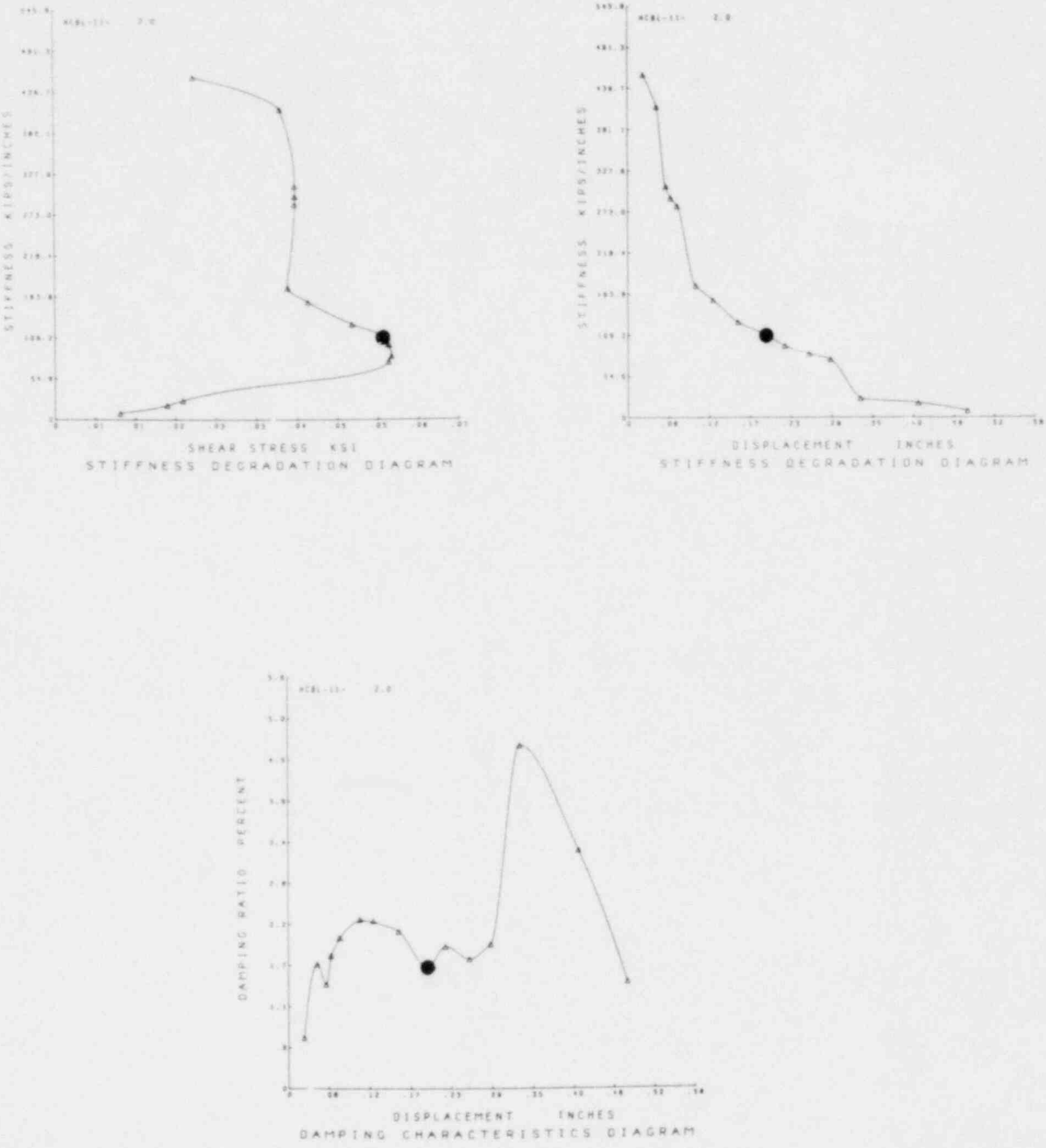

FIG. A.2 CONTINUE HCBL-11-2

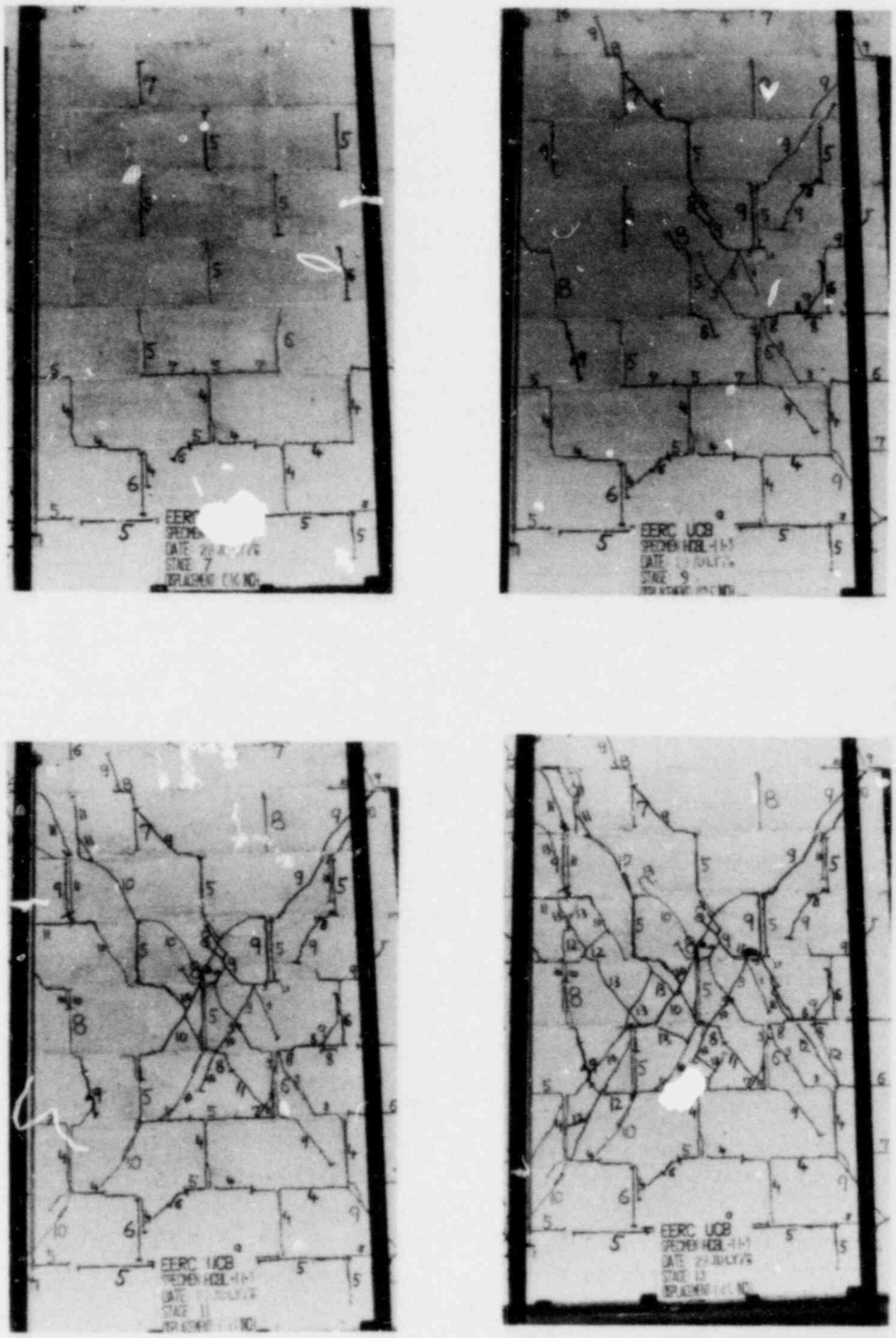

FIG. A.3 SUCCESSIVE CRACK FORMATION
AND EXPERIMENTAL RESULTS
TEST HCBL-11-3

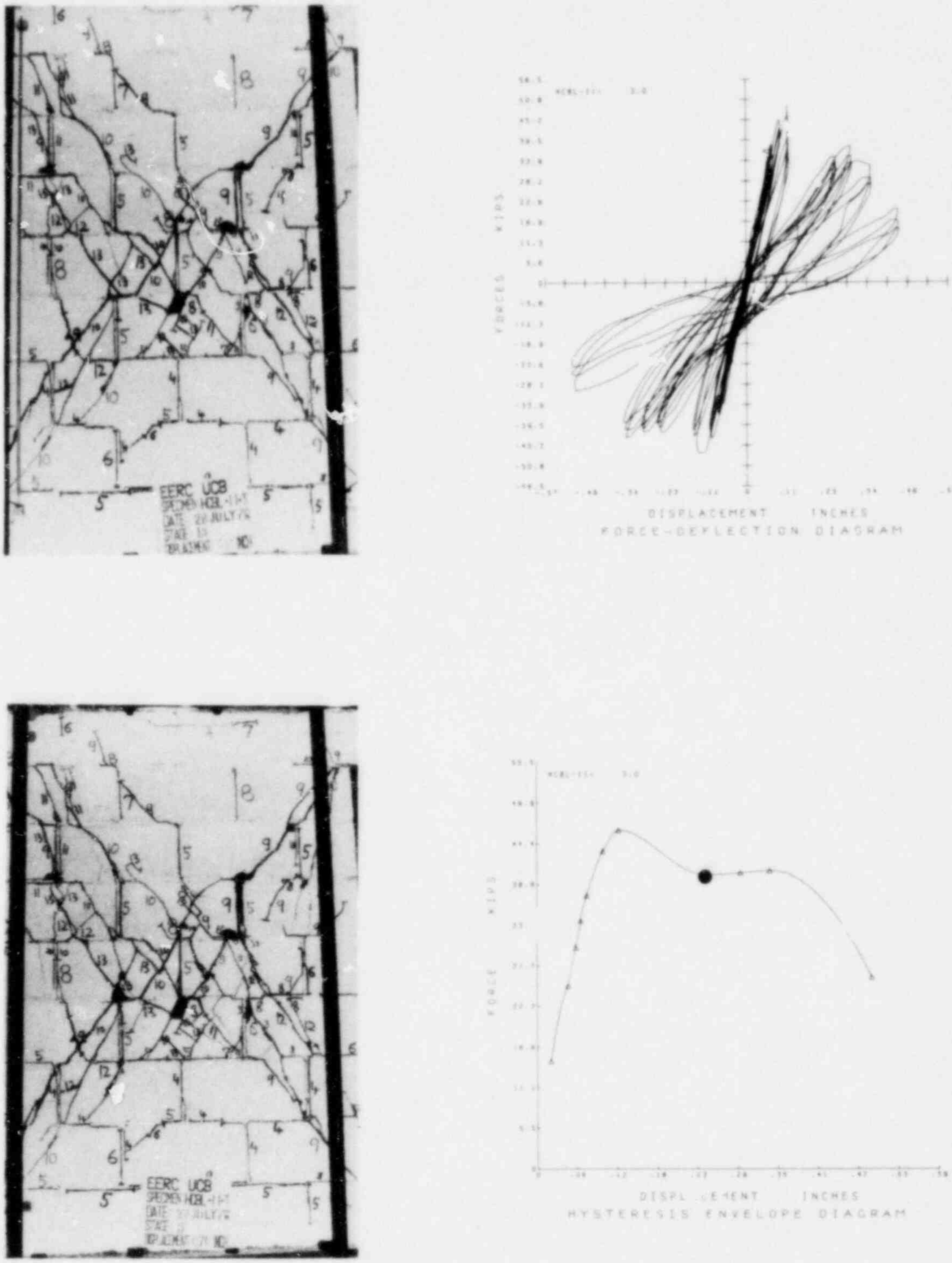

FIG. A.3 CONTINUE HCBL-11-3

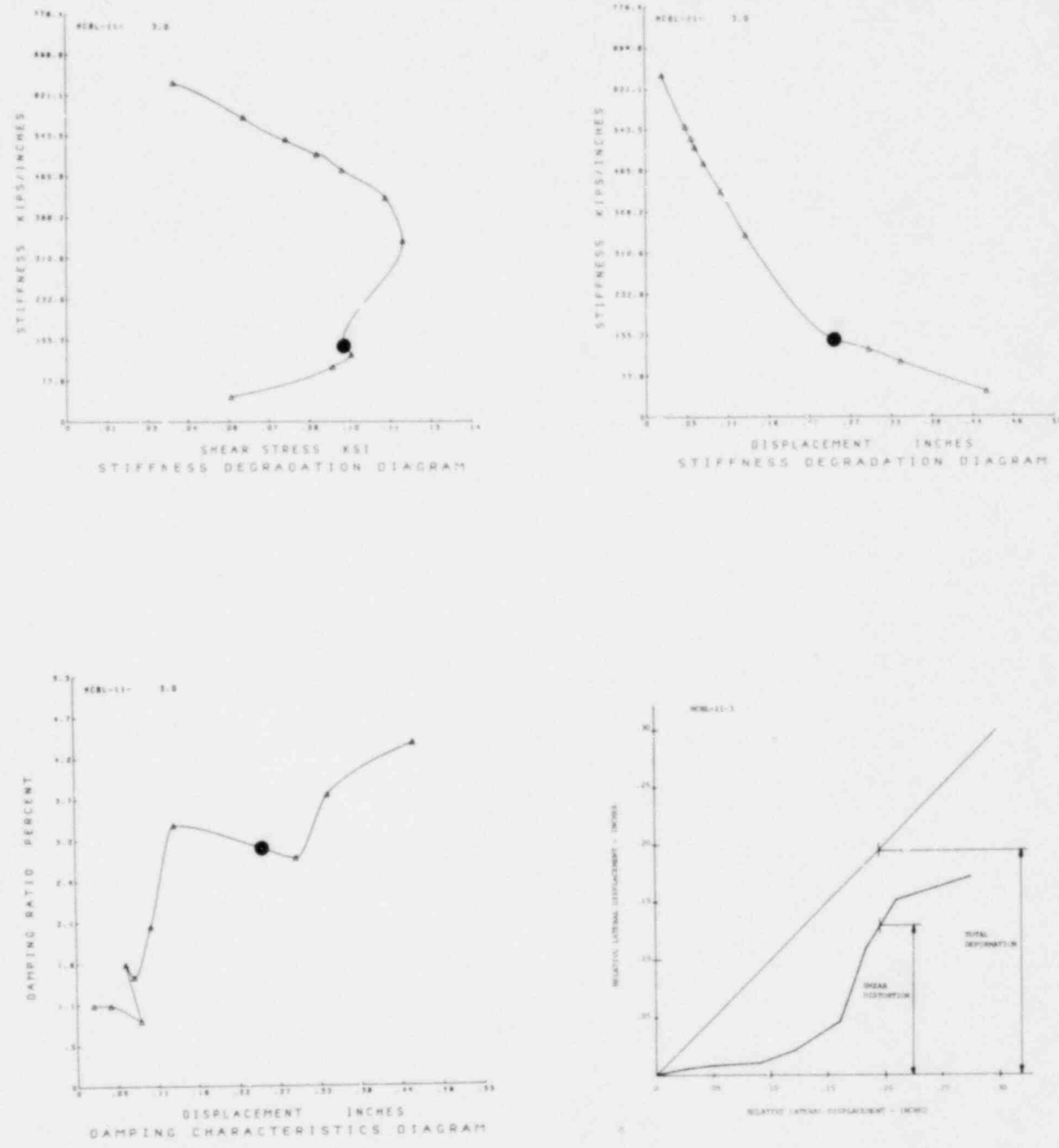

FIG. A.3 CONTINUE HCBL-11-3

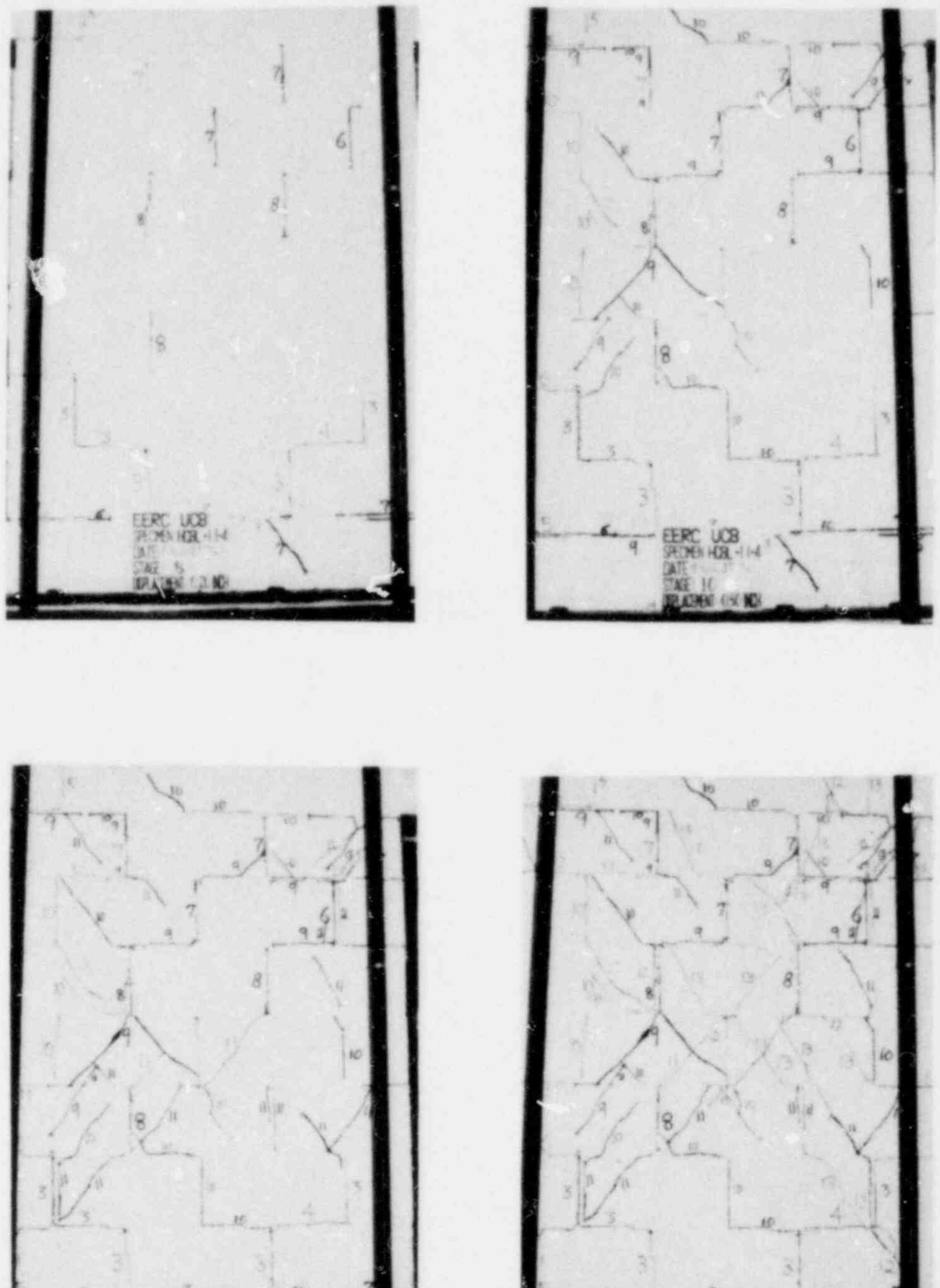

FIG. A.4 SUCCESSIVE CRACK FORMATION
AND EXPERIMENTAL RESULTS
TEST HCBL-11-4

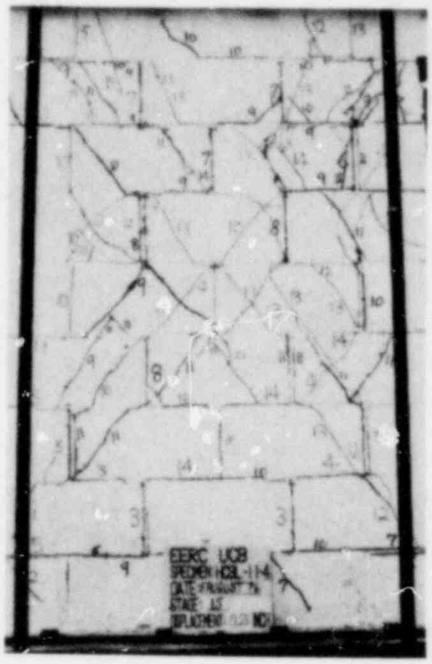

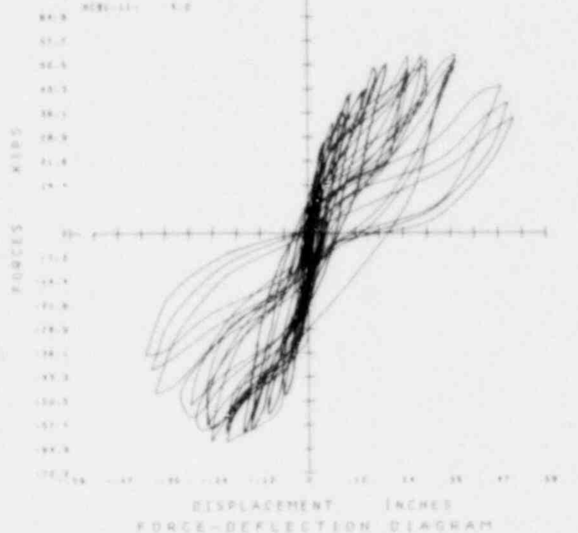

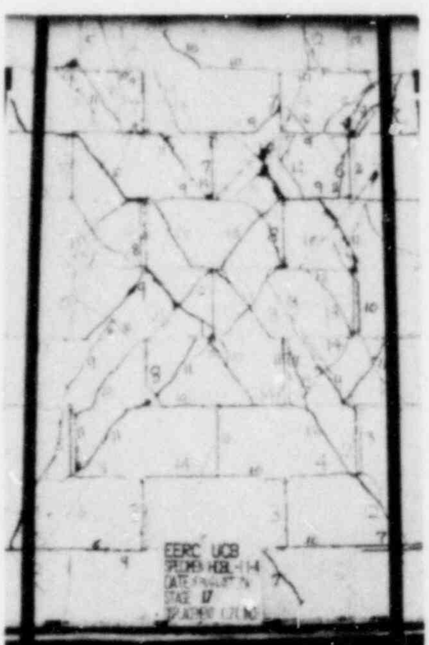

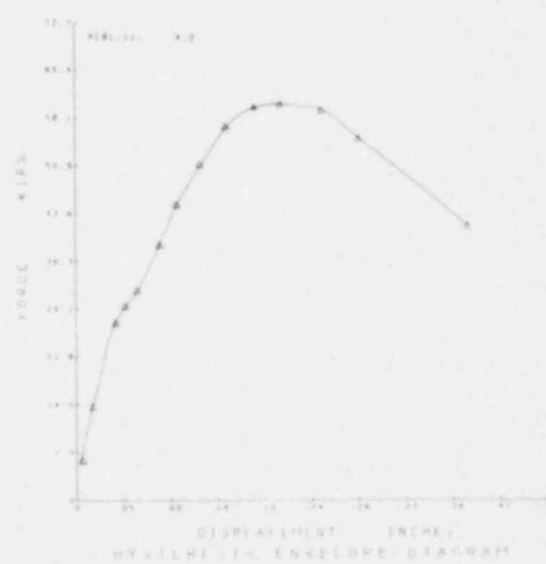

FIG. A.4 CONTINUE HCBL-11-4

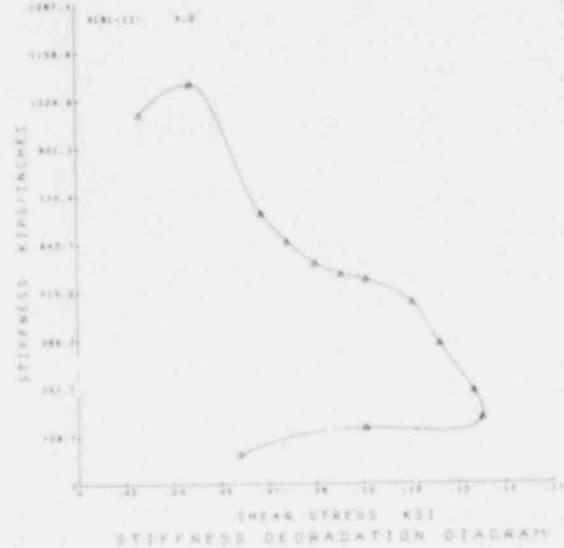

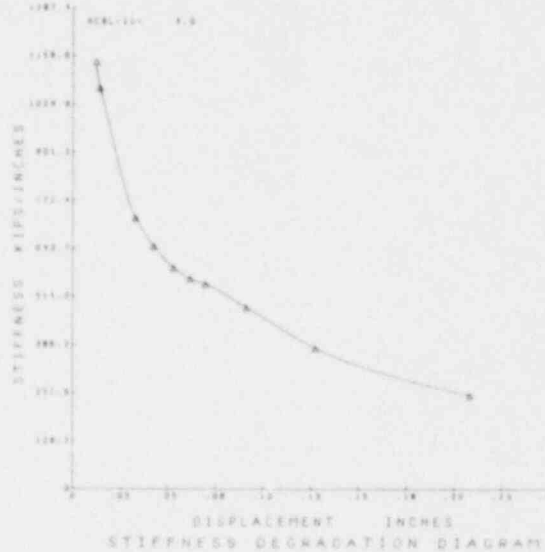

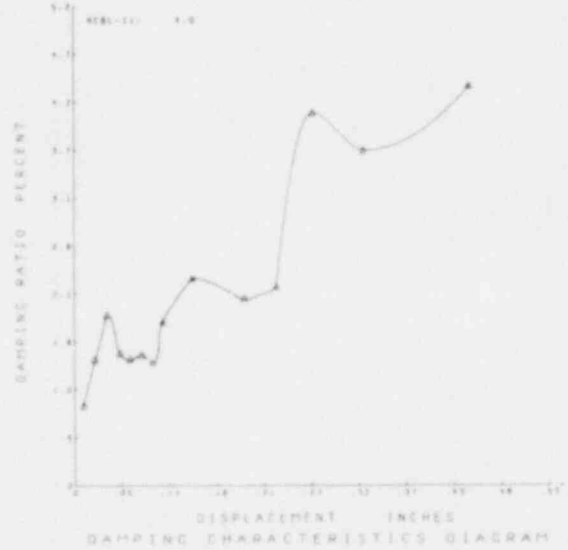

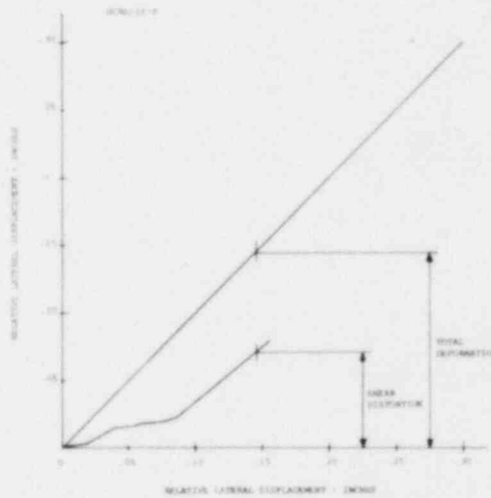

FIG. A.4 CONTINUE HCBL-11-4

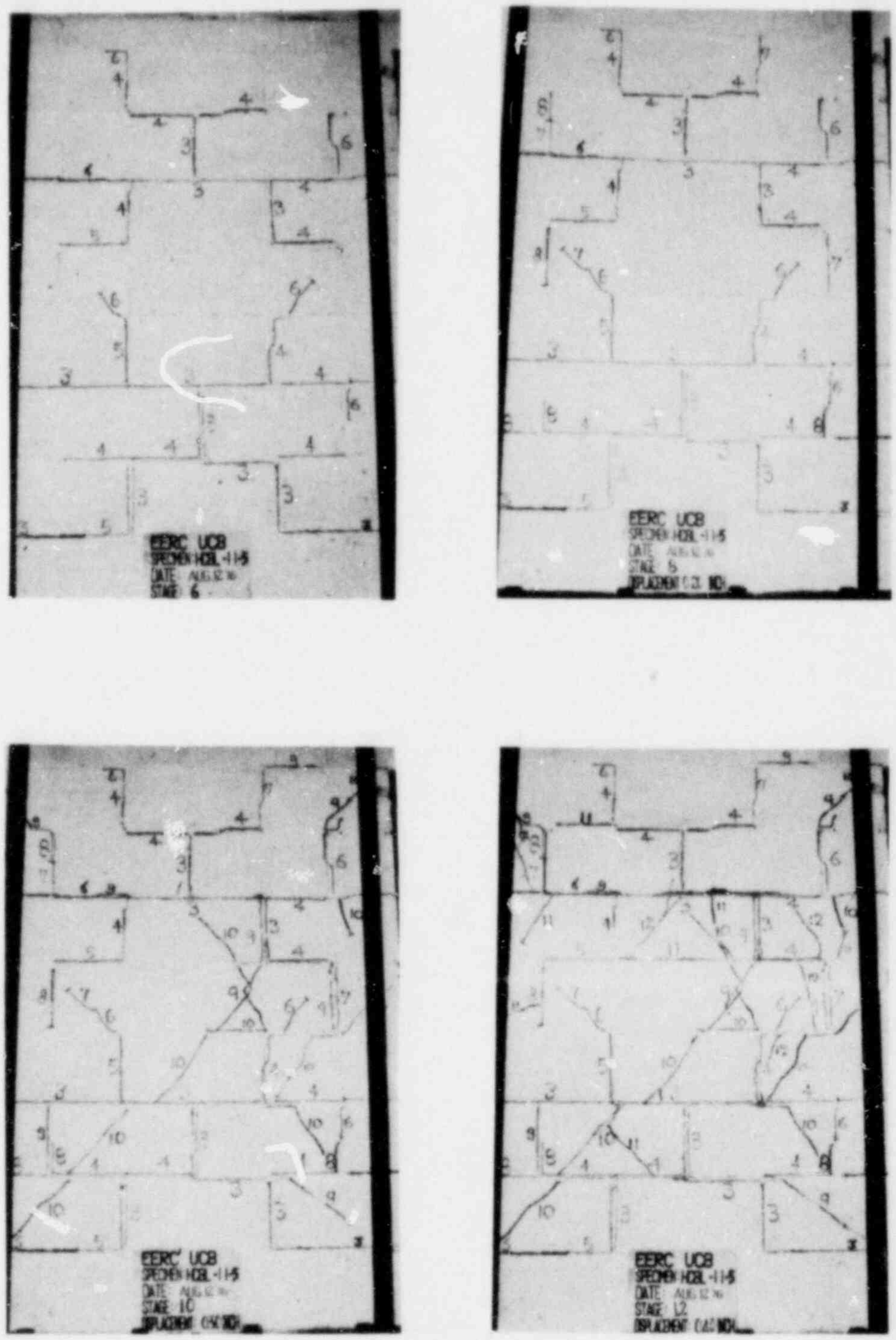

FIG. A.5 SUCCESSIVE CRACK FORMATION
AND EXPERIMENTAL RESULTS
TEST HCBL-11-5

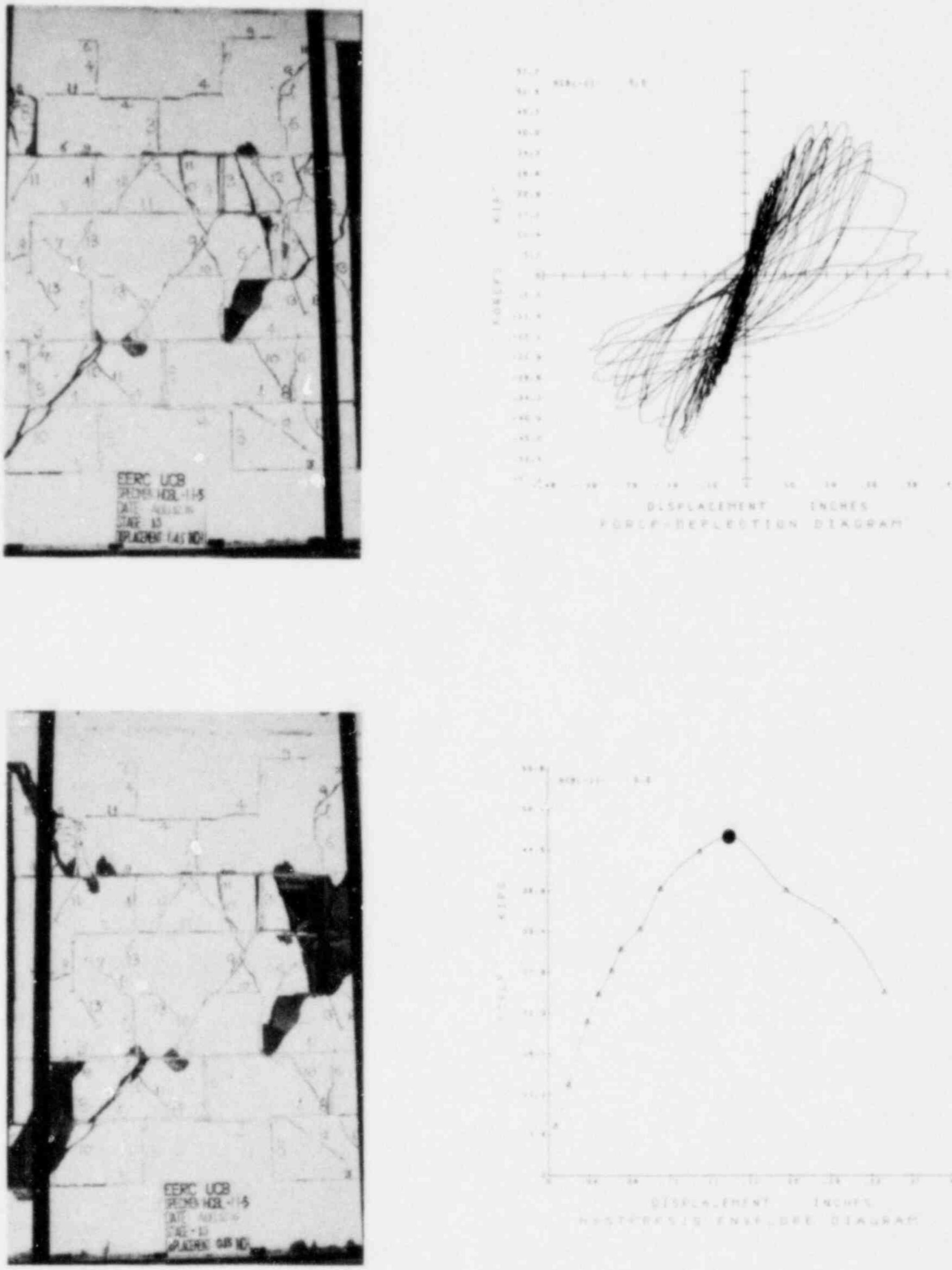

FIG. A.5 CONTINUE HCBL-11-5

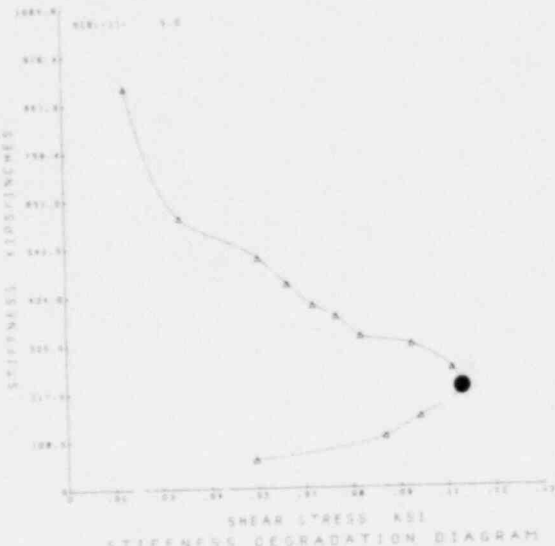

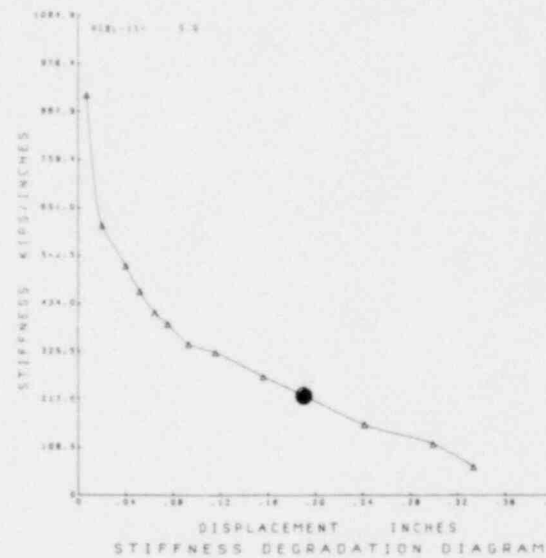

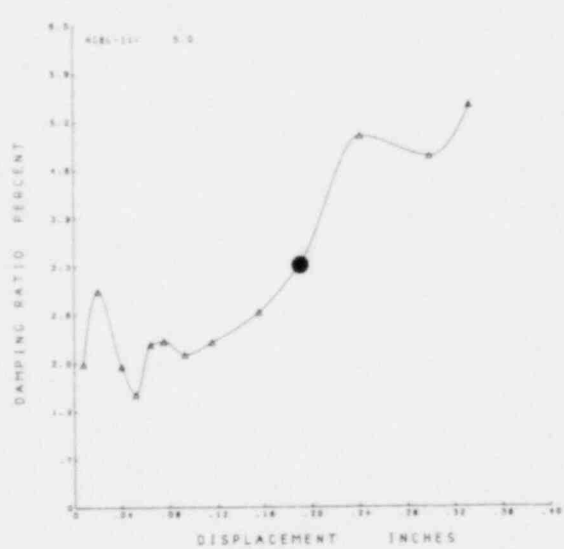

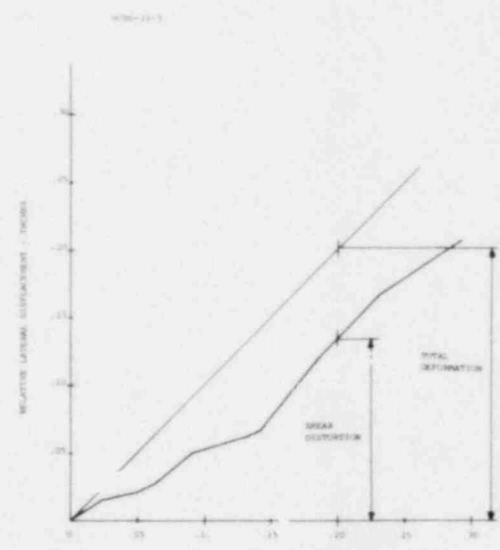

FIG. A.5 CONTINUE HCBL-11-5

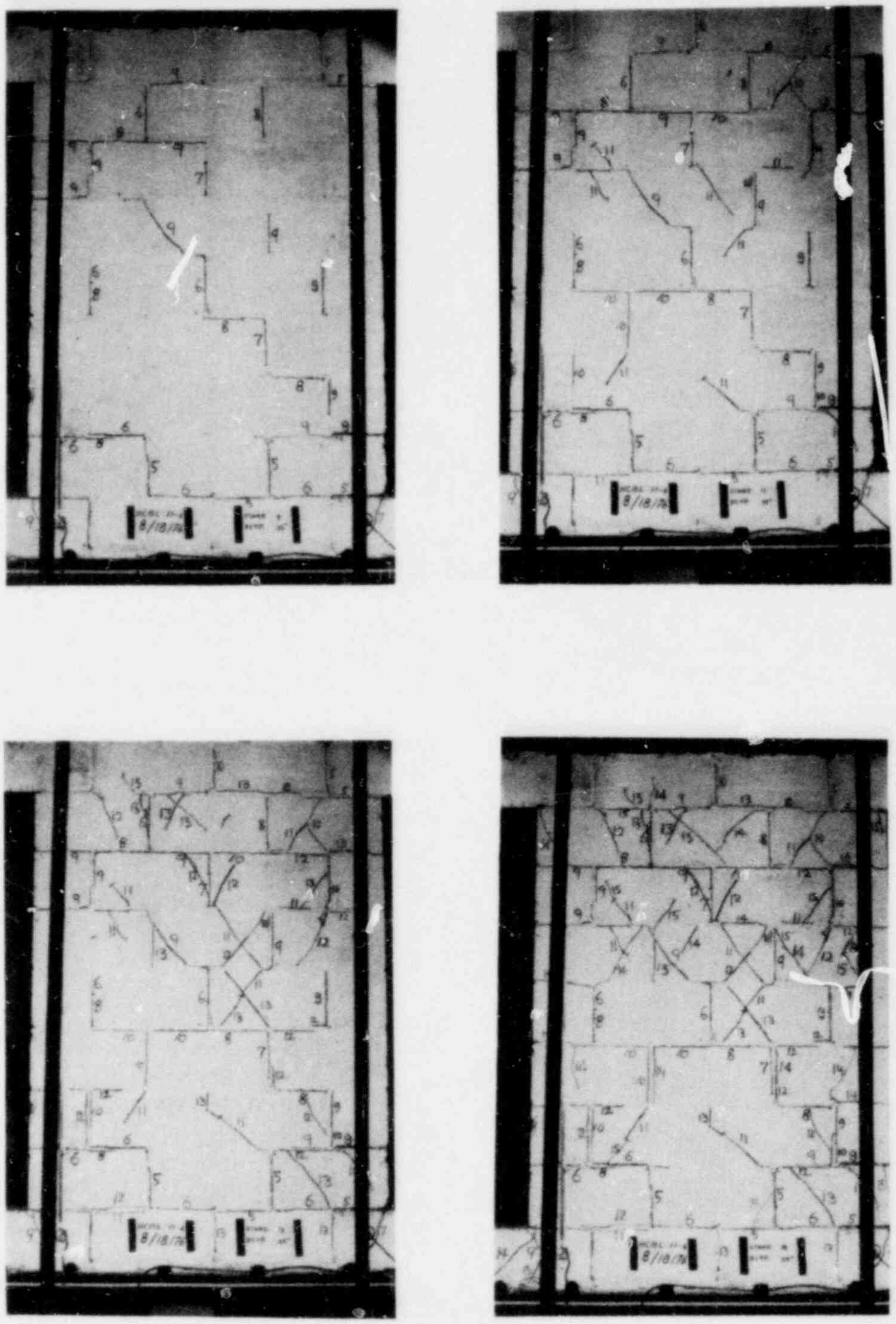

FIG. A.6 SUCCESSIVE CRACK FORMATION
AND EXPERIMENTAL RESULTS
TEST HCBL-11-6

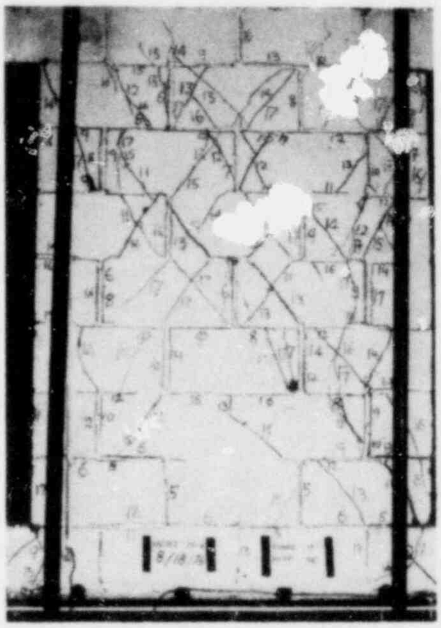

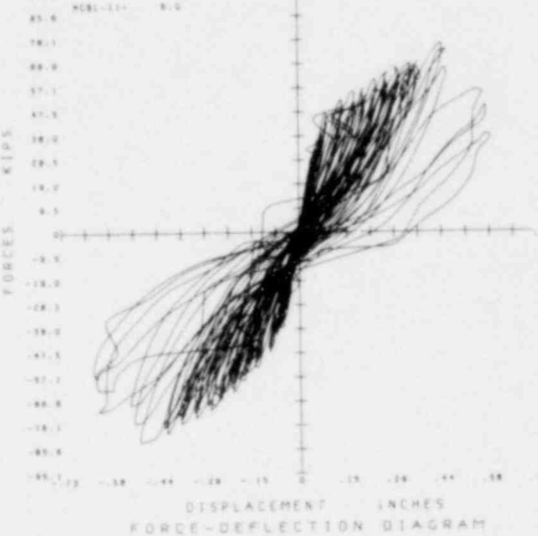

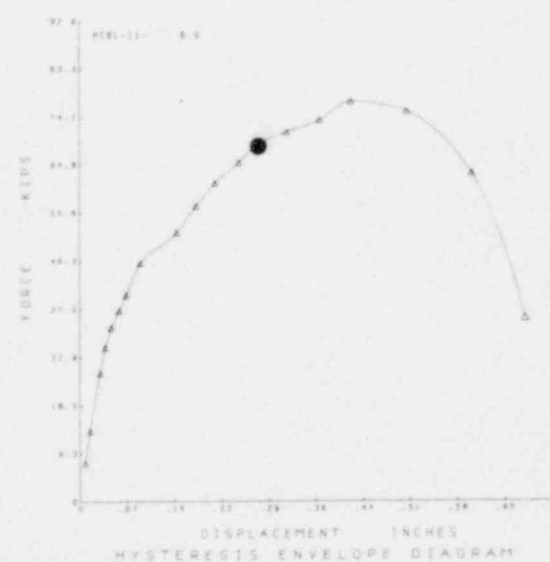

FIG. A.6 CONTINUE HCBL-11-6

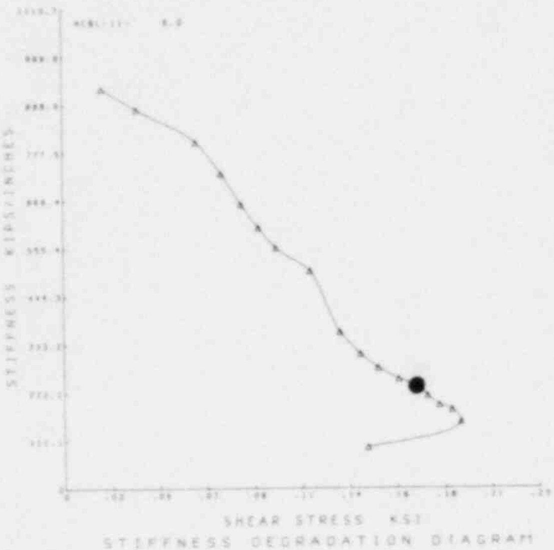

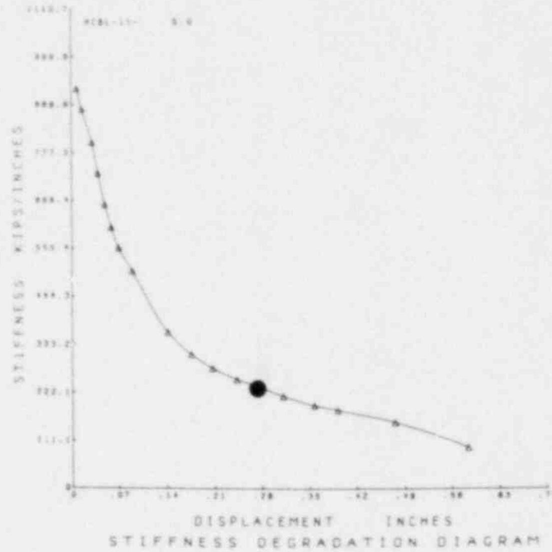

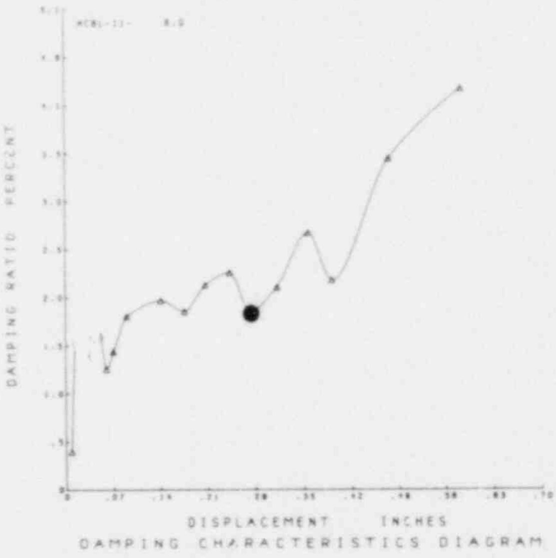

FIG. A.6 CONTINUE HCBL-11-6

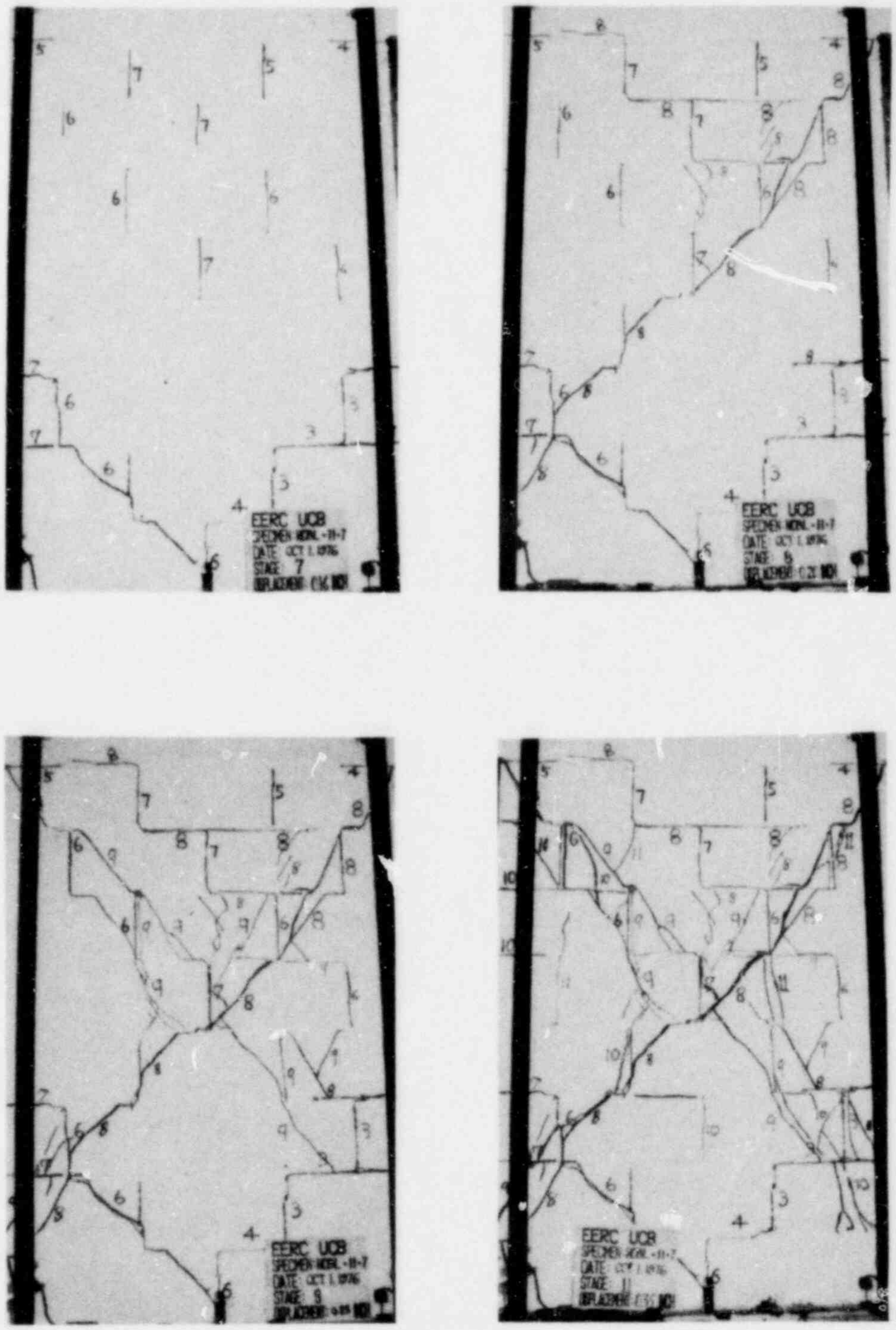

FIG. A.7 SUCCESSIVE CRACK FORMATION
AND EXPERIMENTAL RESULTS
TEST HCBL-11-7

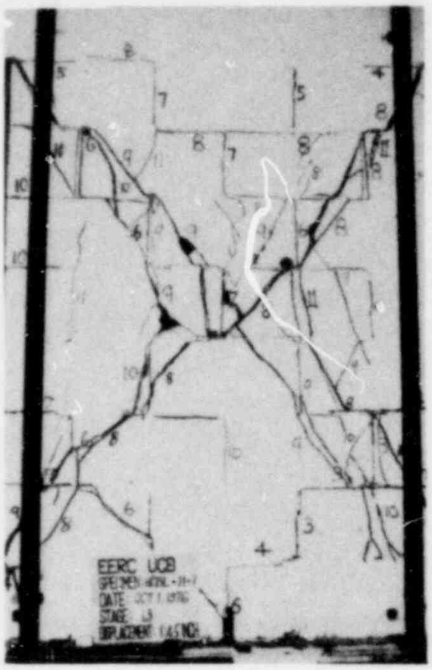

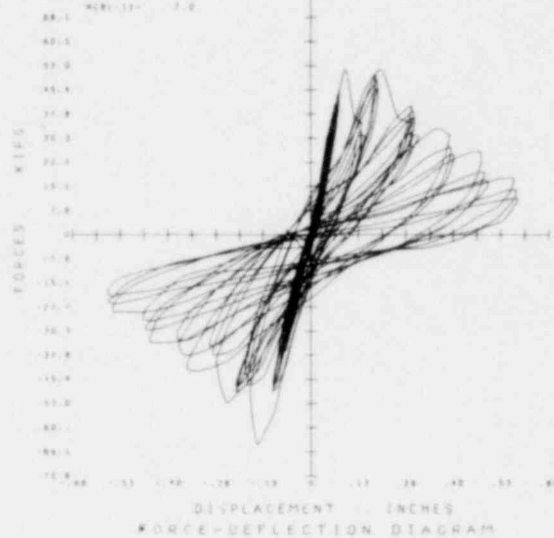

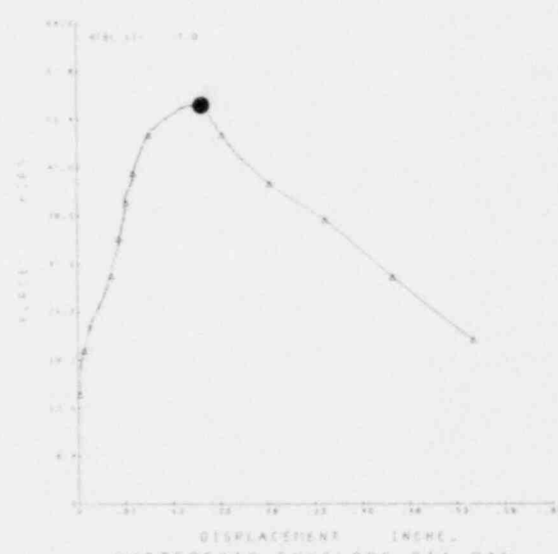

FIG. A.7 CONTINUE HCBL-11-7

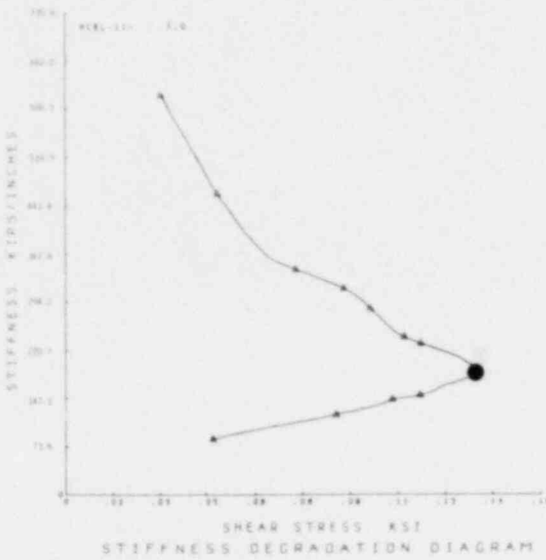

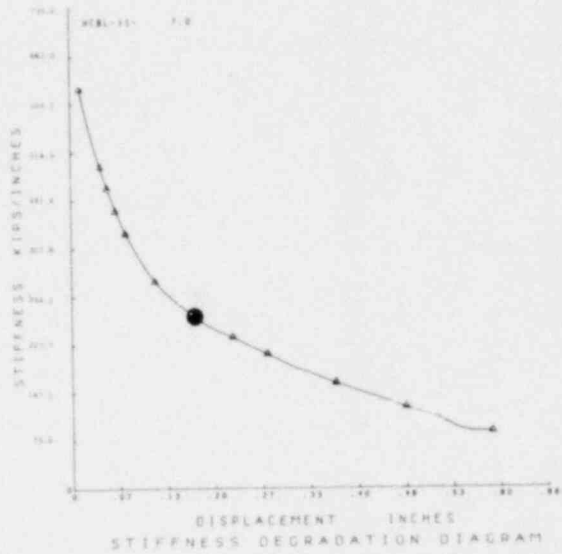

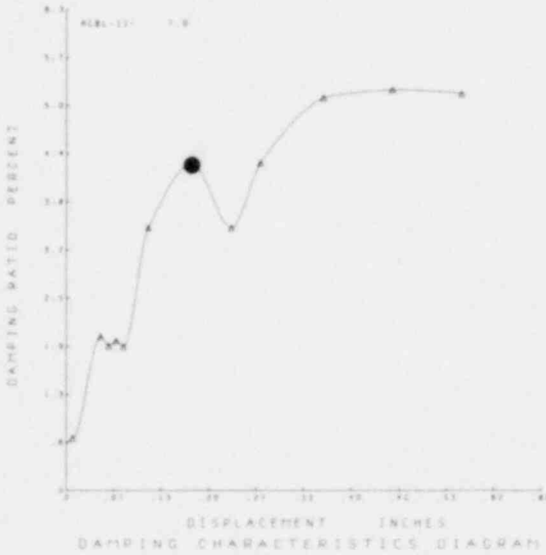

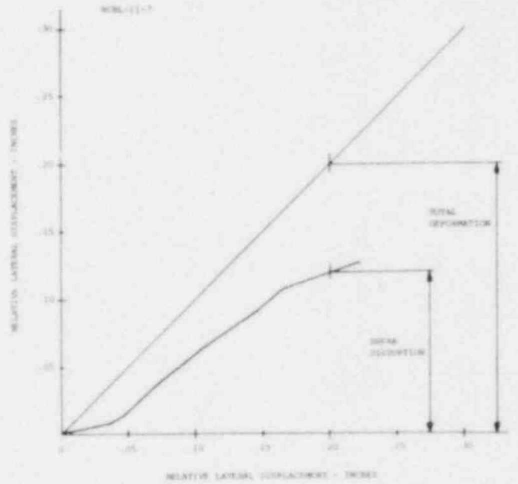

FIG. A.7 CONTINUE HCBL-11-7

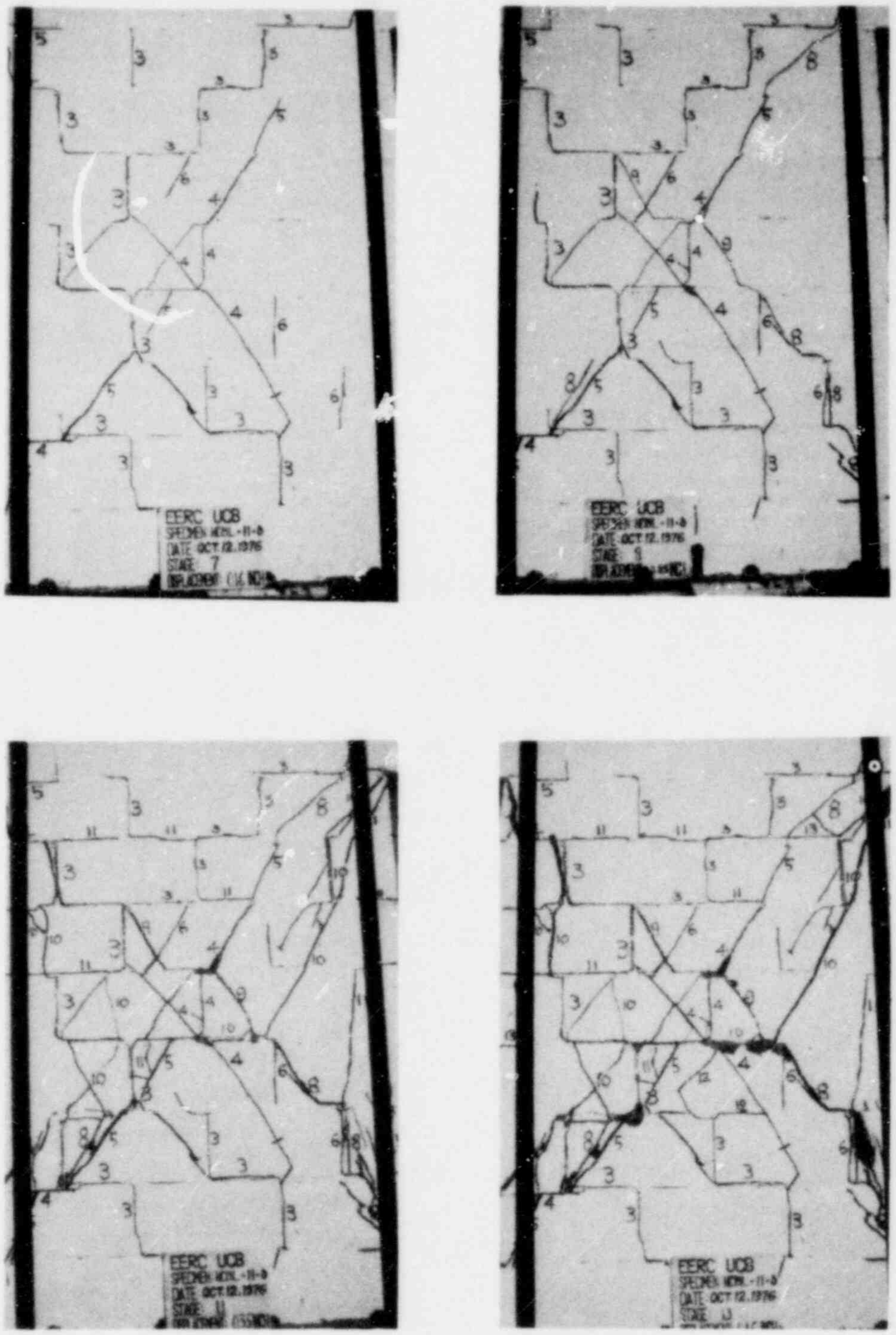

FIG. A.8 SUCCESSIVE CRACK FORMATION
AND EXPERIMENTAL RESULTS
TEST HCBL-11-8

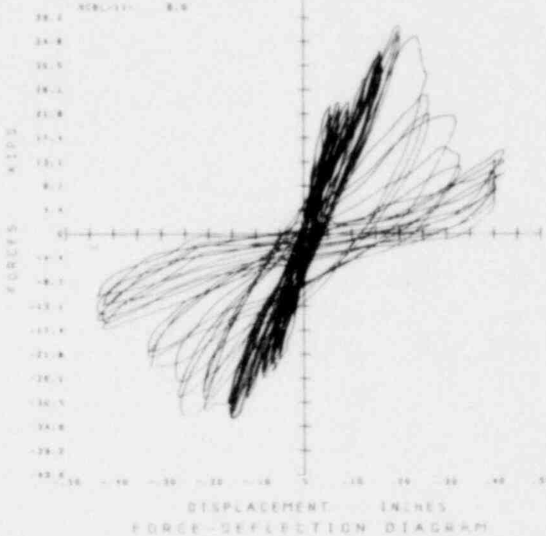

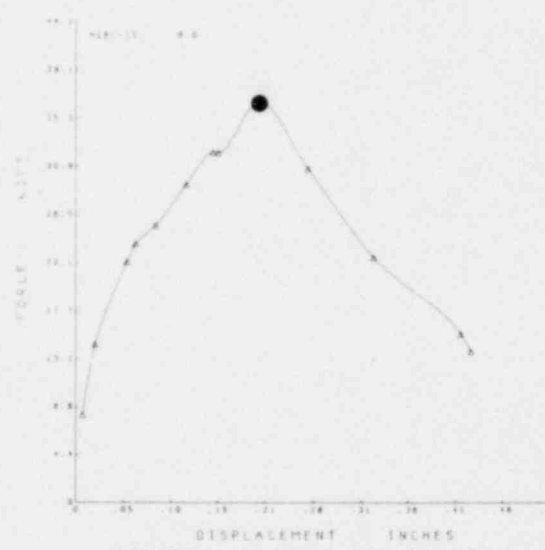

FIG. A.8 CONTINUE HCBL-11-8

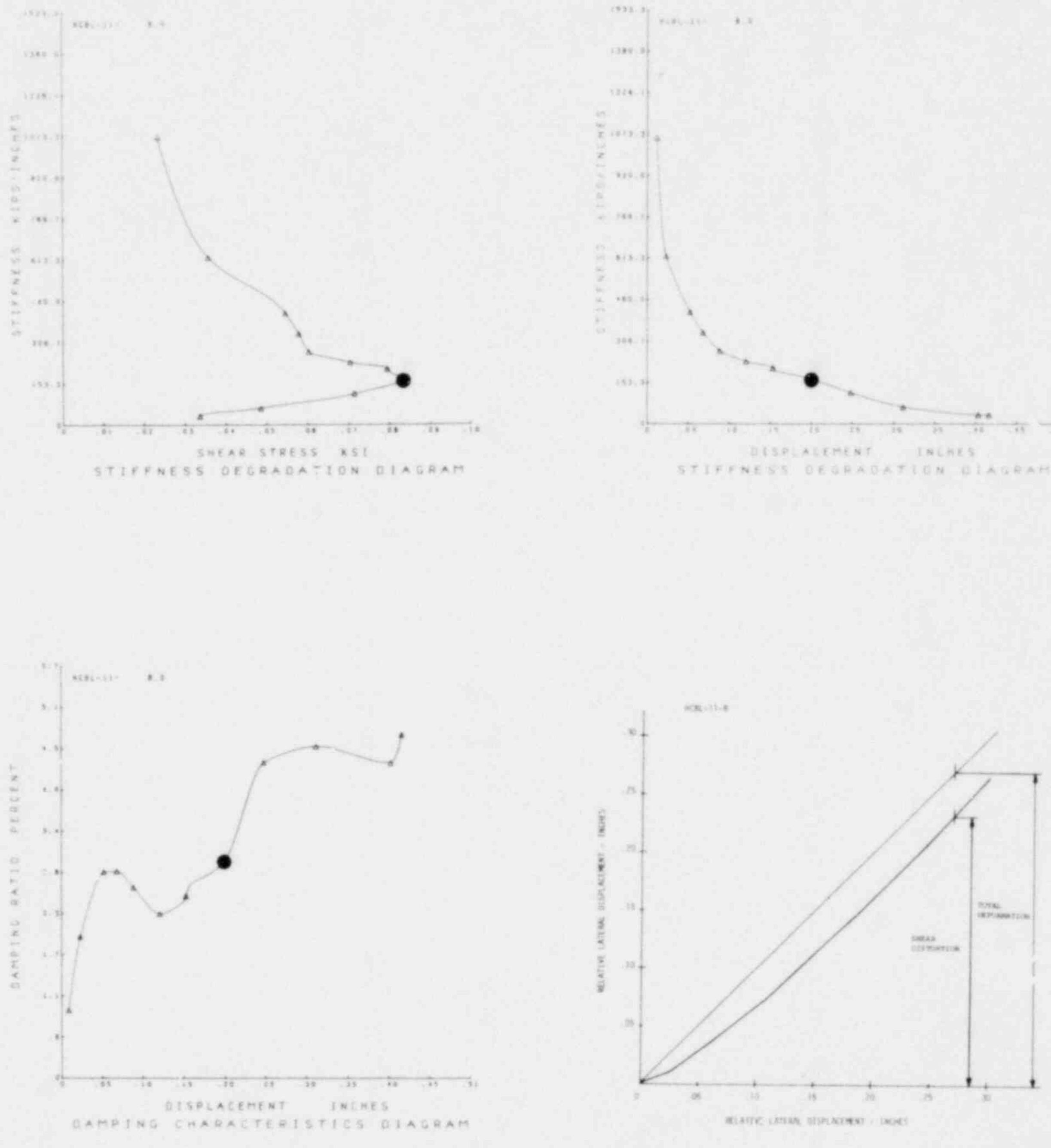

FIG. A.8 CONTINUE HCBL-11-8

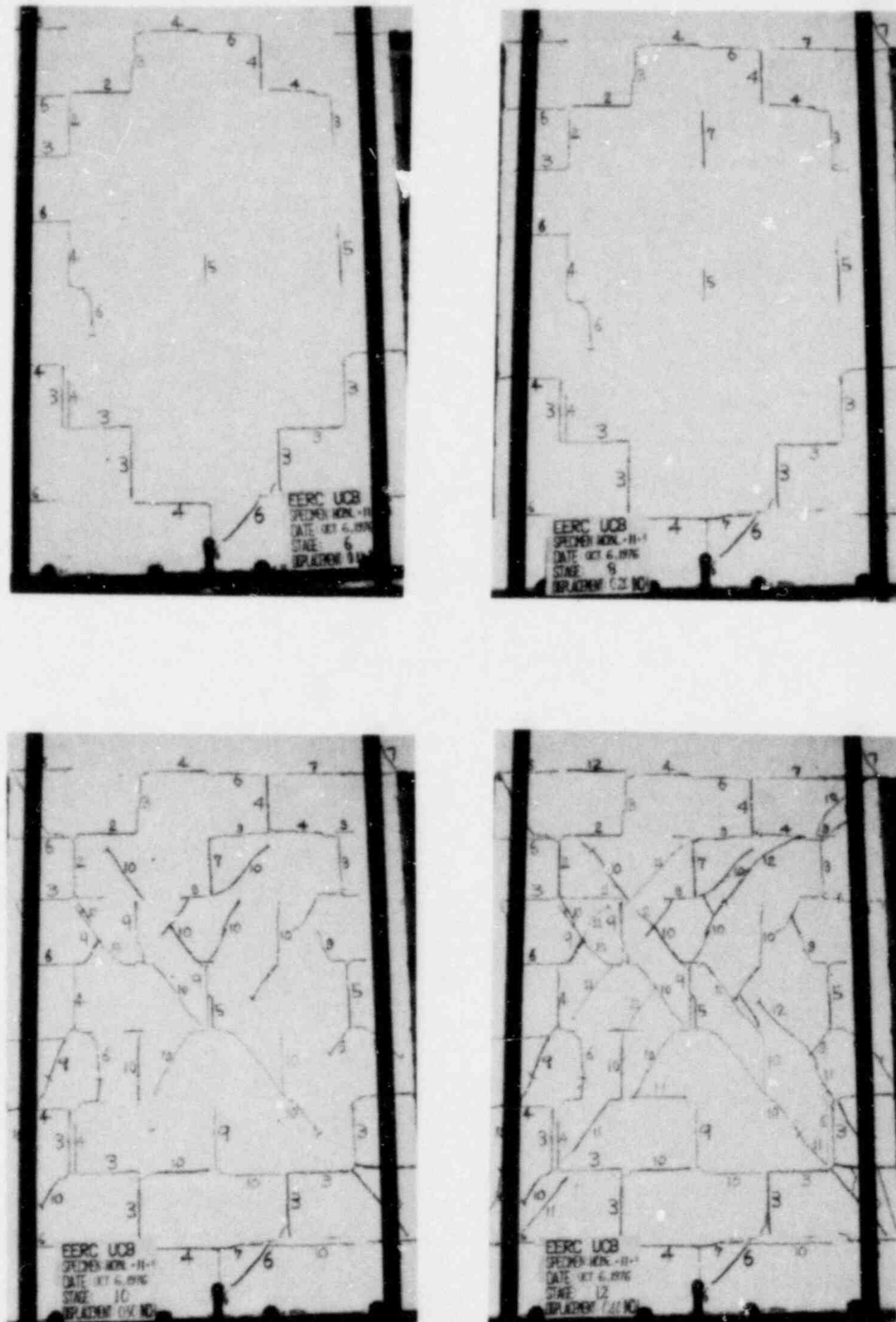

FIG. A.9 SUCCESSIVE CRACK FORMATION
AND EXPERIMENTAL RESULTS
TEST HCBL-11-9

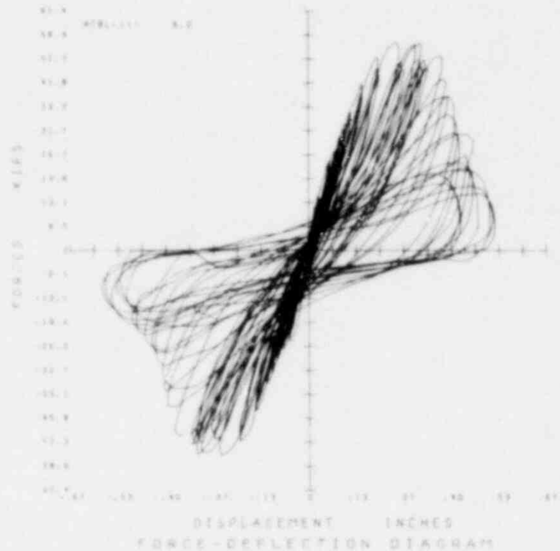

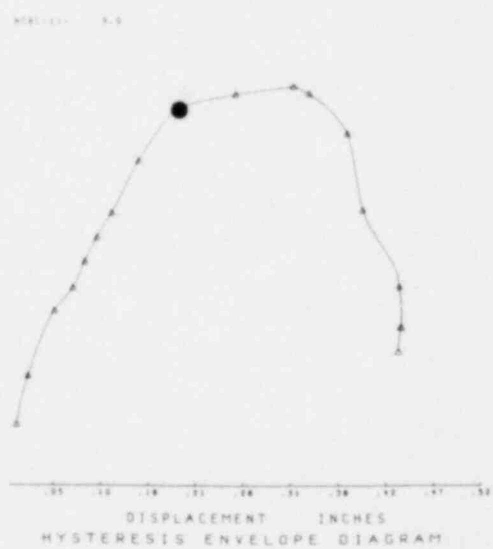

FIG. A.9 CONTINUE HCBL-11-9

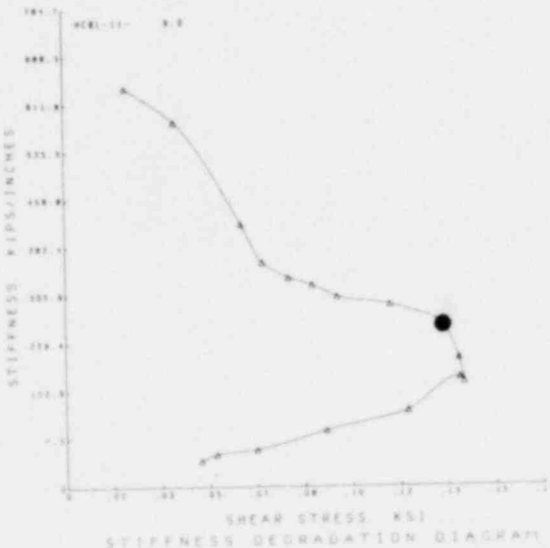

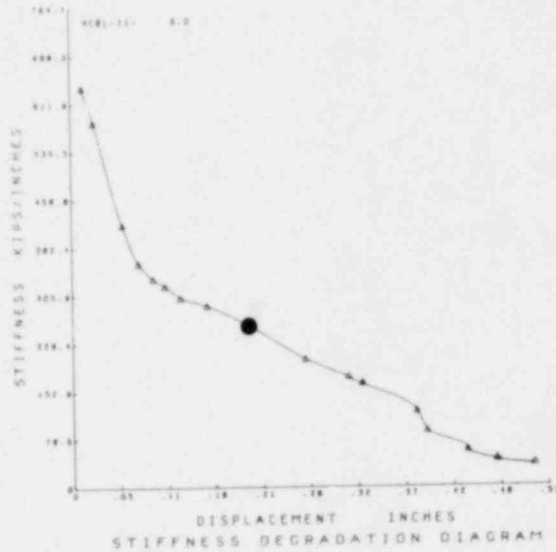

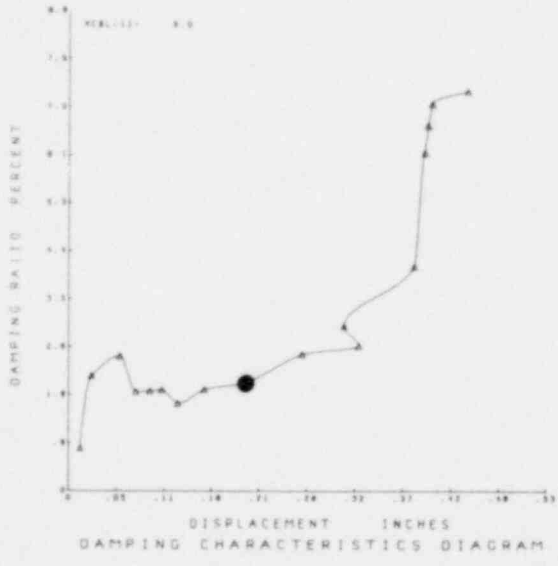

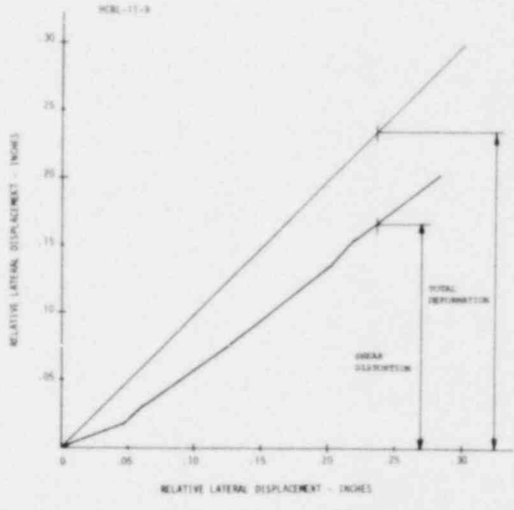

FIG. A.9 CONTINUE HCBL-11-9

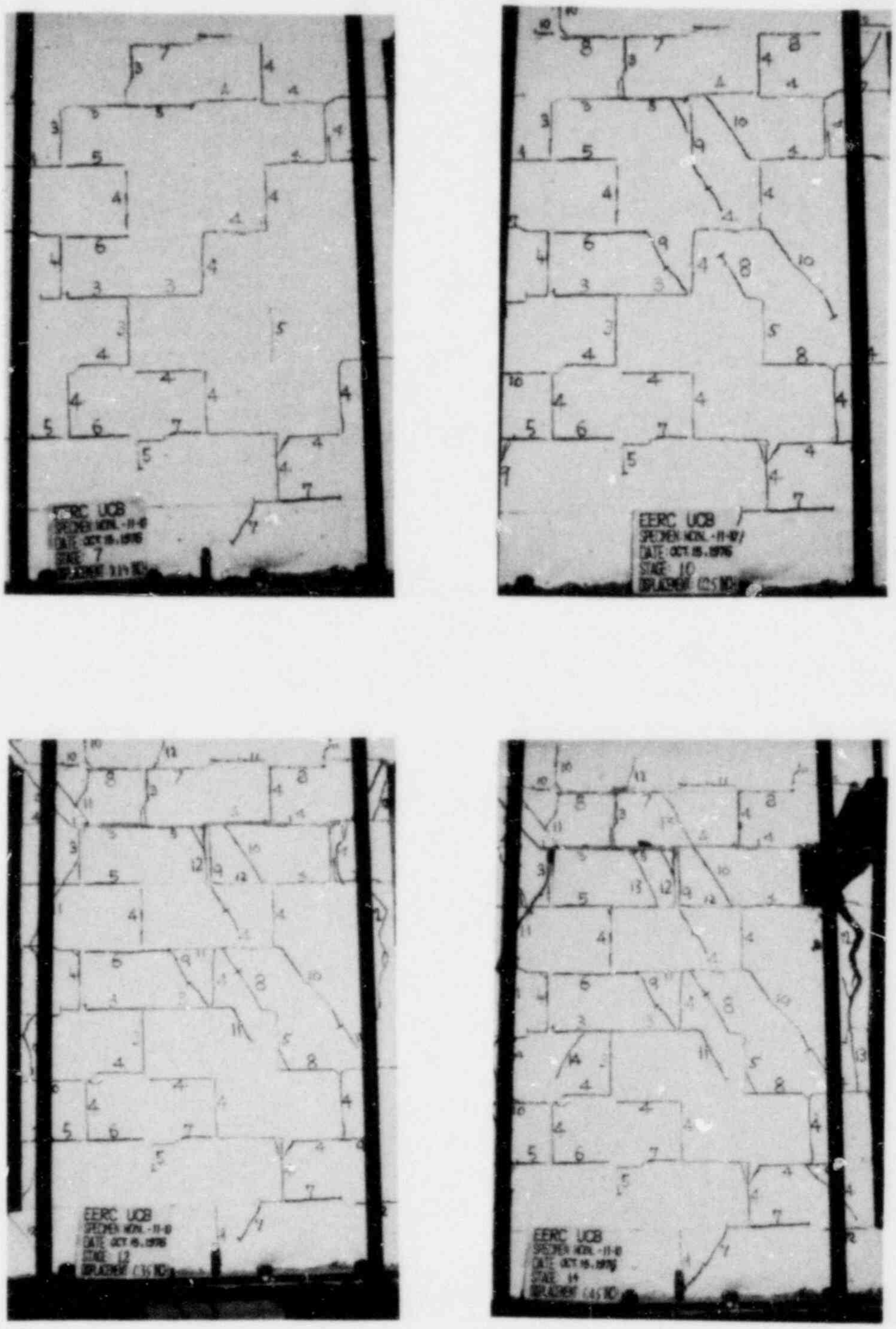

FIG. A.10 SUCCESSIVE CRACK FORMATION
AND EXPERIMENTAL RESULTS
TEST HCBL-11-10

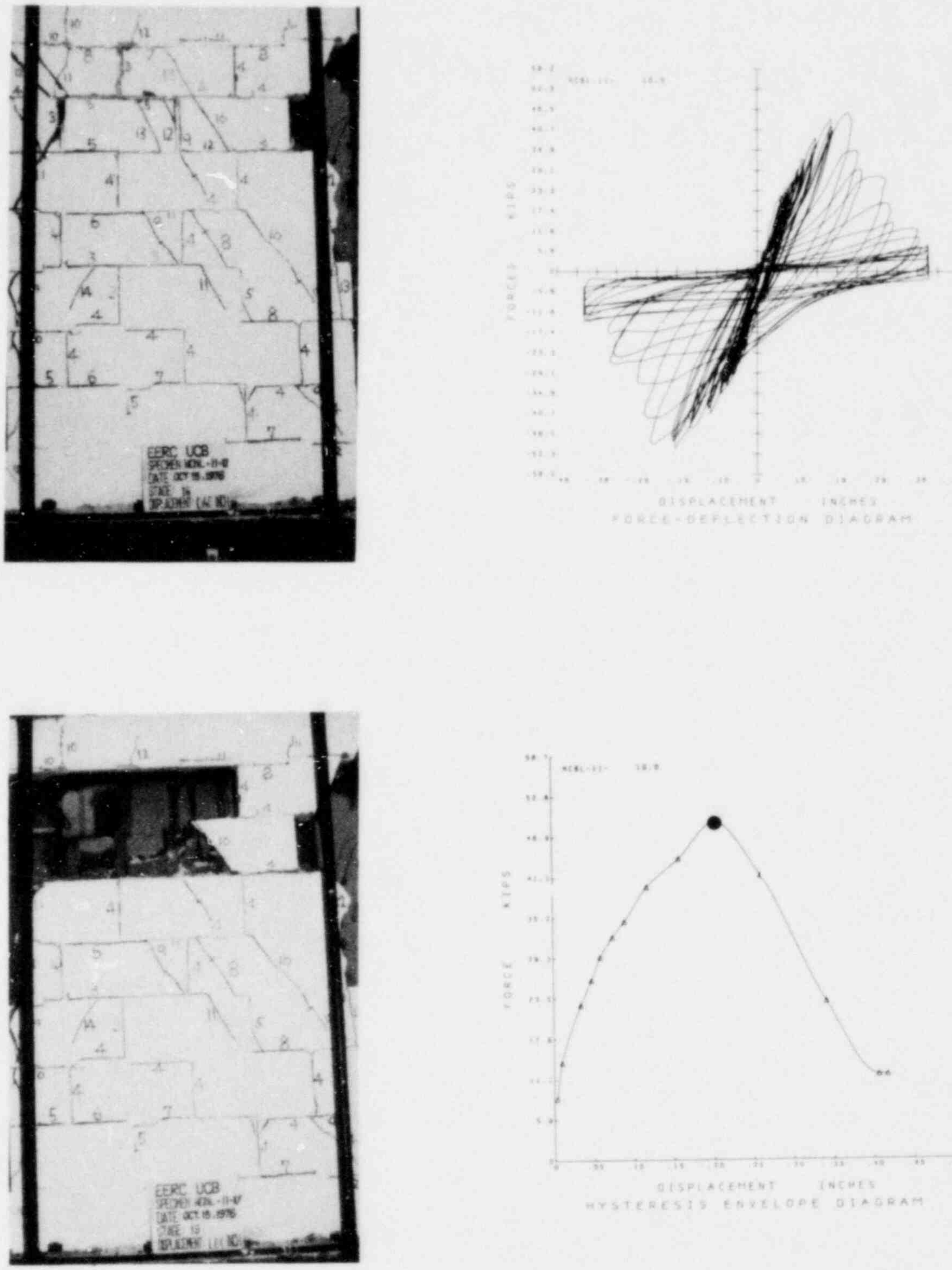

FIG. A.10 CONTINUE HCBL-11-10

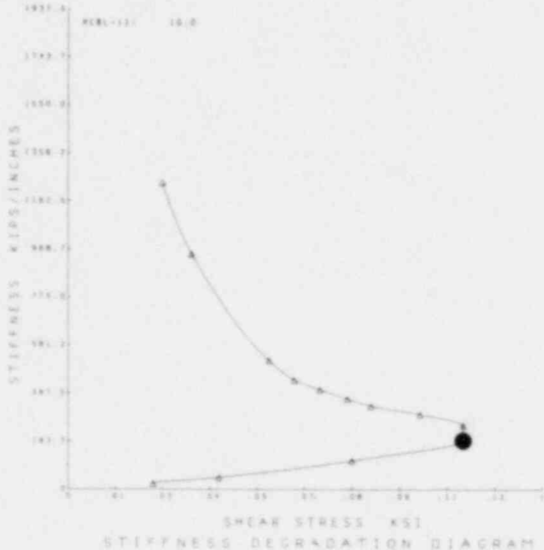

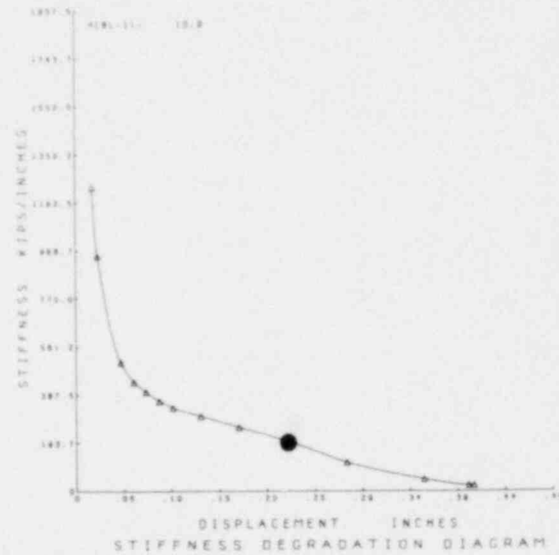

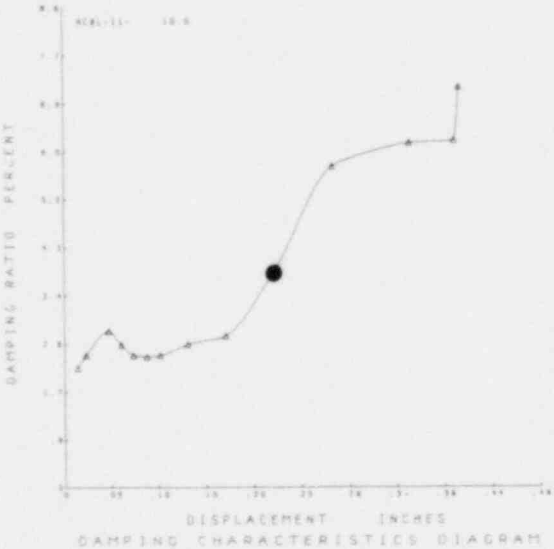

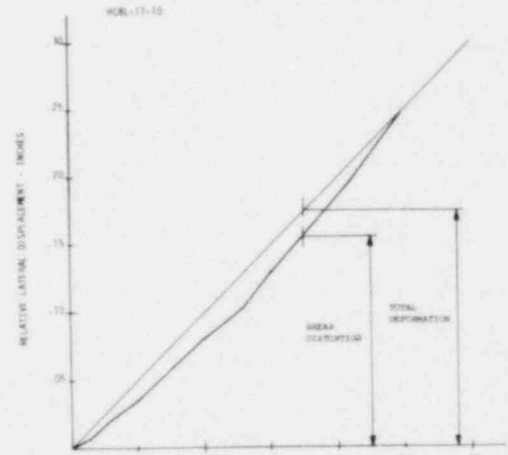

FIG. A.10 CONTINUE HCBL-11-10

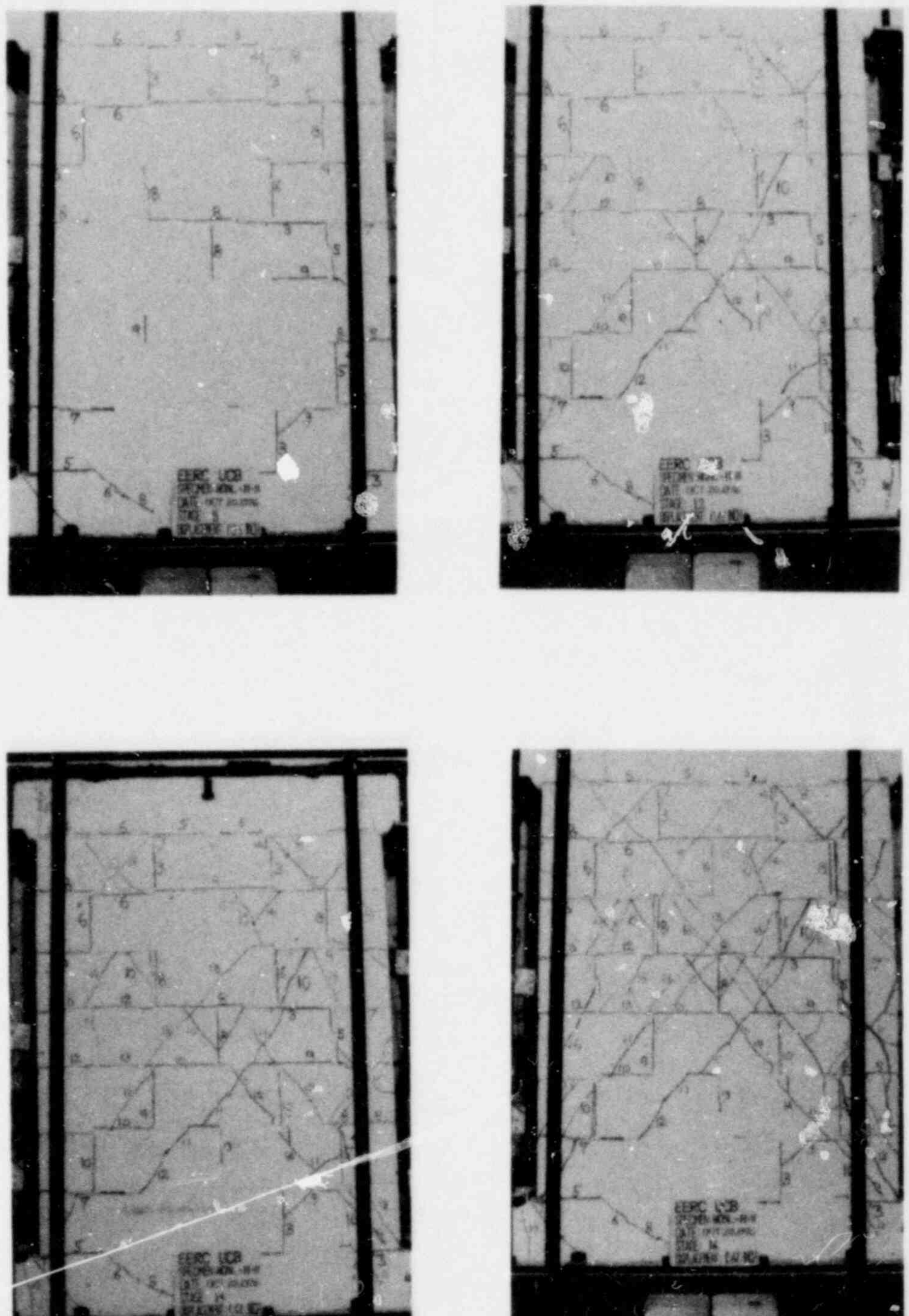

FIG. A.11 SUCCESSIVE CRACK FORMATION
AND EXPERIMENTAL RESULTS
TEST HCBL-11-11

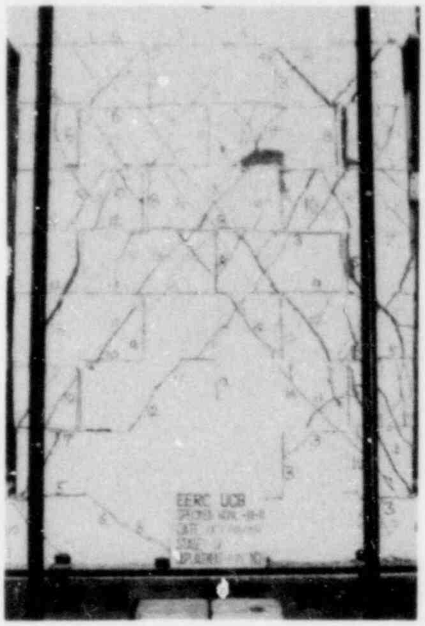

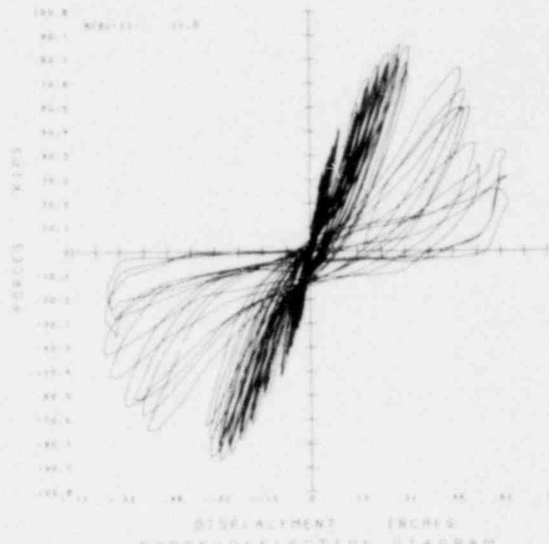

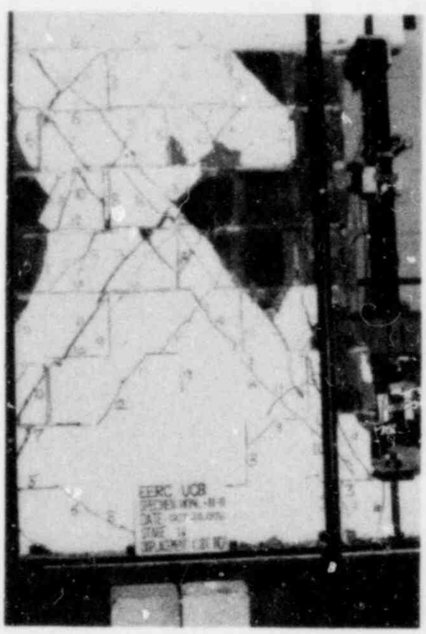

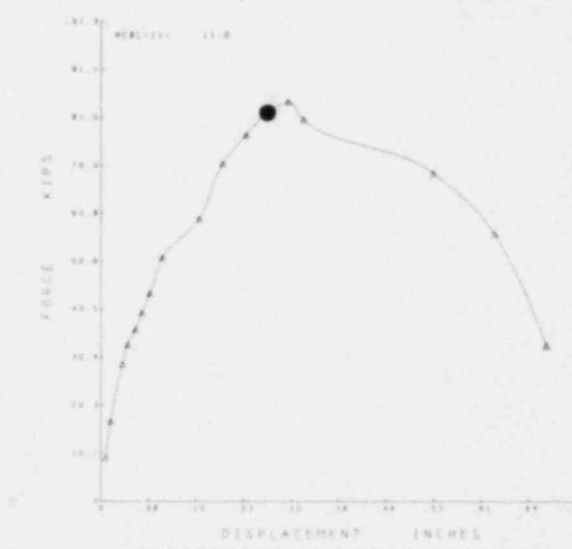

FIG. A.11 CONTINUE HCBL-11-11

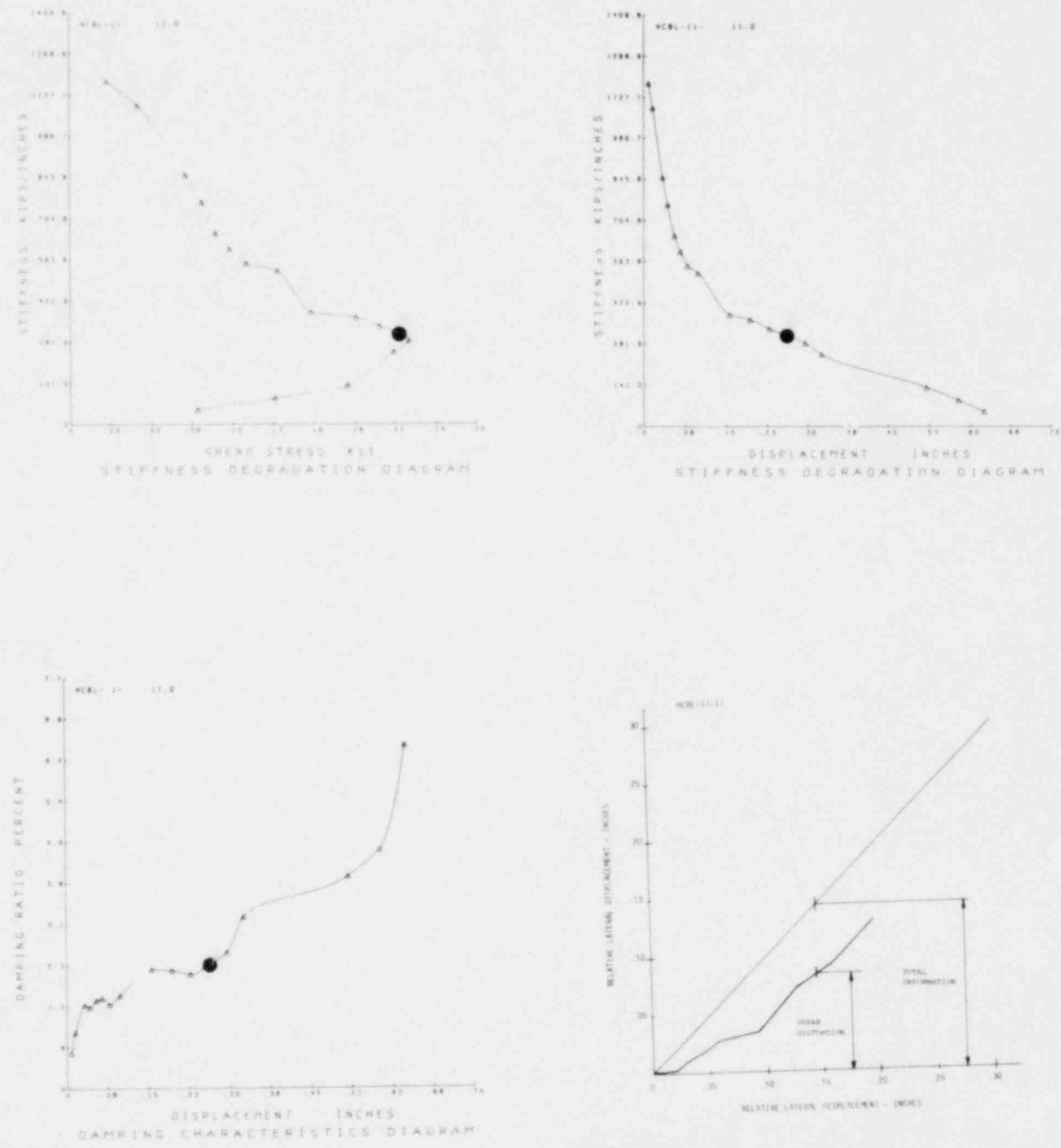

FIG. A.11 CONTINUE HCBL-11-11

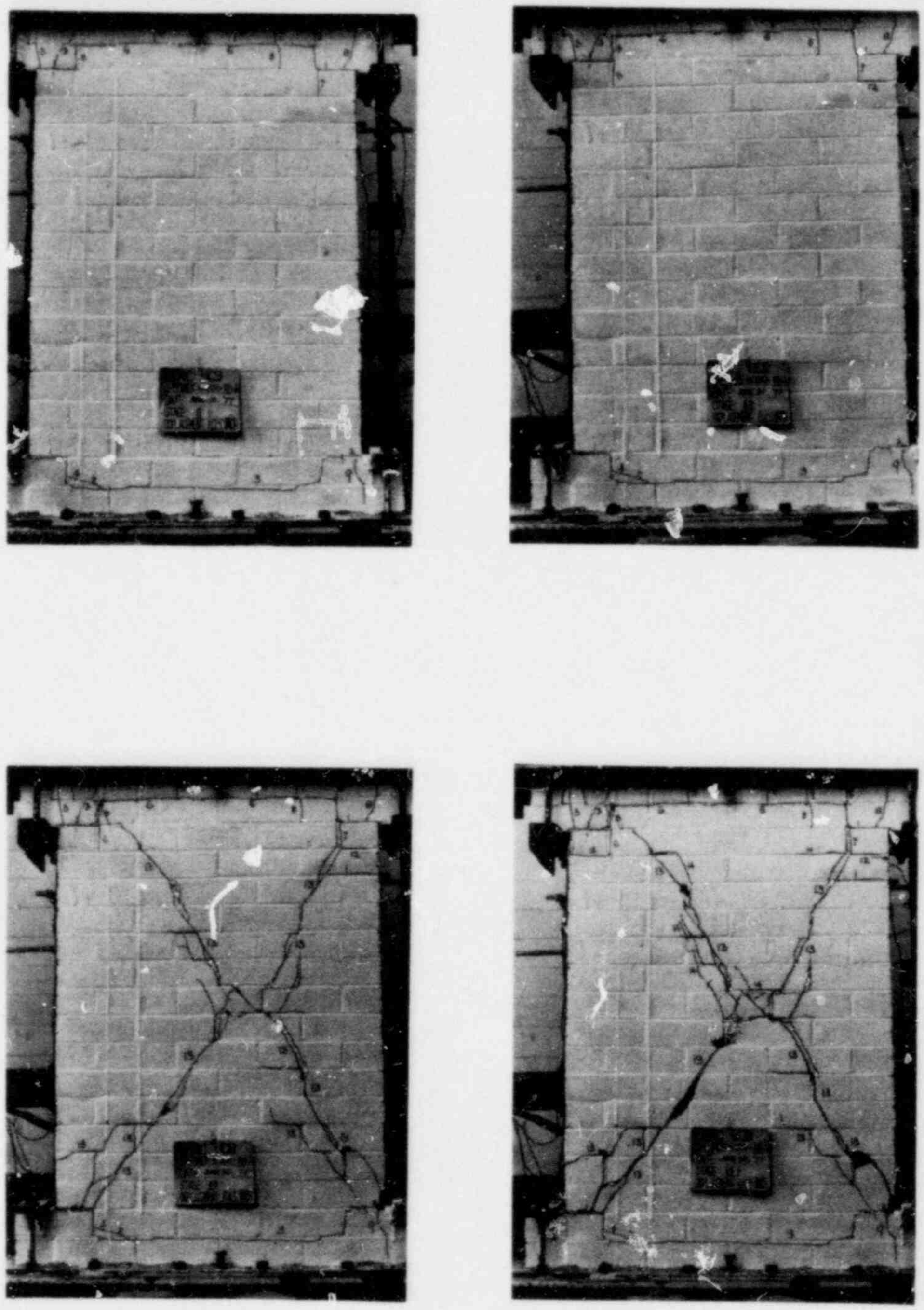

FIG. A.12 SUCCESSIVE CRACK FORMATION
AND EXPERIMENTAL RESULTS
TEST HCBR-11-1

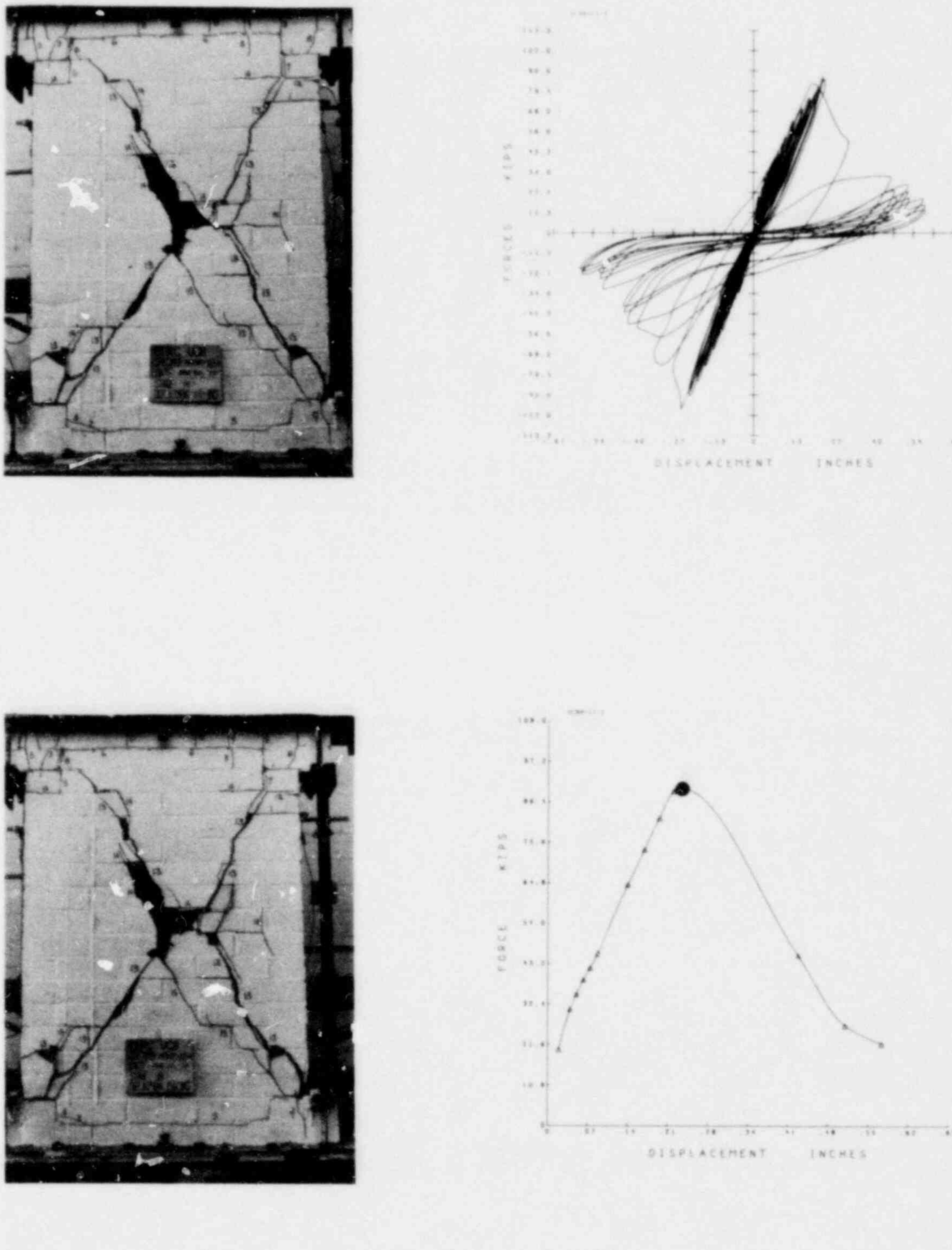

FIG. A.12 CONTINUE HCBR-11-1

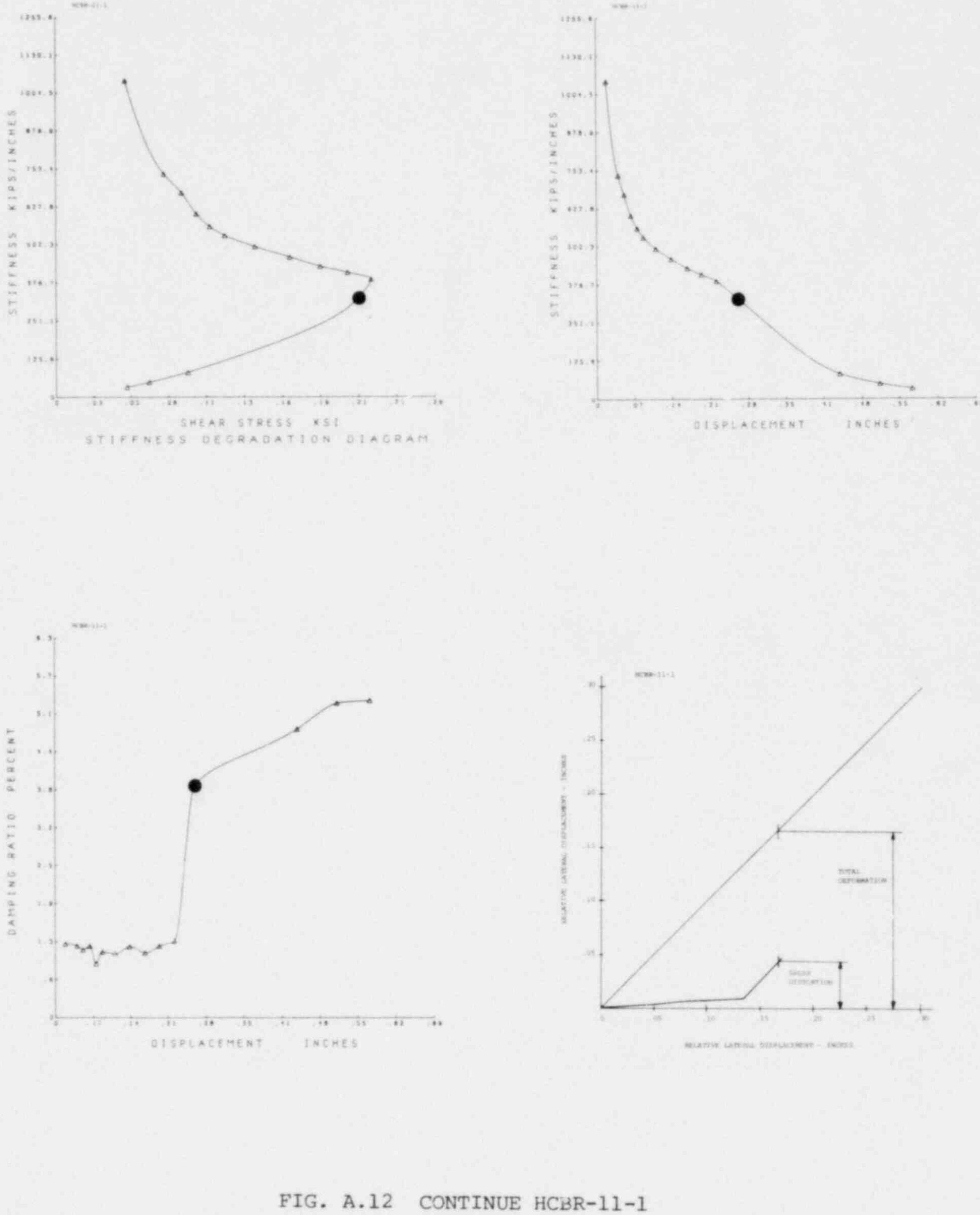

FIG. A.12 CONTINUE HCBR-11-1

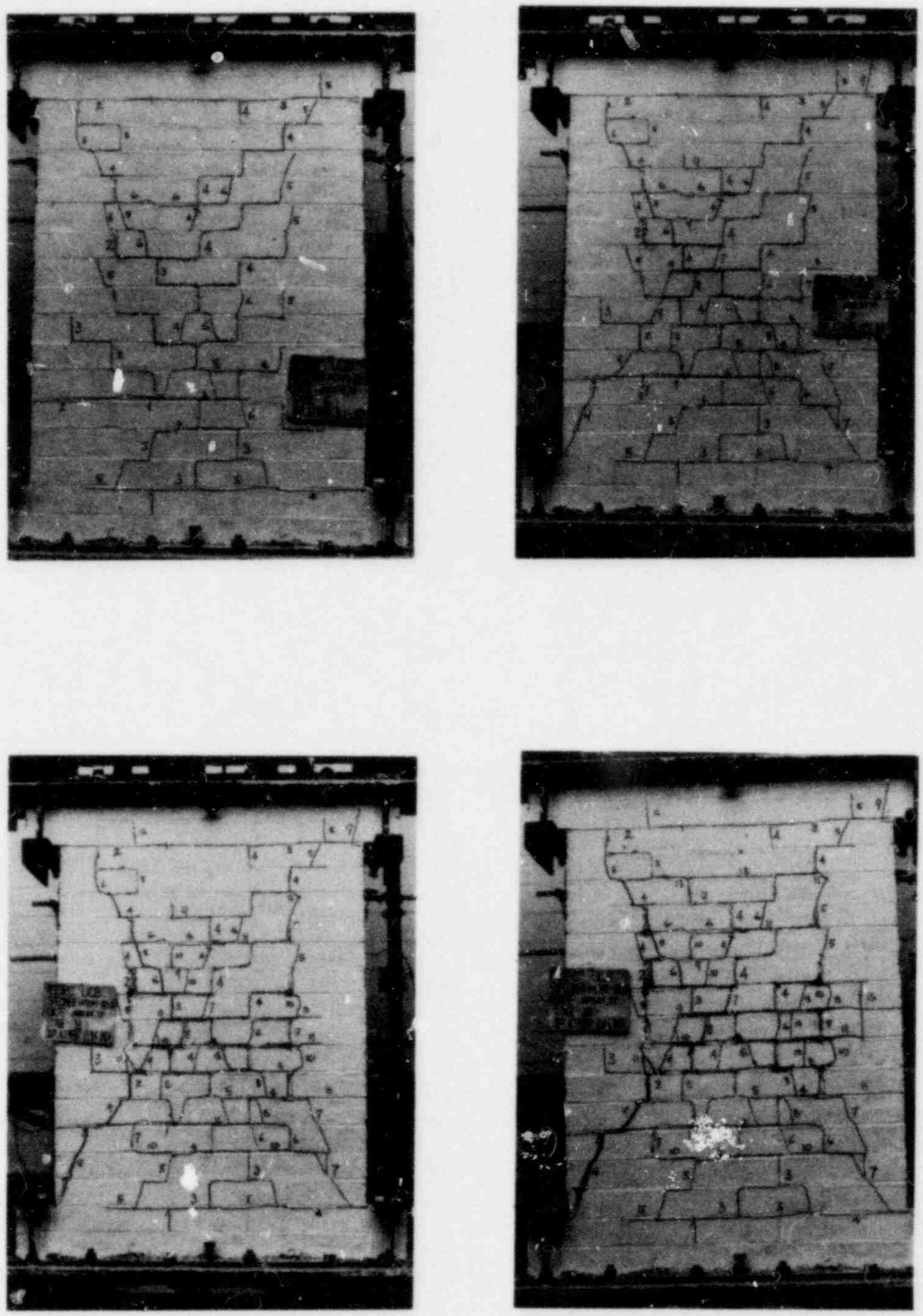

FIG. A.13 SUCCESSIVE CRACK FORMATION
AND EXPERIMENTAL RESULTS
TEST HCBR-11-2

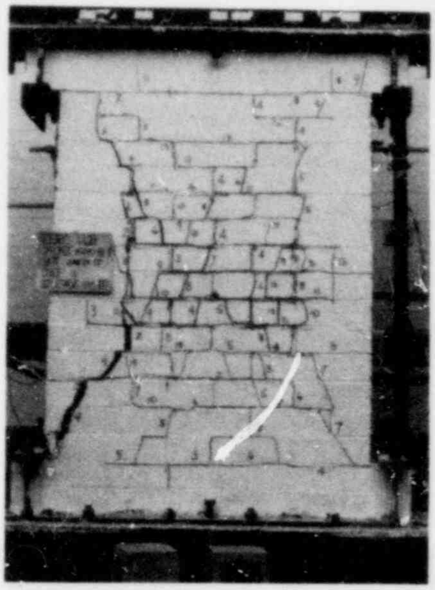

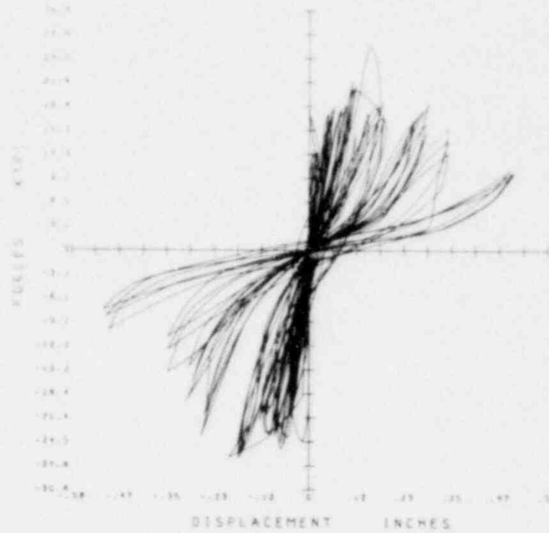

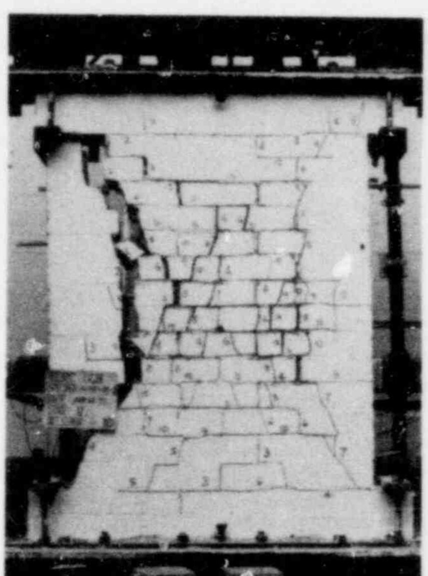

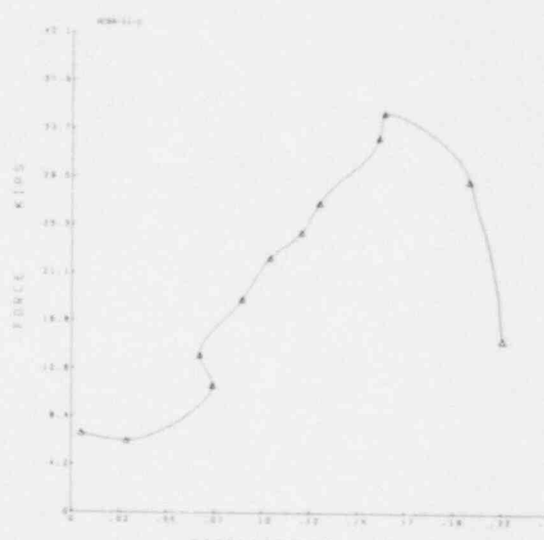

FIG. A.13 CONTINUE HCBR-11-2

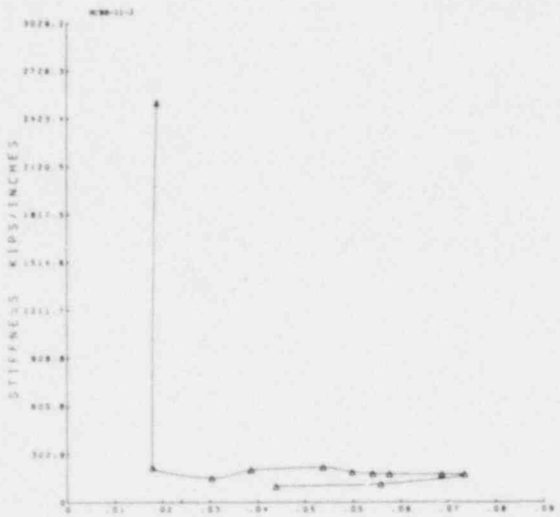

STIFFNESS DEGRADATION DIAGRAM

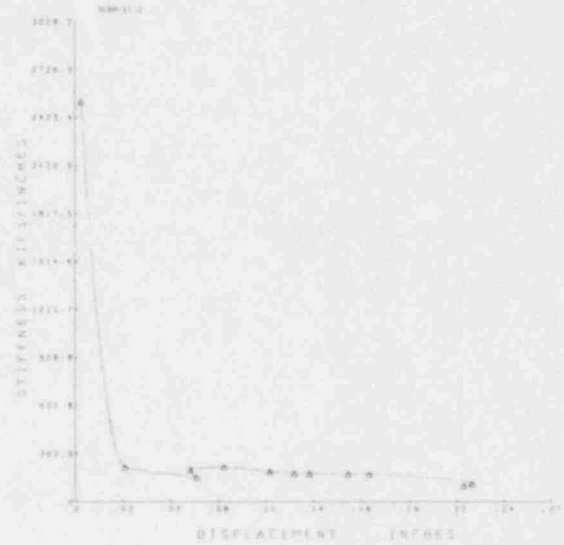

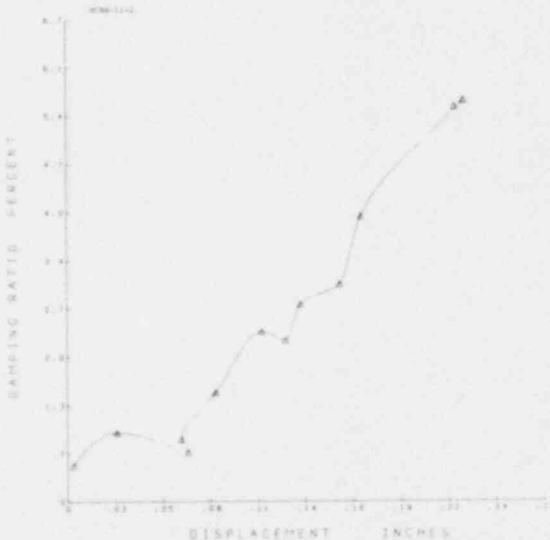

FIG. A.13 CONTINUE HCBR-11-2

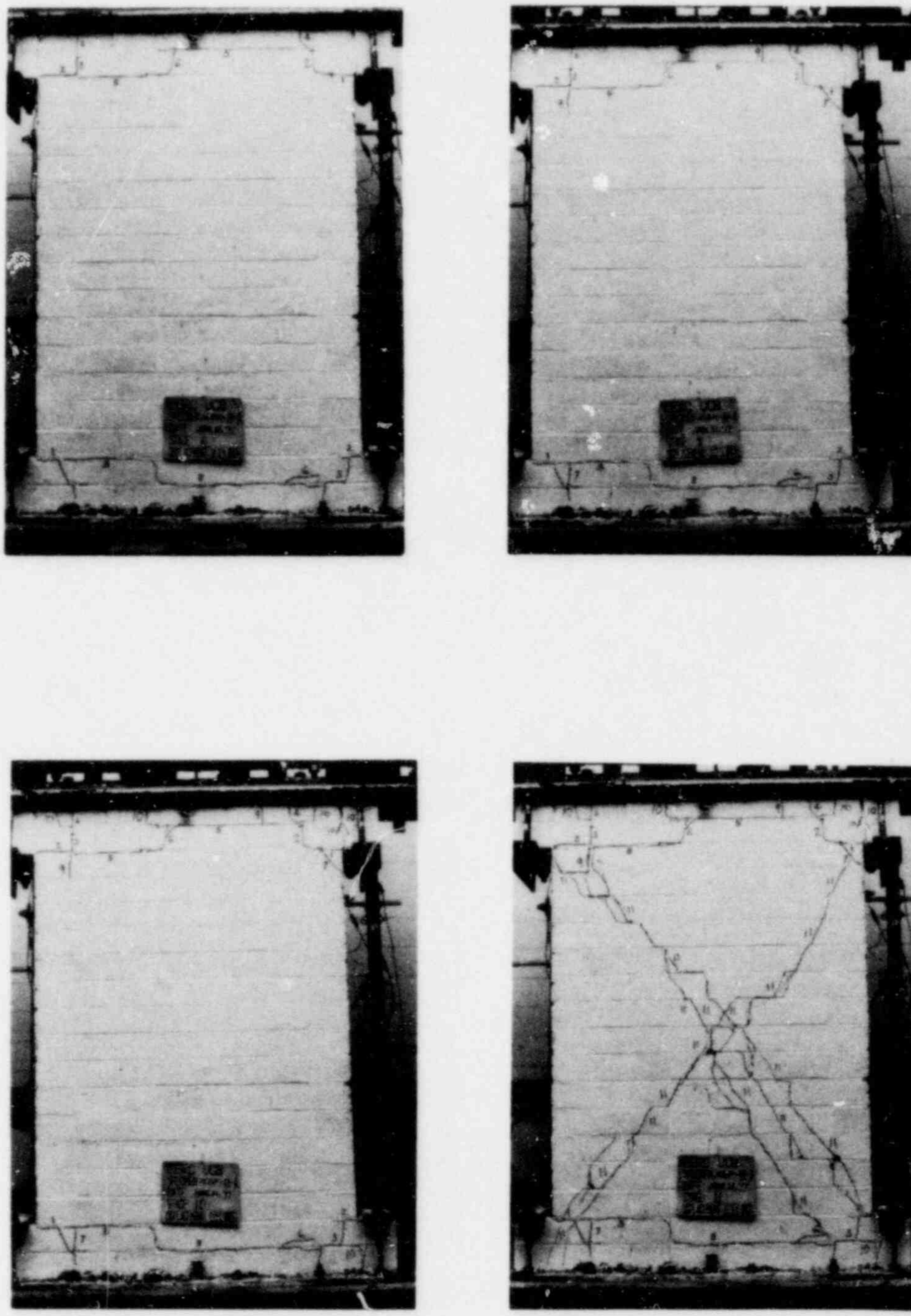

FIG. A.14 SUCCESSIVE CRACK FORMATION
AND EXPERIMENTAL RESULTS
TEST HCBR-11-3

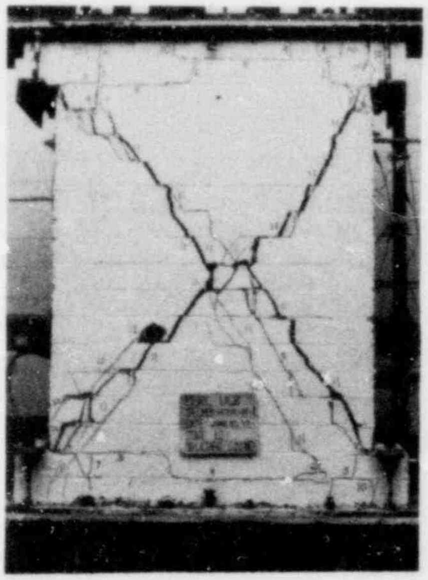

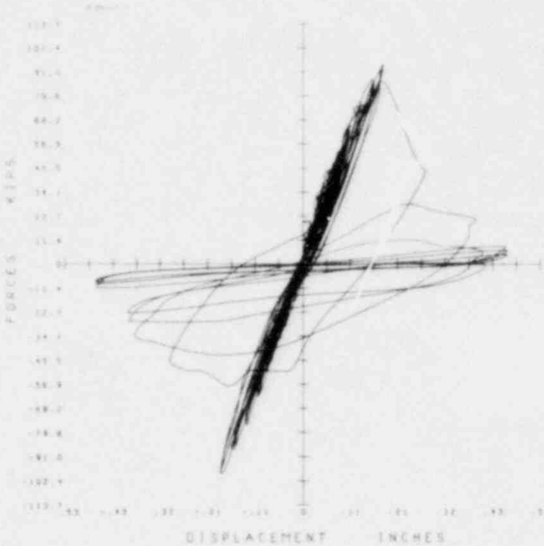

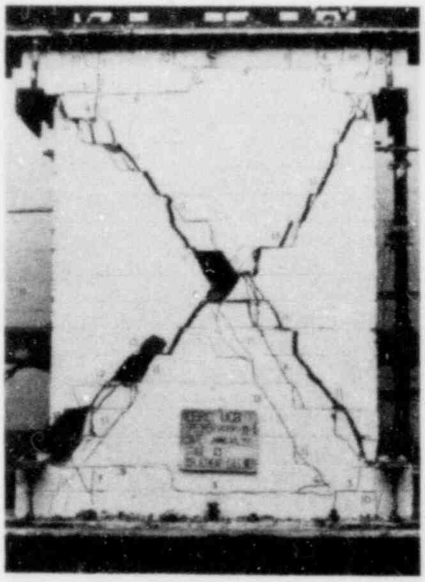

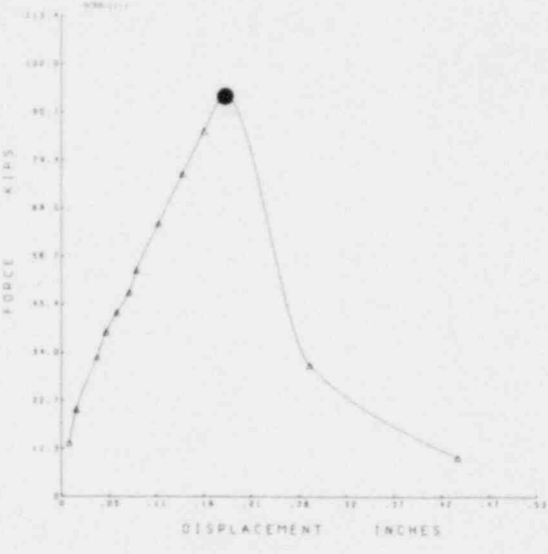

FIG. A.14 CONTINUE HCBR-11-3

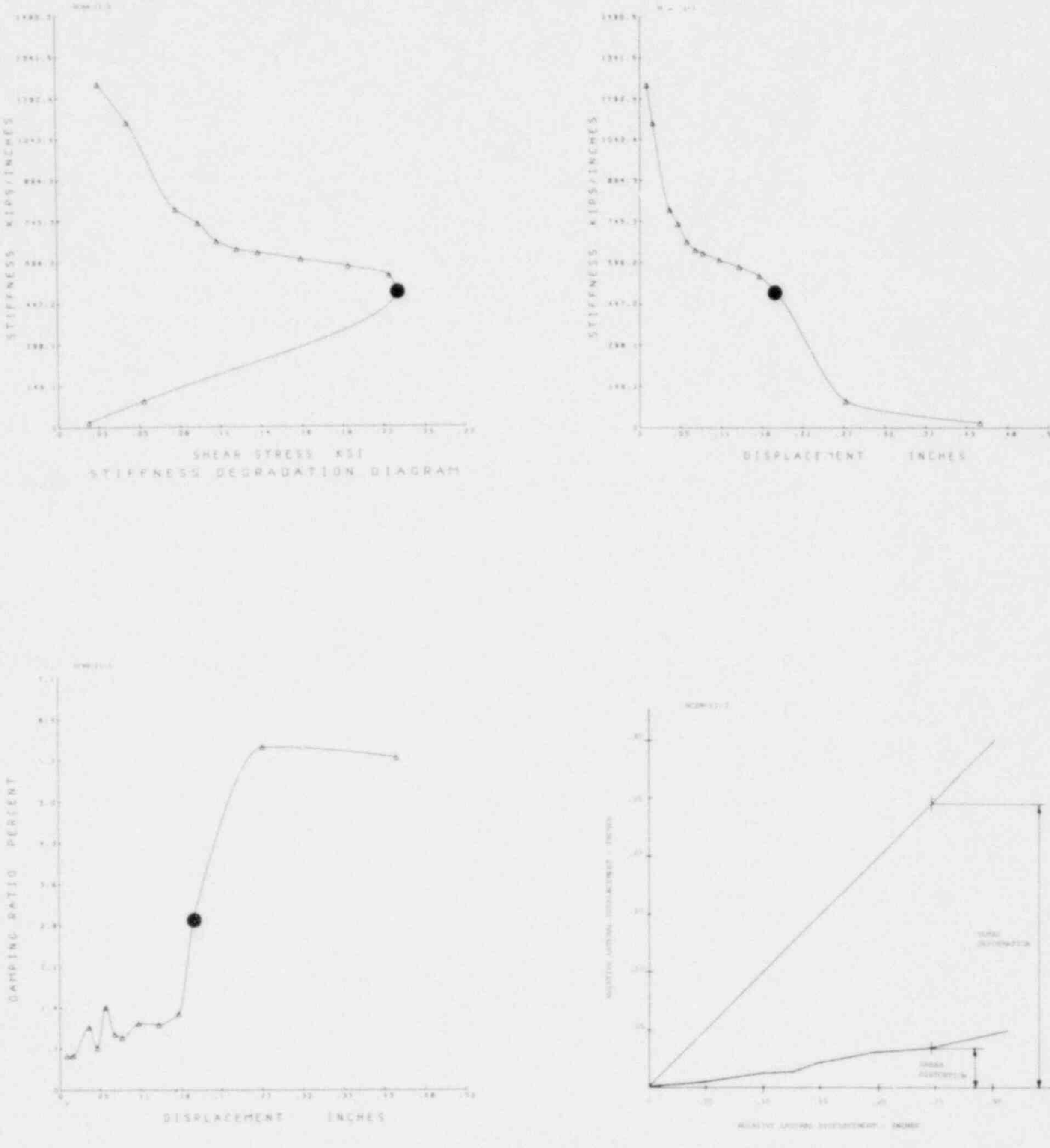

FIG. A.14 CONTINUE HCBR-11-3

FIG. A.15 SUCCESSIVE CRACK FORMATION
AND EXPERIMENTAL RESULTS
TEST HCBR-11-4

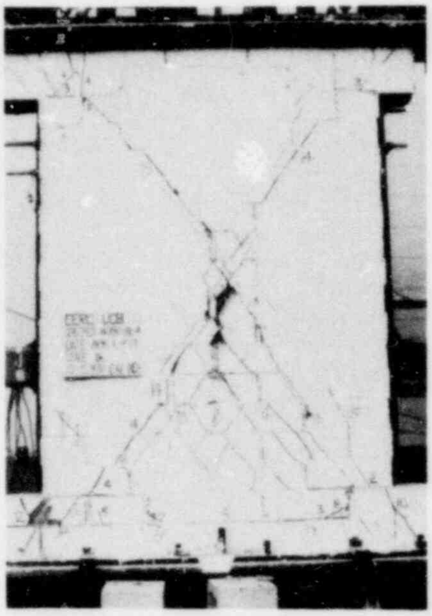

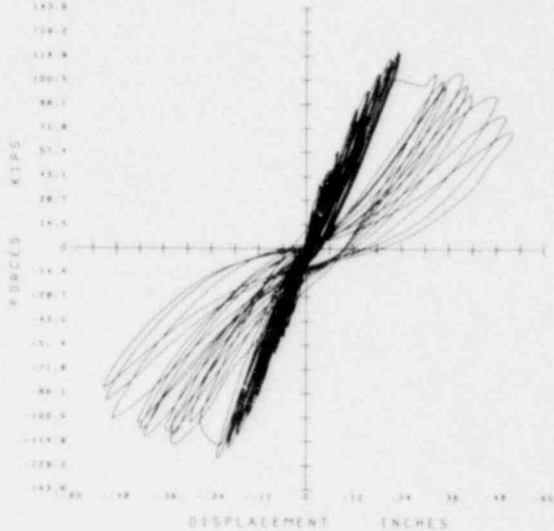

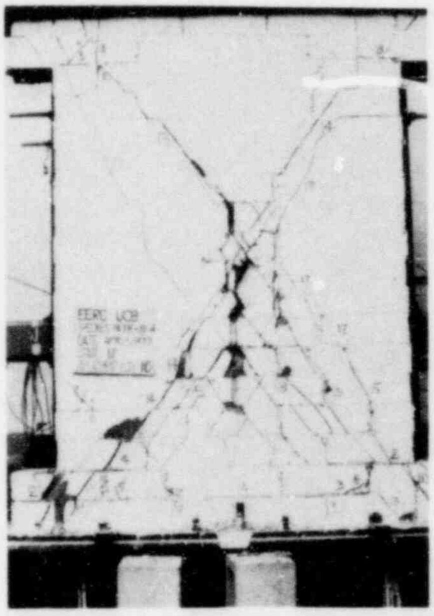

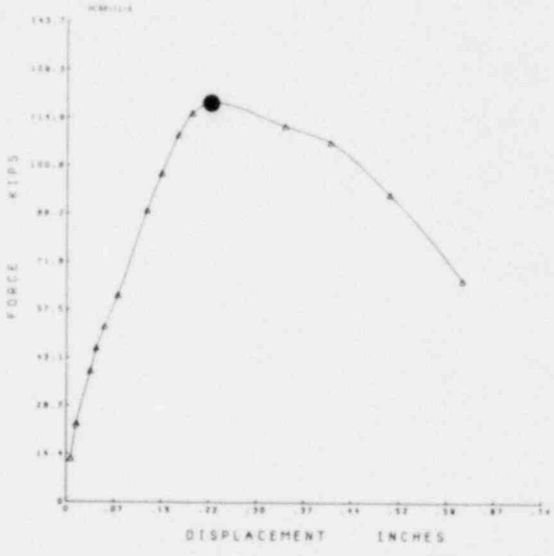

FIG. A.15 CONTINUE HCBR-11-4

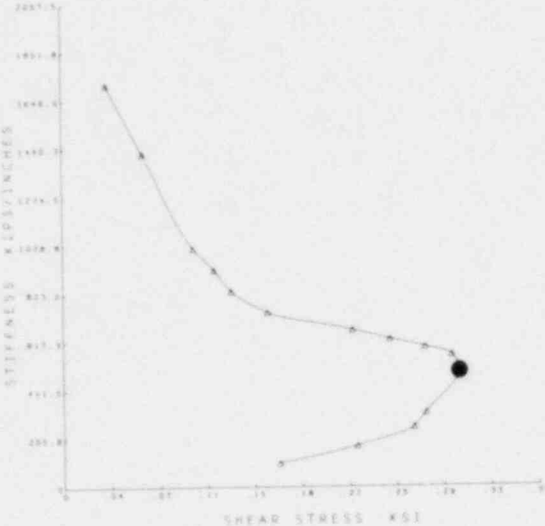

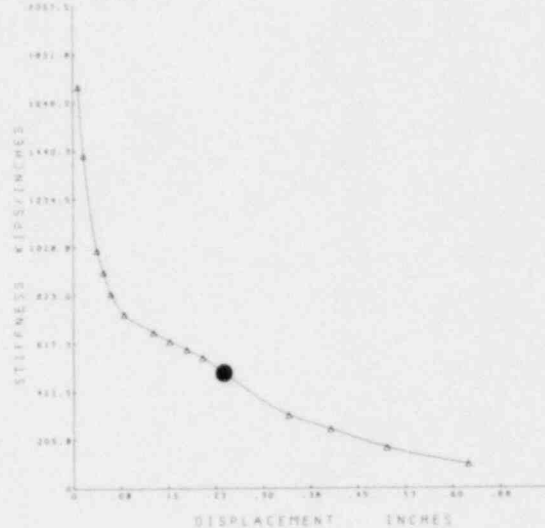

STIFFNESS DEGRADATION DIAGRAM

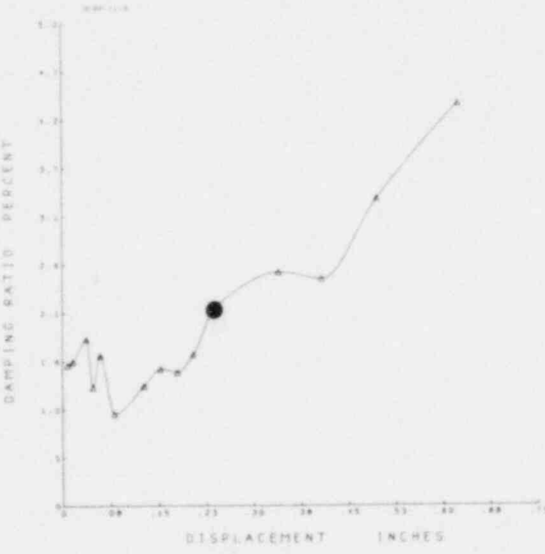

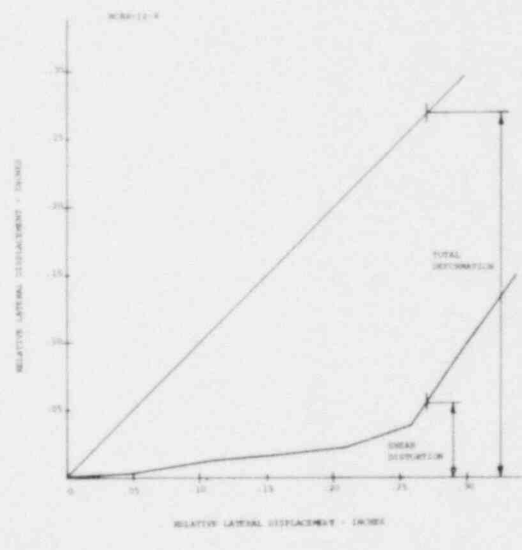

FIG. A.15 CONTINUE HCBR-11-4

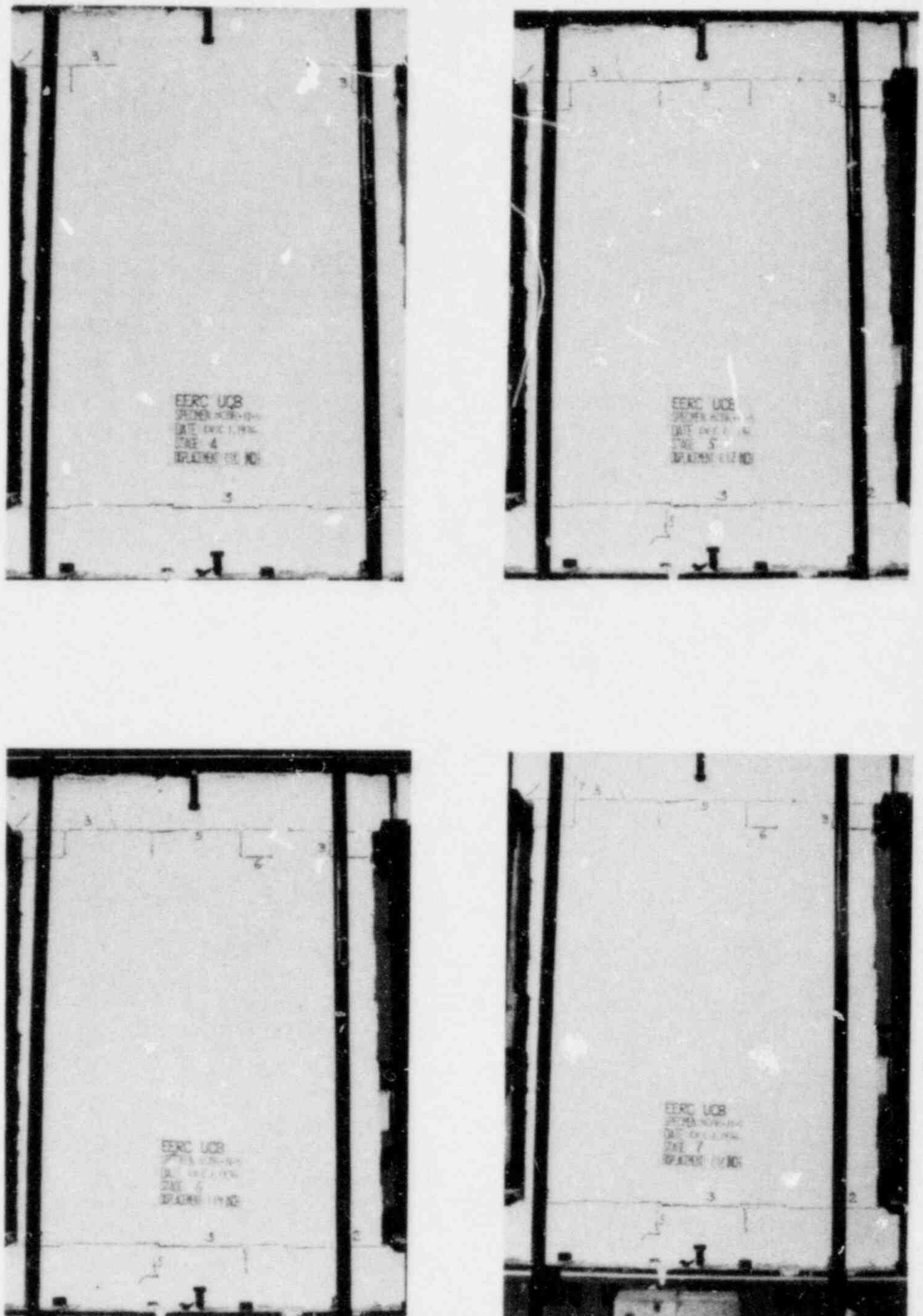

FIG. A.16 SUCCESSIVE CRACK FORMATION
AND EXPERIMENTAL RESULTS
TEST HCBR-11-5

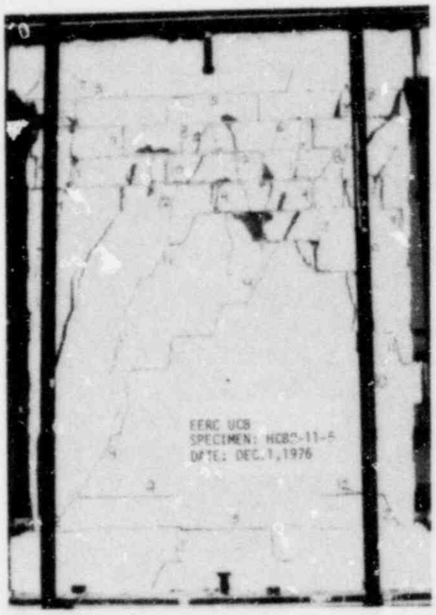

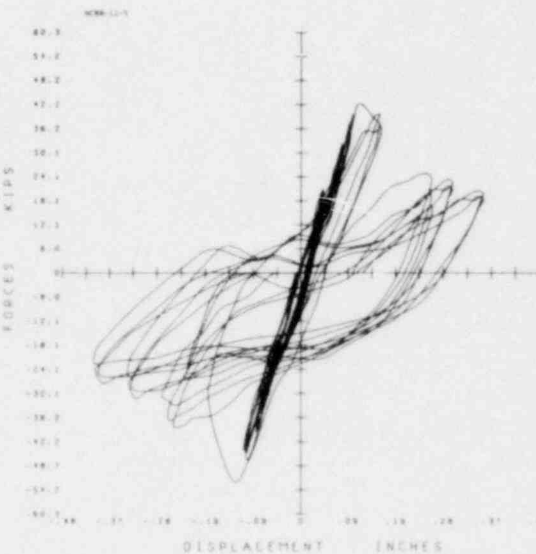

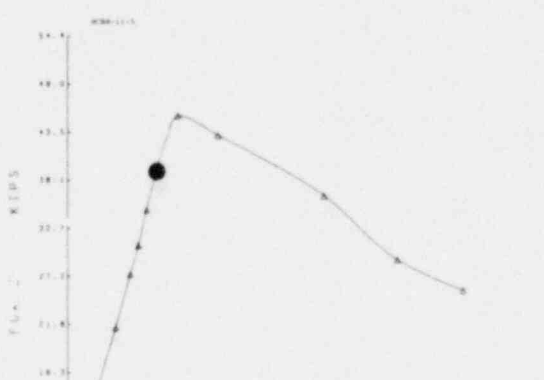

FIG. A.16 CONTINUE HCBR-11-5

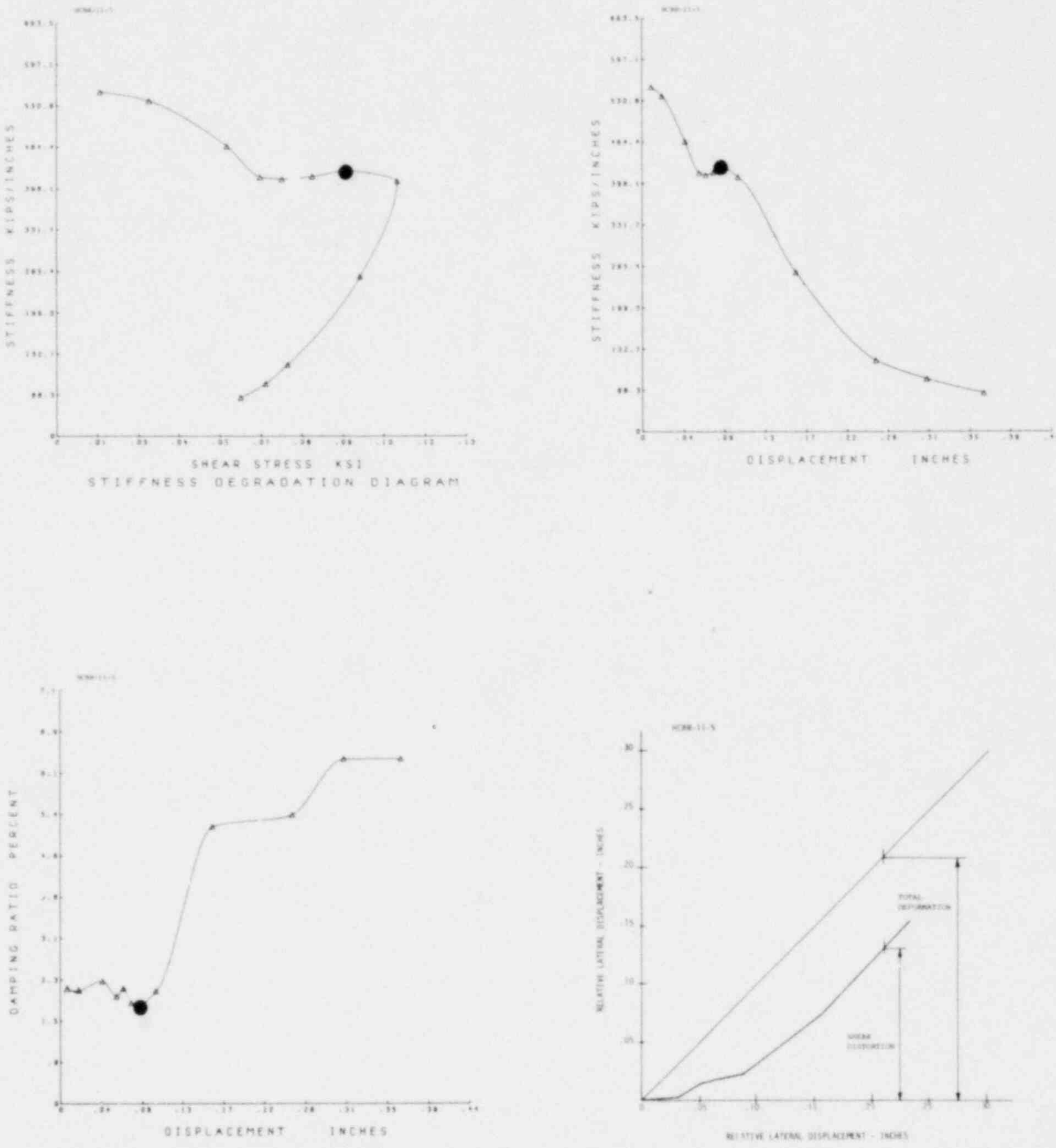

FIG. A.16 CONTINUE HCBR-11-5

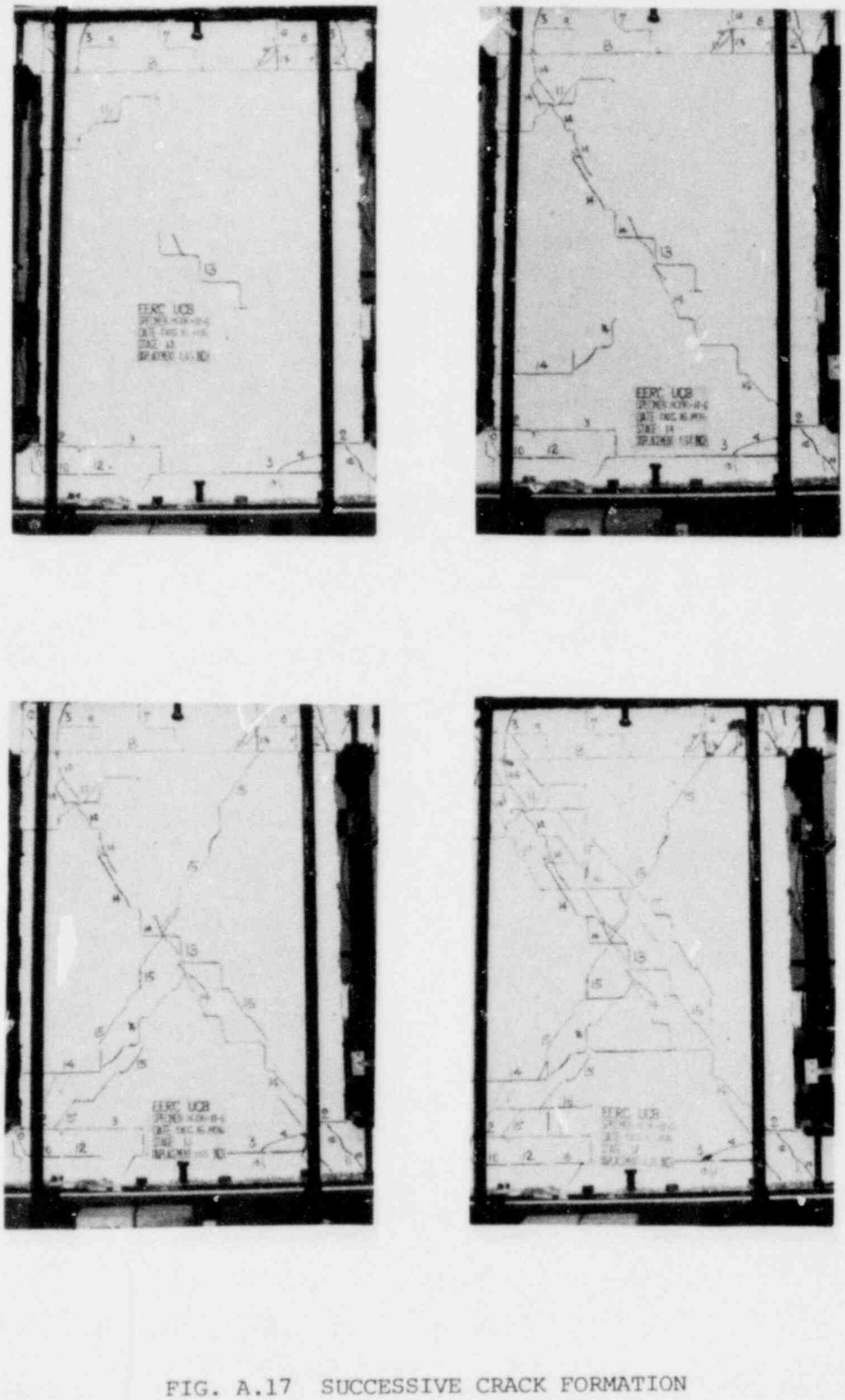

FIG. A.17 SUCCESSIVE CRACK FORMATION
AND EXPERIMENTAL RESULTS
TEST HCBR-11-6

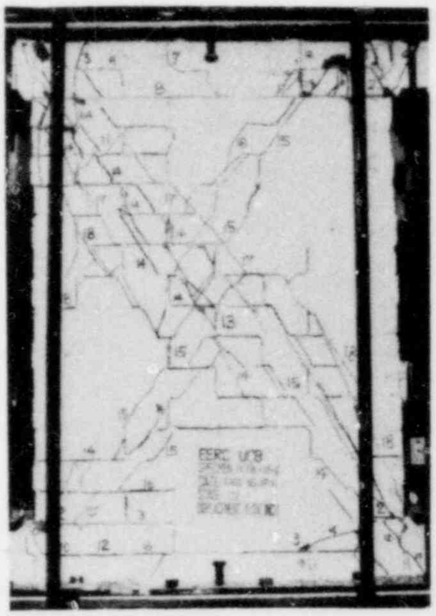

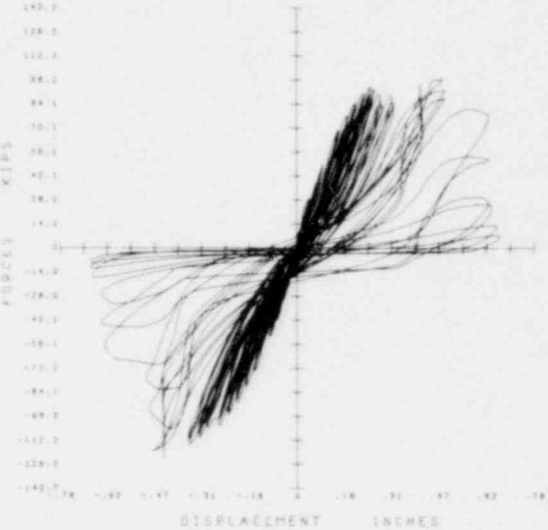

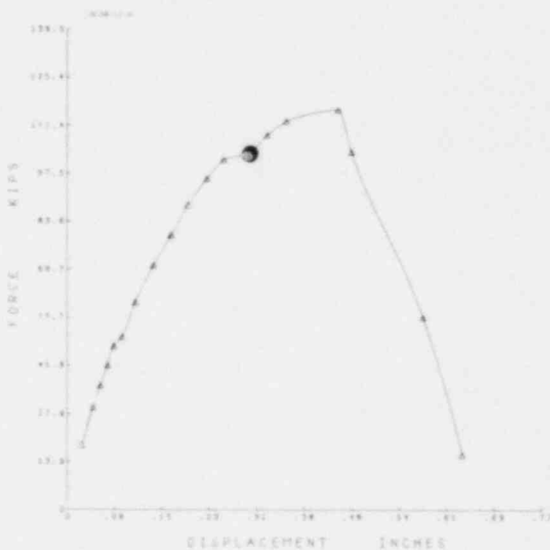

FIG. A.17 CONTINUE HCBR-11-6

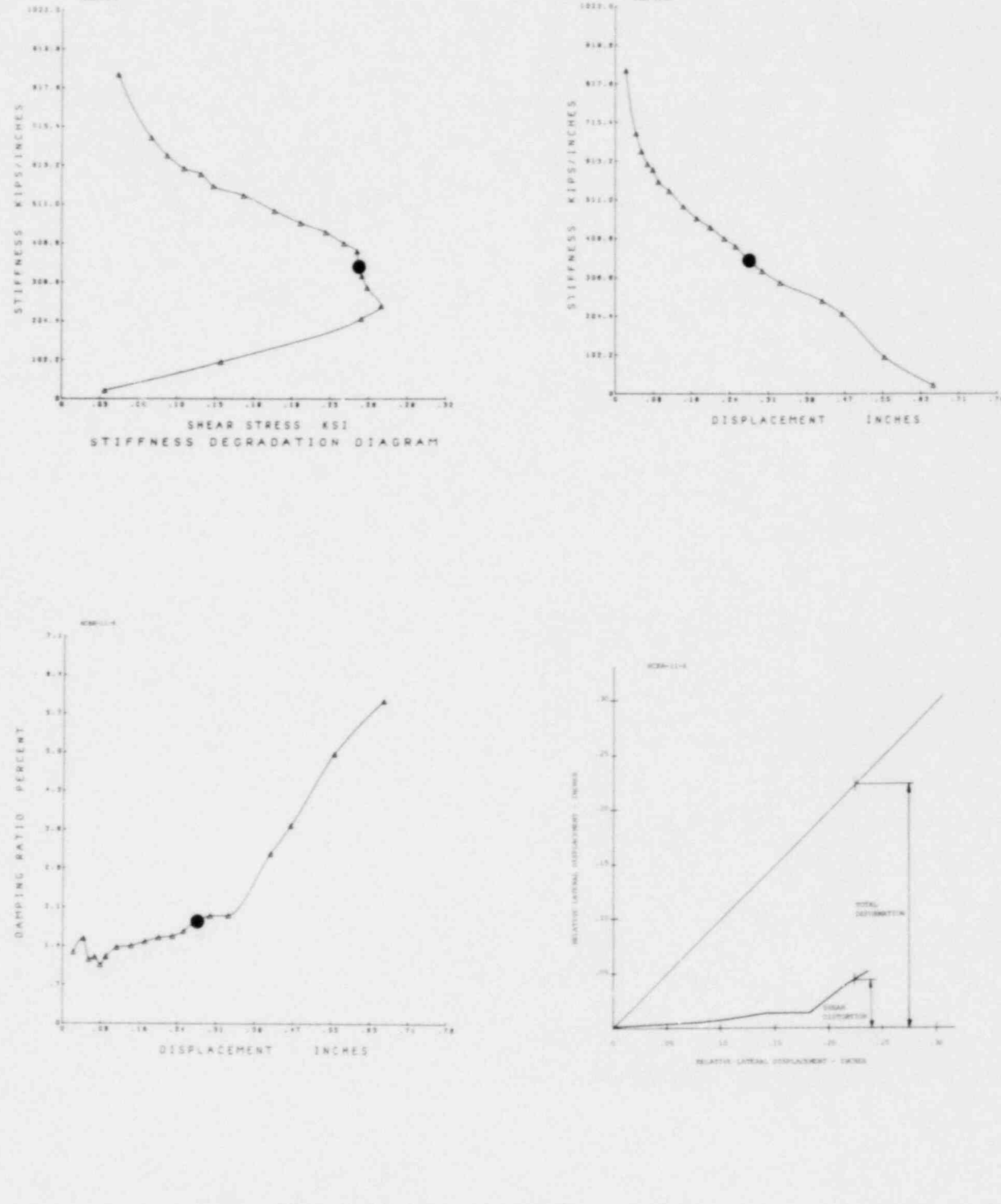

FIG. A.17 CONTINUE HCBR-11-6

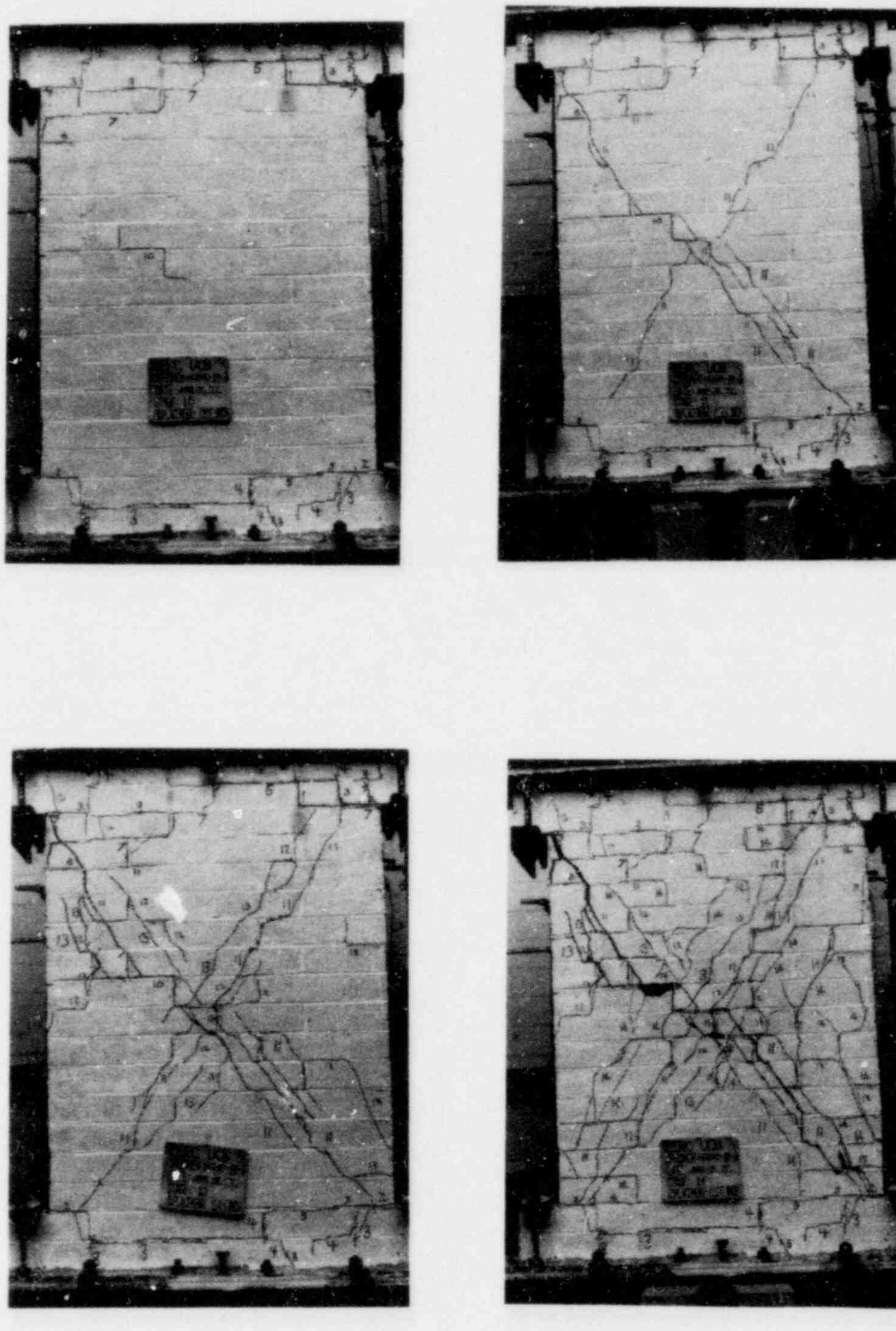

FIG. A.18 SUCCESSIVE CRACK FORMATION
AND EXPERIMENTAL RESULTS
TEST HCBR-11-7

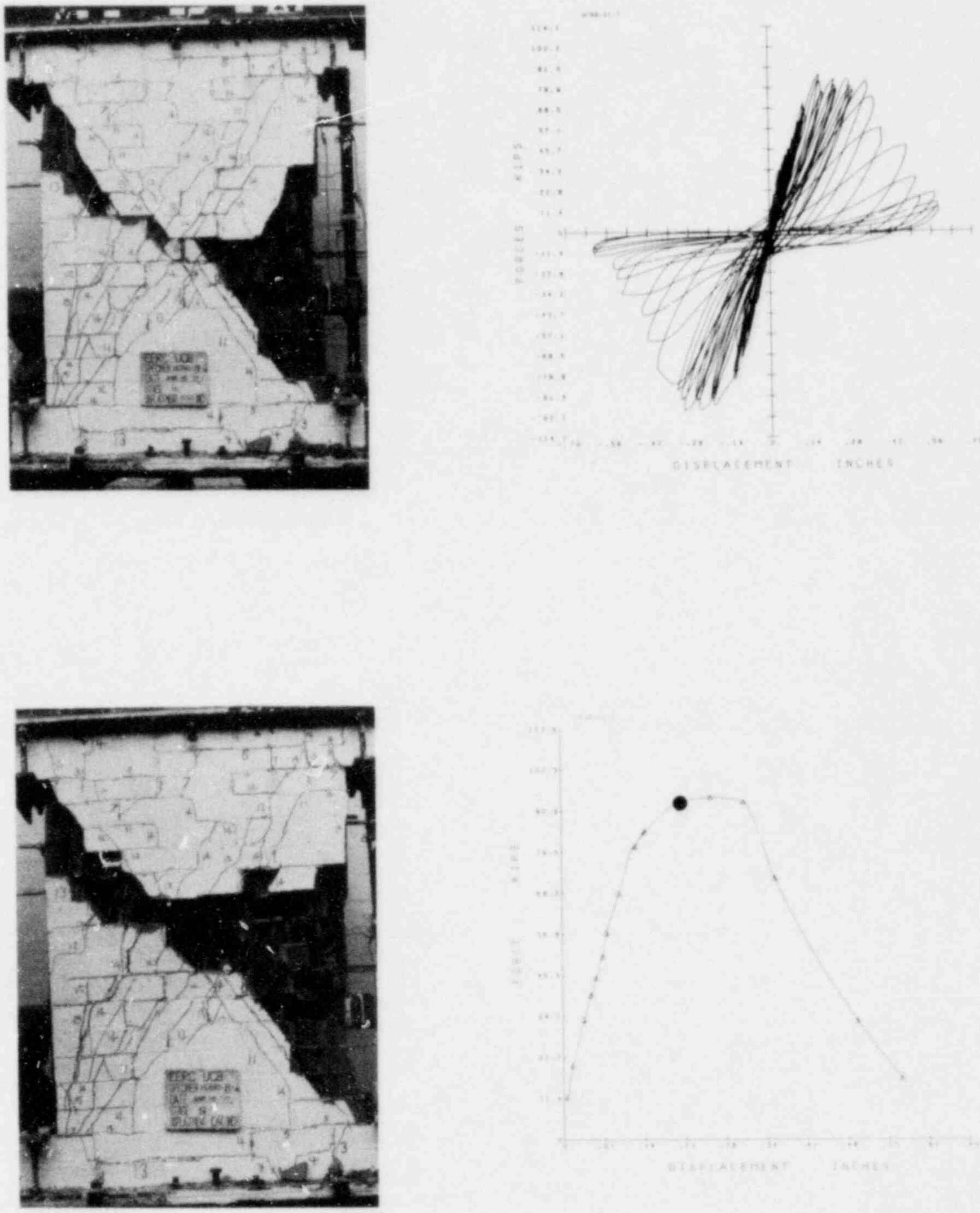

FIG. A.18 CONTINUE HCBR-11-7

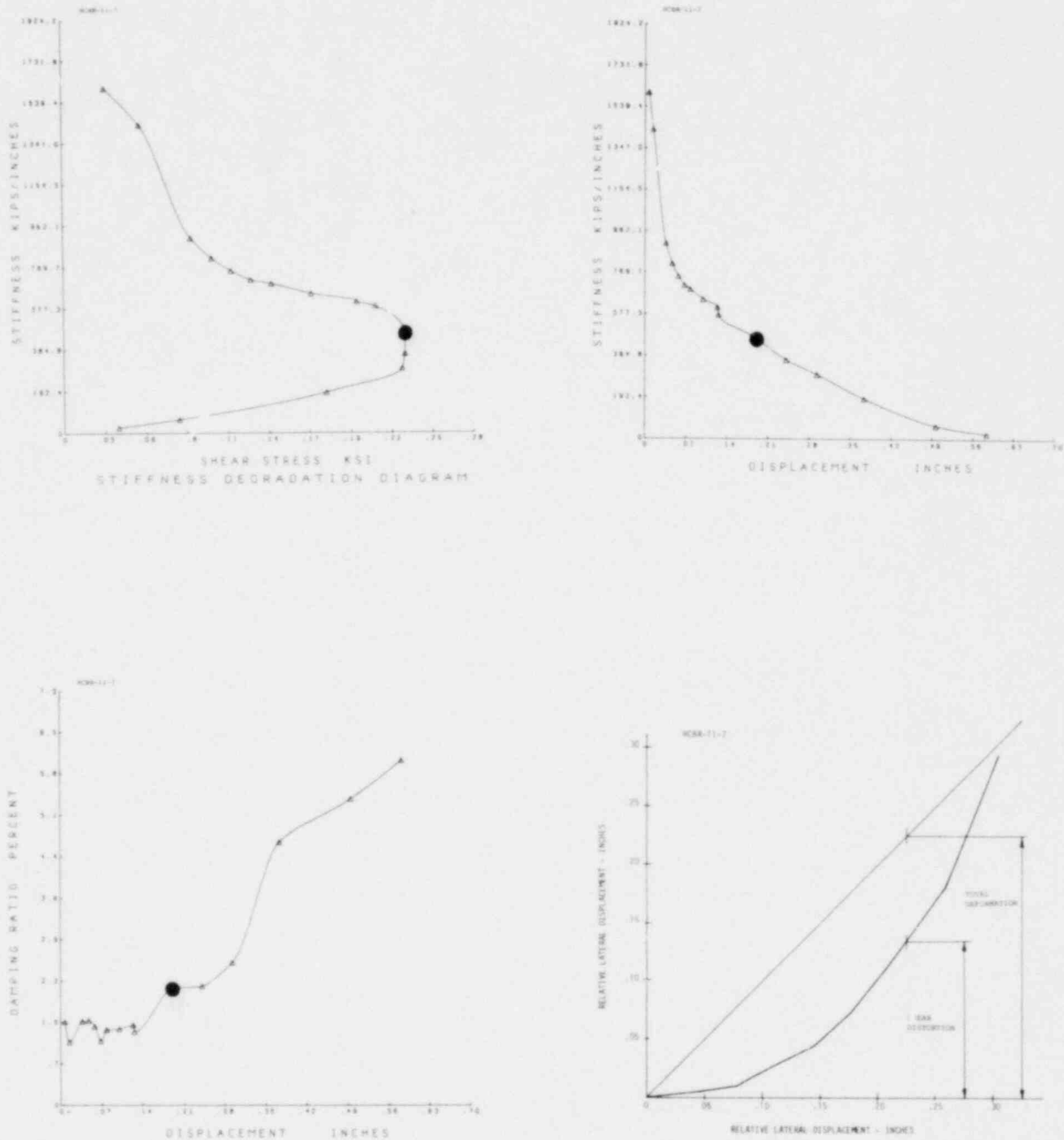

FIG. A.18 CONTINUE HCBR-11-7

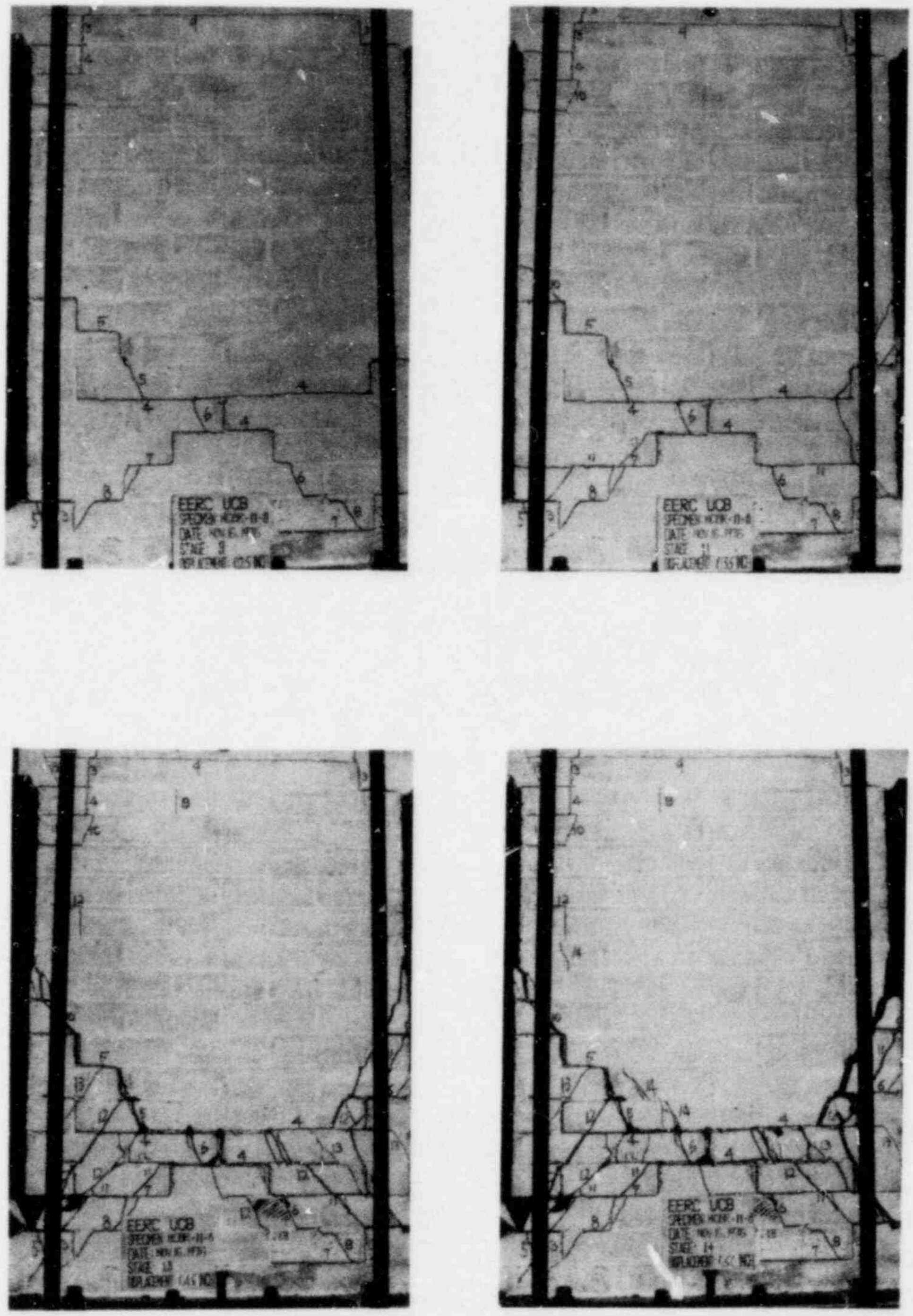

FIG. A.19 SUCCESSIVE CRACK FORMATION AND EXPERIMENTAL RESULTS TEST HCBR-11-8

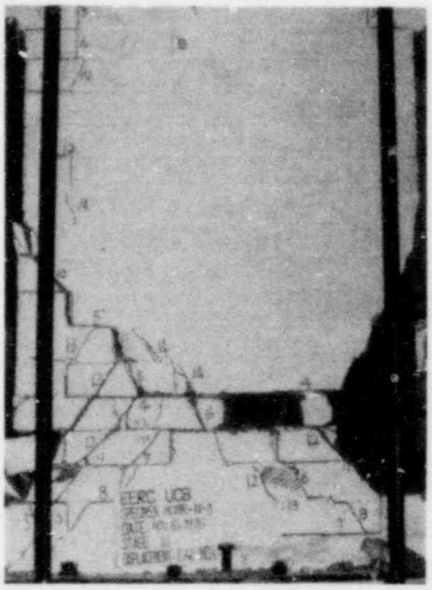

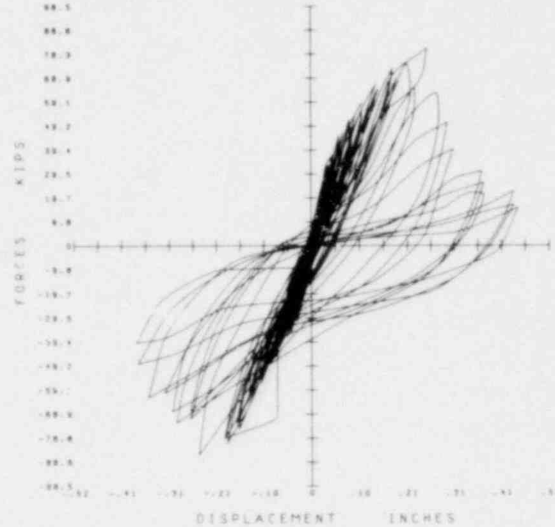

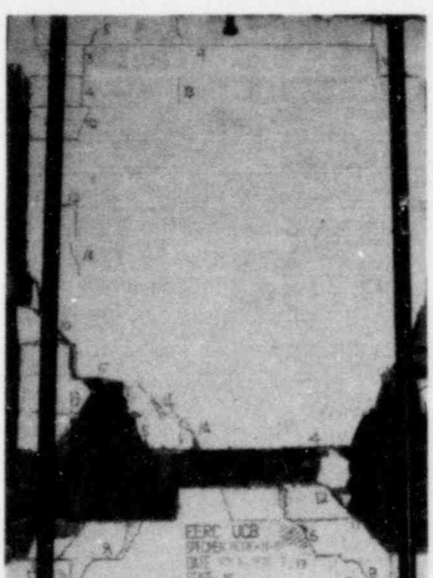

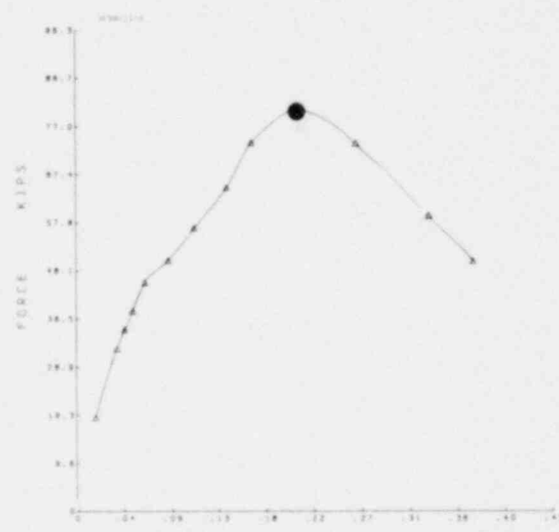

FIG. A.19 CONTINUE HCBR-11-8

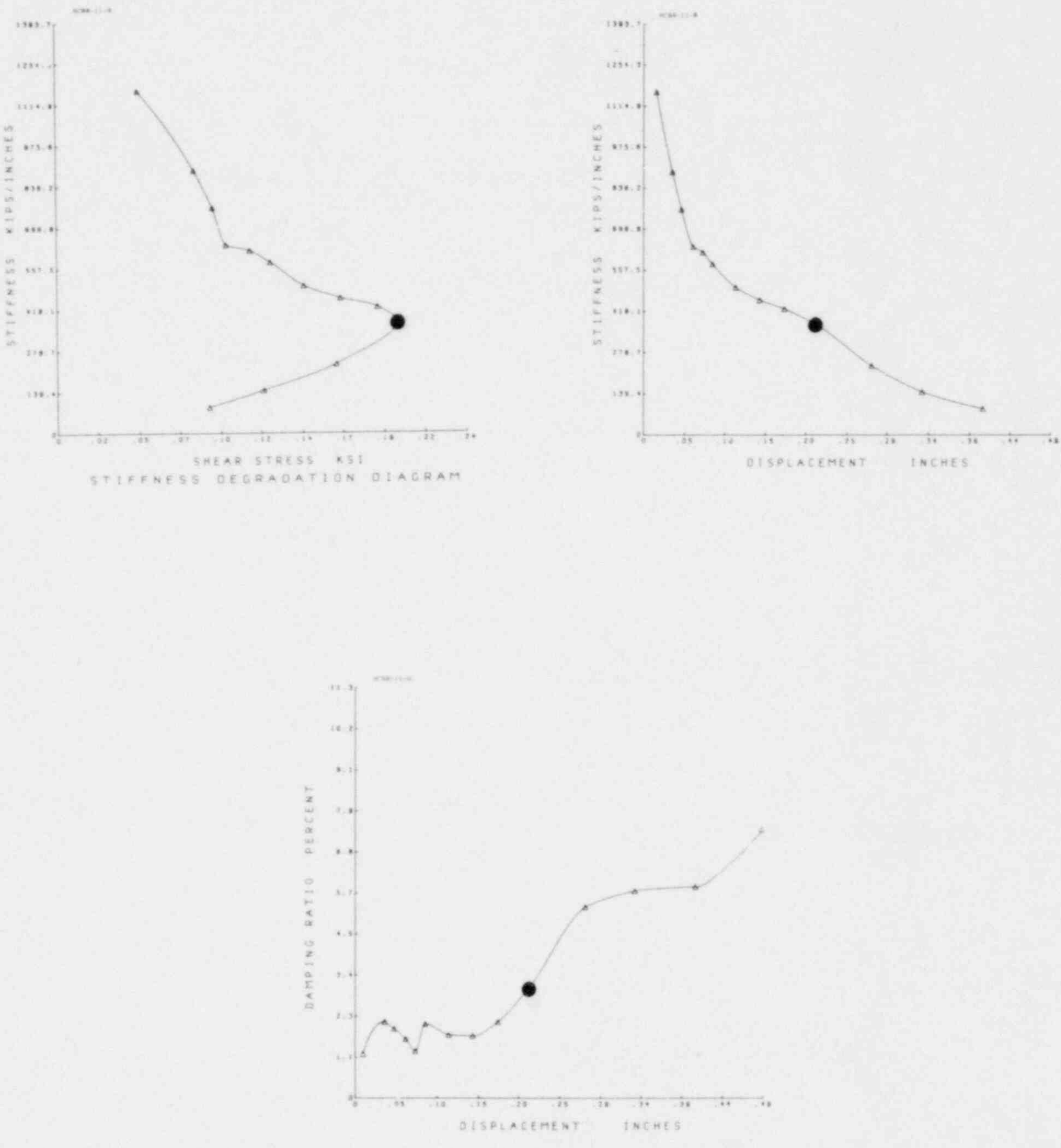

FIG. A.19 CONTINUE HCBR-11-8

FIG. A.20 SUCCESSIVE CRACK FORMATION
AND EXPERIMENTAL RESULTS
TEST HCBR-11-9

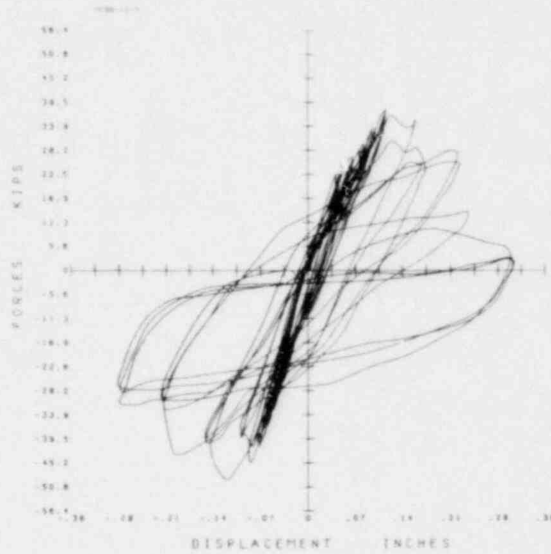

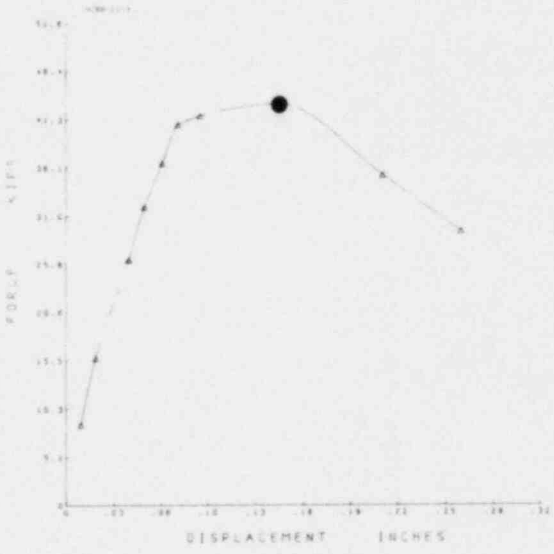

FIG. A.20 CONTINUE HCBR-11-9

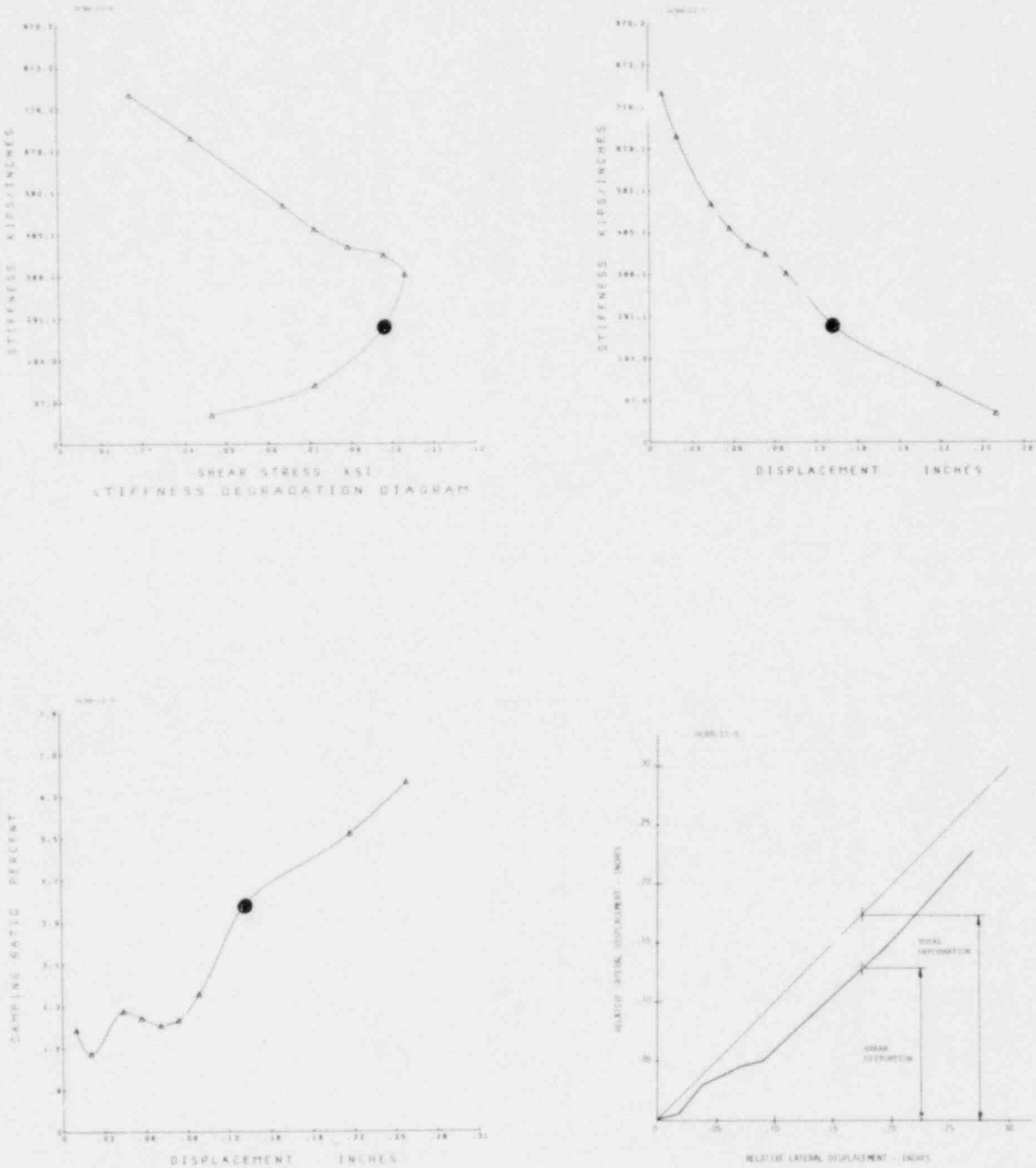

FIG. A.20 CONTINUE HCBR-11-9

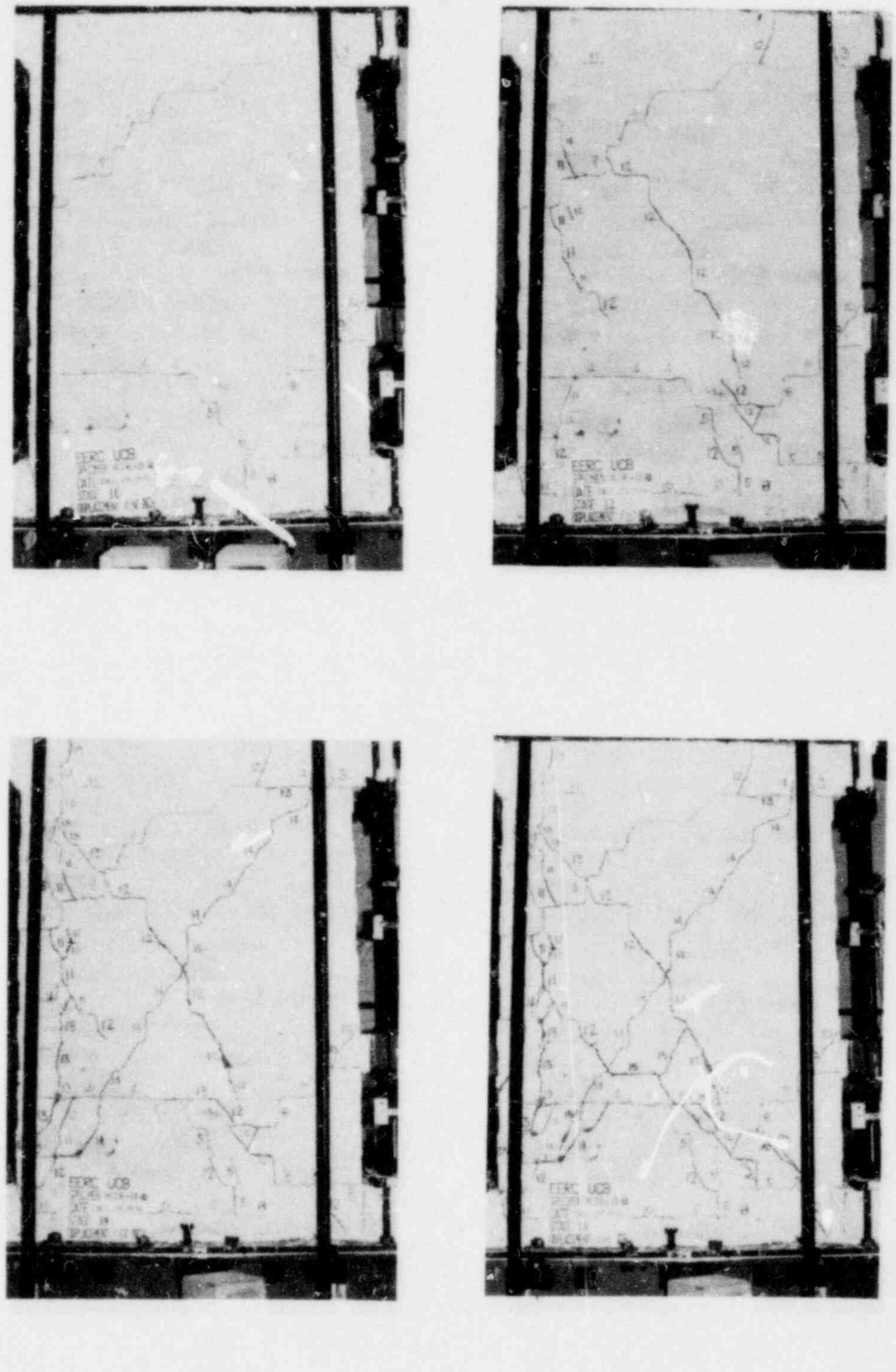

FIG. A.21 SUCCESSIVE CRACK FORMATION
AND EXPERIMENTAL RESULTS
TEST HCBR-11-10

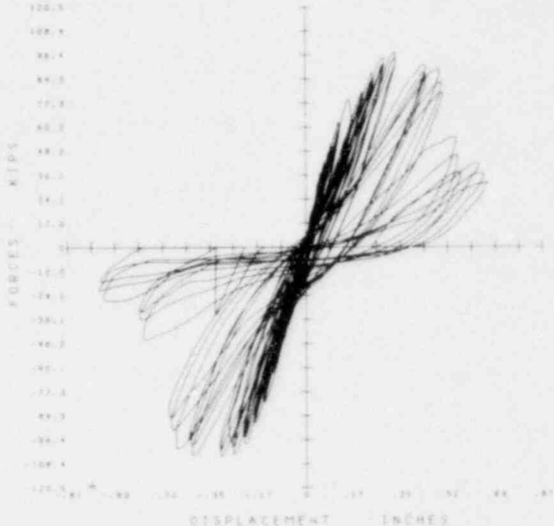

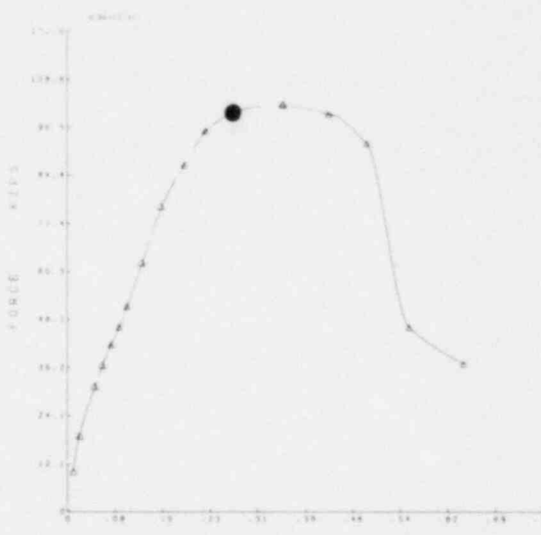

FIG. A.21 CONTINUE HCBR-11-10

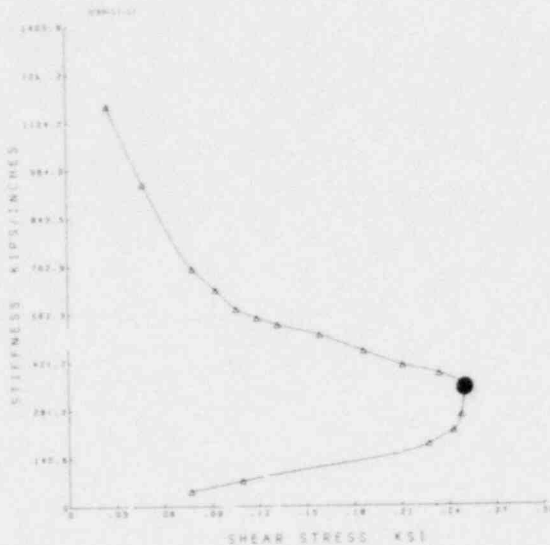

STIFFNESS DEGRADATION DIAGRAM

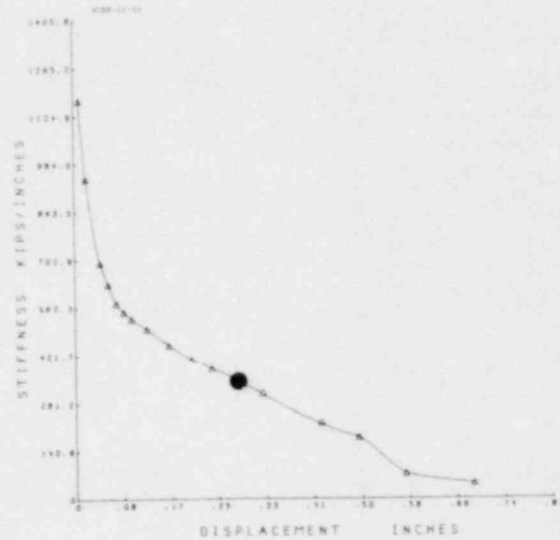

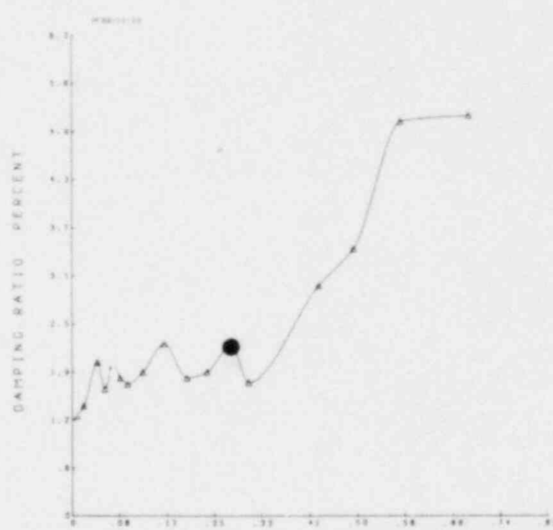

FIG. A.21 CONTINUE HCBR-11-10

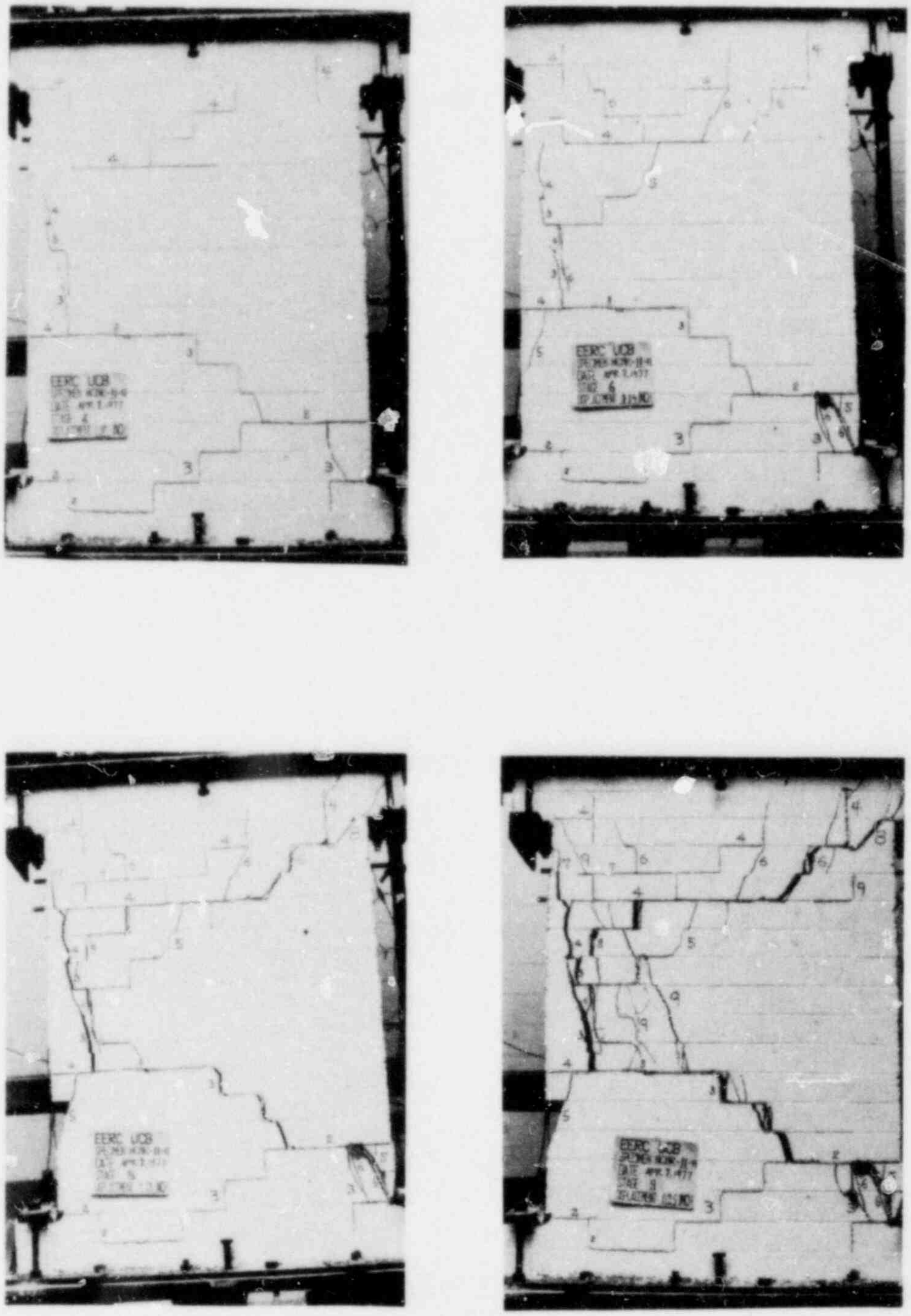

FIG. A.22 SUCCESSIVE CRACK FORMATION
AND EXPERIMENTAL RESULTS
TEST HCBR-11-11

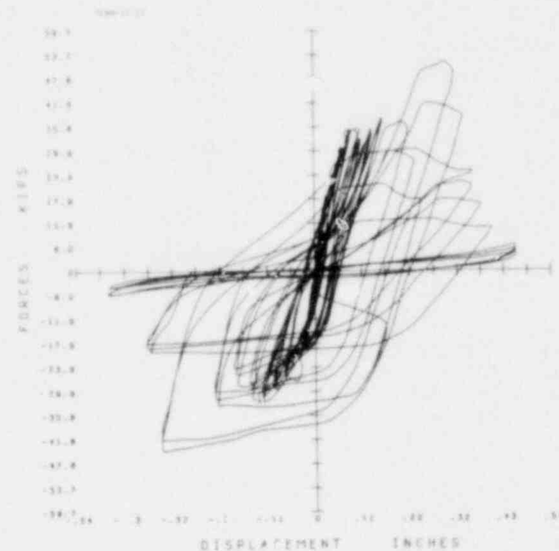

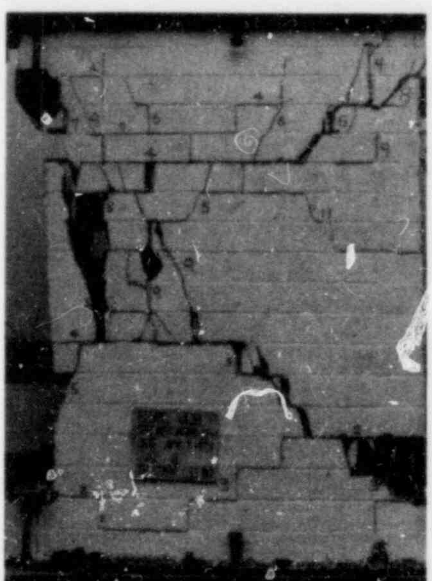

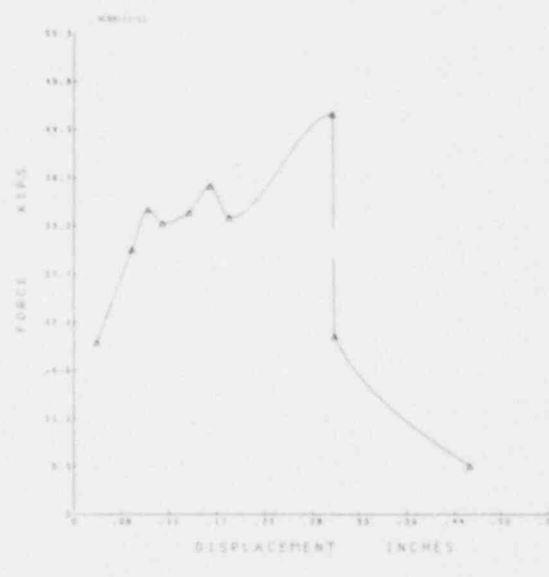

FIG. A.22 CONTINUE HCBR11-11

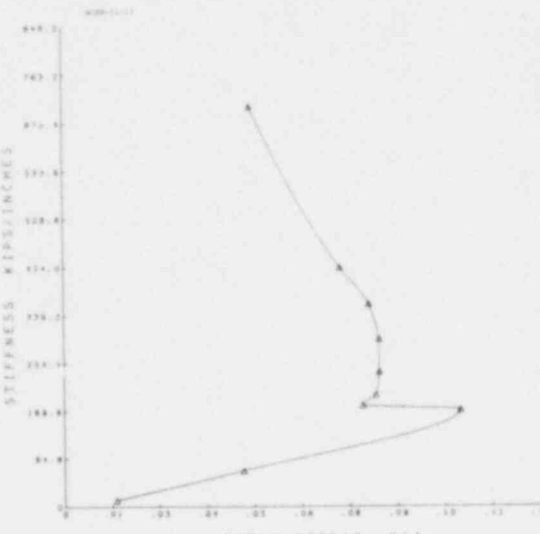

STIFFNESS DEGRADATION DIAGRAM

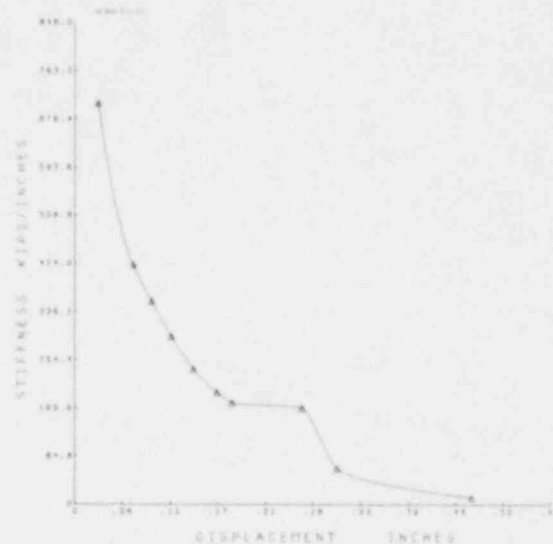

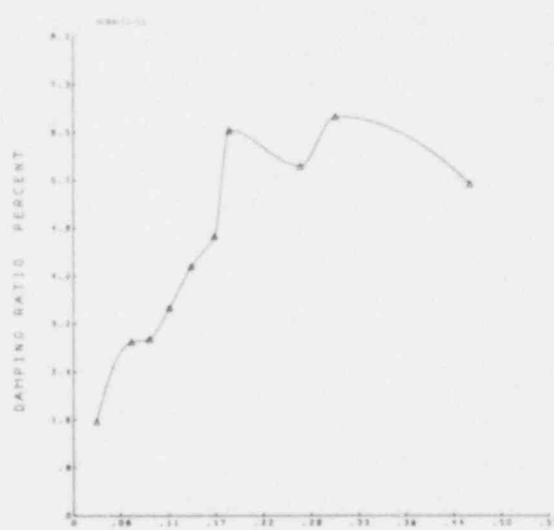

FIG. A.22 CONTINUE HCBR-11-11

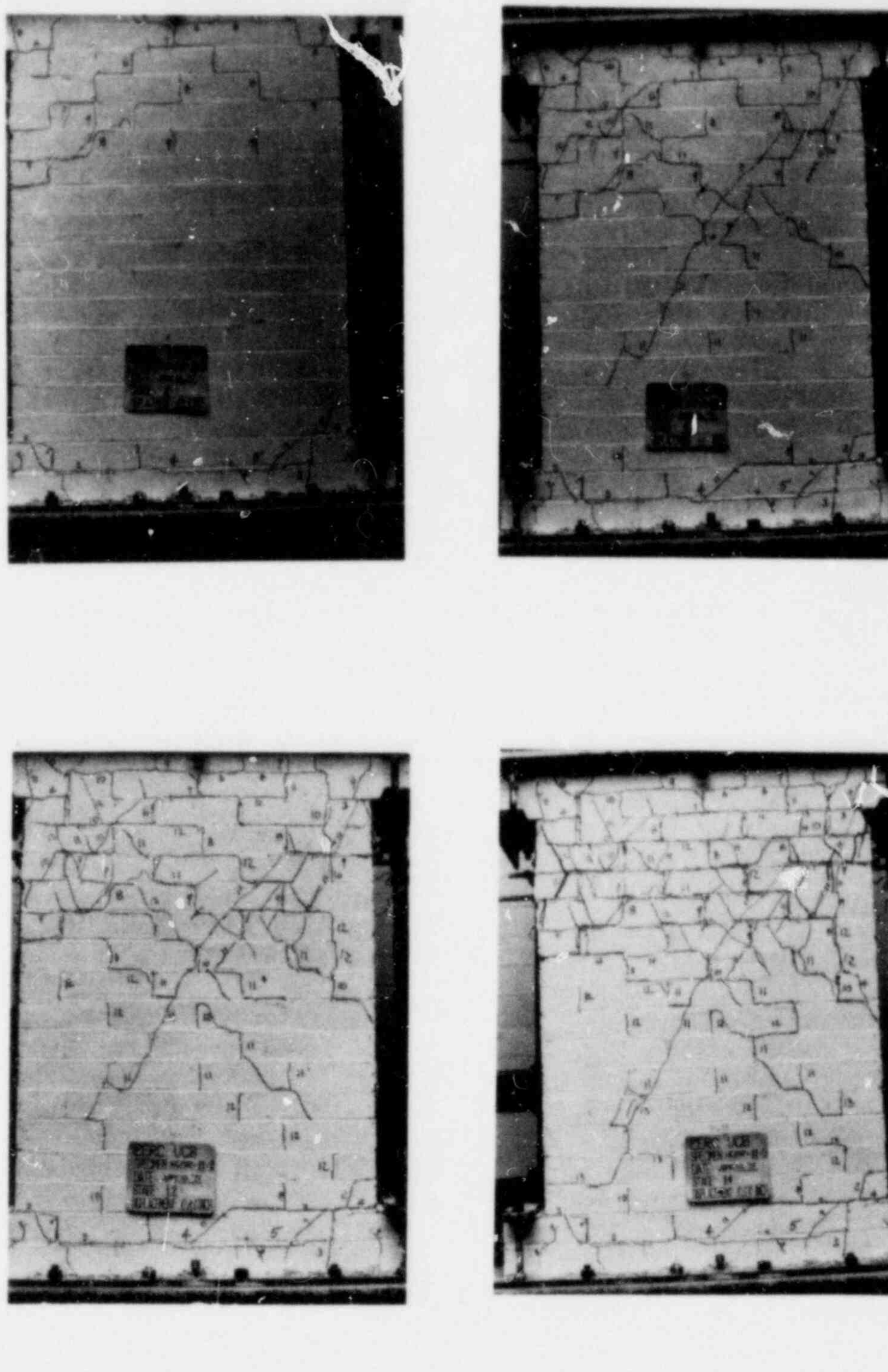

FIG. A.23 SUCCESSIVE CRACK FORMATION
AND EXPERIMENTAL RESULTS
TEST HCBR-11-12

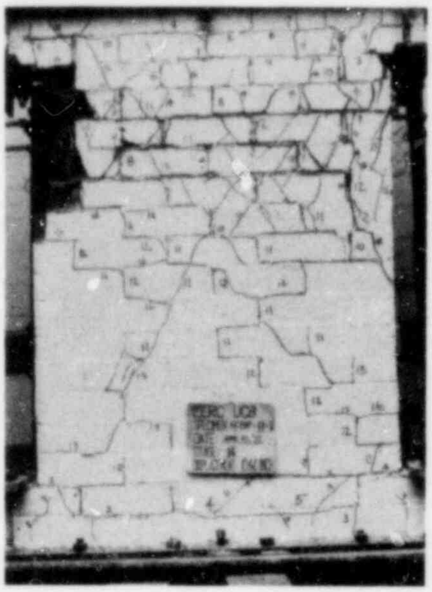

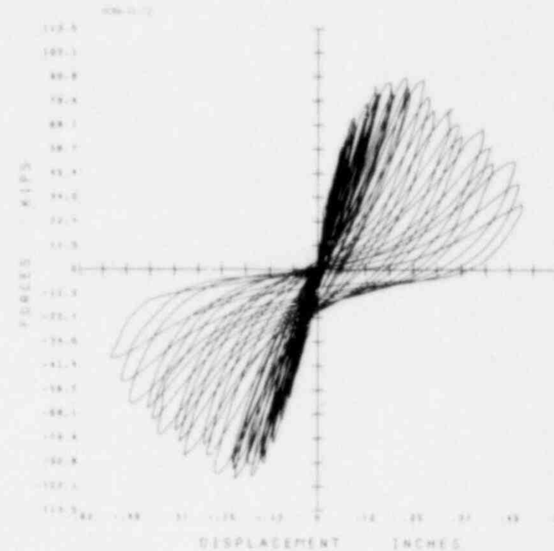

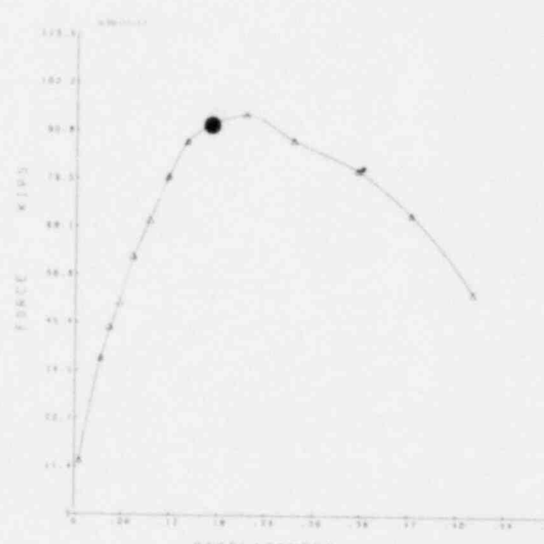

FIG. A.23 CONTINUE HCBR-11-12

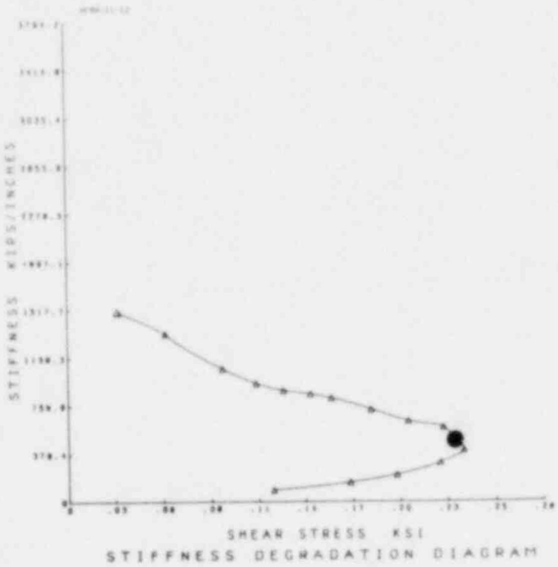

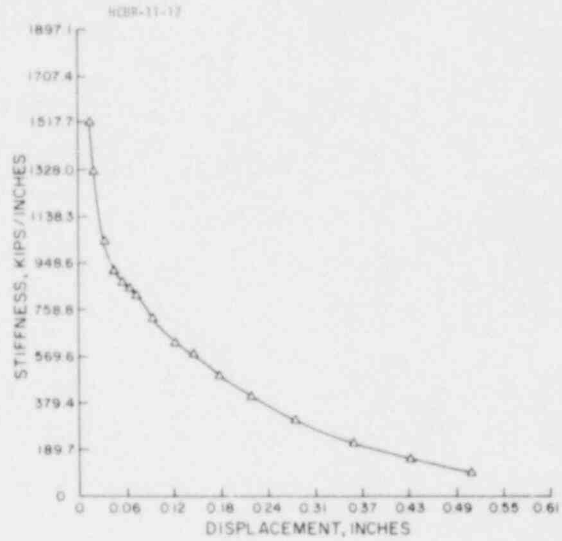

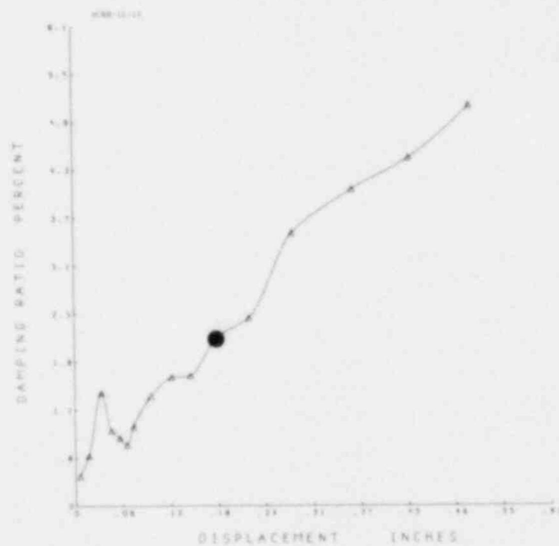

FIG. A.23 CONTINUE HCBR-11-12

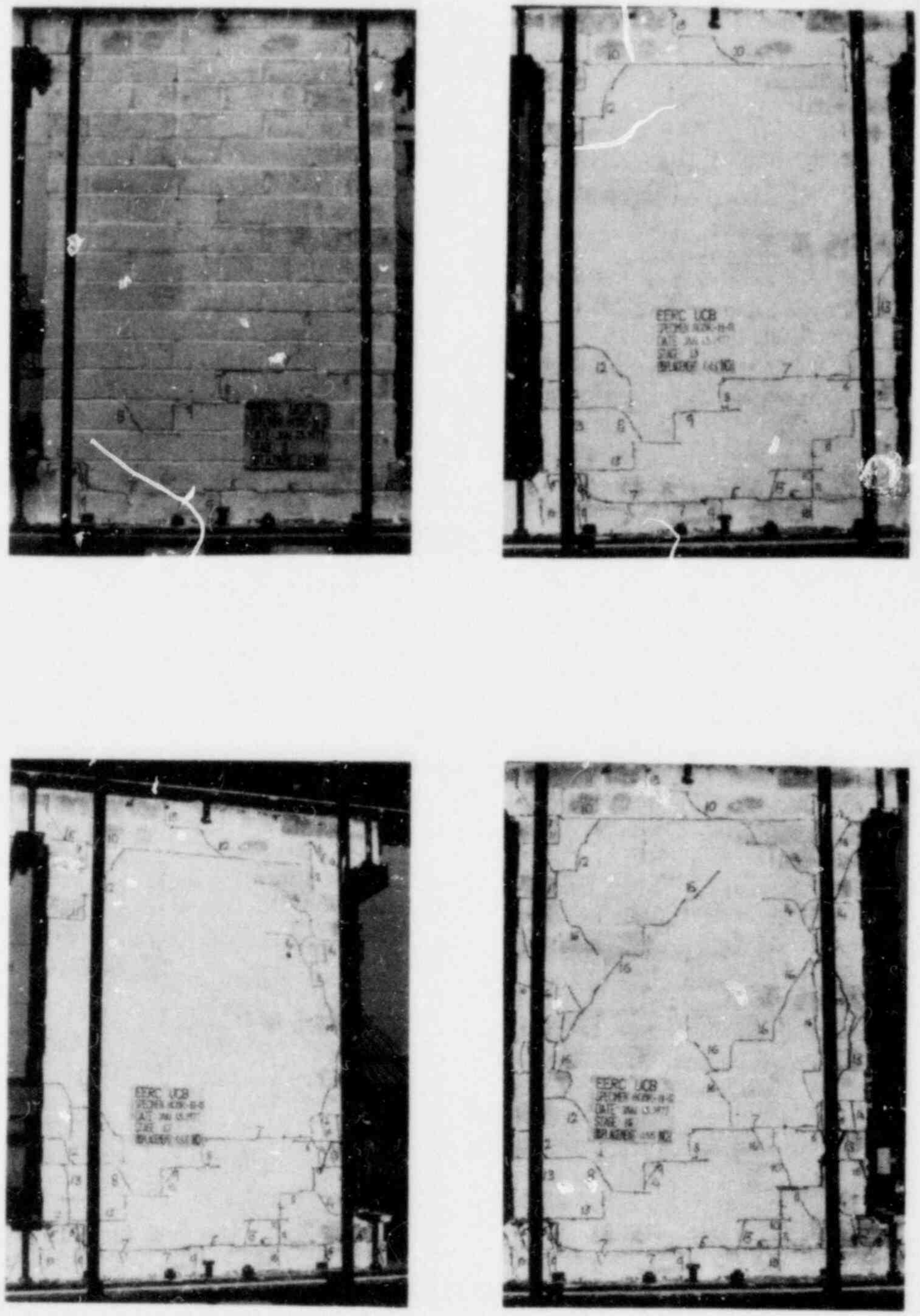

FIG. A.24 SUCCESSIVE CRACK FORMATION
AND EXPERIMENTAL RESULTS
TEST HCBR-11-13

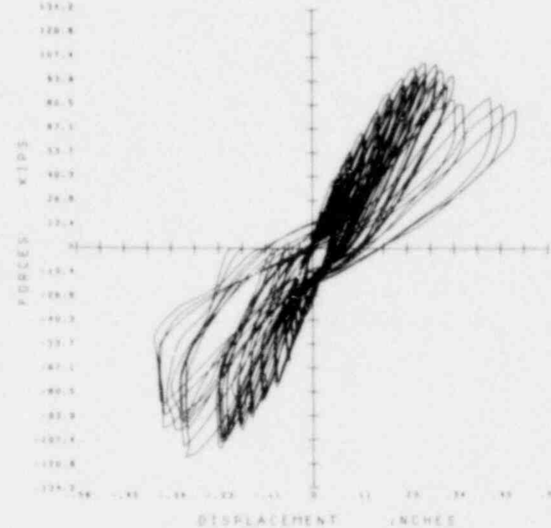

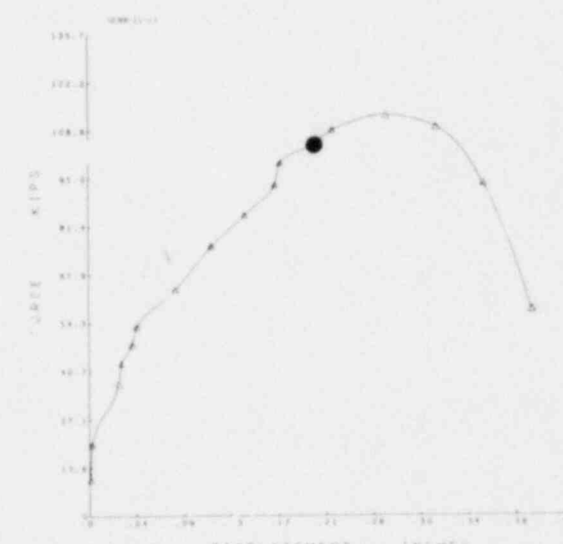

FIG. A.24 CONTINUE HCBR-11-13

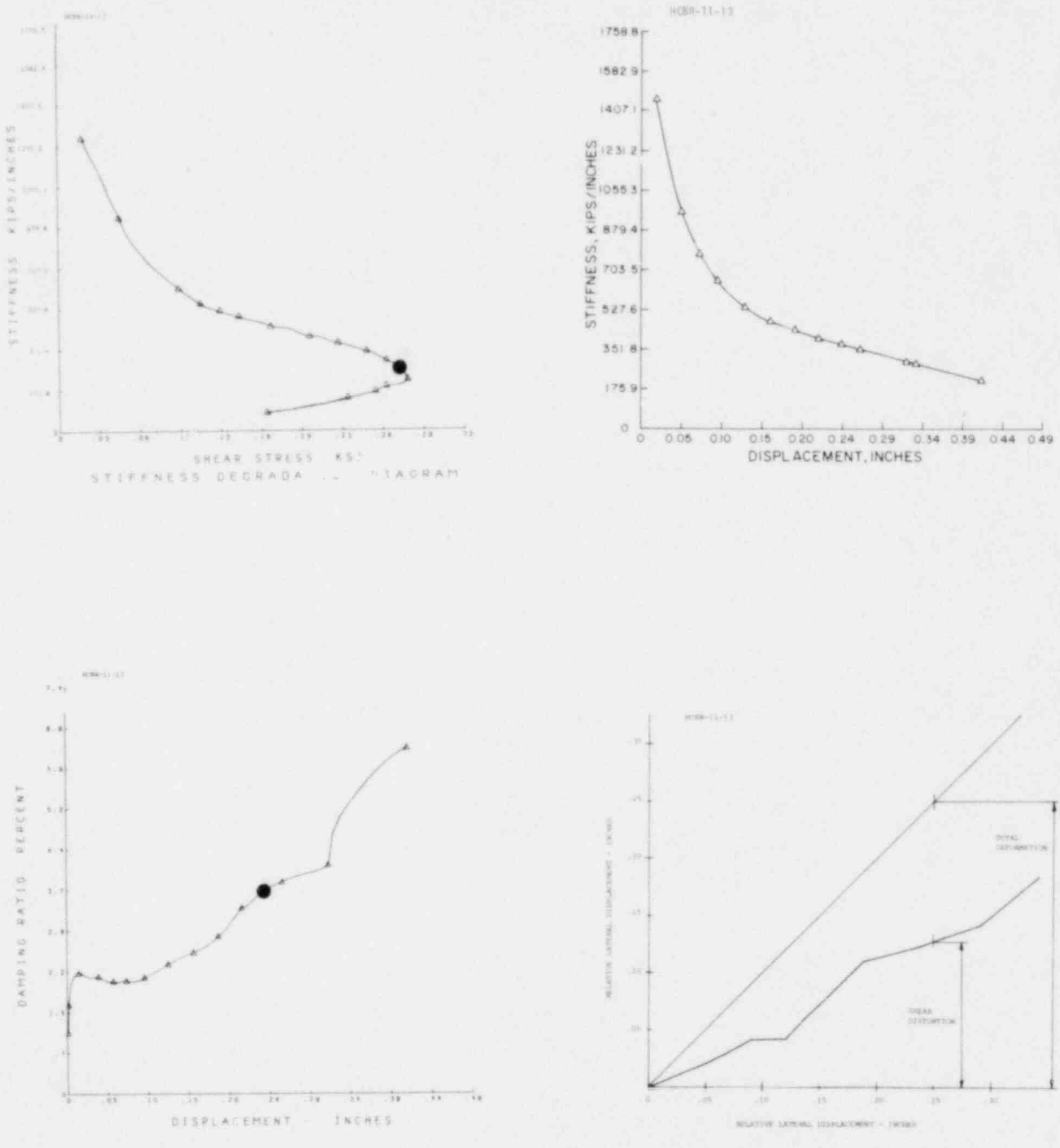

FIG. A.24 CONTINUE HCBR-11-13

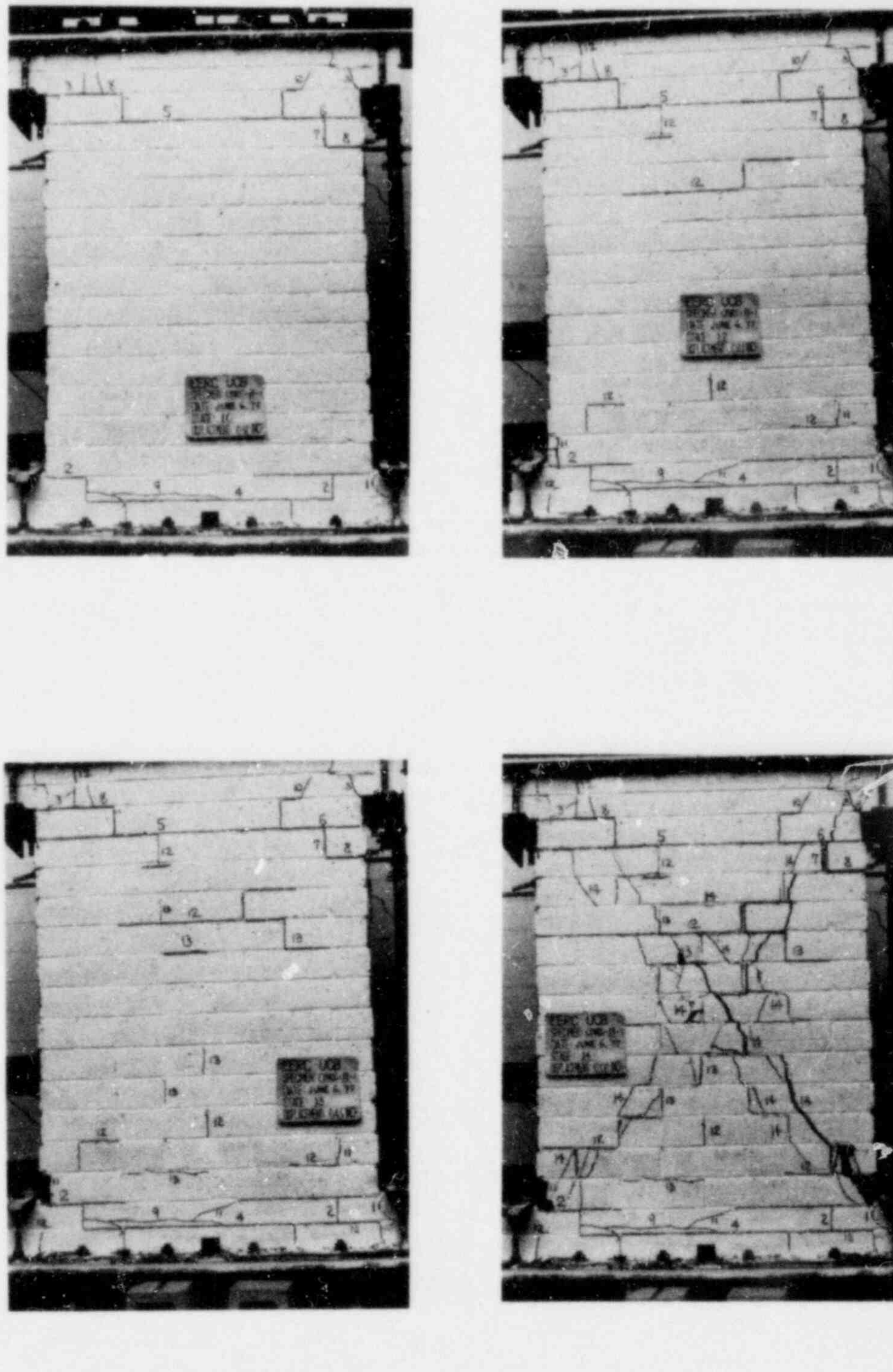

FIG. A.25 SUCCESSIVE CRACK FORMATION
AND EXPERIMENTAL RESULTS
TEST CBRC-11-1

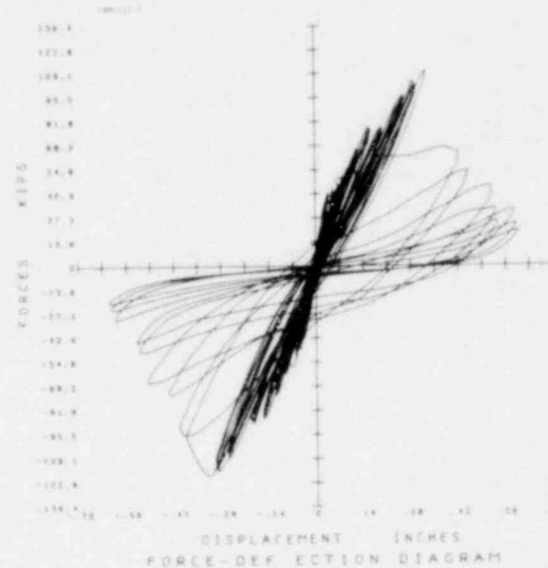

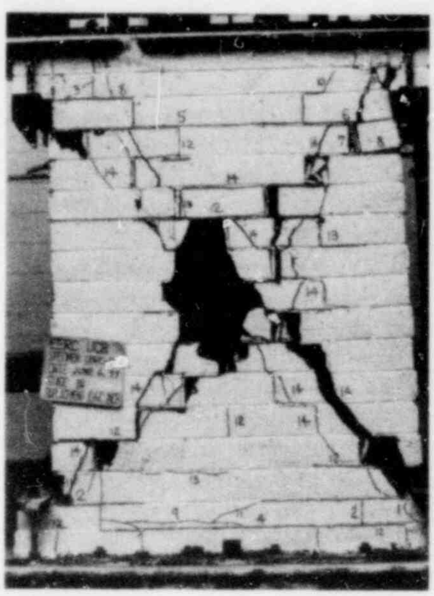

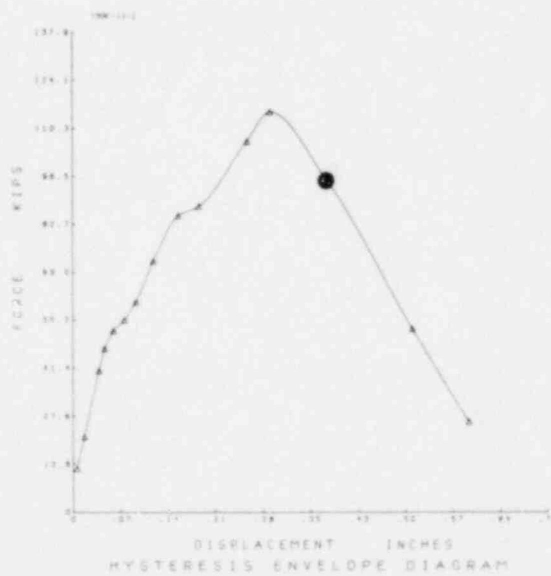

FIG. A.25 CONTINUE CBRC-11-1

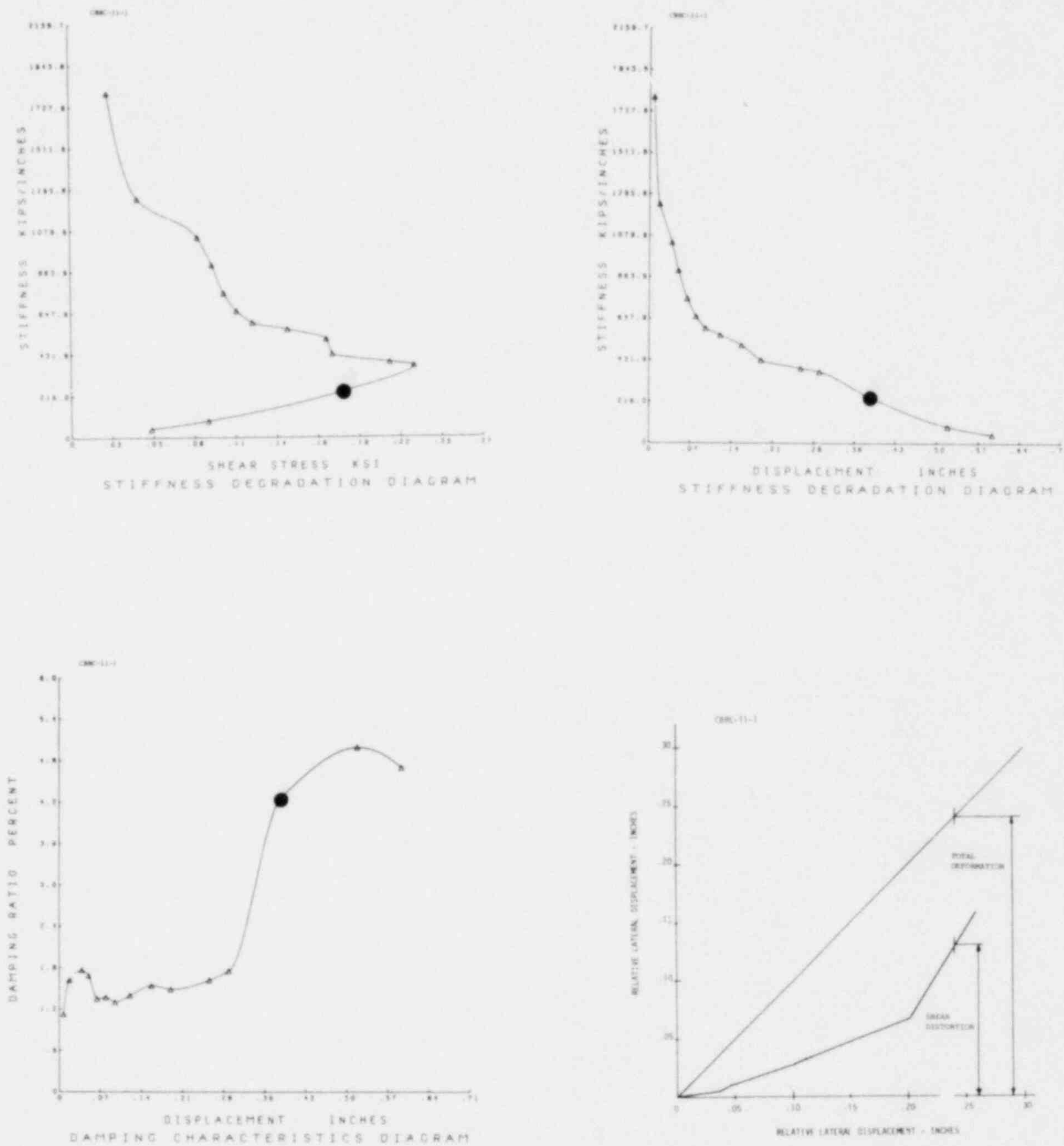

FIG. A.25 CONTINUE CBRC-11-1

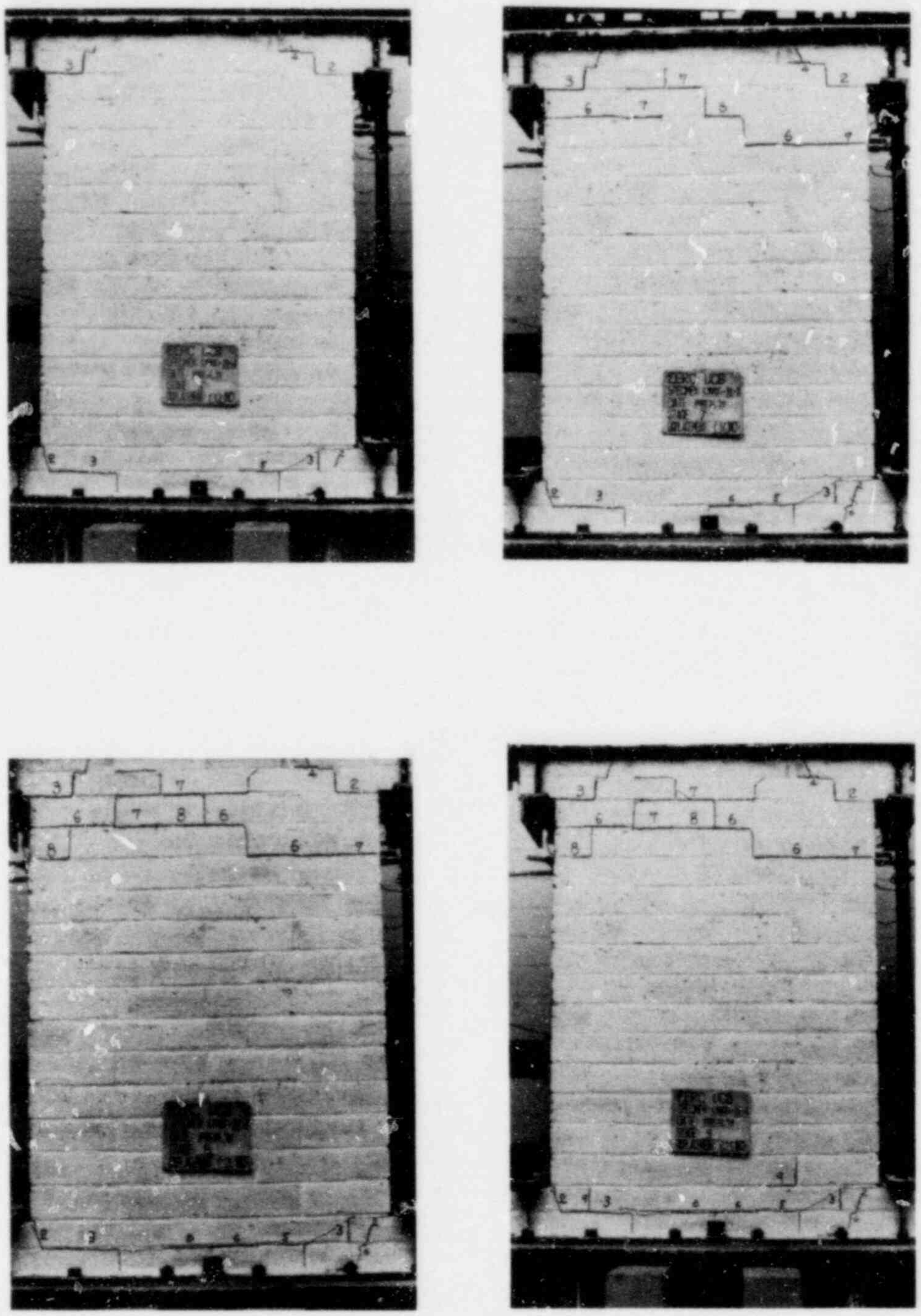

FIG. A.26 SUCCESSIVE CRACK FORMATION
AND EXPERIMENTAL RESULTS
TEST CBRC-11-2

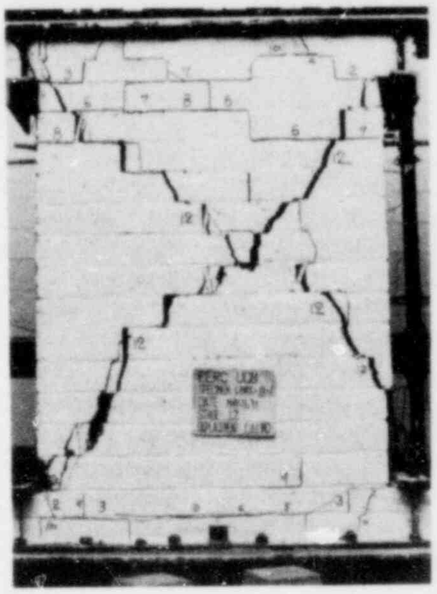

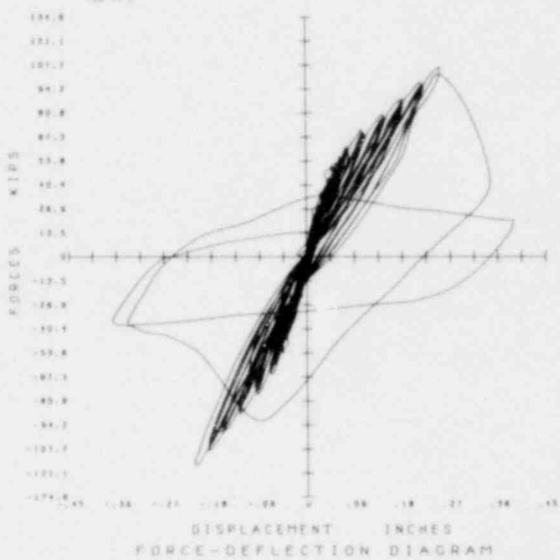

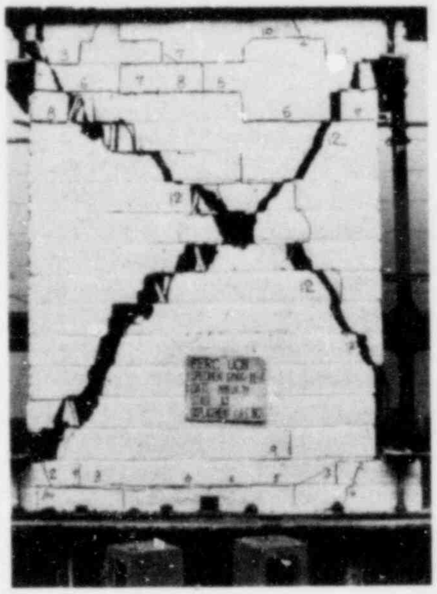

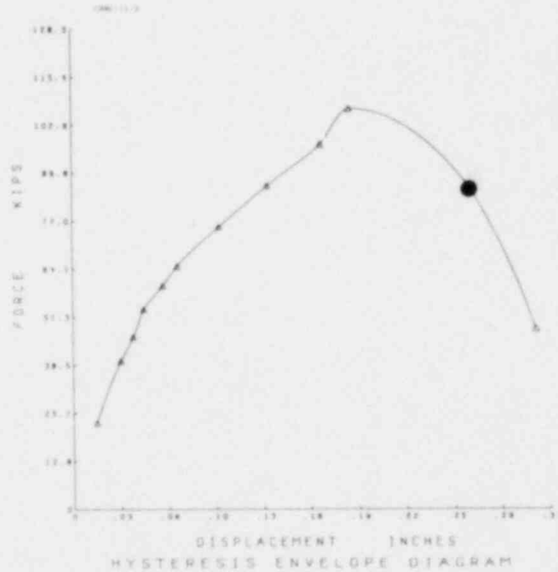

FIG. A.26 CONTINUE CBRC-11-2

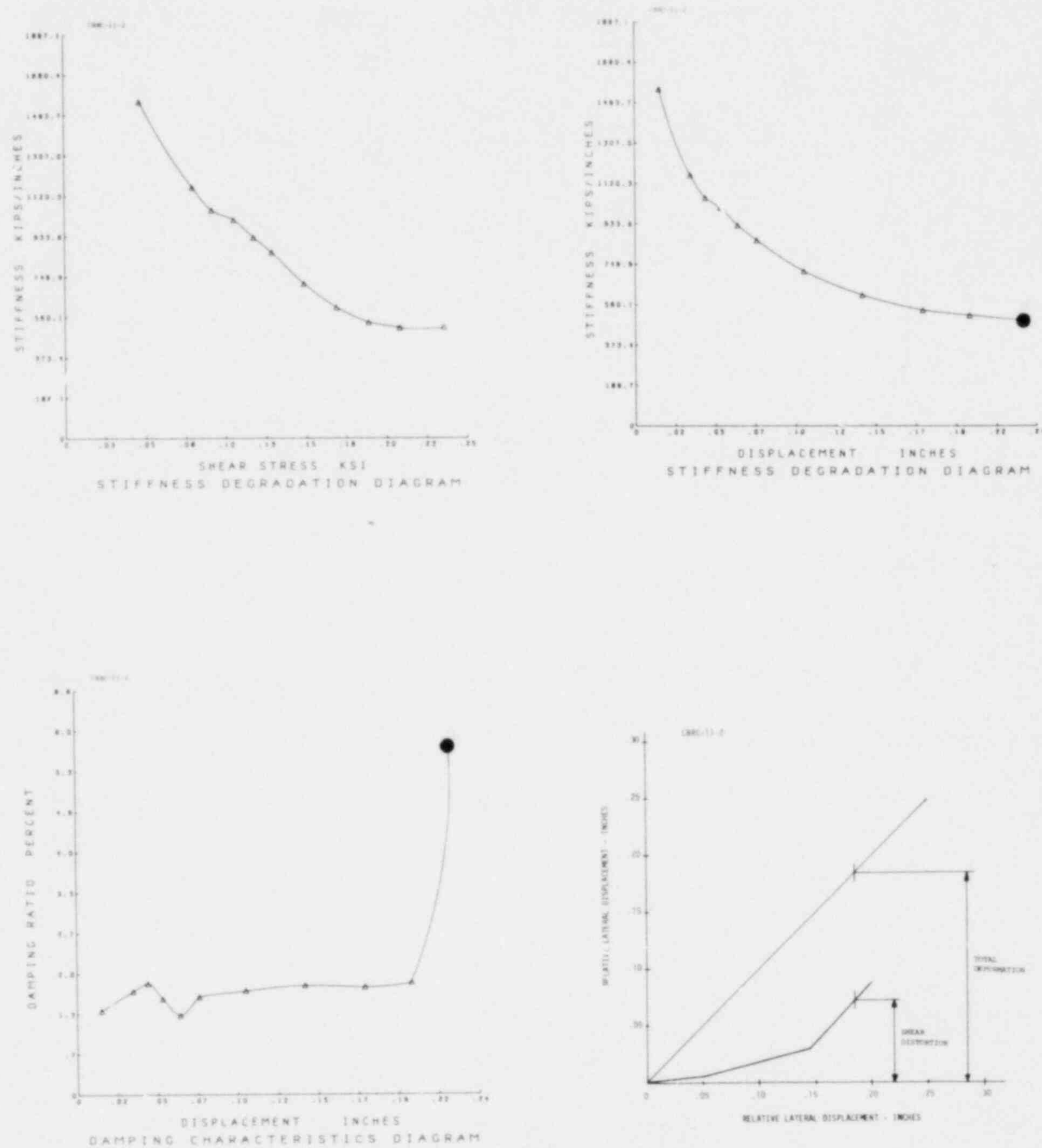

FIG. A.26 CONTINUE CBRC-11-2

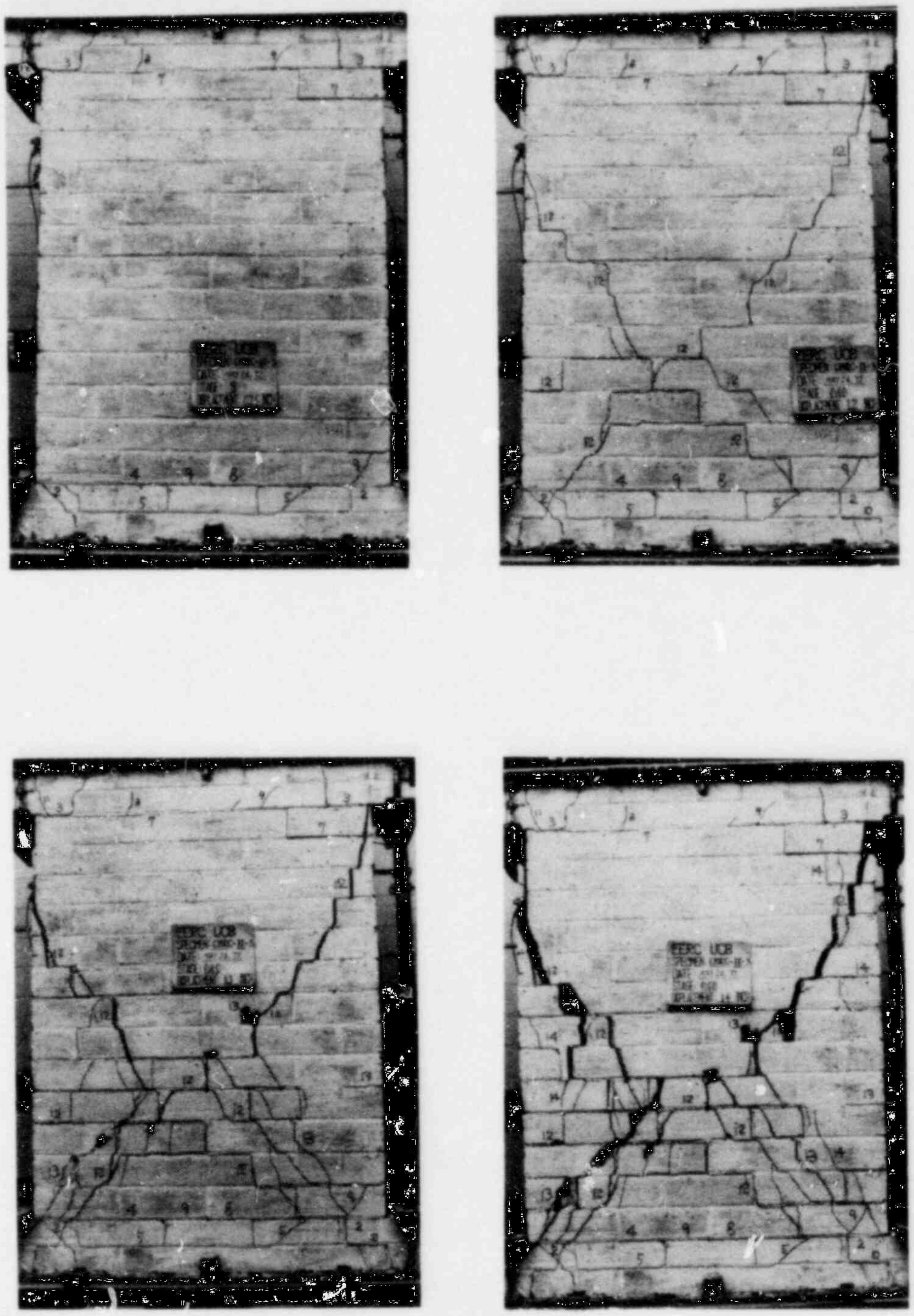

FIG. A.27 SUCCESSIVE CRACK FORMATION
AND EXPERIMENTAL RESULTS
TEST CBRC-11-3

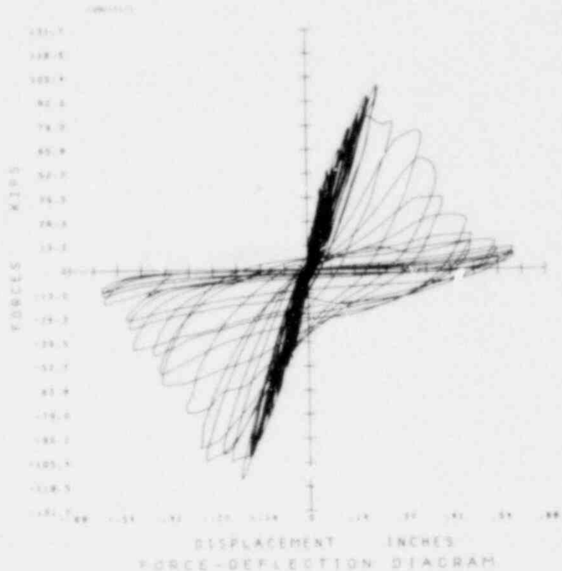

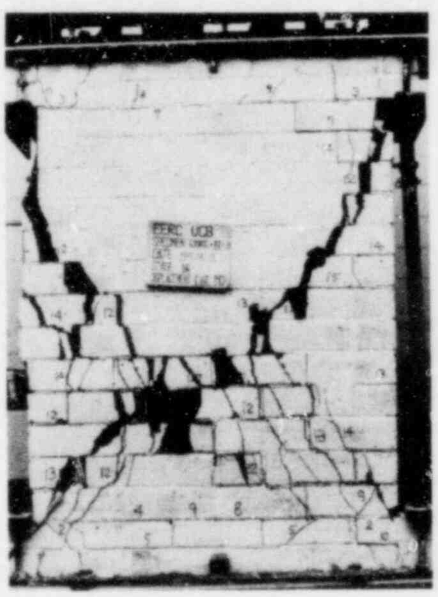

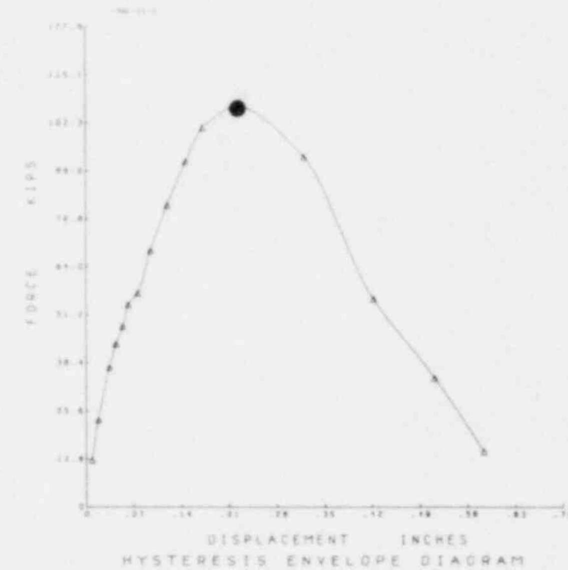

FIG. A.27 CONTINUE CBRC-11-3

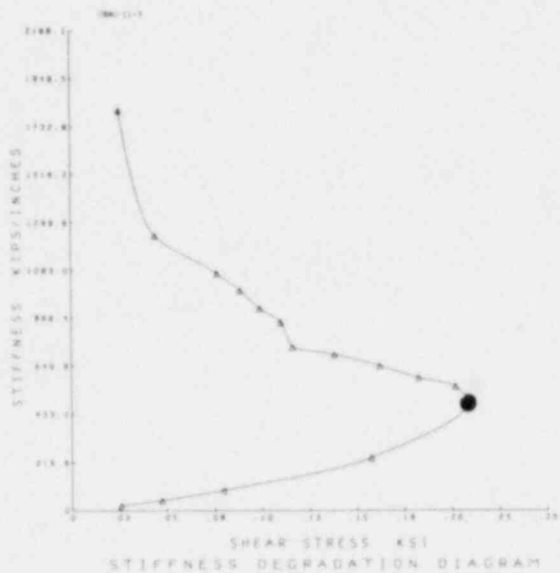

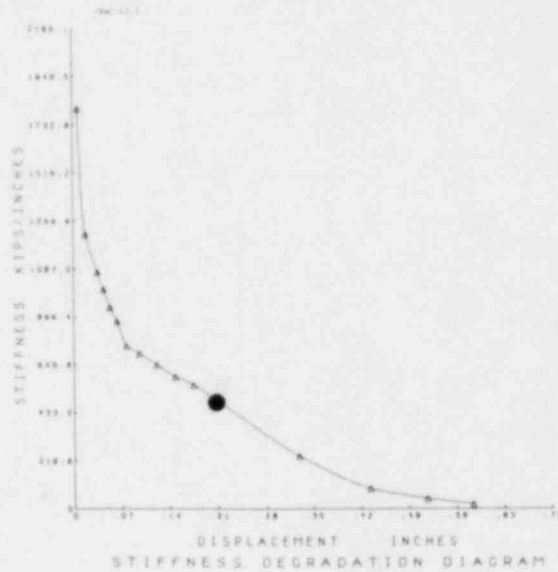

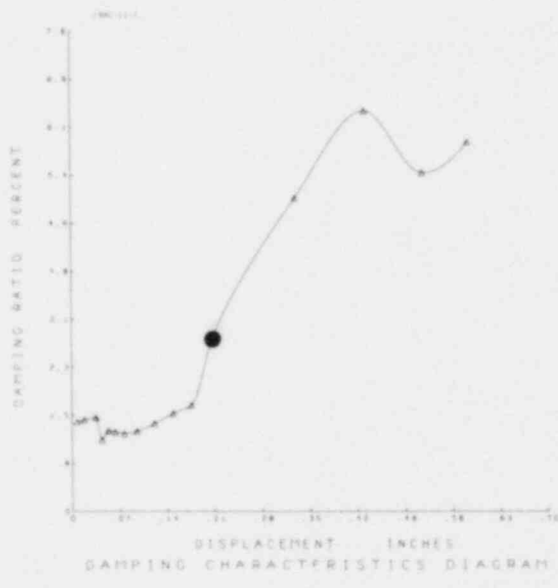

FIG. A.27 CONTINUE CBRC-11-3

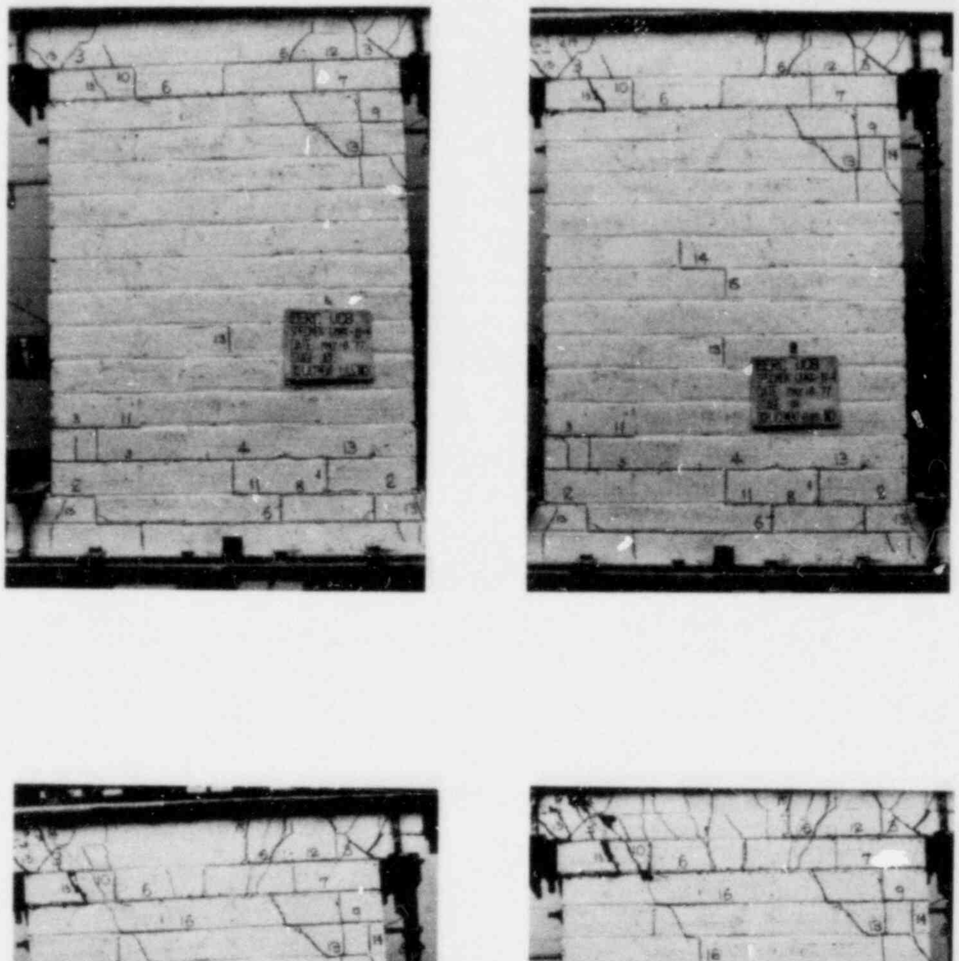

FIG. A.28 SUCCESSIVE CRACK FORMATION
AND EXPERIMENTAL RESULTS
TEST CBRC-11-4

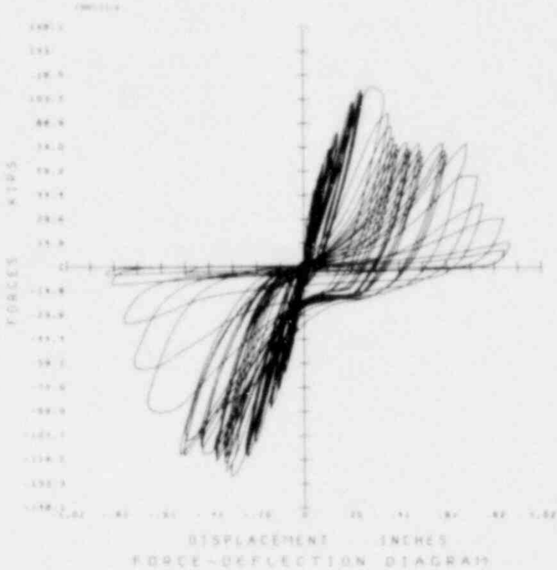

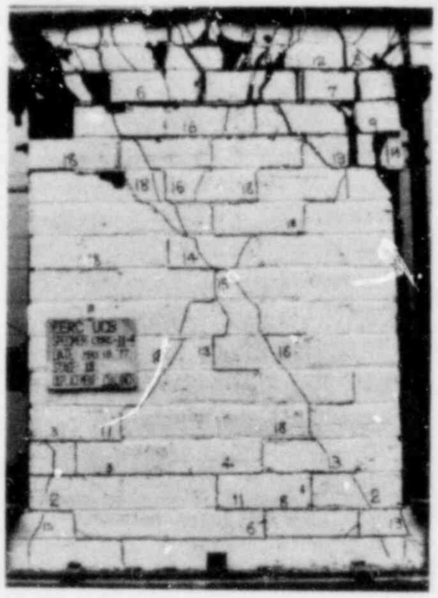

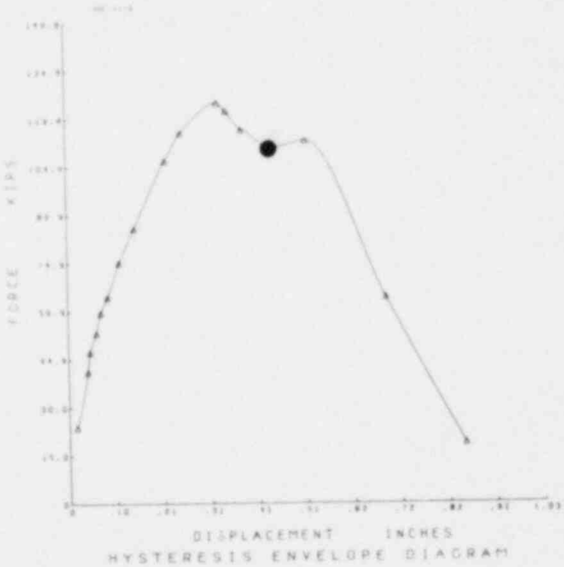

FIG. A.28 CONTINUE CBRC-11-4

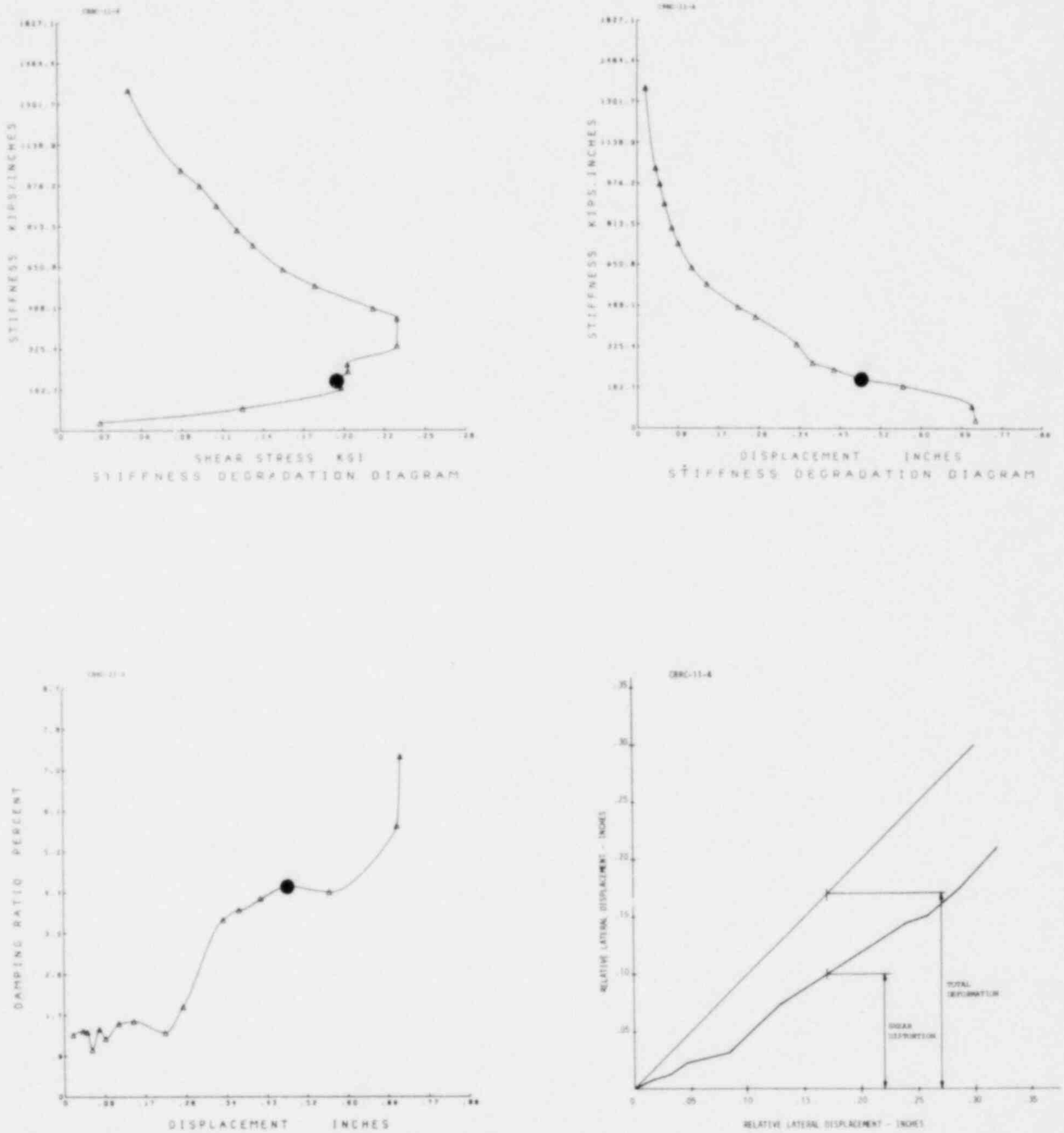

FIG. A.28 CONTINUE CBRC-11-4

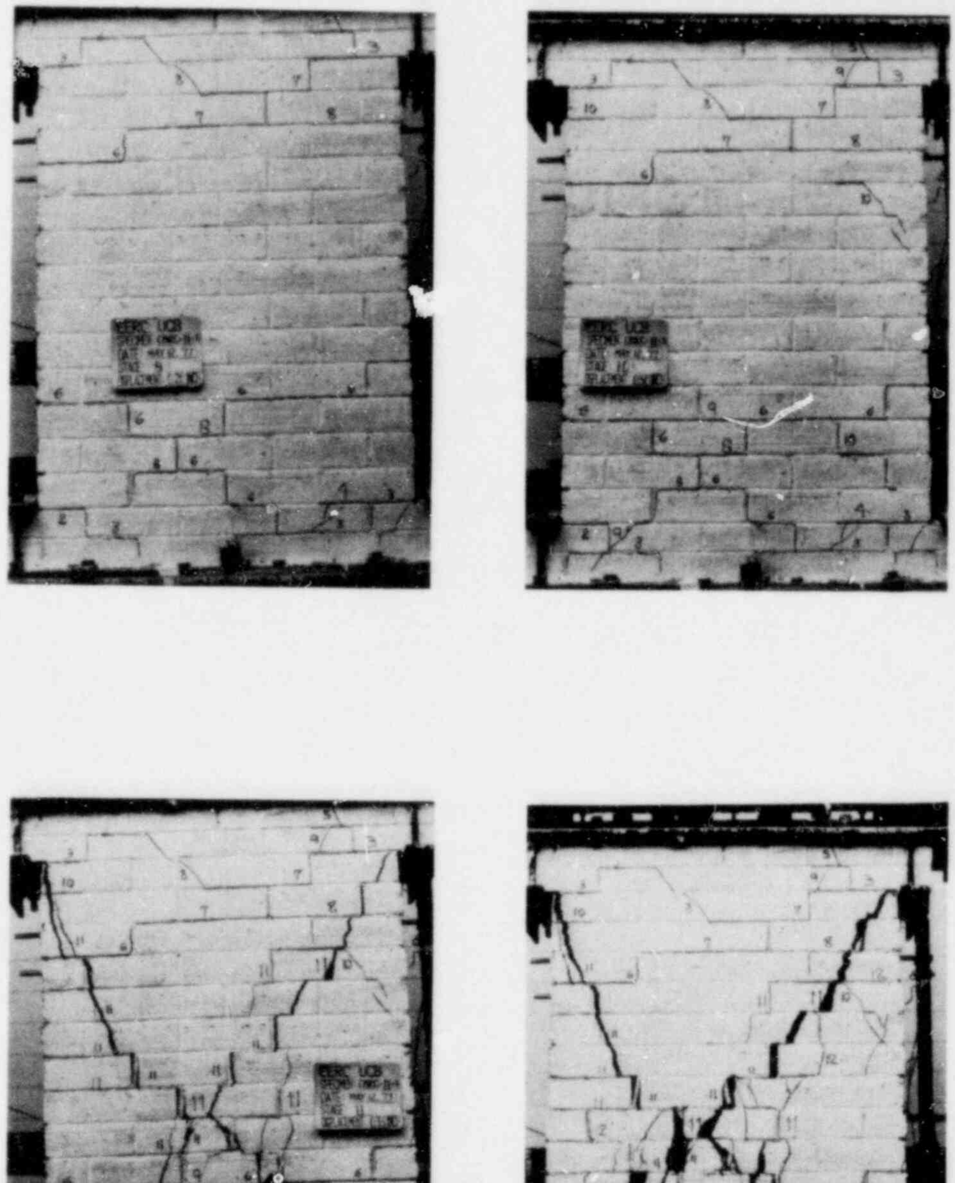

FIG. A.29 SUCCESSIVE CRACK FORMATION
AND EXPERIMENTAL RESULTS
TEST CBRC-11-5

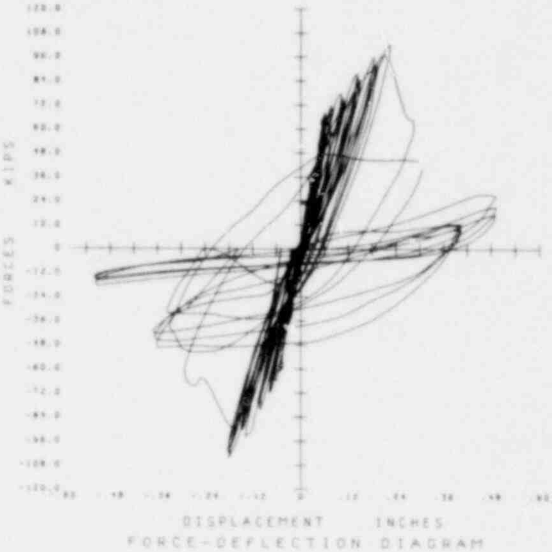

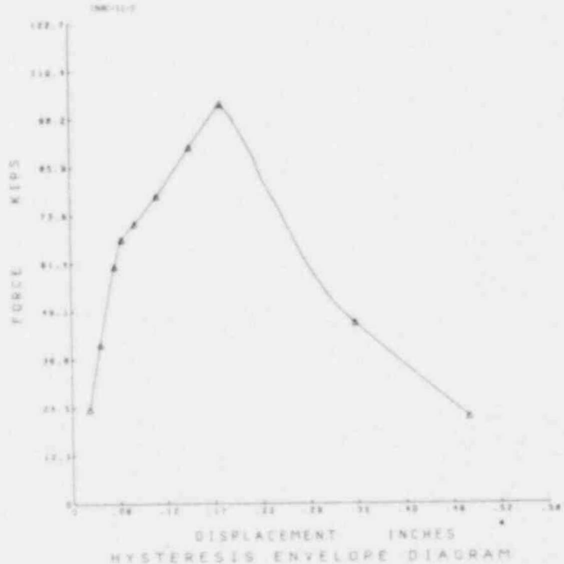

FIG. A.29 CONTINUE CBRC-11-5

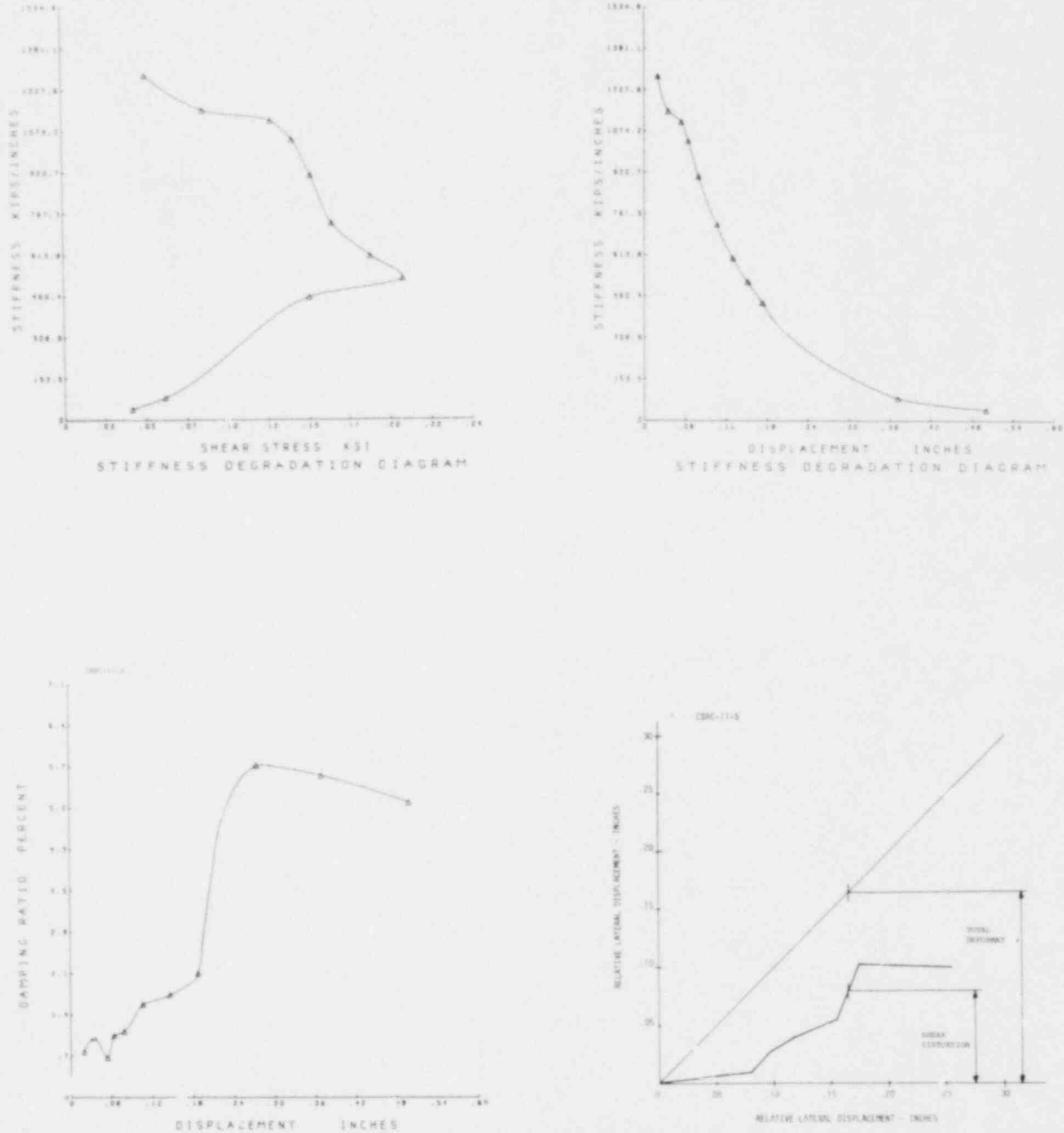

FIG. A.29 CONTINUE CBRC-11-5

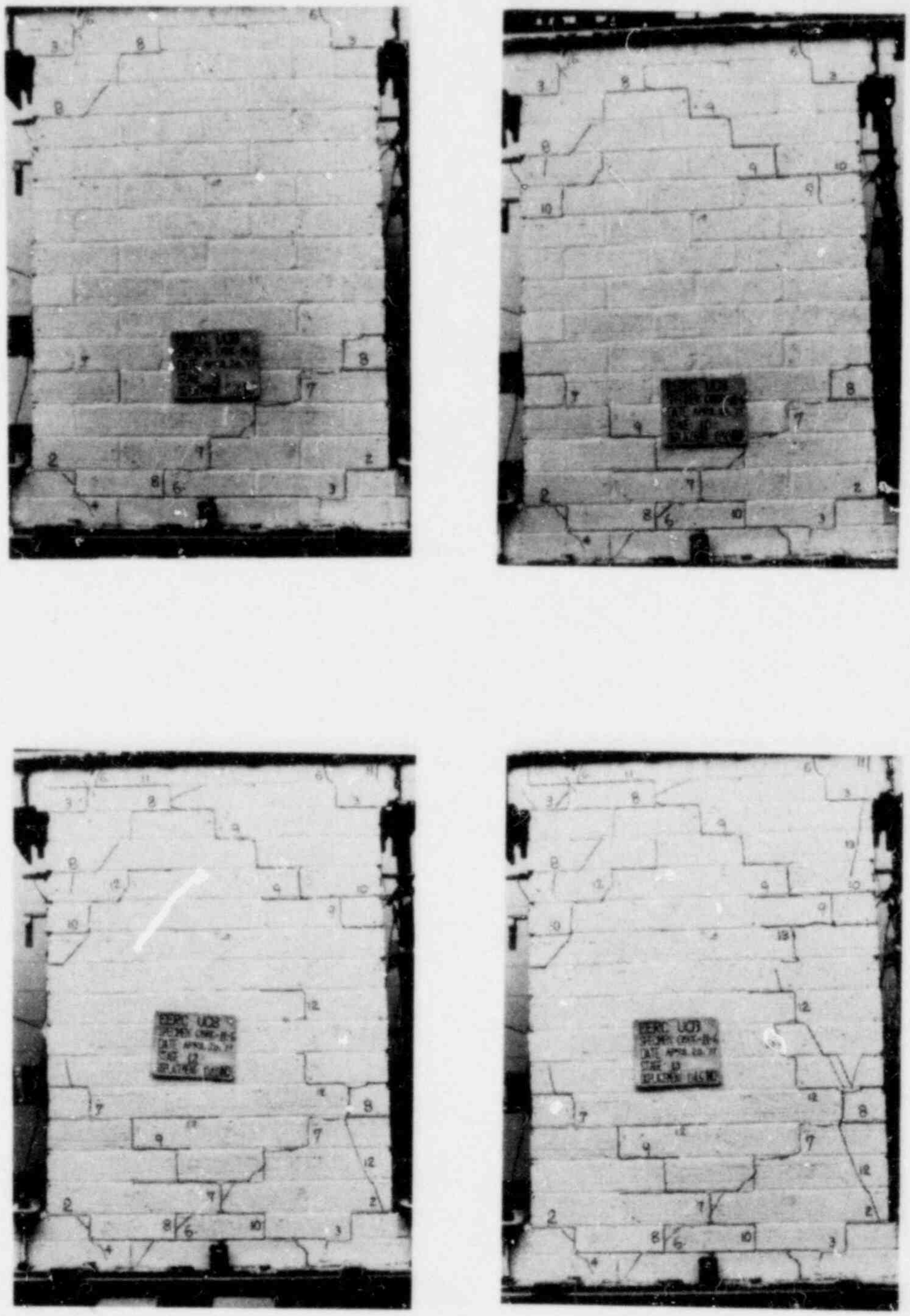

FIG. A.30 SUCCESSIVE CRACK FORMATION
AND EXPERIMENTAL RESULTS
TEST CBRC-11-6

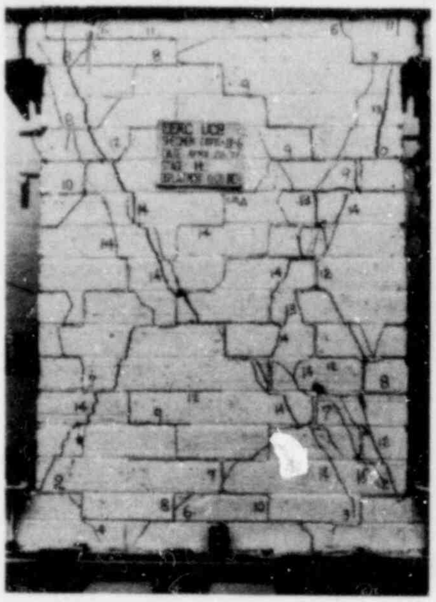

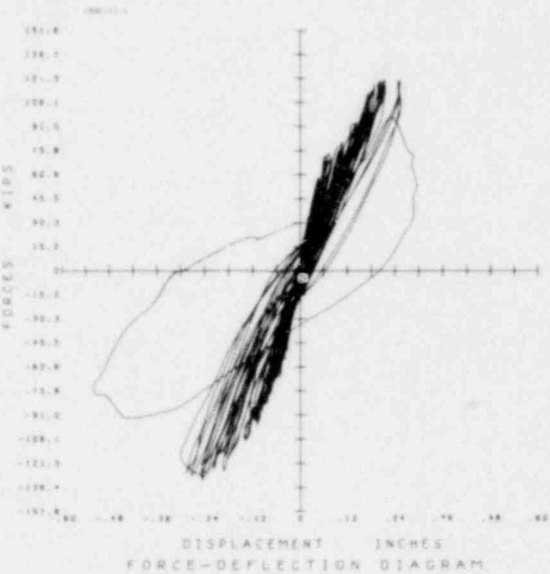

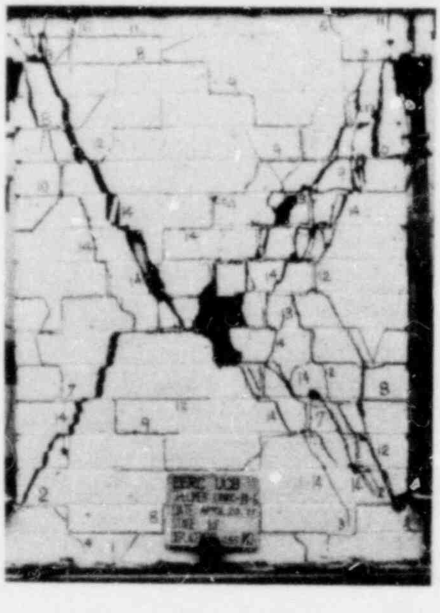

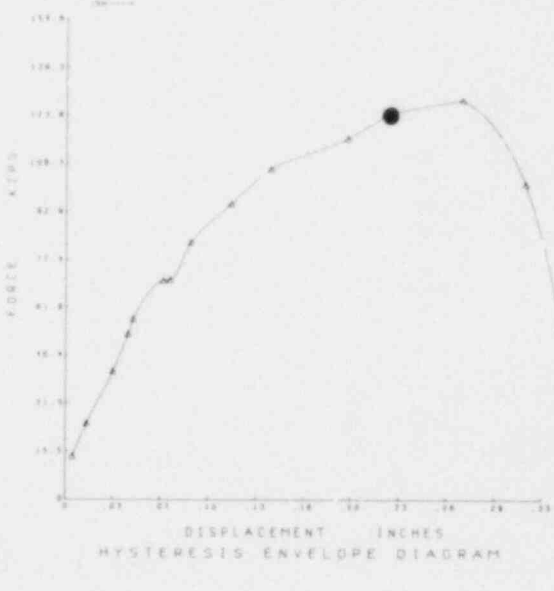

FIG. A.30 CONTINUE CBRC-11-6

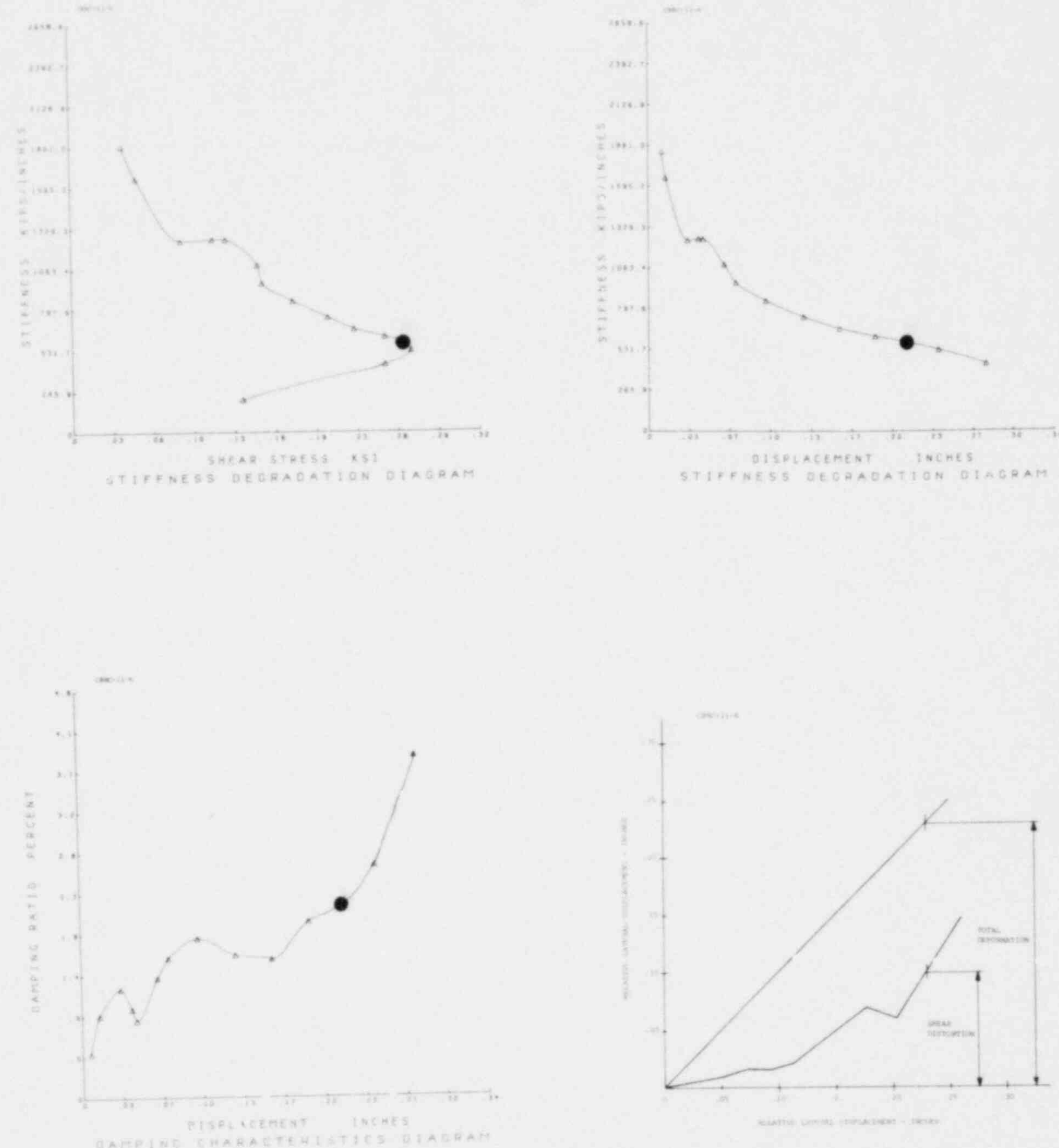

FIG. A.30 CONTINUE CBRC-11-6

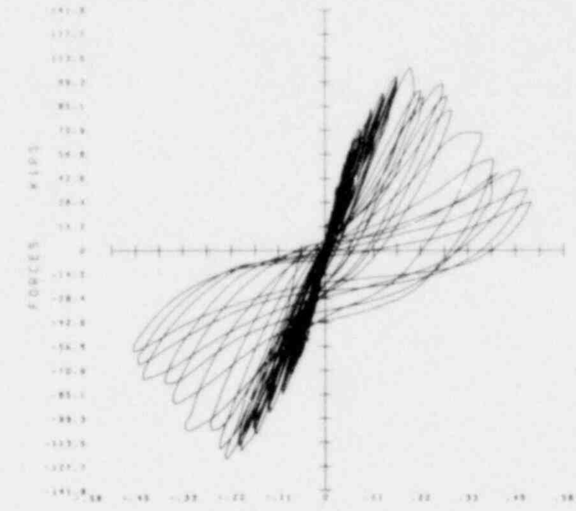

FORCE-DEFLECTION DIAGRAM

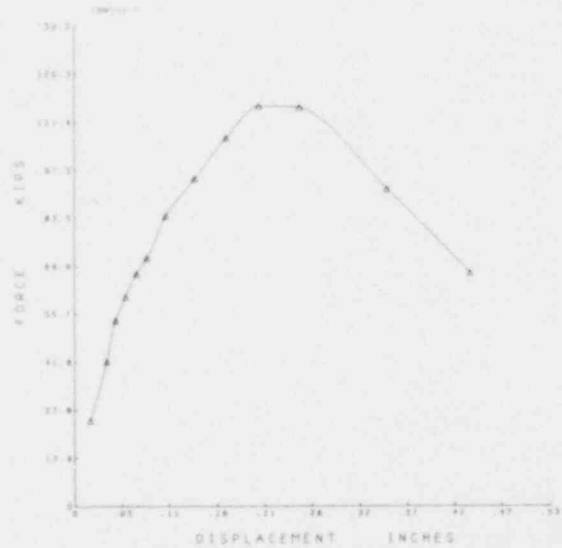

HYSTERESIS ENVELOPE DIAGRAM

FIG. A.31 EXPERIMENTAL RESULTS
TEST CBRC-11-7

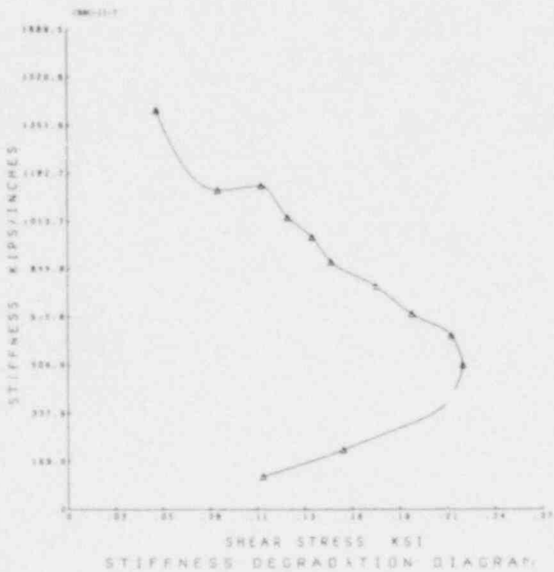

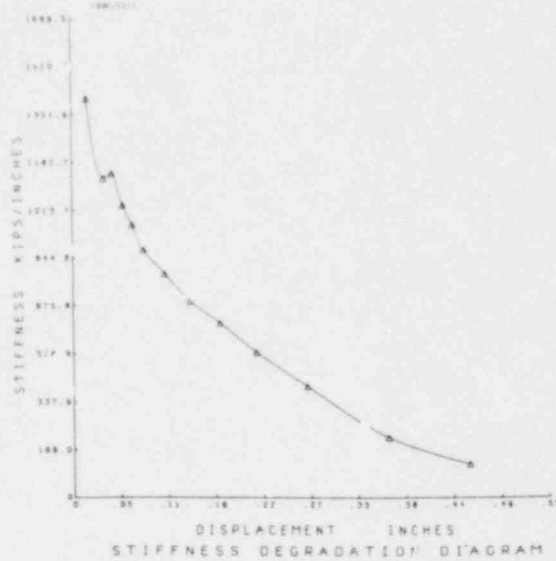

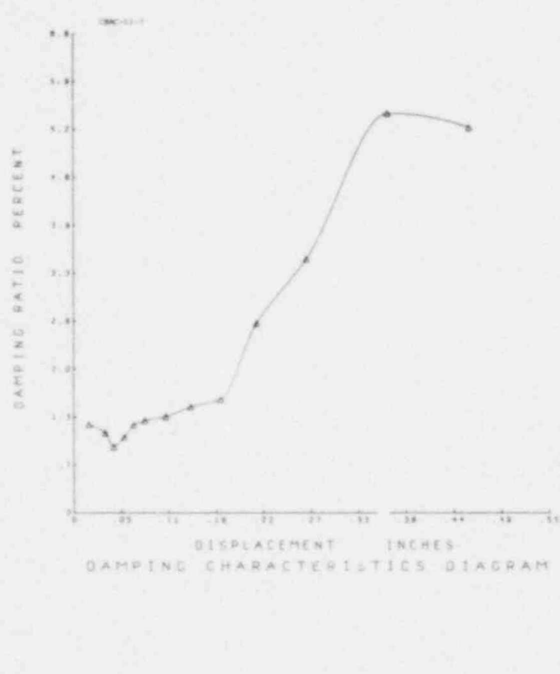

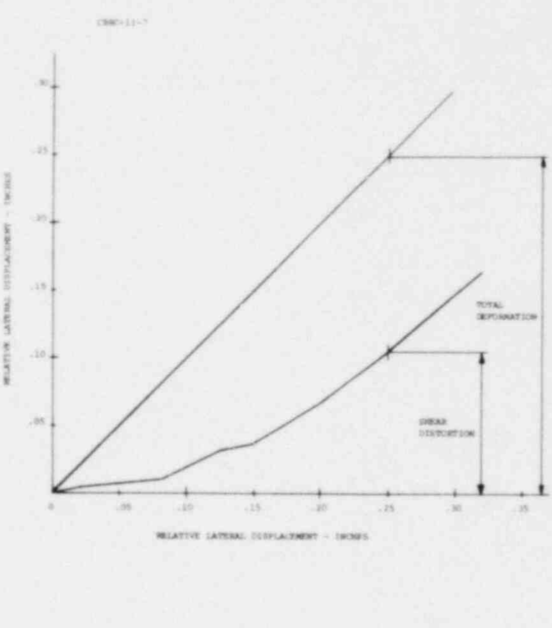

FIG. A.31 CONTINUE CBRC-11-7

EARTHQUAKE ENGINEERING RESEARCH CENTER REPORTS

NOTE: Numbers in parenthesis are Accession Numbers assigned by the National Technical Information Service; these are followed by a price code. Copies of the reports may be ordered from the National Technical Information Service, 5285 Port Royal Road, Springfield, Virginia, 22161. Accession Numbers should be quoted on orders for reports (PB --- ---) and remittance must accompany each order. Reports without this information were not available at time of printing. Upon request, EERC will mail inquirers this information when it becomes available.

EERC 67-1 "Feasibility Study Large-Scale Earthquake Simulator Facility," by J. Penzien, J.G. Bouwkamp, R.W. Clough and D. Rea - 1967 (PB 187 905)A07

EERC 68-1 Unassigned

EERC 68-2 "Inelastic Behavior of Beam-to-Column Subassemblages Under Repeated Loading," by V.V. Bertero - 1968 (PB 184 888)A05

EERC 68-3 "A Graphical Method for Solving the Wave Reflection-Refraction Problem," by H.D. McNiven and Y. Mengi - 1968 (PB 187 943)A03

EERC 68-4 "Dynamic Properties of McKinley School Buildings," by D. Rea, J.G. Bouwkamp and R.W. Clough - 1968 (PB 187 902)A07

EERC 68-5 "Characteristics of Rock Motions During Earthquakes," by H.B. Seed, I.M. Idriss and F.W. Kiefer - 1968 (PB 188 338)A03

EERC 69-1 "Earthquake Engineering Research at Berkeley," - 1969 (PB 187 906)A11

EERC 69-2 "Nonlinear Seismic Response of Earth Structures," by M. Dibaj and J. Penzien - 1969 (PB 187 904)A08

EERC 69-3 "Probabilistic Study of the Behavior of Structures During Earthquakes," by R. Ruiz and J. Penzien - 1969 (PB 187 886)A06

EERC 69-4 "Numerical Solution of Boundary Value Problems in Structural Mechanics by Reduction to an Initial Value Formulation," by N. Distefano and J. [illegible]uiman - 1969 (PB 187 942)A02

EERC 69-5 "Dynamic Programming and the Solution of the Biharmonic Equation," by N. Distefano - 1969 (PB 187 941)A03

EERC 69-6 "Stochastic Analysis of Offshore Tower Structures," by A.K. Malhotra and J. Penzien - 1969 (PB 187 903)A09

EERC 69-7 "Rock Motion Accelerograms for High Magnitude Earthquakes," by H.B. Seed and I.M. Idriss - 1969 (PB 187 940)A02

EERC 69-8 "Structural Dynamics Testing Facilities at the University of California, Berkeley," by R.M. Stephen, J.G. Bouwkamp, R.W. Clough and J. Penzien - 1969 (PB 189 111)A04

EERC 69-9 "Seismic Response of Soil Deposits Underlain by Sloping Rock Boundaries," by H. Dezfulian and H.B. Seed 1969 (PB 189 114)A03

EERC 69-10 "Dynamic Stress Analysis of Axis[illegible]es Under Arbitrary Loading," by S. Ghosh and E.L. Wilson 1969 (PB 189 026)A10

EERC 69-11 "Seismic Behavior of Multistory Frames Designed by Different Philosophies," by J.C. Anderson and V. V. Bertero - 1969 (PB 190 662)A10

EERC 69-12 "Stiffness Degradation of Reinforcing Concrete Members Subjected to Cyclic Flexural Moments," by V.V. Bertero, B. Bresler and H. Ming Liao - 1969 (PB 202 942)A07

EERC 69-13 "Response of Non-Uniform Soil Deposits to Travelling Seismic Waves," by H. Dezfulian and H.B. Seed - 1969 (PB 191 023)A03

EERC 69-14 "Damping Capacity of a Model Steel Structure," by D. Rea, R.W. Clough and J.G. Bouwkamp - 1969 (PB 190 663)A06

EERC 69-15 "Influence of Local Soil Conditions on Building Damage Potential during Earthquakes," by H.B. Seed and I.M. Idriss - 1969 (PB 191 036)A03

EERC 69-16 "The Behavior of Sands Under Seismic Loading Conditions," by M.L. Silver and H.B. Seed - 1969 (AD 714 982)A07

EERC 70-1 "Earthquake Response of Gravity Dams," by A.K. Chopra - 1970 (AD 709 640)A03

EERC 70-2 "Relationships between Soil Conditions and Building Damage in the Caracas Earthquake of July 29, 1967," by H.B. Seed, I.M. Idriss and H. Dezfulian - 1970 (PB 195 762)A05

EERC 70-3 "Cyclic Loading of Full Size Steel Connections," by E.P. Popov and R.M. Stephen - 1970 (PB 213 545)A04

EERC 70-4 "Seismic Analysis of the Charaima Building, Caraballeda, Venezuela," by Subcommittee of the SEAONC Research Committee: V.V. Bertero, P.F. Fratessa, S.A. Mahin, J.H. Sexton, A.C. Scordelis, E.L. Wilson, L.A. Wyllie, H.B. Seed and J. Penzien, Chairman - 1970 (PB 201 455)A06

EERC 70-5 "A Computer Program for Earthquake Analysis of Dams," by A.K. Chopra and P. Chakrabarti - 1970 (AD 723 994)A05

EERC 70-6 "The Propagation of Love Waves Across Non-Horizontally Layered Structures," by J. Lysmer and L.A. Drake 1970 (PB 197 896)A03

EERC 70-7 "Influence of Base Rock Characteristics on Ground Response," by J. Lysmer, H.B. Seed and P.B. Schnabel 1970 (PB 197 897)A03

EERC 70-8 "Applicability of Laboratory Test Procedures for Measuring Soil Liquefaction Characteristics under Cyclic Loading," by H.B. Seed and W.H. Peacock - 1970 (PB 198 016)A03

EERC 70-9 "A Simplified Procedure for Evaluating Soil Liquefaction Potential," by H.B. Seed and I.M. Idriss - 1970 (PB 198 009)A03

EERC 70-10 "Soil Moduli and Damping Factors for Dynamic Response Analysis," by H.B. Seed and I.M. Idriss - 1970 (PB 197 869)A03

EERC 71-1 "Koyna Earthquake of December 11, 1967 and the Performance of Koyna Dam," by A.K. Chopra and P. Chakrabarti 1971 (AD 731 496)A06

EERC 71-2 "Preliminary In-Situ Measurements of Anelastic Absorption in Soils Using a Prototype Earthquake Simulator," by R.D. Borcherdt and P.W. Rodgers - 1971 (PB 201 454)A03

EERC 71-3 "Static and Dynamic Analysis of Inelastic Frame Structures," by F.L. Porter and G.H. Powell - 1971 (PB 210 135)A06

EERC 71-4 "Research Needs in Limit Design of Reinforced Concrete Structures," by V.V. Bertero - 1971 (PB 202 943)A04

EERC 71-5 "Dynamic Behavior of a High-Rise Diagonally Braced Steel Building," by D. Rea, A.A. Shah and J.G. Bouwkamp 1971 (PB 203 584)A06

EERC 71-6 "Dynamic Stress Analysis of Porous Elastic Solids Saturated with Compressible Fluids," by J. Ghaboussi and E. L. Wilson - 1971 (PB 211 396)A06

EERC 71-7 "Inelastic Behavior of Steel Beam-to-Column Subassemblages," by H. Krawinkler, V.V. Bertero and E.P. Popov 1971 (PB 211 335)A14

EERC 71-8 "Modification of Seismograph Records for Effects of Local Soil Conditions," by P. Schnabel, H.B. Seed and J. Lysmer - 1971 (PB 214 450)A03

EERC 72-1 "Static and Earthquake Analysis of Three Dimensional Frame and Shear Wall Buildings," by E.L. Wilson and H.H. Dovey - 1972 (PB 212 904)A05

EERC 72-2 "Accelerations in Rock for Earthquakes in the Western United States," by P.B. Schnabel and H.B. Seed - 1972 (PB 213 100)A03

EERC 72-3 "Elastic-Plastic Earthquake Response of Soil-Building Systems," by T. Minami - 1972 (PB 214 868)A08

EERC 72-4 "Stochastic Inelastic Response of Offshore Towers to Strong Motion Earthquakes," by M.K. Kaul - 1972 (PB 215 713)A05

EERC 72-5 "Cyclic Behavior of Three Reinforced Concrete Flexural Members with High Shear," by E.P. Popov, V.V. Bertero and H. Krawinkler - 1972 (PB 214 555)A05

EERC 72-6 "Earthquake Response of Gravity Dams Including Reservoir Interaction Effects," by P. Chakrabarti and A.K. Chopra - 1972 (AD 762 330)A08

EERC 72-7 "...namic Properties of Pine Flat Dam," by D. Rea, C.Y. Liaw and A.K. Chopra - 1972 (AD 763 928)A05

EERC 72-8 "Three Dimensional Analysis of Building Systems," by E.L. Wilson and H.H. Dovey - 1972 (PB 222 438)A06

EERC 72-9 "Rate of Loading Effects on Uncracked and Repaired Reinforced Concrete Members," by S. Mahin, V.V. Bertero, D. Rea and M. Atalay - 1972 (PB 224 520)A08

EERC 72-10 "Computer Program for Static and Dynamic Analysis of Linear Structural Systems," by E.L. Wilson, K.-J. Bathe, J.E. Peterson and H.H.Dovey - 1972 (PB 220 437)A04

EERC 72-11 "Literature Survey - Seismic Effects on Highway Bridges," by T. Iwasaki, J. Penzien and R.W. Clough - 1972 (PB 215 613)A19

EERC 72-12 "SHAKE-A Computer Program for Earthquake Response Analysis of Horizontally Layered Sites," by P.B. Schnabel and J. Lysmer - 1972 (PB 220 207)A06

EERC 73-1 "Optimal Seismic Design of Multistory Frames," by V.V. Bertero and H. Kamil - 1973

EERC 73-2 "Analysis of the Slides in the San Fernando Dams During the Earthquake of February 9, 1971," by H.B. Seed, K.L. Lee, I.M. Idriss and F. Makdisi - 1973 (PB 223 402)A14

EERC 73-3 "Computer Aided Ultimate Load Design of Unbraced Multistory Steel Frames," by M.B. El-Hafez and G.H. Powell 1973 (PB 248 315)A09

EERC 73-4 "Experimental Investigation into the Seismic Behavior of Critical Regions of Reinforced Concrete Components as Influenced by Moment and Shear," by M. Celebi and J. Penzien - 1973 (PB 215 884)A09

EERC 73-5 "Hysteretic Behavior of Epoxy-Repaired Reinforced Concrete Beams," by M. Celebi and J. Penzien - 1973 (PB 239 568)A03

EERC 73-6 "General Purpose Computer Program for Inelastic Dynamic Response of Plane Structures," by A. Kanaan and G.H. Powell - 1973 (PB 221 260)A08

EERC 73-7 "A Computer Program for Earthquake Analysis of Gravity Dams Including Reservoir Interaction," by P. Chakrabarti and A.K. Chopra - 1973 (AD 766 271)A04

EERC 73-8 "Behavior of Reinforced Concrete Deep Beam-Column Subassemblages Under Cyclic Loads," by O. Küstü and J.G. Bouwkamp - 1973 (PB 246 117)A12

EERC 73-9 "Earthquake Analysis of Structure-Foundation Systems," by A.K. Vaish and A.K. Chopra - 1973 (AD 766 272)A07

EERC 73-10 "Deconvolution of Seismic Response for Linear Systems," by R.B. Reimer - 1973 (PB 227 179)A08

EERC 73-11 "SAP IV: A Structural Analysis Program for Static and Dynamic Response of Linear Systems," by K.-J. Bathe, E.L. Wilson and F.E. Peterson - 1973 (PB 221 967)A09

EERC 73-12 "Analytical Investigations of the Seismic Response of Long, Multiple Span Highway Bridges," by W.S. Tseng and J. Penzien - 1973 (PB 227 816)A10

EERC 73-13 "Earthquake Analysis of Multi-Story Buildings Including Foundation Interaction," by A.K. Chopra and J.A. Gutierrez - 1973 (PB 222 970)A03

EERC 73-14 "ADAP: A Computer Program for Static and Dynamic Analysis of Arch Dams," by R.W. Clough, J.M. Raphael and S. Mojtahedi - 1973 (PB 223 763)A09

EERC 73-15 "Cyclic Plastic Analysis of Structural Steel Joints," by R.B. Pinkney and R.W. Clough - 1973 (PB 226 843)A08

EERC 73-16 "QUAD-4: A Computer Program for Evaluating the Seismic Response of Soil Structures by Variable Damping Finite Element Procedures," by I.M. Idriss, J. Lysmer, R. Hwang and H.B. Seed - 1973 (PB 229 424)A05

EERC 73-17 "Dynamic Behavior of a Multi-Story Pyramid Shaped Building," by R.M. Stephen, J.P. Hollings and J.G. Bouwkamp - 1973 (PB 240 718)A06

EERC 73-18 "Effect of Different Types of Reinforcing on Seismic Behavior of Short Concrete Columns," by V.V. Bertero, J. Hollings, O. Küstü, R.M. Stephen and J.G. Bouwkamp - 1973

EERC 73-19 "Olive View Medical Center Materials Studies, Phase I," by B. Bresler and V.V. Bertero - 1973 (PB 235 986)A06

EERC 73-20 "Linear and Nonlinear Seismic Analysis Computer Programs for Long Multiple-Span Highway Bridges," by W.S. Tseng and J. Penzien - 1973

EERC 73-21 "Constitutive Models for Cyclic Plastic Deformation of Engineering Materials," by J.M. Kelly and P.P. Gillis 1973 (PB 226 024)A03

EERC 73-22 "DRAIN - 2D User's Guide," by G.H. Powell - 1973 (PB 227 016)A05

EERC 73-23 "Earthquake Engineering at Berkeley - 1973," (PB 226 033)A11

EERC 73-24 Unassigned

EERC 73-25 "Earthquake Response of Axisymmetric Tower Structures Surrounded by Water," by C.Y. Liaw and A.K. Chopra 1973 (AD 773 052)A09

EERC 73-26 "Investigation of the Failures of the Olive View Stairtowers During the San Fernando Earthquake and Their Implications on Seismic Design," by V.V. Bertero and R.G. Collins - 1973 (PB 235 106)A13

EERC 73-27 "Further Studies on Seismic Behavior of Steel Beam-Column Subassemblages," by V.V. Bertero, H. Krawinkler and E.P. Popov - 1973 (PB 234 172)A06

EERC 74-1 "Seismic Risk Analysis," by C.S. Oliveira - 1974 (PB 235 920)A06

EERC 74-2 "Settlement and Liquefaction of Sands Under Multi-Directional Shaking," by R. Pyke, C.K. Chan and H.B. Seed 1974

EERC 74-3 "Optimum Design of Earthquake Resistant Shear Buildings," by D. Ray, K.S. Pister and A.K. Chopra - 1974 (PB 231 172)A06

EERC 74-4 "LUSH - A Computer Program for Complex Response Analysis of Soil-Structure Systems," by J. Lysmer, T. Udaka, H.B. Seed and R. Hwang - 1974 (PB 236 796)A05

EERC 74-5 "Sensitivity Analysis for Hysteretic Dynamic Systems: Applications to Earthquake Engineering," by D. Ray 1974 (PB 233 213)A06

EERC 74-6 "Soil Structure Interaction Analyses for Evaluating Seismic Response," by H.B. Seed, J. Lysmer and R. Hwang 1974 (PB 236 519)A04

EERC 74-7 Unassigned

EERC 74-8 "Shaking Table Tests of a Steel Frame - A Progress Report," by R.W. Clough and D. Tang - 1974 (PB 240 269)A03

EERC 74-9 "Hysteretic Behavior of Reinforced Concrete Flexural Members with Special Web Reinforcement," by V.V. Bertero, E.P. Popov and T.Y. Wang - 1974 (PB 236 797)A07

EERC 74-10 "Applications of Reliability-Based, Global Cost Optimization to Design of Earthquake Resistant Structures," by E. Vitiello and K.S. Pister - 1974 (PB 237 231)A06

EERC 74-11 "Liquefaction of Gravelly Soils Under Cyclic Loading Conditions," by R.T. Wong, H.B. Seed and C.K. Chan 1974 (PB 242 042)A03

EERC 74-12 "Site-Dependent Spectra for Earthquake-Resistant Design," by H.B. Seed, C. Ugas and J. Lysmer - 1974 (PB 240 953)A03

EERC 74-13 "Earthquake Simulator Study of a Reinforced Concrete Frame," by P. Hidalgo and R.W. Clough - 1974 (PB 241 944)A13

EERC 74-14 "Nonlinear Earthquake Response of Concrete Gravity Dams," by N. Pal - 1974 (AD/A 006 583)A06

EERC 74-15 "Modeling and Identification in Nonlinear Structural Dynamics - I. One Degree of Freedom Models," by N. Distefano and A. Rath - 1974 (PB 241 548)A06

EERC 75-1 "Determination of Seismic Design Criteria for the Dumbarton Bridge Replacement Structure, Vol. I: Description, Theory and Analytical Modeling of Bridge and Parameters," by F. Baron and S.-H. Pang - 1975 (PB 259 407)A15

EERC 75-2 "Determination of Seismic Design Criteria for the Dumbarton Bridge Replacement Structure, Vol. II: Numerical Studies and Establishment of Seismic Design Criteria," by F. Baron and S.-H. Pang - 1975 (PB 259 408)A11 (For set of EERC 75-1 and 75-2 (PB 259 406))

EERC 75-3 "Seismic Risk Analysis for a Site and a Metropolitan Area," by C.S. Oliveira - 1975 (PB 248 134)A09

EERC 75-4 "Analytical Investigations of Seismic Response of Short, Single or Multiple-Span Highway Bridges," by M.-C. Chen and J. Penzien - 1975 (PB 241 454)A09

EERC 75-5 "An Evaluation of Some Methods for Predicting Seismic Behavior of Reinforced Concrete Buildings," by S.A. Mahin and V.V. Bertero - 1975 (PB 246 306)A16

EERC 75-6 "Earthquake Simulator Study of a Steel Frame Structure, Vol. I: Experimental Results," by R.W. Clough and D.T. Tang - 1975 (PB 243 981)A13

EERC 75-7 "Dynamic Properties of San Bernardino Intake Tower," by D. Rea, C.-Y. Liaw and A.K. Chopra - 1975 (AD/A008 406) A05

EERC 75-8 "Seismic Studies of the Articulation for the Dumbarton Bridge Replacement Structure, Vol. I: Description, Theory and Analytical Modeling of Bridge Components," by F. Baron and R.E. Hamati - 1975 (PB 251 539)A07

EERC 75-9 "Seismic Studies of the Articulation for the Dumbarton Bridge Replacement Structure, Vol. 2: Numerical Studies of Steel and Concrete Girder Alternates," by F. Baron and R.E. Hamati - 1975 (PB 251 540)A10

EERC 75-10 "Static and Dynamic Analysis of Nonlinear Structures," by D.P. Mondkar and G.H. Powell - 1975 (PB 242 434)A08

EERC 75-11 "Hysteretic Behavior of Steel Columns," by E.P. Popov, V.V. Bertero and S. Chandramouli - 1975 (PB 252 365)A11

EERC 75-12 "Earthquake Engineering Research Center Library Printed Catalog," - 1975 (PB 243 711)A26

EERC 75-13 "Three Dimensional Analysis of Building Systems (Extended Version)," by E.L. Wilson, J.P. Hollings and H.H. Dovey - 1975 (PB 243 989)A07

EERC 75-14 "Determination of Soil Liquefaction Characteristics by Large-Scale Laboratory Tests," by P. De Alba, C.K. Chan and H.B. Seed - 1975 (NUREG 0027)A08

EERC 75-15 "A Literature Survey - Compressive, Tensile, Bond and Shear Strength of Masonry," by R.L. Mayes and R.W. Clough - 1975 (PB 246 292)A10

EERC 75-16 "Hysteretic Behavior of Ductile Moment Resisting Reinforced Concrete Frame Components," by V.V. Bertero and E.P. Popov - 1975 (PB 246 388)A05

EERC 75-17 "Relationships Between Maximum Acceleration, Maximum Velocity, Distance from Source, Local Site Conditions for Moderately Strong Earthquakes," by H.B. Seed, R. Murarka, J. Lysmer and I.M. Idriss - 1975 (PB 248 172)A03

EERC 75-18 "The Effects of Method of Sample Preparation on the Cyclic Stress-Strain Behavior of Sands," by J. Mulilis, C.K. Chan and H.B. Seed - 1975 (Summarized in EERC 75-28)

EERC 75-19 "The Seismic Behavior of Critical Regions of Reinforced Concrete Components as Influenced by Moment, Shear and Axial Force," by M.B. Atalay and J. Penzien - 1975 (PB 258 842)A11

EERC 75-20 "Dynamic Properties of an Eleven Story Masonry Building," by R.M. Stephen, J.P. Hollings, J.G. Bouwkamp and D. Jurukovski - 1975 (PB 246 945)A04

EERC 75-21 "State-of-the-Art in Seismic Strength of Masonry - An Evaluation and Review," by R.L. Mayes and R.W. Clough 1975 (PB 249 040)A07

EERC 75-22 "Frequency Dependent Stiffness Matrices for Viscoelastic Half-Plane Foundations," by A.K. Chopra, P. Chakrabarti and G. Dasgupta - 1975 (PB 248 121)A07

EERC 75-23 "Hysteretic Behavior of Reinforced Concrete Framed Walls," by T.Y. Wong, V.V. Bertero and E.P. Popov - 1975

EERC 75-24 "Testing Facility for Subassemblages of Frame-Wall Structural Systems," by V.V. Bertero, E.P. Popov and T. Endo - 1975

EERC 75-25 "Influence of Seismic History on the Liquefaction Characteristics of Sands," by H.B. Seed, K. Mori and C.K. Chan - 1975 (Summarized in EERC 75-28)

EERC 75-26 "The Generation and Dissipation of Pore Water Pressures during Soil Liquefaction," by H.B. Seed, P.P. Martin and J. Lysmer - 1975 (PB 252 648)A03

EERC 75-27 "Identification of Research Needs for Improving Aseismic Design of Building Structures," by V.V. Bertero 1975 (PB 248 136)A05

EERC 75-28 "Evaluation of Soil Liquefaction Potential during Earthquakes," by H.B. Seed, I. Arango and C.K. Chan - 1975 (NUREG 0026)A13

EERC 75-29 "Representation of Irregular Stress Time Histories by Equivalent Uniform Stress Series in Liquefaction Analyses," by H.B. Seed, I.M. Idriss, F. Makdisi and N. Banerjee - 1975 (PB 252 635)A03

EERC 75-30 "FLUSH - A Computer Program for Approximate 3-D Analysis of Soil-Structure Interaction Problems," by J. Lysmer, T. Udaka, C.-F. Tsai and H.B. Seed - 1975 (PB 259 332)A07

EERC 75-31 "ALUSH - A Computer Program for Seismic Response Analysis of Axisymmetric Soil-Structure Systems," by E. Berger, J. Lysmer and H.B. Seed - 1975

EERC 75-32 "TRIP and TRAVEL - Computer Programs for Soil-Structure Interaction Analysis with Horizontally Travelling Waves," by T. Udaka, J. Lysmer and H.B. Seed - 1975

EERC 75-33 "Predicting the Performance of Structures in Regions of High Seismicity," by J. Penzien - 1975 (PB 248 130)A03

EERC 75-34 "Efficient Finite Element Analysis of Seismic Structure - Soil - Direction," by J. Lysmer, H.B. Seed, T. Udaka, R.N. Hwang and C.-F. Tsai - 1975 (PB 253 570)A03

EERC 75-35 "The Dynamic Behavior of a First Story Girder of a Three-Story Steel Frame Subjected to Earthquake Loading," by R.W. Clough and L.-Y. Li - 1975 (PB 248 841)A05

EERC 75-36 "Earthquake Simulator Study of a Steel Frame Structure, Volume II - Analytical Results," by D.T. Tang - 1975 (PB 252 926)A10

EERC 75-37 "ANSR-I General Purpose Computer Program for Analysis of Non-Linear Structural Response," by D.P. Mondkar and G.H. Powell - 1975 (PB 252 386)A08

EERC 75-38 "Nonlinear Response Spectra for Probabilistic Seismic Design and Damage Assessment of Reinforced Concrete Structures," by M. Murakami and J. Penzien - 1975 (PB 259 530)A05

EERC 75-39 "Study of a Method of Feasible Directions for Optimal Elastic Design of Frame Structures Subjected to Earthquake Loading," by N.D. Walker and K.S. Pister - 1975 (PB 257 781)A06

EERC 75-40 "An Alternative Representation of the Elastic-Viscoelastic Analogy," by G. Dasgupta and J.L. Sackman - 1975 (PB 252 173)A03

EERC 75-41 "Effect of Multi-Directional Shaking on Liquefaction of Sands," by H.B. Seed, R. Pyke and G.R. Martin - 1975 (PB 258 78[illegible] A03

EERC 76-1 "Strength and Ductility Evaluation of Existing Low-Rise Reinforced Concrete Buildings - Screening Method," by T. Okada and B. Bresler - 1976 (PB 257 906)A11

EERC 76-2 "Experimental and Analytical Studies on the Hysteretic Behavior of Reinforced Concrete Rectangular and T-Beams," by S.-Y.M. Ma, E.P. Popov and V.V. Bertero - 1976 (PB 260 843)A12

EERC 76-3 "[illegible]mic Behavior of a Multistory Triangular-Shaped Building," by J. Petrovski, R.M. Stephen, E. Gartenbaum [illegible].G. Bouwkamp - 1976

EERC 76-4 "Earthquake Induced Deformations of Earth Dams," by N. Serff and H.B. Seed - 1976

EERC 76-5 "Analysis and Design of Tube-Type Tall Building Structures," by H. de Clercq and G.H. Powell - 1976 (PB 252 220) A10

EERC 76-6 "Time and Frequency Domain Analysis of Three-Dimensional Ground Motions, San Fernando Earthquake," by T. Kubo and J. Penzien (PB 260 556)A11

EERC 76-7 "Expected Performance of Uniform Building Code Design Masonry Structures," by R.L. Mayes, Y. Omote, S.W. Chen and R.W. Clough - 1976

EERC 76-8 "Cyclic Shear Tests on Concrete Masonry Piers," Part I - Test Results," by R.L. Mayes, Y. Omote and R.W. Clough - 1976 (PB 264 424)A06

EERC 76-9 "A Substructure Method for Earthquake Analysis of Structure - Soil Interaction," by J.A. Gutierrez and A.K. Chopra - 1976 (PB 257 783)A08

EERC 76-10 "Stabilization of Potentially Liquefiable Sand Deposits using Gravel Drain Systems," by H.B. Seed and J.R. Booker - 1976 (PB 258 820)A04

EERC 76-11 "Influence of Design and Analysis Assumptions on Computed Inelastic Response of Moderately Tall Frames," by G.H. Powell and D.G. Row - 1976

EERC 76-12 "Sensitivity Analysis for Hysteretic Dynamic Systems: Theory and Applications," by D. Ray, K.S. Pister and E. Polak - 1976 (PB 262 859)A04

EERC 76-13 "Coupled Lateral Torsional Response of Buildings to Ground Shaking," by C.L. Kan and A.K. Chopra - 1976 (PB 257 907)A09

EERC 76-14 "Seismic Analyses of the Banco de America," by V.V. Bertero, S.A. Mahin and J.A. Hollings - 1976

EERC 76-15 "Reinforced Concrete Frame 2: Seismic Testing and Analytical Correlation," by R.W. Clough and J. Gidwani - 1976 (PB 261 323)A08

EERC 76-16 "Cyclic Shear Tests on Masonry Piers, Part II - Analysis of Test Results," by R.L. Mayes, Y. Omote and R.W. Clough - 1976

EERC 76-17 "Structural Steel Bracing Systems: Behavior Under Cyclic Loading," by E.P. Popov, K. Takanashi and C.W. Roeder - 1976 (PB 260 715)A05

EERC 76-18 "Experimental Model Studies on Seismic Response of High Curved Overcrossings," by D. Williams and W.G. Godden - 1976

EERC 76-19 "Effects of Non-Uniform Seismic Disturbances on the Dumbarton Bridge Replacement Structure," by F. Baron and R.E. Hamati - 1976

EERC 76-20 "Investigation of the Inelastic Characteristics of a Single Story Steel Structure Using System Identification and Shaking Table Experiments," by V.C. Matzen and H.D. McNiven - 1976 (PB 258 453)A07

EERC 76-21 "Capacity of Columns with Splice Imperfections," by E.P. Popov, R.M. Stephen and R. Philbrick - 1976 (PB 260 378)A04

EERC 76-22 "Response of the Olive View Hospital Main Building during the San Fernando Earthquake," by S. A. Mahin, R. Collins, A.K. Chopra and V.V. Bertero - 1976

EERC 76-23 "A Study on the Major Factors Influencing the Strength of Masonry Prisms," by N.M. Mostaghel, R.L. Mayes, R. W. Clough and S.W. Chen - 1976

EERC 76-24 "GADFLEA - A Computer Program for the Analysis of Pore Pressure Generation and Dissipation during Cyclic or Earthquake Loading," by J.R. Booker, M.S. Rahman and H.B. Seed - 1976 (PB 263 947)A04

EERC 76-25 "Rehabilitation of an Existing Building: A Case Study," by B. Bresler and J. Axley - 1976

EERC 76-26 "Correlative Investigations on Theoretical and Experimental Dynamic Behavior of a Model Bridge Structure," by K. Kawashima and J. Penzien - 1976 (PB 263 388)A11

EERC 76-27 "Earthquake Response of Coupled Shear Wall Buildings," by T. Srichatrapimuk - 1976 (PB 265 157)A07

EERC 76-28 "Tensile Capacity of Partial Penetration Welds," by E.P. Popov and R.M. Stephen - 1976 (PB 262 899)A03

EERC 76-29 "Analysis and Design of Numerical Integration Methods in Structural Dynamics," by H.M. Hilber - 1976 (PB 264 410)A06

EERC 76-30 "Contribution of a Floor System to the Dynamic Characteristics of Reinforced Concrete Buildings," by L.J. Edgar and V.V. Bertero - 1976

EERC 76-31 "The Effects of Seismic Disturbances on the Golden Gate Bridge," by F. Baron, M. Arikan and R.E. Hamati - 1976

EERC 76-32 "Infilled Frames in Earthquake Resistant Construction," by R.E. Klingner and V.V. Bertero - 1976 (PB 265 892)A13

UCB/EERC-77/01 "PLUSH - A Computer Program for Probabilistic Finite Element Analysis of Seismic Soil-Structure Interaction," by M.P. Romo Organista, J. Lysmer and H.B. Seed - 1977

UCB/EERC-77/02 "Soil-Structure Interaction Effects at the Humboldt Bay Power Plant in the Ferndale Earthquake of June 7, 1975," by J.E. Valera, H.B. Seed, C.F. Tsai and J. Lysmer - 1977 (PB 265 795)A04

UCB/EERC-77/03 "Influence of Sample Disturbance on Sand Response to Cyclic Loading," by K. Mori, H.B. Seed and C.K. Chan - 1977 (PB 267 352)A04

UCB/EERC-77/04 "Seismological Studies of Strong Motion Records," by J. Shoja-Taheri - 1977 (PB 269 655)A10

UCB/EERC-77/05 "Testing Facility for Coupled-Shear Walls," by L. Li-Hyung, V.V. Bertero and E.P. Popov - 1977

UCB/EERC-77/06 "Developing Methodologies for Evaluating the Earthquake Safety of Existing Buildings," by No. 1 - B. Bresler; No. 2 - B. Bresler, T. Okada and D. Zisling; No. 3 - T. Okada and B. Bresler; No. 4 - V.V. Bertero and B. Bresler - 1977 (PB 267 354)A08

UCB/EERC-77/07 "A Literature Survey - Transverse Strength of Masonry Walls," by Y. Omote, R.L. Mayes, S.W. Chen and R.W. Clough - 1977 (PB 277 933)A07

UCB/EERC-77/08 "DRAIN-TABS: A Computer Program for Inelastic Earthquake Response of Three Dimensional Buildings," by R. Guendelman-Israel and G.H. Powell - 1977 (PB 270 693)A07

UCB/EERC-77/09 "SUBWALL: A Special Purpose Finite Element Computer Program for Practical Elastic Analysis and Design of Structural Walls with Substructure Option," by D.Q. Le, H. Peterson and E.P. Popov - 1977 (PB 270 567)A05

UCB/EERC-77/10 "Experimental Evaluation of Seismic Design Methods for Broad Cylindrical Tanks," by D.P. Clough (PB 272 280)A13

UCB/EERC-77/11 "Earthquake Engineering Research at Berkeley - 1976," - 1977 (PB 273 507)A09

UCB/EERC-77/12 "Automated Design of Earthquake Resistant Multistory Steel Building Frames," by N.D. Walker, Jr. - 1977 (PB 276 526)A09

UCB/EERC-77/13 "Concrete Confined by Rectangular Hoops Subjected to Axial Loads," by J. Vallenas, V.V. Bertero and E.P. Popov - 1977 (PB 275 165)A06

UCB/EERC-77/14 "Seismic Strain Induced in the Ground During Earthquakes," by Y. Sugimura - 1977 (PB 284 201)A04

UCB/EERC-77/15 "Bond Deterioration under Generalized Loading," by V.V. Bertero, E.P. Popov and S. Viwathanatepa - 1977

UCB/EERC-77/16 "Computer Aided Optimum Design of Ductile Reinforced Concrete Moment Resisting Frames," by S.W. Zagajeski and V.V. Bertero - 1977 (PB 280 137)A07

UCB/EERC-77/17 "Earthquake Simulation Testing of a Stepping Frame with Energy-Absorbing Devices," by J.M. Kelly and D.F. Tsztoo - 1977 (PB 273 506)A04

UCB/EERC-77/18 "Inelastic Behavior of Eccentrically Braced Steel Frames under Cyclic Loadings," by C.W. Roeder and E.P. Popov - 1977 (PB 275 526)A15

UCB/EERC-77/19 "A Symplified Procedure for Estimating Earthquake-Induced Deformations in Dams and Embankments," by F.I. Makdisi and H.B. Seed - 1977 (PB 276 820) A04

UCB/EERC-77/20 "The Performance of Earth Dams during Earthquakes," by H.B. Seed, F.I. Makdisi and P. de Alba - 1977 (PB 276 821)A04

UCB/EERC-77/21 "Dynamic Plastic Analysis Using Stress Resultant Finite Element Formulation," by P. Lukkunapvasit and J.M. Kelly - 1977 (PB 275 453)A04

UCB/EERC-77/22 "Preliminary Experimental Study of Seismic Uplift of a Steel Frame," by R.W. Clough and A.A. Huckelbridge 1977 (PB 278 769)A08

UCB/EERC-77/23 "Earthquake Simulator Tests of a Nine-Story Steel Frame with Columns Allowed to Uplift," by A.A. Huckelbridge - 1977 (PB 277 944)A09

UCB/EERC-77/24 "Nonlinear Soil-Structure Interaction of Skew Highway Bridges," by M.-C. Chen and J. Penzien - 1977 (PB 276 176)A07

UCB/EERC-77/25 "Seismic Analysis of an Offshore Structure Supported on Pile Foundations," by D.D.-N. Liou and J. Penzien 1977 (PB 283 180)A06

UCB/EERC-77/26 "Dynamic Stiffness Matrices for Homogeneous Viscoelastic Half-Planes," by G. Dasgupta and A.K. Chopra - 1977 (PB 279 654)A06

UCB/EERC-77/27 "A Practical Soft Story Earthquake Isolation System," by J.M. Kelly and J.M. Eidinger - 1977 (PB 276 814)A07

UCB/EERC-77/28 "Seismic Safety of Existing Buildings and Incentives for Hazard Mitigation in San Francisco: An Exploratory Study," by A.J. Meltsner - 1977 (PB 281 970)A05

UCB/EERC-77/29 "Dynamic Analysis of Electrohydraulic Shaking Tables," by D. Rea, S. Abedi-Hayati and Y. Takahashi 1977 (PB 282 569)A04

UCB/EERC-77/30 "An Approach for Improving Seismic - Resistant Behavior of Reinforced Concrete Interior Joints," by B. Galunic, V.V. Bertero and E.P. Popov - 1977

UCB/EERC-78/01 "The Development of Energy-Absorbing Devices for Aseismic Base Isolation Systems," by J.M. Kelly and D.F. Tsztoo 1978 (PB 284 978)A04

UCB/EERC-78/02 "Effect of Tensile Prestrain on the Cyclic Response of Structural Steel Connections," by J.G. Bouwkamp and A. Mukhopadhyay - 1978

UCB/EERC-78/03 "Experimental Results of an Earthquake Isolation System using Natural Rubber Bearings," by J.M. Eidinger and J.M. Kelly - 1978

UCB/EERC-78/04 "Seismic Behavior of Tall Liquid Storage Tanks," by A. Niwa 1978

UCB/EERC-78/05 "Hysteretic Behavior of Reinforced Concrete Columns Subjected to High Axial and Cyclic Shear Forces," by S.W. Zagajeski, V.V. Bertero and J.G. Bouwkamp - 1978

UCB/EERC-78/06 "Inelastic Beam-Column Elements for the ANSR-I Program," by A. Riahi, D.G. Row and G.H. Powell - 1978

UCB/EERC-78/07 "Studies of Structural Response to Earthquake Ground Motion," by O.A. Lopez and A.K. Chopra - 1978

UCB/EERC-78/08 "A Laboratory Study of the Fluid-Structure Interaction of Submerged Tanks and Caissons in Earthquakes," by R.C. Byrd - 1978 (PB 284 957)A08

UCB/EERC-78/09 "Models for Evaluating Damageability of Structures," by I. Sakamoto and B. Bresler - 1978

UCB/EERC-78/10 "Seismic Performance of Secondary Structural Elements," by I. Sakamoto - 1978

UCB/EERC-78/11 Case Study--Seismic Safety Evaluation of a Reinforced Concrete School Building," by J. Axley and B. Bresler 1978

UCB/EERC-78/12 "Potential Damageability in Existing Buildings," by T. Blejwas and B. Bresler - 1978

UCB/EERC-78/13 "Dynamic Behavior of a Pedestal Base Multistory Building," by R. M. Stephen, E. L. Wilson, J. G. Bouwkamp and M. Button - 1978

UCB/EERC-78/14 "Seismic Response of Bridges - Case Studies," by R.A. Imbsen, V. Nutt and J. Penzien - 1978

UCB/EERC-78/15 "A Substructure Technique for Nonlinear Static and Dynamic Analysis," by D.G. Row and G.H. Powell - 1978

UCB/EERC-78/16 "Seismic Performance of Nonstructural and Secondary Structural Elements," by Isao Sakamoto - 1978

UCB/EERC-78/17 "Model for Evaluating Damageability of Structures," by Isao Sakamoto and B. Bresler - 1978

UCB/EERC-78/18 "Response of K-Braced Steel Frame Models to Lateral Loads," by J.G. Bouwkamp, R.M. Stephen and E.P. Popov - 1978

UCB/EERC-78/19 "Rational Design Methods for Light Equipment in Structures Subjected to Ground Motion," by Jerome L. Sackman and James M. Kelly - 1978

UCB/EERC-78/20 "Testing of a Wind Restraint for Aseismic Base Isolation," by James M. Kelly and Daniel E. Chitty - 1978

UCB/EERC-78/21 "APOLLO A Computer Program for the Analysis of Pore Pressure Generation and Dissipation in Horizontal Sand Layers During Cyclic or Earthquake Loading," by Philippe P. Martin and H. Bolton Seed - 1978

UCB/EERC-78/22 "Optimal Design of an Earthquake Isolation System," by M.A. Bhatti, K.S. Pister and E. Polak - 1978

UCB/EERC-78/23 "MASH A Computer Program for the Non-Linear Analysis of Vertically Propagating Shear Waves in Horizontally Layered Deposits," by Philippe P. Martin and H. Bolton Seed - 1978

UCB/EERC-78/24 "Investigation of the Elastic Characteristics of a Three Story Steel Frame Using System Identification," by Izak Kaya and Hugh D. McNiven - 1978

UCB/EERC-78/25 "Investigation of the Nonlinear Characteristics of a Three-Story Steel Frame Using System Identification," by I. Kaya and H.D. McNiven - 1978

UCB/EERC-78/26 "Studies of Strong Ground Motion in Taiwan," by Y.M. Hsiung, B.A. Bolt and J. Penzien - 1978

UCB/EERC-78/27 "Cyclic Loading Tests of Masonry Single Piers Volume 1 - Height to Width Ratio of 2," by P.A. Hidalgo, R.L. Mayes, H.D. McNiven & R.W. Clough - 1978

UCB/EERC-78/28 "Cyclic Loading Tests of Masonry Single Piers Volume 2 - Height to Width Radio of 1," by S.-W.J.Chen, P.A. Hidalgo, R.L. Mayes, R.W. Clough & H.D. McNiven - 1978

For sale by the National Technical Information Service, U. S. Department of Commerce, Springfield, Virginia 22161.

See back of report for up to date listing of EERC reports.